RAS 14166

UNITED STATES OF AMERICA
NUCLEAR REGULATORY COMMISSION
OFFICE OF THE SECRETARY

ATOMIC SAFETY AND LICENSING BOARD

Before Administrative Judges:
E. Roy Hawkens, Chair
Dr. Paul B. Abramson
Dr. Anthony J. Baratta

In the Matter of	)	
	)	
AMERGEN ENERGY COMPANY, LLC	)	
	)	Docket No. 50-0219-LR
(License Renewal for the Oyster Creek Nuclear Generating Station)	)	
	)	

PREFILED SUR-REBUTTAL WRITTEN TESTIMONY OF DR. RUDOLF H. HAUSLER REGARDING CITIZENS' DRYWELL CONTENTION

On behalf of Citizens, Dr. Rudolf H. Hausler hereby submits the following sur-rebuttal testimony regarding Citizens' contention.

Q1. Have you reviewed the rebuttal testimony of AmerGen and the NRC Staff in this case?

A1. Yes I have.

Q2. What is your overall reaction to AmerGen's rebuttal testimony?

A2. Overall, I think AmerGen is now trying to disavow its own data because they show that it is likely the drywell does not meet the acceptance criteria. If, as Amergen has alleged, the exterior measurements are not numerous enough to characterize the state of the drywell, and, as AmerGen has admitted and is obvious, the interior measurements are not representative of the drywell, then there is no reasonable assurance that any margin will exist at the start of any period of extended operation. Indeed, the NRC Staff experts have provided candid testimony stating that if my contour plots provided with the initial testimony are right, the drywell no longer meets

Template=SECY-055

SECY-02

the ASME code requirements. In this round of testimony I show that those contour plots probably underestimated the severity of the corrosion and AmerGen's assessment broadly agrees with mine, even though it suffers from numerous errors and is very crude. Thus, based on the testimony so far, I reasonably conclude that the critical effective factor of safety during refueling is less than the 1.9 that NRC Staff estimated. NRC Staff Rebuttal Test. at A.28. Because AmerGen has stated that the required factor is 2.0, AmerGen Rebuttal Test. Part 2 at A.6, I conclude that in its current state, the plant would not meet the safety requirements at the start of any period of extended operation.

Q3. Have you prepared a memorandum to accompany this testimony?

A3. Yes. The memorandum contained in Citizens' Ex. 61 deals with issues concerning the comparison between AmerGen's latest assessment of the external UT results and my own. It broadly shows that there is no major disagreement among the parties on how to treat the data, but my analysis is more sophisticated than AmerGen's and more objective and less error-prone. It is therefore more reliable. Both analyses show that the drywell does not meet the local area acceptance criterion, as might be expected given NRC Staff's conclusion that the factor of safety is now below which is acceptable. Therefore, the argument that contouring the data is somehow inappropriate is not only flatly wrong, it also largely irrelevant. Finally, my latest analysis confirms previous indications that areas of severe corrosion probably exist at the edges of the bays, in the areas considered by AmerGen to be most vulnerable to buckling. AmerGen Rebuttal Test. Part 2 at A.4. Because NRC's estimate of 1.9 was based on my previous analysis, my latest analysis shows that the factor of safety during refueling is probably considerably less than 1.9.

Q4. Is it correct that the GE sensitivity study modeled a contiguous area of 3 feet by 3 feet in each Bay that was less than 0.736 inches?

A4. No, in the GE sensitivity study, AmerGen Ex. 39, the tray-shaped cut-out that was thinner than 0.736 inches was 1.5 feet by 3 feet (6 elements by 12 elements) in total with a centre area of 0.5 feet by 1 foot (2 elements by 4 elements) which was modeled as both 0.536 inches thick and 0.636 inches thick. The cut-outs reduced the buckling capacity by 9.5% and 3.9% respectively. It is unclear to me whether the boundary conditions also led to the implicit inclusion of a second area of the same size in the adjacent Bay. However, what is critical is that the *continuous* area

thinner than 0.736 inches per bay modeled was only 4.5 square feet, not 9 square feet. Therefore, I believe that if the data are to be analyzed Bay by Bay, the maximum permissible *contiguous* area thinner than 0.736 inches in each bay should be less than 4.5 square feet. As discussed in my latest memorandum (Citizens' Exhibit 61) areas much larger than this have been estimated to be present by my analysis and by Amergen's. Thus, I believe that far from showing that the drywell meets the local area acceptance criterion to a high degree of certainty, AmerGen's own analysis, reinforced by my own, shows that there is little doubt that the drywell fails the local area acceptance criterion.

Q5. To your knowledge, is Citizens' Exhibit 61 and this testimony, true and accurate?

A5. Yes, Citizens' Exhibit 61 and this testimony provide, to the best of my knowledge, true and accurate statements of my responses to AmerGen and the NRC Staff. I should point out that in Citizens' Exhibit 61 I have refined my previous analysis in various ways in response to AmerGen's criticism. These revisions are spelled out in detail in the Exhibit. Because the revised calculations in Citizens' Exhibit 61 are the most accurate, these should be regarded as definitive.

Q6. Has AmerGen's and NRC Staff's rebuttal testimony changed your opinions regarding the state of the drywell shell?

A6. No, in fact for the reasons explained before, the rebuttal testimony reinforces my view that AmerGen has failed to establish reasonable assurance that the drywell meets the safety requirements.

Q7. Do AmerGen's analyses of the external data actually demonstrate compliance with the local area acceptance criteria?

A7. No, AmerGen's latest analysis actually demonstrates non-compliance with even the least stringent version of the local area acceptance criterion. Most obviously the assessment shows an area larger than 3 feet by 3 feet in Bay 1 that has an average thickness of 0.699 inches. *See* AmerGen Ex. 16 at 34, Citizens Ex. 61 at Fig. 1 (area illustrated on AmerGen Ex. 16 Figs. 1-2 and 1-7 is actually approximately 36 inches by 42 inches even though it is labeled as 36 inches by 36 inches). If the area were actually 36 inches by 36 inches, it would not encompass the

points that are shown to be inside it on AmerGen Ex. 16 Fig. 1-2. Furthermore, additional extrapolation of the data for Bay 13 shows that it is likely that a large continuous band of corrosion extends all the way across the Bay and is thinnest at the edge of the Bay, precisely where the drywell is most vulnerable to buckling. Citizens' Ex. 61, Figure 4. This area fails the local acceptance criterion for multiple reasons explained in detail in Citizens' Ex. 61.

Q8. Would you have included the internal data into the contouring if you had the coordinates at which the internal data was taken?

A8. Yes, but it was very difficult to finalize the location of the external points due to various discrepancies. Apart from AmerGen Ex. 28 (the map of all the points), which is too small and is not to scale, I have not seen any plots or data sheets that combine the internal and the external measurements. However I would welcome a contouring analysis that includes both the internal data (including the trench data) and the external measurements. Finally, I note that AmerGen's analysis of the 2006 external data also ignored the internal measurements, presumably for similar reasons. Instead of complaining that I did not do this, AmerGen should have done what it suggests should be done in its own analysis. I further question whether AmerGen's statements about internal grids being inches from the external points are valid because I have not seen a good table of data giving comparable coordinates for all the measured points.

Q9. Looking at AmerGen's allegations in their Rebuttal Test. Part 3 at A.2, does including the other grid data invalidate your argument?

A9. No, in Citizens' Ex. 61 I have revised the Figure to include the data cited by AmerGen. The revised Figure shows that the internal grid data are highly variable from grid to grid because some grids are in more severely corroded areas than others. It also shows that in this Bay the average of the external measurements is approximately the same as the average of the grid data at 11'3" but is quite a lot lower than the trench data. This really shows first that there is a lot of spatial variation in the corrosion in each Bay that cannot be captured by the internal girds at 11'3". It also illustrates that the external measurements are not biased to the thin side by very much. Finally, I don't think there can be any dispute that the internal grids in Bay 1 do not represent the thickness of that Bay, because the bathtub ring in that Bay is below the 11'3" level. Bay 13 also appears to suffer from a similar problem.

Q10. Which data is and is not capable of showing whether the local area acceptance criterion is met?

A.10. The internal grid measurements are certainly not useful for this purpose because they only consist of a few 6 inch by 6 inch grids taken at an elevation which is above the worst of the corrosion in many Bays. Similarly, the trench measurements were only taken in two lightly corroded Bays and therefore cannot assist with finding margins for the most corroded local areas. Therefore, in principle, only the external measurements could show whether the local area acceptance criterion is met. Consistent with this approach, AmerGen has tried (but failed) to convince us that the external data show compliance with the local acceptance criteria. E.g. AmerGen Ex. 16. Contradicting AmerGen Ex. 16, AmerGen now apparently alleges the external data cannot be compared to the local acceptance criterion. AmerGen Rebuttal Test. Part 3 at A.2. If this were true, AmerGen would not be able to determine whether the local acceptance criterion is met and would therefore have no reasonable assurance of meeting safety requirements.

Q11. Does AmerGen confuse the concepts of systematic error and random error in AmerGen Rebuttal Test. Part 3 at A.6 and 7?

A11. Yes. In the past the measurements have two kinds of error, systematic error and random error. Essentially, random error is when the errors in different measurements are uncorrelated, whereas systematic error results when there are correlations between the errors. In simple terms, random error is noise in the data, while systematic error is bias in the data. For both the external measurements in 1992 and the internal measurements in 1996, AmerGen has alleged and acknowledged, respectively, that there were systematic errors in the data. Unlike random error, systematic errors do not reduce the uncertainty of the mean as more data is taken. The sources of error that AmerGen has listed in AmerGen Rebuttal Test. Part 3 at A.6 could be sources of both random and systematic error and it is important to distinguish between the two, which AmerGen fails to do. In addition, the conclusion in AmerGen Rebuttal Test. Part 3 at A.7 that systematic error is not significant because the data are averaged over multiple sampling events and it is associated with a random variable is flatly wrong for multiple reasons, most importantly because more sampling does not eliminate or reduce certain systematic errors. (What AmerGen proposes

here is to confound random and systematic error again after the Analysis of Variance has separated them). Moreover, assessments of significance require comparison of one number to another. In the absence of any quantification of errors, AmerGen's conclusion is virtually meaningless. Finally, it has been agreed that systematic bias of around 0.016 inches was observed in the 1996 internal measurements. The error analysis fails to acknowledge that such a problem could recur and should be accounted for statistically.

Q12. Is AmerGen Rebuttal Test. Part 3 A17 correctly stated?

A12. No. The 95% confidence interval is approximately twice the standard error. Using a confidence interval of one standard error gives rise to a confidence level of 67%, which would be insufficient to maintain reasonable assurance that the ASME code and the acceptance criteria are met. Here, the Board asked for 95% confidence limits, but AmerGen appears to be trying to argue that 67% confidence limits are sufficient, without directly stating it.

Q13. Is AmerGen Rebuttal Test. Part 3 A20 correct?

A13. No. AmerGen takes account of possible systematic error when deciding whether corrosion is "significant" over time. In addition, in evaluating the 2006 external data, AmerGen specifically looked for systematic error. AmerGen Ex. 4. Furthermore, it is important to explicitly account for possible systematic error when evaluating the thickness measurements.

Q14. Is AmerGen Rebuttal Test. Part 3 A22 correct?

A14. No. Requiring that the average of a parameter meet a requirement without placing any limits on the confidence intervals of the mean is a recipe for allowing components to fail. To prevent failures we must be concerned with behavior that is unlikely but nonetheless could occur. AmerGen' answer unequivocally demonstrates that they do not understand some of the most basic principles of statistics: While data are (may be) randomly distributed about the sample mean with a frequency distribution resembling a Gaussian distribution, the sample means are equally distributed about the true mean of the population (according the to "central limit theorem). Therefore it makes sense to ask the question bout the lower (or higher) mean value within the 5% limits, because it might actually better represent the true mean than the measured mean. This is not idle speculation because if one has only one set of data, and hence only one

measured mean, the true mean may indeed lay somewhere under the Gaussian distribution curve for all "measured means", event though only one such mean had been experimentally determined. . At minimum in this context we believe the lower 95% confidence limit should be used for the observed mean. Requiring this limit to meet the acceptance requirements would mean that in one out of forty instances, the components could be below the requirements without us knowing it. Thus, if a single power plant were required to meet more than 40 acceptance criteria using the lower 95% confidence limit of the measured data, there would be a statistical likelihood that one of the parameters would be in violation. In contrast, allowing the calculated mean of the measurements to go as low as the acceptance criterion would mean that in 50% of instances the components would be thinner than estimated and would violate the requirements. This would mean that 20 of the 40 parameters would likely be below requirements. Because each power plant must meet many different criteria using measured data, even taking a 95% confidence interval could be too little. Using a 50% confidence interval makes it virtually certain that mainly unknown failures to meet safety requirements would exist at each plant. That would hardly provide reasonable assurance that the plants are meeting safety requirements.

Q15. Is AmerGen Rebuttal Test. Part 3 A29 correct?

A15. No. We believe AmerGen should compare the lower 95% confidence limit of the averages (means) of the internal grids minus an allowance for possible systematic error to the acceptance criterion. This procedure would not ignore any data at all; it merely avoids the statistical likelihood that the results appear to be better than they really are.

Q16. Is AmerGen Rebuttal Test. Part 3 A31 correct?

A16. No. To clarify, my assumption was that the standard error of the mean was 0.03. Thus the lower 95% confidence interval for the mean is approximately the (stated hypothetical) mean minus two times 0.03. This is another example of AmerGen's multiple attempts to misread and misrepresent statements.

Q17. Is AmerGen Rebuttal Test. Part 3 A32 correct?

A17. We have looked at the data from Bay 17 again. There were indeed two internal grid measurements, 17 A and 17D. 17 A reflects the more severe corrosion only at the highest

elevations (not what one would have expected) , 17 D on the other hand mirrors the corrosion observed in the trench, but only at lower elevation. We have now combined all data in Figure 5 of Citizens' Ex. 61 and hope that the elevation data as reported were in fact the correct ones. When looking at that figure, one must remember that the data are only plotted as a function of the vertical distance from the bottom of the sandbed, but no doubt the data are not in the same lateral positions. Rather than "our argument falling apart " (namely that "internal grid measurements do not reflect the true corrosion of the sand bed"), Figure 5 of the memorandum fully supports the notion that no single set of measurements fully represents the extent of corrosion in the sandbed. However, I also think that one needs to look first and foremost at the most serious corrosion damage, because there is the greatest danger of failure. This is often located below the 11'3" height where the internal grids are taken.

Q18. What are the ramifications of AmerGen Rebuttal Test. Part 3 A38 and 39?

A18. It is hard to understand how one could be reasonably certain that the measurements indicate compliance with an acceptance criterion without being able to make a numerical estimate of the value that parameter and also estimating the possible error associate with the numerical value. However, leaving this issue aside, if AmerGen really does not calculate the margins above the local area acceptance criterion, then there is no assurance that the monitoring frequency is based on the narrowest margin. At present AmerGen is assuming that the smallest margin is 0.064 inches which was derived from the internal grids, but according to A38 and 39 it cannot verify this assumption because it has not estimated the margin above the local area acceptance criterion. This is obviously unacceptable.

Q.19 Do you agree with AmerGen Rebuttal Test. Part 3 A41?

A19. Not completely. AmerGen's suggested approach to having an imperfect data set is to ignore it, even though AmerGen itself had the power to take better data. Furthermore, the analogy is completely wrong. As discussed in A. 14above, we believe the lower 95% confidence interval of estimates of each acceptance parameter must be compared to each acceptance criterion. For the mean thickness, this means the lower 95% confidence interval of the estimate of the mean should be compared to 0.736 inches. Although we have acknowledged at the time (based on the available documents and AmerGen's insistence) that the external data may be

biased somewhat low, we believe this bias provides assurance that systematic bias will not result in the plant violating the acceptance criterion for the mean. We have, however, never intimated, contrary to AmerGen, that averages obtained over a small area might be representative of the structure as a whole. Finally, I find it strange that AmerGen states here that extreme value statistics should be used to analyze the external data set and not averaging, when Amergen's own analysis of the external data, carried out by Mr. Tamburro, used simple averaging. I think I may point out at this time that AmerGen is not familiar with extreme value statistics, or else they would not make the statements they do in A 41 final paragraph. The use of extreme value statistics does not depend on whether the data set is biased toward low values or not. It only depends on whether the frequency distribution is Gaussian or exponential.

Q20. Do you agree with AmerGen Rebuttal Test. Part 3 A43?

A20. Not completely. Although I agree that scanning across the ground location is a good idea, in the initial report AmerGen did not use the thinnest measured reading as the basis for its initial evaluation. As it now appears to admit in A.44, this was a serious mistake. Furthermore, I note that the scan across the locations was only carried out for a few locations in four Bays. AmerGen has not explained why such a scan was not carried out at the other locations. The results from the scans clearly show that the results are highly variable and without such a scan any claim to have measured even the local thin spots on the drywell is invalid.

Q21. Do you agree with AmerGen Rebuttal Test. Part 3 A46?

A21. No. I make the same assumptions as Mr. Tamburro, I just used a better method to estimate the thin areas. As I show in Citizens' Ex. 61, AmerGen's position is founded on a non-rigorous analysis that should have concluded that at least Bays 1 and 13 fail the local area acceptance criterion.

Q22. Please comment on AmerGen Rebuttal Test. Part 3 A47 and 48.

A22. I recognized that my calculations presented in Citizens Ex. 13 had some shortcomings. As discussed in my rebuttal testimony A8, I therefore revised the calculations and presented the results in Citizens' Exhibit 38. I believe that my estimate of the standard deviation based on duplicate or triplicate measurements and reported there is the best estimate that we have,

although I agree that it would have been more ideal if AmerGen had gathered more data. Here, I believe AmerGen is allowing the perfect to become the enemy of the useful. While one can always criticize calculations based on imperfect data, the task here is to test whether the drywell meets the acceptance criteria with the required degree of confidence. That can only be done if we estimate the uncertainty in the measurements using statistics. I find the whole tone of AmerGen's statistical testimony rather strange. Instead of actually analyzing the data available, AmerGen seems to suggest the data is not good enough to be analyzed, forgetting that it designed the sampling strategy and should have considered how it was going to analyze the results before they were taken. It is hardly useful to spend time and money taking data which is then cannot be used for the purpose intended, which was to show whether the drywell met the local area acceptance criteria.

Q23. Do you agree with AmerGen Rebuttal Test. Part 3 A50 to 51?

A23. No, as I previously testified the micrometer results in Bay 13 actually show a surface roughness of 0.1 inches and because scans were not conducted at every location to find the locally thinnest point, it is inappropriate to make any correction for roughness. Instead AmerGen should use the raw results that it measured. Please note, that with all the talk about "evaluation thickness", starting with Calc. 24 Rev.0, Mr. Tamburro in his latest discussion (Calc. 24, Rev. 2) largely used the actual lowest measurements, thus demonstrating that these unfounded corrections for surface roughness are irrelevant.

Q24. Do you agree with AmerGen Rebuttal Test. Part 3, Section IV?

A24. No. My issues with the latest analysis of the external measurements are set out in detail in Citizens' Ex. 61. The page reference in Rev.1 to the assumption that all areas that are thinner than 0.736 inches are also less than 2 inches in extent is AmerGen Ex. 18 at 11, 13. In addition, AmerGen tries to imply that all the points were ground, which is incorrect. Furthermore, I note that Mr. Tamburro must have used some other method to derive the areas presented in the latest calculation, which are not all 36 inches by 36 inches. Finally, Mr. Tamburro's method effectively assumed that no areas larger than 36 inches by 36 inches that are on average thinner than 0.736 inches would exist. If he had used a 37 inch by 37 inch square or rectangular geometries and applied the same method he would have found a number of areas that are on

average thinner than 0.736 inches and are also larger than nine square feet, violating the least stringent acceptance criterion alleged by AmerGen.

Q25. Do you agree with AmerGen Rebuttal Test. Part 4 A4 and 5?

A25. Not completely. Citizens' Ex. 50 showed that the metal tape and strippable coating is not always effective in preventing significant leaks.

Q26. Do you agree with AmerGen Rebuttal Test. Part 4 A14?

A26. No. It is misleading to conclude too much from the leakage observed in the 2006 outage. Because Citizens' Ex. 50 showed that the metal tape and strippable coating is not always effective in preventing significant leaks, it is not possible to say that the trough drain capacity cannot be exceeded. Furthermore, Citizens Exs. 48 and 49 showed that the trough drain was found to be in a deteriorated condition in 1996 and it is subject to high temperatures which can degrade the concrete it is made of. Thus, it is not speculation to suggest that similar degradation could occur in the future.

Q27. Do you have other comments on Part 4 of AmerGen's rebuttal testimony?

A27. Yes. For the reasons I stated previously, the evaporation estimate provided by AmerGen is hopelessly over optimistic. Although I agree that coating failure is first manifested by pinpoint rusting and rust staining, the issue is how quickly more widespread failure could occur. I believe it is possible that such widespread failure could occur between coating inspections, which I understand are every four years. I note that AmerGen now suggests that the coating will require "proper maintenance" to last further decades. AmerGen Rebuttal Test. Part 4 A8. This is an acknowledgement by AmerGen that it is reasonable to expect some coating failures, which will require repair. With regard to the cracking of the epoxy floor, photographs show that the cracks were more widespread than AmerGen suggests in AmerGen Rebuttal Test. Part 4 A9. However, the key point is that in this very environment the floor epoxy cracked. Although the failure mechanisms for the thin epoxy coating on the shell are somewhat different, this is nonetheless a salutary lesson that it is necessary to regularly verify that the coating is working effectively, through both UT measurements and visual inspections.

Q27. Do you have any comments on Part 6 of AmerGen's rebuttal testimony?

A27. Yes. In A10, AmerGen mistakenly over-concludes from the UT measurements for the small area of the embedded region that was revealed. In fact, interior corrosion is most likely to occur in spurts at elevations that are in the sand bed region. Measurements in the embedded region cannot show lack of corrosion in the sandbed region. In A13, Gordon disputes the assessment of AmerGen's technical reviewer even though he carried out no new calculations in response to the comment. This is strange because at the time he said the "requested calculation" to respond to the comment was "rather straightforward." Citizens Ex. 36. He fails to explain why he did not make this calculation and continues to fail to present any quantitative response to the comment. Finally, I note that Gordon now does not say that corrosion has been arrested, as AmerGen did earlier, but rather the corrosion rate is "near zero." However, once again this answer lacks quantification. For example if the margins are 0.02 inches or less, a very small corrosion rate of 0.01 inches per year could consume the margin in two years, making that rate highly significant.

Q28. Turning to NRC Staff Rebuttal Test. A26, do you believe that "long grooves of corrosion" are present?

A28. The observations often refer to a "bathtub ring." I have used the term "long grooves of corrosion" to describe the "bathtub ring." Does using a different name for the same feature has any effect on the reality of what is there? More seriously though, Figure 5 of Citizen's Exhibit 61 shows that an abrupt decrease in wall thickness of 250 – 400 mils (22 – 35% of wall thickness) occurs over a vertical distance of about 2 to 3 inches. Then the trench data indicate that wall thinning continues to the bottom of the sandbed, although to a lesser extent. Maybe one should describe this as a horizontal "trough" rather than a groove, but clearly the distinction is one of width rather than depth.

Q28. Looking at NRC Staff Rebuttal Test. A27, do you have any comment?

A28. Yes. As AmerGen has pointed out, the contour plots cannot be very precise because they are based on only a few points and there are large areas of the drywell for which we have no measurements or incomplete measurements. In my latest calculations I have used various extrapolation techniques to make up for the lack of data. Although the results are extrapolations and therefore subject to interpretation, they provide the best estimates that I am able to produce

from the data we have. I do not believe it would be appropriate to measure the areas below certain thresholds from these plots very accurately. Instead, the plots provide a visual indication of how big the areas below each threshold are. Citizens Ex. 61 Figure 4 shows the extrapolated corrosion in Bay 13. It is clear from this plot that the area below 0.736 inches is large and cannot be bounded by a 3 feet by 3 feet square. Thus, I believe the local area acceptance criterion is violated by these data.

Q29. Looking at NRC Staff Rebuttal Test. A28, do you have any comment?

A29. Yes, I find it quite surprising that the applicant is arguing that it must meet the ASME code requirement of 2.0 during refueling, but the regulator appears to be saying that compliance with the ASME code is not required. I will leave it to the lawyers to argue about what is legally required, but note that it is very unusual to have the regulator leading the charge to relax standards that the licensee thought it had to meet.

Q30. Looking at NRC Staff Rebuttal Test. A31, do you have any comment?

A30. Yes. I wholeheartedly agree with this answer. This is precisely why AmerGen cannot continue to rely on the regression technique to determine the potential rate of future corrosion.

Q31. Looking at NRC Staff Rebuttal Test. A35, do you have any comment?

A31. Yes. Because it is difficult to predict the lifetime of the coating and it has already had a service life of 15 years, it is not reasonable to assume it will not fail during any extended period of operation.

Q32. Looking at NRC Staff Rebuttal Test. A36, do you have any comment?

A32. Yes. The very early stages of degradation below a coating will not be seen by visual inspection. Obviously, at some point the degradation becomes visible.

Q33. Looking at NRC Staff Rebuttal Test. A37 regarding the difference between pitting corrosion and general corrosion, do you have any comment?

A33. Yes. It is of course no surprise that different technicians or scientists should have different opinions about corrosion mechanism, because after all it is not long since pinhole

corrosion on organic coatings was likened to pinhole corrosion on metallic coatings, a comparison which we determined not too long ago was totally unjustified. Nevertheless, the corrosion rate on or in pinholes depends on mass transfer in or out of the pit. For corrosion to occur one needs first of all water, and then a corrodent, such as oxygen, and some sort of access to the metal surface. As corrosion takes place, corrosion products are formed. These will eventually put pressure on the coating to the point it first blisters and then cracks (depending on the physical properties of the coating). When the coating breaks open (often as a boil breaks open) access of corrodent, water, electrolyte etc. is facilitated, i.e. all mass transfer is accelerated and hence corrosion. Is this mechanism an over-simplification? Yes, because the details depend on a plethora of shifting parameters. However, the principle is correct, how processes occur over time (the kinetics) varies.

Q34. Looking at NRC Staff Rebuttal Test. A38 regarding the extent of the areas that are thinner than 0.736 inches do you have any comment?

A34. Yes. Having said that the NRC Staff did not rely on an estimate that the total area thinner than 0.736 inches was 0.68 square feet, the NRC Staff then erroneously draws a conclusion about the *maximum* area that could be thinner than 0.736 inches from the knowledge that the *minimum* such area that is 0.68 square feet. This is of course entirely illogical and irrelevant because the extent of the contiguous areas that are thinner than 0.736 inches is highly restricted to 4.5 square feet per Bay or less.

Q35. Looking at NRC Staff Rebuttal Test. A39 regarding the use of the acceptance criteria do you have any comment?

A35. Yes. This answer confirms that the cut-out areas in the sensitivity study were designed to "bound all degradation." Because both my analysis and AmerGen's now show that the corrosion is no longer bounded by these cut-outs, the modeling no longer shows that the degradation is acceptable, if indeed it ever did.

Q36. Looking at NRC Staff Rebuttal Test. A40 regarding the use of the external data do you have any comment?

A36. Yes. Because the internal grids are clearly placed above the worst corrosion in the most

corroded Bays it is not reasonable to rely on the internal measurements to estimate the drywell average thickness in every Bay. Even though the external measurements are slightly biased to the thin side and are admittedly incomplete, we have no other data to use estimate the thickness of the most corroded Bays. The initial question is not whether corrosion is ongoing, it is what is the current margin. Furthermore, AmerGen is no longer saying that corrosion has been arrested. I am puzzled by the reference to the "Staff's conclusion about the extent of corrosion." To date, the Staff have not stated any conclusions about the extent of severe corrosion except to say that is larger than 0.68 square feet and smaller than 700 feet. However, I am pleased to note that the Staff did not rely on the grid measurements to determine the extent of corrosion, although I am unclear which measurements they did rely upon, because they appear to criticize me for using the external measurements.

Q37. Looking at NRC Staff Rebuttal Test. Response 8 regarding the failure to take account of systematic error do you have any comment?

A37. Yes. I believe it is important to make an allowance of 0.01 to 0.02 inches for systematic error in the internal measurements because such error was observed at least once and possibly on two occasions in the past. For the 2006 external measurements, I have decided that it is reasonable to make no such allowance because there has at least been some attempt to bias the sampling locations to the thin side and the measurement technique seems robust.

Q38. Looking at NRC Staff Rebuttal Test. A11 (on page 26) regarding the calculation of the corrosion rate do you have any comment?

A38. Yes. It is not conservative to assume a linear corrosion rate of 2 mils per year. Experience from when the sand was in place shows that corrosion can happen much more quickly than that. The reason the observed rate from 1986 to 2006 in the trenches is so low is not known, but is probably due in part to the fact that the trenches were excavated in two of the least corroded Bays. Unfortunately, AmerGen has not presented any data analysis of the trench measurements and I have had limited time to spend on this issue. In the absence of a detailed analysis of the data, a more conservative but still reasonable assumption is that most of this corrosion was caused by degradation from the interior in fits and starts around refueling outages.

Q39. Looking at NRC Staff Rebuttal Test. Response 12(d) regarding the use of the contour plots do you have any comment?

A39. Yes. I would refer you to my previous answer in which I said NRC Staff are trying to be too precise here. The contour plots are designed to allow a better estimate for the extent of the areas thinner than 0.736 inches than merely greater than 0.68 square feet, but smaller than 700 square feet, which is all the Staff has said. They are also more accurate than AmerGen's estimate given in Rev. 2 of the 24 Calc. (AmerGen Ex. 16), which is that the extent of the areas thinner than 0.736 inches is approximately 21 square feet (at least 9 sq. feet in Bay 1, *id.* at 34, 1 sq. foot in Bay 13, *id.* at 62, 1 sq. foot in Bay 15, *id.* at 79, 1 sq. foot in Bay 17, *id.* at 89, and 9 sq. feet in Bay 19. *Id.* at 93)

Q40. In summary, are you convinced that the drywell will meet safety requirements during any extended period of operation?

A40. No. NRC Staff and AmerGen have created confusion and contradictions, which makes it difficult to show what the current situation is or how it could change in the future. However, I believe that it is likely that the drywell shell fails even the least stringent version of the local area acceptance criterion and the lower 95% confidence limit of the mean derived from the external results also violates the acceptance criterion for the mean in some Bays. Finally, I also believe the very local area acceptance criterion of 0.49 inches could be violated, based on extreme value statistics. Furthermore, all parties now agree that future corrosion could occur, but there is no certainty about the rate at which this could occur. Thus, it makes sense to err on the side of caution in selecting a monitoring frequency. To date, neither AmerGen nor NRC has justified a monitoring interval of once every four years was selected or how it was justified. In the absence of any further information, and if AmerGen could establish that some margin is available, I would recommend more frequent monitoring than once every four years, which should be calculated by taking the minimum values derived from dividing the amount by which the lower 95% confidence limit of the measured data for each acceptance parameter exceeds each acceptance criterion by a conservative estimate of the corrosion rate. A reasonably cautious estimate of the possible combined corrosion rate from the interior and the exterior is approximately 0.05 inches per year.

Q41. Have you now completed your sur-rebuttal testimony?

A41. Yes.

In accordance with 28 U.S.C. § 1746, I state under penalty of perjury that the foregoing is true and correct.

Rudolf H. Hausler — 9-13-2001

Dr. Rudolf H. Hausler — Date

UNITED STATES OF AMERICA
BEFORE THE NUCLEAR REGULATORY COMMISSION
OFFICE OF THE SECRETARY

In the Matter of	)	
	)	Docket No. 50-0219-LR
AMERGEN ENERGY COMPANY, LLC	)	
	)	ASLB No. 06-844-01-LR
(License Renewal for the Oyster Creek	)	
Nuclear Generating Station)	)	September 14, 2007
	)	

CERTIFICATE OF SERVICE

I, Richard Webster, of full age, certify as follows:

I hereby certify that on September 14, 2007, I caused Citizen's sur-rebuttal filing in the above captioned matter to be served via email, Federal Express (as indicated) and U.S. Postal Service (as indicated) on the following:

Secretary of the Commission (Email and original and 2 copies via U.S Postal Service)
United States Nuclear Regulatory Commission
Washington, DC 20555-0001
Attention: Rulemaking and Adjudications Staff
E-mail: HEARINGDOCKET@NRC.GOV

Administrative Judge
E. Roy Hawkens, Chair (Email and Federal Express)
Atomic Safety and Licensing Board Panel
Mail Stop – T-3 F23
United States Nuclear Regulatory Commission
Washington, DC 20555-0001
E-mail: erh@nrc.gov

Administrative Judge
Dr. Paul B. Abramson (Email and Federal Express)
Atomic Safety and Licensing Board Panel
Mail Stop – T-3 F23
United States Nuclear Regulatory Commission
Washington, DC 20555-0001
E-mail: pba@nrc.gov

Administrative Judge
Dr. Anthony J. Baratta (Email and Federal Express)
Atomic Safety and Licensing Board Panel
Mail Stop – T-3 F23
United States Nuclear Regulatory Commission
Washington, DC 20555-0001
E-mail: ajb5@nrc.gov

Law Clerk
Debra Wolf (Email and Federal Express)
Atomic Safety & Licensing Board Panel
Mail Stop – T-3 F23
U.S. Nuclear Regulatory Commission
Washington, DC 20555-0001
E-mail: DAW1@nrc.gov

Office of General Counsel (Email and U.S. Postal Service)
United States Nuclear Regulatory Commission
Washington, DC 20555-0001
E-mail: OGCMAILCENTER@NRC.GOV

Mitzi Young (Email and Federal Express)
U.S. Nuclear Regulatory Commission
Office of the General Counsel
Mail Stop: O-15 D21
Washington, DC 20555-0001
E-mail: may@nrc.gov

Mary C. Baty (Email and Federal Express)
U.S. Nuclear Regulatory Commission
Office of the General Counsel
Mail Stop: O-15 D21
Washington, DC 20555-0001
E-mail: mcb1@nrc.gov

Alex S. Polonsky, Esq. (Email and Federal Express)
Morgan, Lewis, & Bockius LLP
1111 Pennsylvania Avenue, NW
Washington, DC 20004
E-mail: apolonsky@morganlewis.com

Kathryn M. Sutton, Esq. (Email and Federal Express)
Morgan, Lewis, & Bockius LLP
1111 Pennsylvania Avenue, NW
Washington, DC 20004
E-mail: ksutton@morganlewis.com

Donald Silverman, Esq. (Email and Federal Express)
Morgan, Lewis, & Bockius LLP
1111 Pennsylvania Avenue, NW
Washington, DC 20004
E-mail: dsilverman@morganlewis.com

J. Bradley Fewell (Email and U.S. Postal Service)
Exelon Corporation
200 Exelon Way, Suite 200
Kennett Square, PA 19348
E-mail: bradley.fewell@exceloncorp.com

John Covino, DAG (Email and U.S. Postal Service)
State of New Jersey
Department of Law and Public Safety
Office of the Attorney General
Hughes Justice Complex
25 West Market Street
P.O. Box 093
Trenton, NJ 08625
E-mail: john.corvino@dol.lps.state.nj.us

Valerie Gray (Email)
State of New Jersey
Department of Law and Public Safety
Office of the Attorney General
Hughes Justice Complex
25 West Market Street
P.O. Box 093
Trenton, NJ 08625
E-mail: valerie.gray@dol.lps.state.nj.us.

Paul Gunter (Email and U.S. Postal Service)
c/o Nuclear Information and Resource Service
6930 Carroll Ave., Suite 340
Takoma Park, MD 20912-4446
E-mail: paul@beyondnuclear.org

Edith Gbur (Email)
Jersey Shore Nuclear Watch, Inc.
364 Costa Mesa Drive. Toms River, New Jersey 08757
E-mail: gburl@comcast.net

Paula Gotsch (Email)
GRAMMIES
205 6th Avenue
Normandy Beach, New Jersey 08723
E-mail: paulagotsch@verizon.net

Jeff Tittel (Email)
New Jersey Sierra Club
139 West Hanover Street
Trenton New Jersey 08618
E-mail: Jeff.Tittel@sierraclub.org

Peggy Sturmfels (Email)
New Jersey Environmental Federation
1002 Ocean Avenue
Belmar, New Jersey 07319
E-mail: psturmfels@cleanwater.org

Signed: 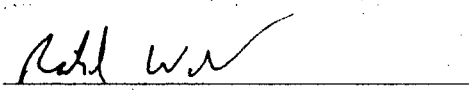
Richard Webster

Dated: September 14, 2007

UNITED STATES OF AMERICA
NUCLEAR REGULATORY COMMISSION
OFFICE OF THE SECRETARY

ATOMIC SAFETY AND LICENSING BOARD

Before Administrative Judges:
E. Roy Hawkens, Chair
Dr. Paul B. Abramson
Dr. Anthony J. Baratta

In the Matter of	)	
	)	Docket No. 50-219
AMERGEN ENERGY COMPANY, LLC	)	
OYSTER CREEK NUCLEAR	)	
GENERATING STATION	)	
	)	September 14, 2007
License Renewal for Oyster Creek Nuclear	)	
Generating Station	)	
	)	

CITIZENS' SUR-REBUTTAL - BRIEFS AND EXHIBITS

UNITED STATES OF AMERICA
NUCLEAR REGULATORY COMMISSION
OFFICE OF THE SECRETARY

ATOMIC SAFETY AND LICENSING BOARD

Before Administrative Judges:
E. Roy Hawkens, Chair
Dr. Paul B. Abramson
Dr. Anthony J. Baratta

In the Matter of	)	
	)	Docket No. 50-219
AMERGEN ENERGY COMPANY, LLC	)	
OYSTER CREEK NUCLEAR	)	
GENERATING STATION	)	
	)	September 14, 2007
License Renewal for Oyster Creek Nuclear	)	
Generating Station	)	
	)	

CITIZENS' REPLY TO AMERGEN AND NRC STAFF REBUTTAL TESTIMONY

PRELIMINARY STATEMENT

In accordance with an Order from the Atomic Safety and Licensing Board (the "Board"), dated April 17, 2007, this response Brief to the Initial Statements of Position filed by American Energy Company LLC ("AmerGen") and NRC Staff is submitted on behalf of Nuclear Information and Resource Service, Jersey Shore Nuclear Watch, Inc., Grandmothers, Mothers and More for Energy Safety, New Jersey Public Interest Research Group, New Jersey Sierra Club, and New Jersey Environmental Federation (collectively "Citizens").

AmerGen has now affirmatively sworn that it is unable to quantitatively estimate the margins above the local area acceptance criteria. This is very surprising because, as

the Atomic Safety and Licesing Board (the "Board") has already found, to estimate the required monitoring frequency, it is essential to estimate the smallest margin and the certainty that the margin is really as large as estimated. Without any quantitative estimate of the margin above the local area acceptance criterion, there can be no justification for basing the monitoring frequency on the margin above the acceptance criteria for mean thickness. Thus, AmerGen has sworn that it will unable to meet its burden in this proceeding.

In addition, Dr. Hausler has shown that the drywell does not meet the least stringent local area acceptance criterion and there is less than 95% certainty that the drywell complies with the other criteria. In this round of testimony he further shows that AmerGen's own assessment is merely a crude approximation of the contouring approach that he has employed. Furthermore, responding to Amergen's testimony on how it analyzed the external data and criticisms of his methods, Dr. Hausler shows that both analyses confirm that even the least stringent version of the local area acceptance criterion is violated. Because the drywell is now beyond the state that was evaluated as acceptable by NRC in 1992 and in 2006, it no longer meets the Current Licensing Basis ("CLB").

Finally, the NRC Staff have admitted that the drywell shell fails an ASME code requirement, if Dr. Hausler's initial assessment of the corrosion using the external measurements is correct. Because this requirement forms part of the CLB, a critical question is whether Dr. Hausler's initial analysis is valid. Responding to this question in this round of testimony, Dr. Hausler shows that his initial assessment was in fact quite

conservative and the areas of severe corrosion are probably considerably larger than previously predicted. Thus, there is now little doubt that the drywell fails the CLB.

A nuclear power plant cannot be relicensed unless there is reasonable assurance that it meets the CLB. Based on the record before the Board, AmerGen's application to relicense the Oyster Creek Nuclear Generating Station ("Oyster Creek") should be denied because AmerGen has affirmatively stated that it cannot meet its burden in this proceeding and, even though they are not required to carry the burden of proof, Citizens have proven that the drywell shell fails to meet the acceptance criteria and an applicable ASME code requirement and is therefore beyond the CLB.

ARGUMENT

I. Additional Response To Board Question 11(a) Regarding The Term Reasonable Assurance

On September 12, 2007, the Memorandum and Order from the Licensing Board made it plain that it still had questions about the issue of confidence and reasonable assurance. Citizens stated in their previous filing that in the context of initial licensing, the United States Court of Appeals for the District of Columbia found no error when a licensing board equated "reasonable assurance" with a "clear preponderance of the evidence" and rejected claims that reasonable assurance means "beyond a reasonable doubt." *North Anna Environmental Coalition v. NRC*, 533 F.2d 655, 667-68 (D.C. Cir. 1976). In the more specific context of corrosion at Oyster Creek, both the reactor operator and NRC staff have regarded 95% confidence as a good yardstick for reasonable assurance. Using case law about the reliability of scientific testimony, this brief shows 95% confidence is normally the minimum accepted by the scientific community and the federal courts.

First of all, a "confidence interval tells us if the results of a given study are statistically significant at a particular confidence level." *Merrell Dow Pharmaceuticals, Inc., v. Havner*, 953 S.W.2d 706, 723 (Tex. Sup. Ct 1997). Furthermore, Havner decided that 95% confidence is normally the minimum required to establish facts as scientifically proven:

> The generally accepted significance level or confidence level in epidemiological studies is 95%, meaning that if the study were repeated numerous times, the confidence interval would indicate the range of relative risk values that would result 95% of the time. *See DeLuca v. Merrell Dow Pharms., Inc.*, 791 F.Supp. 1042, 1046 (D.N.J.1992), *aff'd*, 6 F.3d 778 (3d Cir.1993); Linda A. Bailey et al., *Reference Guide on Epidemiology, in* FEDERAL JUDICIAL CENTER, REFERENCE MANUAL ON SCIENTIFIC EVIDENCE at 153 (1994); Michael Dore, *A Proposed Standard For Evaluating the Use of Epidemiological Evidence in Toxic Tort and other Personal Injury Cases,* 28 HOW. L.J. 677, 693 (1985); Melissa Moore Thompson, *Causal Inference in Epidemiology: Implications for Toxic Tort Litigation,* 71 N.C. L.REV. 247, 256 (1992). Virtually all the published, peer-reviewed studies on Bendectin have a confidence level of at least 95%. Although one of the Havners' witnesses, Dr. Swan, advocated the use of a 90% confidence level (10 in 100 chance of error), she and other of the Havners' witnesses conceded that 95% is the generally accepted level.

Id. at 723-24.

Havner further stated that the federal courts should use 95% confidence as the minimum acceptable for scientific testimony:

> We think it unwise to depart from the methodology that is at present generally accepted among epidemiologists. *See generally* Bert Black, *The Supreme Court's View of Science: Has* Daubert *Exorcised the Certainty Demon?,* 15 CARDOZO L.REV. 2129, 2135 (1994) (stating that " '[a]lmost all thoughtful scientists would agree ... that [a significance level of five percent] is a reasonable general standard'" (quoting Amicus Curiae Brief of Professor Alvan R. Feinstein in Support of Respondent at 16, *Daubert v. Merrell Dow Pharms., Inc.*, 509 U.S. 579, 113 S. Ct. 2786, 125 L.Ed.2d 469 (1993) (No. 92-102))). Accordingly, we should not widen the boundaries at which courts will acknowledge a statistically significant association beyond the 95% level to 90% or lower values.

Id. at 724.

Even more relevantly, the use of 95% confidence intervals was advocated by federal government scientists in *US v. Chase*, where the court found credible "the testimony of the government's experts that the use of 95% confidence interval is a standard approach that is generally accepted in the scientific community." *US v. Chase*, 2005 WL 757259, 6 (D.C. Super); *See generally,* DATABASE LIMITATIONS ON THE EVIDENTIARY VALUE OF FORENSIC MITOCHONDRIAL DNA EVIDENCE, 43 Am. Crim. L. Rev. 53, 88+ (2006).

Thus, plaintiffs seeking redress through monetary damages suits must establish their scientific theories with greater than 95% confidence for those theories to be admissible in evidence, because that is the standard generally required by the scientific community. As a corollary, the cases show that a scientific conclusion that is less than 95% certain is generally not fit to address to a jury. Because a scientific assessment with less than 95% certainty would not be good enough to allow a single injured plaintiff that has already been injured to seek redress in federal court, it also cannot be good enough to avert nuclear accidents that could cause harm to thousands of people. It is therefore essential that the NRC make nuclear plant operators prove their scientific theories to at least the 95% confidence required in federal court.

More specifically, to meet the "not inimical" standard in the AEA, the NRC must only permit licensee to use reliable scientific evidence. Federal courts have already decided that scientific proof to less than 95% confidence is unreliable. Therefore, to establish reasonable assurance of compliance with the ASME code a licensee must be able to show with 95% confidence that it has margins over minimum requirements.

II. AmerGen Has Testified It Cannot Meet Its Burden Regarding Margins

The Board has already stated that it expected AmerGen to show to a known confidence level that the drywell shell will not violate the minimum thickness requirements in the interval between UT inspections taking into account the variance of the data. Board Order dated July 11, 2007 at 4.

AmerGen has now testified that it cannot calculate the numerical margin above two of its alleged thickness requirements for the thinnest 12 inch by 12 inch area on the shell and the thinnest 3 feet by 3 feet area on the shell. In addition, it has testified it cannot calculate the margin above the alleged requirement that the largest contiguous area that is thinner than 0.736 inches is less than 3 feet by 3 feet. If AmerGen cannot even calculate these margins, it also cannot possibly estimate the uncertainty in the derived margin. Thus, AmerGen has actually testified under oath that it cannot meet its burden in this proceeding and now finds itself woefully short of meeting the expectations of the Board.

III. Citizens Have Proved That The Drywell Violates The CLB

Even though Citizens do not bear the burden of proof, they have gone beyond what is required of them and proved that the Oyster Creek drywell violates the CLB. Dr. Hausler has previously shown that the drywell does not meet the least stringent local area acceptance criterion and there is less than 95% certainty that the drywell complies with the other criteria. In this round of testimony he further shows that AmerGen's own assessment is merely a crude approximation of the contouring approach that he has employed. Furthermore, responding to AmerGen's testimony on how it analyzed the external data and AmerGen's criticisms of his methods, Dr. Hausler shows that both

analyses confirm that even the least stringent version of the local area acceptance criterion is violated. In 1992, the drywell shell was evaluated as acceptable by NRC, provided the areas thinner than 0.736 inches were "highly localized." At that time, this requirement was incorporated into the CLB. In spring 2007, the SER evaluated the shell as acceptable, provided the areas within each Bay that are thinner than 0.736 inches are within, at most, a 3 feet by 3 feet cut-out shape. It is unclear if this requirement became part of the CLB. In any event, because the areas of the shell thinner than 0.736 inches go beyond a 3 feet by 3 feet square on the drywell, they are no longer highly localized and therefore the drywell shell no longer meets the CLB.

Finally, the NRC Staff have admitted that the drywell shell fails an ASME code requirement for a safety factor of 2.0 during refueling, if Dr. Hausler's initial assessment of the corrosion using the external measurements is correct. Because this requirement forms part of the CLB, a critical question is whether Dr. Hausler's initial analysis is valid. Responding to this question in this round of testimony, Dr. Hausler shows that his initial assessment was in fact quite conservative and the areas of severe corrosion are probably considerably larger than previously predicted. Thus, there is now little doubt that the drywell not only fails the CLB because the areas of severe corrosion are not highly localized, it also fails the CLB because the factor of safety during refueling is less than the required minimum of 2.0.

IV. Minimum Monitoring Frequency Is More Than Once Per Year

Finally, even if the Board accepts AmerGen's arguments that the margin above the acceptance criterion for mean thickness is the most limiting margin,[1] that margin is

[1] AmerGen has only made this argument implicitly by repeatedly citing 0.064 inches as the limiting margin and failing to mention the other acceptance requirements. Presumably the reason that AmerGen has never

currently 0.064 inches at the mid-range estimate,[2] and the grand standard error should be used, this translates into a margin of approximately 0.044 inches at the lower 95% confidence limit, including an allowance of 0.01 inches for possible systematic error.[3] *See* AmerGen Ex. 25 at 2 (minimum mean thickness is 0.800 inches, minimum required is 0.736 inches, and grand standard error of mean for grid 19A is 0.05 inches). Future corrosion rates after refueling outages are up to 0.01 inches per year from the interior and 0.039 inches per year from the exterior. The total corrosion rate could therefore be approximately 0.05 inches per year. This means that, at minimum, a UT monitoring frequency of greater than once per year is required.

---

stated the margins above the local area acceptance criteria is because it has testified that it cannot calculate those margins. There is therefore no evidence to support the argument that the margin above mean thickness requirements is the most limiting.

[2] To accept this value, the Board would have to ignore the lower estimates of the mean thickness produced from analyses of the external data.

[3] Citizens Ex. 37 at 11-12, justifies this allowance.

CONCLUSION

For the foregoing reasons, AmerGen's application to relicense the Oyster Creek Nuclear Generating Station should be denied. In the alternative, should the Board decide to allow the relicensing to proceed, it must ensure that AmerGen meets the burden the Board has set forth and then calculate the monitoring interval based on the minimum established margins.

Respectfully submitted

Richard Webster, Esq
RUTGERS ENVIRONMENTAL
LAW CLINIC
Attorneys for Petitioners

Dated: September 14, 2007

CITIZENS' EXHIBIT LIST ON SUR-REBUTTAL

No.	Exhibit	Other Reference
1	GPU Nuclear, Drywell Steel Shell Plate Thickness Reduction (July 21, 1995).	Citizen's Exhibit NC 8
2	Partial Cross Section of Drywell and Torus.	Citizen's Exhibit NC 10
3	Memorandum from Peter Tamburro on the Unclear Documentation of Calculation C-1302-187-5320-024 (AR 00461639 Report) (Mar. 30, 2006).	Exhibit ANC 8
4*	Exelon Nuclear, Calculation C-1302-187-5320-024 Revision 1: O.C. Drywell Ext. UT Evaluation in Sandbed (Jan. 12, 1993).	AmerGen's Exhibit 3
5*	Exelon Nuclear, Calculation C-1302-187-E310-041 Revision 0: Statistical Analysis of Drywell Vessel Sandbed Thickness Data 1992, 1994, 1996, and 2006 (Dec. 12, 2006).	Exhibit SJA 1
6	Affidavit of Peter Tamburro, Mar. 26, 2007.	
7	AmerGen, NRC Information Request: Audit Question Numbers AMP-141, 210, 356 (Apr. 5, 2006).	Citizen's Exhibit NC 1
8*	AmerGen, Passport 00546049 07 (AR A2152754 E09): Water Found in Drywell Trench 5 - UT Data Evaluation (Nov. 7, 2006).	Exhibit SJA 2

* Citizens understand that these exhibits marked with a * will be provided by AmerGen, however, if AmerGen fails to submit these exhibits as anticipated they will be submitted by the Citizens at a later date.

9	Structural Integrity Associates, Inc., Statistical Analysis of Oyster Creek Drywell Thickness Data (Jan. 4, 2007).	AmerGen's Exhibit 4
10	AmerGen, NRC Information Request: Audit Question Numbers AMP-357, 356, 210 (Jan. 24, 2006 and Feb. 16, 2006).	Citizen's Exhibit NC 2
11	Email from Peter Tamburro to Ahmed Ouaou (June 6, 2006, 14:03 EST).	OCLR00013624-13625
12	Memorandum from Dr. Rudolf Hausler, Apr. 25, 2007 (Redacted).	
13	Memorandum from Dr. Rudolf Hausler, July 19, 2007.	
14	AmerGen, Reference Material to the ACRS: Photograph of the Sand Bed Region (1992).	Exhibit SJA 3
15	Transcript of Nuclear Regulatory Commission Proceedings, Advisory Committee on Reactor Safeguards Subcommittee on Plant License Renewal Oyster Creek Generating Station (Jan. 18, 2007) (Excerpted Pages: p.1-10, p.132-144, p.207-224, p. 353-358).	
16	Transcript of Nuclear Regulatory Commission Proceedings, Advisory Committee on Reactor Safeguards Meeting of Plant License Renewal Subcommittee (Oct. 3, 2006) (Excerpted Pages: p.1-8, p.59-63).	
17	Email from Steven Hutchins to John Hufnagel Jr., with Drywell White Papers attachment (Sept. 18, 2006, 16:51 EST).	OCLR00013714 - 13734
18	Affidavit of Jon R. Cavallo, Mar. 26, 2007.	

19	AmerGen, Action Request: Determine the Proper Sealant for Drywell Sandbed Floor Voids (Oct. 23, 2006).	Exhibit ANC 5
20	Letter from Richard J. Conte, Chief Engineering Branch 1, Nuclear Regulatory Commission, to Richard Webster, Esq., Rutgers Environmental Law Clinic (Nov. 9, 2006).	Exhibit ANC 6
21	Letter from J.C. Devine, Jr., Vice President of Technical Functions, GPU Nuclear, to the Nuclear Regulatory Commission (Dec. 5, 1990) (Attachment 3; GPUN Detailed Summary Addressing Water Intrusion and Leakage Effects Related to the Oyster Creek Drywell).	OCLR00029270-29283
22	GPU Nuclear, Clearing of the Oyster Creek Drywell Sand Bed Drains (Feb. 15, 1989).	OCLR00028912-28918
23	AmerGen, Disclosed Document Relating to Drywell Leakage.	OCLR00013354
24	Transcript of Nuclear Regulatory Commission Proceedings, Advisory Committee on Reactor Safeguards 539th Meeting (Feb. 1, 2007) (Excerpted Pages: p.1-3, p. 172-177, p. 217-224).	
25	Letter from the Nuclear Regulatory Commission to C. Crane (Jan. 17, 2007) ("Inspection Report").	ML070170396
26	Email from Steven Dunsmuir, FIN/Operations RO, Exelon Corp., to Howie Ray, et al. (Oct. 22, 2006, 04:52 EST).	OCLR00014454-14455
27	Email from Tom Quintenz to Kevin Muggleston, et al. (Feb. 1, 2006, 17:02 EST).	OCLR00013629
28	GPU Nuclear, Evaluation of February 1990 Drywell UT Examination Data (Mar. 8, 1990).	Citizen's Exhibit NC 9

29	Affidavit of Gordon, Mar. 26, 2007.	
30	Letter from Jill Lipoti, Director Division of Environmental Safety and Health, New Jersey Dept. of Environmental Protection, to Dr. Pao-Tsin Kuo, Director Division of License Renewal, U.S. Nuclear Regulatory Commission (Apr. 26, 2007).	
31*	AmerGen, Calculation Sheet C-1302-187-5300-01.	
32*	GPU Nuclear, Calculation Sheet C-1302-187-5320-024 Revision 0: Oyster Creek Drywell Exterior Evaluation in Sandbed (1993).	Citizen's Exhibit NC 3
33*	Exelon Nuclear, Calculation C-1302-187-5320-024 Revision 2: O.C. Drywell Ext. UT Evaluation in Sandbed (Mar. 18, 2007).	
34*	ACRS Information Packet (Dec. 2006).	Exhibit ANC 2
35	Letter from AmerGen to the NRC (2103-06-20426) (Dec. 3, 2006) (Excerpted Pages: Dec. 3, 2006 Letter, p.1-3, p. 9-15, p. 17-24).	Exhibit ANC 1
36	Email from Caroline Schlaseman, MPR Associates, Inc., to Howie Ray (Nov. 2, 2006, 12:09 EST).	OCLR00015433-15434
37	Background and Statement of Facts	Attachment 5 to Hausler Initial Testimony
38	Memorandum from Dr. Rudolf Hausler, Subject: Response To The Questions About Statistics (Aug. 16, 2007).	

39 Memorandum from Dr. Rudolf Hausler, Subject: Further Discussion of the Nature of the Corroded Surfaces and The Residual Wall Thickness of the Oyster Creek Dry Well (Aug. 16, 2007).

40. Email from William Russell to Frederick Polaski, et al., Subject: Challenge Board #1 additional comment (Nov. 30, 2006, 9:48 EST), attached to email from John Hufnagel Jr. to Ahmed Ouaou, et al. (Nov. 30, 2006 10:41 EST).

41. GPU Nuclear, Technical Functions Safety/Environmental Determination and 50.59 Review (Jan. 5, 1993).

42. Email from Peter Tamburro to Ahmed Ouaou, Cc Howie Ray, et al., Subject: Surface Are (sic) of the Drywell in the sand bed (Apr. 3, 2006 3:24 PM).

43. Email from John O'Rourke to Michael Gallagher, et al., Subject: External Inspections of DW in Sandbed Region (Oct. 10, 2006 8:08 AM), attached to email from John Hufnagel to John O'Rourke (Oct. 10, 2006 8:10 AM).

44. Memorandum, GPU Nuclear from K. L. Whitmore, Civil/Structural Mgr. to J. C. Flynn, Manager, Special Projects, Engineering Projects, Subject: Inspection of drywell sand bed region and access holes (Jan. 28, 1993).

45. AmerGen Technical Evaluation 330592-27-27 (Apr. 20, 2007).

46. Email from John O'Rourke to Marcos Herrera, Cc Michael Gallagher et al., Subject: Oyster Creek Drywell Thickness to be Used for Base Case Analysis, with OYSTER CREEK DRYWELL THICKNESSES, Rev2.doc attachment (Feb. 28, 2007 7:20 PM).

47. Issue # 00557180, Exelon Nuclear Issue - Statement of Confirmation, Originator: Kathy Barnes (Nov. 13, 2006).

48. Email from Tom Quintenz to John O'Rourke, Subject: Notes of video inspection results of trough area with Video Inspection of Concrete Trough Notes November 1996 with attachment (Oct. 10, 2006 2:26 PM).

49. GPU Nuclear, Material Nonconformance Report (Oct. 27, 1986).

50. Memorandum, GPU Nuclear from R. Miranda, Engineer, Technical Functions to Distribution, Subject: 14R Reactor Cavity Leak Detection Effort (Feb. 1, 1993).

51. Sketches showing ultrasonic and "Echo to Echo" techniques, and explanations of sketches.

52. E-mail from Tom Quintenz to Ahmed Ouaou & John Hufnagel, Jr. (September 20, 2006 2:02 EST) OCLR00013796
AR 00547236 Report OCLR00013846

53. Letter from Alexander W. Dromerick to John J. Barton (November 19, 1991)

54. Letter from Alexander W. Dromerick to John J. Barton (September 2, 1993) ML011210012

55. Memorandum from Goutam Bagchi from John F. Stolz dated April 9, 1992, with attached Safety Evaluation Report with supporting analysis by Brookhaven National Laboratories

56. Letter from Alexander W. Dromerick to John J. Barton (April 24, 1992)

57. Letter from J.C. DeVine to NRC (May 26, 1992)

58. Letter from Alexander W. Dromerick to John J. Barton (June 30, 1992)

59. Letter from H.S. Mehta to Dr. Stephen Tumminelli (December 11, 1992)

60. Sandia Report on Structural Integrity Analysis of the Degraded Drywell Containment of Oyster Creek Nuclear Generating Station.

61. Memorandum from Rudolf H. Hausler to Richard Webster, Esq., Subject: Further Discussion of the External Corrosion on the Drywall Shell in the Sandbed Region. (September 13, 2007).

62. Transcript excerpt from the Official Transcript of Proceedings, Nuclear Regulatory Commission - Advisory Committee on Reactor Safeguards, http://www.nrc.gov/reading-rm/doc-collections/acrs/tr/fullcommittee/2001/ac010906.html (last visited Sept. 13, 2007) (transcript excerpt from the 485th Meeting held on September 6, 2001).

63. Diagram of Oyster Creek Lower Drywell / Sandbed Region.

64. E-mails ending in e-mail from Gordon to Licina, dated October 24, 2006 (redacted to be non-proprietary)

65. E-mail from O'Rourke to Herrera, dated February 7, 2007 (redacted to be non-proprietary)

Exhibit 52

E-mail from Tom Quintenz to Ahmed Ouaou & John Hufnagel, Jr.
(September 20, 2006 2:02 EST) OCLR00013796

&

AR 00547236 Report OCLR00013846

From:	Quintenz, Tom <Tom.Quintenz@exeloncorp.com>
Sent:	Wednesday, September 20, 2006 2:02 PM
To:	Ouaou, Ahmed <u999ao2@ucm.com>; Hufnagel Jr, John G <u000jgh@ucm.com>
Cc:	Tamburro, Peter <u777p0t@ucm.com>; Warfel Sr, Donald B <u001dbw@ucm.com>; O'Rourke, John F. <t925jfo@ucm.com>
Subject:	RE: Inspection of Sand Bed Drain Lines

I am responding to my action item from Dave Ryan that this is not a commitment, but must remain in scope for the outage.

----Original Message----
From: Ouaou, Ahmed
Sent: Wednesday, September 20, 2006 1:36 PM
To: Quintenz, Tom; Hufnagel Jr, John G
Cc: Tamburro, Peter; Warfel Sr, Donald B; O'Rourke, John F.
Subject: RE: Inspection of Sand Bed Drain Lines

I'll discuss with Don and John O' during turn over. I also think it is a good idea to look at the drains and sandbed floor for debris that could get into the drains when the coating in the bays with drains is inspected. It is not a commitment to check the drains; but we would not look good if we flood the sandbed because the drains are plugged

----Original Message----
From: Quintenz, Tom
Sent: Friday, September 15, 2006 5:36 PM
To: Hufnagel Jr, John G
Cc: Ouaou, Ahmed; Tamburro, Peter
Subject: RE: Inspection of Sand Bed Drain Lines

With regard to the suggested check of the configuration, suggest that we agree on the change and have the KS program engineer issue a revision to the appropriate recurring task(s) to implement the requirement.

----Original Message----
From: Hufnagel Jr, John G
Sent: Friday, September 15, 2006 5:03 PM
To: Quintenz, Tom
Cc: Ouaou, Ahmed; Tamburro, Peter
Subject: RE: Inspection of Sand Bed Drain Lines

I agree with your assessment. I also reviewed the June 20, 2006 letter which responded to NRC concerns outlined in the June 1 Public meeting, and as expected, found no commitment to inspect the sand bed drain lines for blockage.

As a separate but related point, do we have a recurring task to ensure that the tubing that goes from the sand bed drain to the poly bottles is intact? It seems we should verify the integrity of this configuration on some regular interval, even if it is not a commitment.

- John.

-----Original Message---

From: Quintenz, Tom

Sent: Friday, September 15, 2006 4:29 PM

To: Hufnagel Jr, John G

Cc: Ouaou, Ahmed; Tamburro, Peter

Subject: *Inspection of Sand Bed Drain Lines*

John, Please confirm the following conclusion relative to the sand bed drain line inspection. This is needed to satisfy an action item I received from an outage planning meeting this week. Thanks.

Conclusion: It appears the inspection of the sand bed drain lines for blockage is not currently a commitment. This is based on my review of the current A.5 table of commitments, review of the July 7, 2006 letter to the NRC, and discussions with Ahmed Ouaou. Examination of the trough drain for blockage is a commitment and is contained in our table of commitments and is specifically listed in the July 7, 2006 letter. I have attached a copy of the letter for your reference if needed.

<< File: 2130-06-20358 Additional Appendix A Clarifications - 7-7-06.pdf >>

AR 00547236 Report

Aff Fac:	Oyster Creek	**AR Type:**	CR	**Status:**	APPROVED
Aff Unit:	NA	**Owed To:**	ACAPALL	**Due Date:**	11/20/2006
Aff System:	167			**Event Date:**	10/21/2006
CR Level/Class:	/			**Disc Date:**	10/21/2006
How Discovered:	H02			**Orig Date:**	10/21/2006
WR/PIMS AR:		**Component #:**			

Action Request Details

Subject: DEBRIS LOCATED IN BAYS 7 AND 11 SANDBED DRAIN LINES

Description:

Originator: PETER TAMBURRO Supv Contacted: Howie Ray

Condition Description:
Inspection of the Sandbed Drain Lines in accordance with Specification IS-328227-004 Rev. 13 showed that the drain line in bay 7 has debris, which could cause blockage of this line. The debris looks like loose concrete. This does not meet the acceptance criteria in the specification per section 3.2.5.2.

In addition the inspection of the drain line in bay 11 shows some loose debris in the bottom of the line directly downstream of the first elbow. However the line is not blocked and meets the acceptance criteria.

Operability

The purpose of the drain lines is to route water in the sandbed from the drywell vessel. At this time the remaining 4 lines are capable of performing this function. In addition since the line in bay 7 is not completely blocked it too would partially perform its function by draining the sandbed. So far in 1R21 no water has entered the sandbed.

Engineering has inspected the 5 bottles every day since the beginning of the outage (R2088495). To date no water has been found in any of the bottles or on the floor outside the sandbed bays.

Also Engineering and/or NDE have inspected all 10 Drywell Sandbed bays. To date no water or moisture has been observed in these bays and the coating is in good condition..

Engineering will continue to monitor (on a daily basis) the trough drain line for changes in flow rate and the five polyvinyl bottles for water.

Immediate actions taken:
Informed Howie Ray and the Engineering Control Center

Recommended Actions:

1) Continue to monitor the five poly bottles and trough drain line daily per our commitments

2) Recommend cleaning the drain lines in bays 7 and 11.

Operable Basis:

Reportable Basis:

Assignments

Assign #:	01	**Assigned To:**		**Status:**	AWAIT/C
Aff Fac:	Oyster Creek	**Prim Grp:**	ACAPALL	**Due Date:**	10/26/2006
Assign Type:	TRKG	**Sec Grp:**		**Orig Due Date:**	pp/pp/pppp
Priority:					
Schedule Ref:					
Unit Condition:					
Subject/Description:	DEBRIS LOCATED IN BAYS 7 AND 11 SANDBED DRAIN LINES				

Exhibit 52

E-mail from Tom Quintenz to Ahmed Ouaou & John Hufnagel, Jr.
(September 20, 2006 2:02 EST) OCLR00013796

&

AR 00547236 Report OCLR00013846

From:	Quintenz, Tom <Tom.Quintenz@exeloncorp.com>
Sent:	Wednesday, September 20, 2006 2:02 PM
To:	Ouaou, Ahmed <u999ao2@ucm.com>; Hufnagel Jr, John G <u000jgh@ucm.com>
Cc:	Tamburro, Peter <u777p0t@ucm.com>; Warfel Sr, Donald B <u001dbw@ucm.com>; O'Rourke, John F. <t925jfo@ucm.com>
Subject:	RE: Inspection of Sand Bed Drain Lines

I am responding to my action item from Dave Ryan that this is not a commitment, but must remain in scope for the outage.

-----Original Message-----
From: Ouaou, Ahmed
Sent: Wednesday, September 20, 2006 1:36 PM
To: Quintenz, Tom; Hufnagel Jr, John G
Cc: Tamburro, Peter; Warfel Sr, Donald B; O'Rourke, John F.
Subject: RE: Inspection of Sand Bed Drain Lines

I'll discuss with Don and John O' during turn over. I also think it is a good idea to look at the drains and sandbed floor for debris that could get into the drains when the coating in the bays with drains is inspected. It is not a commitment to check the drains; but we would not look good if we flood the sandbed because the drains are plugged

-----Original Message-----
From: Quintenz, Tom
Sent: Friday, September 15, 2006 5:36 PM
To: Hufnagel Jr, John G
Cc: Ouaou, Ahmed; Tamburro, Peter
Subject: RE: Inspection of Sand Bed Drain Lines

With regard to the suggested check of the configuration, suggest that we agree on the change and have the KS program engineer issue a revision to the appropriate recurring task(s) to implement the requirement.

-----Original Message-----
From: Hufnagel Jr, John G
Sent: Friday, September 15, 2006 5:03 PM
To: Quintenz, Tom
Cc: Ouaou, Ahmed; Tamburro, Peter
Subject: RE: Inspection of Sand Bed Drain Lines

I agree with your assessment. I also reviewed the June 20, 2006 letter which responded to NRC concerns outlined in the June 1 Public meeting, and as expected, found no commitment to inspect the sand bed drain lines for blockage.

As a separate but related point, do we have a recurring task to ensure that the tubing that goes from the sand bed drain to the poly bottles is intact? It seems we should verify the integrity of this configuration on some regular interval, even if it is not a commitment.

- John.

-----Original Message----

From: Quintenz, Tom

Sent: Friday, September 15, 2006 4:29 PM

To: Hufnagel Jr, John G

Cc: Ouaou, Ahmed; Tamburro, Peter

Subject: Inspection of Sand Bed Drain Lines

John, Please confirm the following conclusion relative to the sand bed drain line inspection. This is needed to satisfy an action item I received from an outage planning meeting this week. Thanks.

Conclusion: It appears the inspection of the sand bed drain lines for blockage is not currently a commitment. This is based on my review of the current A.5 table of commitments, review of the July 7, 2006 letter to the NRC, and discussions with Ahmed Ouaou. Examination of the trough drain for blockage is a commitment and is contained in our table of commitments and is specifically listed in the July 7, 2006 letter. I have attached a copy of the letter for your reference if needed.

<< File: 2130-06-20358 Additional Appendix A Clarifications - 7-7-06.pdf >>

AR 00547236 Report

Aff Fac:	Oyster Creek	**AR Type:**	CR	**Status:**	APPROVED
Aff Unit:	NA	**Owed To:**	ACAPALL	**Due Date:**	11/20/2006
Aff System:	187			**Event Date:**	10/21/2006
CR Level/Class:	/			**Disc Date:**	10/21/2006
How Discovered:	H02			**Orig Date:**	10/21/2006
WR/PIMS AR:		**Component #:**			

Action Request Details

Subject: DEBRIS LOCATED IN BAYS 7 AND 11 SANDBED DRAIN LINES

Description:

Originator: PETER TAMBURRO Supv Contacted: Howie Ray

Condition Description:
Inspection of the Sandbed Drain Lines in accordance with Specification IS-328227-004 Rev. 13 showed that the drain line in bay 7 has debris, which could cause blockage of this line. The debris looks like loose concrete. This does not meet the acceptance criteria in the specification per section 3.2.5.2.

In addition the inspection of the drain line in bay 11 shows some loose debris in the bottom of the line directly downstream of the first elbow. However the line is not blocked and meets the acceptance criteria.

Operability

The purpose of the drain lines is to route water in the sandbed from the drywell vessel. At this time the remaining 4 lines are capable of performing this function. In addition since the line in bay 7 is not completely blocked it too would partially perform its function by draining the sandbed. So far in 1R21 no water has entered the sandbed.

Engineering has inspected the 5 bottles every day since the beginning of the outage (R2088495). To date no water has been found in any of the bottles or on the floor outside the sandbed bays.

Also Engineering and/or NDE have inspected all 10 Drywell Sandbed bays. To date no water or moisture has been observed in these bays and the coating is in good condition..

Engineering will continue to monitor (on a daily basis) the trough drain line for changes in flow rate and the five polyvinyl bottles for water.

Immediate actions taken:
Informed Howie Ray and the Engineering Control Center

Recommended Actions:

1) Continue to monitor the five poly bottles and trough drain line daily per our commitments

2) Recommend cleaning the drain lines in bays 7 and 11.

Operable Basis:

Reportable Basis:

Assignments

Assign #:	01	**Assigned To:**		**Status:**	AWAIT/C
Aff Fac:	Oyster Creek	**Prim Grp:**	ACAPALL	**Due Date:**	10/26/2006
Assign Type:	TRKG	**Sec Grp:**		**Orig Due Date:**	pp/pp/pppp
Priority:					
Schedule Ref:					
Unit Condition:					
Subject/Description:	DEBRIS LOCATED IN SAYS 7 AND 11 SANDBED DRAIN LINES				

Exhibit 53

Letter from Alexander W. Dromerick to John J. Barton
(November 19, 1991)

Docket File

UNITED STATES
NUCLEAR REGULATORY COMMISSION
WASHINGTON, D. C. 20555

November 19, 1991

Docket No. 50-219

Mr. John J. Barton, Vice President
and Director
GPU Nuclear Corporation
Oyster Creek Nuclear Generating Station
Post Office Box 388
Forked River, New Jersey 08731

Dear Mr. Barton:

SUBJECT: CLARIFICATION OF STAFF POSITION ON EVALUATION OF STRUCTURAL INTEGRITY OF A DEGRADED STEEL CONTAINMENT (TAC NO M79166)

References:
1. Letter to J. J. Barton from A. W. Dromerick providing the subject staff's position dated September 3, 1991.
2. Letter to NRC from GPU Nuclear Corporation providing the response to staff's position dated October 9, 1991.

In a letter of October 9, 1991 (Reference 2), GPU Nuclear Corporation (GPUN) provided responses to the staff position on the evaluation of the structural integrity of a degraded steel containment. It appears from the responses that GPUN differs with the staff's position, specifically on the application of ASME subsection NE-3213.10. Enclosed is the staff's review of GPUN's response. It clarifies the staff's position and requires GPUN to provide additional information to aid in a final resolution of staff's concerns.

We request that the information be provided within 30 days of receipt of this letter. If you have any questions regarding this request, please contact me.

DF01

The requirements of this letter affect fewer than 10 respondents, and therefore, are not subject to Office of Management review under P.L. 97-511.

Sincerely,

/s/

Alexander W. Dromerick, Sr. Project Manager
Project Directorate I-4
Division of Reactor Projects - I/II
Office of Nuclear Reactor Regulation

Enclosure:
As stated

cc: See next page

Distribution:
Docket File
NRC & Local PDRs
PD I-4 Plant
SVarga
JCalvo
SNorris
ADromerick
OGC
EJordan
GBagchi
RRothman
ACRS (10)
CWHehl

OFC	:PDI-4:LA	:PDI-4:PM	:PDI-4:D	:	:
NAME	:SNorris:cn	:ADromerick:cn	:JFStolz	:	:
DATE	:11/20 /91	:11/20 /91	:11/20 /91	:	:

OFFICIAL RECORD COPY
Document Name: TAC NO. 79166

REVIEW OF GPUN'S RESPONSE OF OCTOBER 9, 1991
RELATED TO THE
STAFF'S POSITION ON EVALUATION OF
DEGRADED STEEL CONTAINMENT
AT OYSTER CREEK

The staff has reviewed GPU Nuclear Corporation's (GPUN) response of October 9, 1991 to the staff's position on the evaluation of the structural integrity of a degraded steel containment. It is to be noted that this staff position is to be applied generically in the evaluation of steel containments which are degraded, not specifically to the Oyster Creek steel drywell. The staff's position is based on technical criteria that conform to the spirit and intent of ASME subsection NE-3213.10. NE is the design part of the ASME code and cannot be directly applied to the situation of inservice degradation without the exercise of engineering judgment. By considering the corroded area as equivalent to a discontinuity as indicated in NE-3212.10, great caution must be exercised. It should be understood that the discontinuity as created by corrosion is not the same as the "designed" discontinuity such as a change in shell thicknesses, the presence of a bracket or a penetration as envisioned in the code. The basic characteristic of the discontinuity due to corrosion is irregularity, e.g. variation in thickness and extent of corroded areas. In view of the above observation, the NE 3312.10 stipulation cannot be applied indiscriminately to a corroded steel containment. NE-3312.10 specifies the limit of the discontinuity region in which the stresses can be greater than 1.1 Smc. The code does not specify the outside limit of the region which is contiguous to and supports the discontinuity and in which the stresses vary from 1.1 Smc to 1.0 Smc. This should be expected because this outside limit varies with the configuration of the discontinuity and the loading. Therefore, the lack of specific stipulation in the code in this respect should be understood and should not be construed to allow the stress limit of 1.1 Smc to be applied universally throughout the containment shell. The staff position is not, in any way, more restrictive than the stipulation in the ASME Code.

The staff is well aware of the extensive examinations and analysis performed on the Oyster Creek drywell as reported by GPUN. GPUN has repeatedly claimed that the Oyster Creek drywell has been examined thoroughly and the condition of the drywell is fully understood with a 95% confidence level. On the basis of this claim, the staff has requested GPUN to determine the extent of each corroded area. The staff is not requesting any additional physical examination. However, on the basis of the information available, GPUN should present in a figure the known areas of corrosion with the critical stresses (general primary membrane stress or local primary membrane stress) identified. The purpose of such an action is to determine the behavior of the drywell especially at and around the corroded areas. By comparing the calculated stresses of the drywell shell at and around corroded areas with the code allowables the staff can reasonably determine the adequacy of the licensee's proposed actions.

Exhibit 54

Letter from Alexander W. Dromerick to John J. Barton
(September 2, 1993) ML011210012

September 2, 1993

Docket No. 50-219

Distribution:
Docket File
NRC & Local PDRs
PD I-4 Plant
SVarga (14E4)
JCalvo (14A2)
SNorris
ADromerick
OGC (15B18)
EJordan (MNBB 3701)
ACRS (10)(P-315)
OPA (17A3)
JFRogge, RI

Mr. John J. Barton
Vice President and Director
GPU Nuclear Corporation
Oyster Creek Nuclear Generating Station
Post Office Box 388
Forked River, New Jersey 08731

Dear Mr. Barton:

SUBJECT: OYSTER CREEK NUCLEAR GENERATING STATION - ENVIRONMENTAL ASSESSMENT (TAC NO. M81093)

Enclosed is a copy of the Environmental Assessment and Finding of No Significant Impact which relates to your submittal dated July 22, 1991, as supplemented February 14, 1992, August 19, 1992, and July 12, 1993, requesting a license amendment to revise Technical Specification 5.2.A to change the current containment drywell pressure of 62 psig to the new design pressure of 44 psig and the current containment drywell temperatures of 175 °F to the new design temperature of 292 °F. Related changes to Technical Specification Bases are also proposed. Unrelated editorial changes to the Bases of Technical Specification 3.4 and 3.5 are also proposed.

The assessment is being forwarded to the Office of the Federal Register for publication.

Sincerely,

Original signed by:

Alexander W. Dromerick, Sr. Project Manager
Project Directorate I-4
Division of Reactor Projects - I/II
Office of Nuclear Reactor Regulation

Enclosure:
As stated

cc w/enclosure:
See next page

9309140346

OFFICE	LA:PDI-4	PM:PDI-4	D:PDI-4	OGC	
NAME	SNorris	ADromerick:cn	JStolz	[redacted]	
DATE	7/19/93	7/19/93	7/19/93	7/17/93	/ /

OFFICIAL RECORD COPY
Document Name: G:\DROMERIC\M81093.EA 8/2/93

220068

DF01

UNITED STATES
NUCLEAR REGULATORY COMMISSION
WASHINGTON, D.C. 20555-0001

September 2, 1993

Docket No. 50-219

Mr. John J. Barton
Vice President and Director
GPU Nuclear Corporation
Oyster Creek Nuclear Generating Station
Post Office Box 388
Forked River, New Jersey 08731

Dear Mr. Barton:

SUBJECT: OYSTER CREEK NUCLEAR GENERATING STATION - ENVIRONMENTAL ASSESSMENT (TAC NO. M81093)

Enclosed is a copy of the Environmental Assessment and Finding of No Significant Impact which relates to your submittal dated July 22, 1991, as supplemented February 14, 1992, August 19, 1992, and July 12, 1993, requesting a license amendment to revise Technical Specification 5.2.A to change the current containment drywell pressure of 62 psig to the new design pressure of 44 psig and the current containment drywell temperatures of 175 °F to the new design temperature of 292 °F. Related changes to Technical Specification Bases are also proposed. Unrelated editorial changes to the Bases of Technical Specification 3.4 and 3.5 are also proposed.

The assessment is being forwarded to the Office of the Federal Register for publication.

Sincerely,

Alexander W. Dromerick

Alexander W. Dromerick, Sr. Project Manager
Project Directorate I-4
Division of Reactor Projects - I/II
Office of Nuclear Reactor Regulation

Enclosure:
As stated

cc w/enclosure:
See next page

Mr. John J. Barton
GPU Nuclear Corporation

Oyster Creek Nuclear
Generating Station

cc:

Ernest L. Blake, Jr., Esquire
Shaw, Pittman, Potts & Trowbridge
2300 N Street, NW.
Washington, DC 20037

Resident Inspector
c/o U.S. Nuclear Regulatory Commission
Post Office Box 445
Forked River, New Jersey 08731

Regional Administrator, Region I
U.S. Nuclear Regulatory Commission
475 Allendale Road
King of Prussia, Pennsylvania 19406

Kent Tosch, Chief
New Jersey Department of
Environmental Protection
Bureau of Nuclear Engineering
CN 415
Trenton, New Jersey 08625

BWR Licensing Manager
GPU Nuclear Corporation
1 Upper Pond Road
Parsippany, New Jersey 07054

Mayor
Lacey Township
818 West Lacey Road
Forked River, New Jersey 08731

Licensing Manager
Oyster Creek Nuclear Generating Station
Mail Stop: Site Emergency Bldg.
Post Office Box 388
Forked River, New Jersey 08731

UNITED STATES NUCLEAR REGULATORY COMMISSION

GPU NUCLEAR CORPORATION

JERSEY CENTRAL POWER & LIGHT COMPANY

DOCKET NO. 50-219

ENVIRONMENTAL ASSESSMENT AND

FINDING OF NO SIGNIFICANT IMPACT

The U.S. Nuclear Regulatory Commission (NRC or the Commission) is considering issuance of an amendment to Facility Operating License No. DPR-16 issued to GPU Nuclear Corporation, et al. (the licensee), for operation of the Oyster Creek Nuclear Generating Station, located in Ocean County, New Jersey.

ENVIRONMENTAL ASSESSMENT

Identification of the Proposed Action:

The proposed amendment would revise Technical Specification 5.2.A to change the current containment drywell pressure of 62 psig to the new design pressure of 44 psig and the current containment drywell temperatures of 175 °F to the new design temperature of 292 °F. Related changes to Technical Specification Bases are also proposed. Unrelated editorial changes to the bases of Technical Specification 3.4 and 3.5 are also proposed.

The proposed amendment is in accordance with GPU Nuclear Corporation's application dated July 22, 1991, as supplemented February 14, 1992, August 19, 1992, and July 12, 1993.

Need for the Proposed Action:

The proposed changes to the Facility Operating License are needed because it is a part of GPU Nuclear Corporation's comprehensive program to address the corrosion of the Oyster Creek drywell.

Environmental Impacts of the Proposed Action:

The Commission has completed its evaluation of the licensee's proposal to change the current containment drywell pressure of 62 psig to the new design pressure of 44 psig and the current containment drywell temperatures of 175 °F to the new design temperature of 292 °F. The licensee also proposes to change the related Technical Specification Bases.

Based on its review of the licensee's analyses and the licensee's statement that the analyses have been performed in accordance with the Standard Review Plan, the staff finds that the licensee's proposed change to reduce the current containment drywell pressure of 62 psig to the new design pressure of 44 psig and the current containment drywell temperatures of 175 °F to the new design temperature of 292 °F is acceptable. The Commission has determined that the proposed changes do not alter any initial conditions

Exhibit 55

Memorandum from Goutam Bagchi from John F. Stolz dated April 9, 1992, with attached Safety Evaluation Report with supporting analysis by Brookhaven National Laboratories

APR 09 1992

MEMORANDUM FOR: John F. Stolz, Director
Project Directorate 1-4
Division of Reactor Projects I/II
Office of Nuclear Reactor Regulation

FROM: Goutam Bagchi, Chief
Structural and Geosciences Branch
Division of Engineering Technology
Office of Nuclear Reactor Regulation

SUBJECT: EVALUATION REPORT ON STRUCTURAL INTEGRITY OF THE OYSTER CREEK DRYWELL

Plant Name: Oyster Creek Nuclear Generating Station
Applicant: GPU Nuclear Corporation
Docket No.: 50-219
Review Status: Complete
Tac No.: M79166

The Structural and Geosciences Branch (ESGB) has completed the review and evaluation of the stress analyses and stability analyses reports of the corroded drywell with and without the sand bed. Our evaluation report together with a SALP is contained in the enclosure. The licensee used the analyses to justify the removal of the sand from the sand bed region. Even though the staff, with the assistance of consultants from Brookhaven National Laboratory (BNL), concurred with licensee's conclusion that the drywell meets the ASME Section III Subsection NE requirements, it is essential that the licensee continue UT thickness measurements at refueling outages and at outages of opportunity for the life of the plant.

The review is performed by C. P. Tan of Geosciences Section of ESGB with the assistance of BNL.

/S/
Goutam Bagchi, Chief
Structural and Geosciences Branch
Division of Engineering Technology

Enclosure:
As stated

cc: J. E. Richardson
B. D. Liaw
A. Dromerick

DISTRIBUTION:	ESGB:DET	ESGB:DET	ESGB:DET
Central File	CPTan:db	RRothman	GBagchi
ESGB R/F	03/30/92*	03/30/92*	04/8/92
CPTan			
RRothman	EMCB:DET		
GBagchi	JWiggins		
JWiggins	04/9/92	*SEE PREVIOUS CONCURRENCE	

SAFETY EVALUATION REPORT
OYSTER CREEK NUCLEAR GENERATING STATION
DRYWELL STRUCTURAL INTEGRITY
STRUCTURAL AND GEOSCIENCES BRANCH

I. INTRODUCTION

In 1986 the steel drywell at Oyster Creek Nuclear Generating Station (OCNGS) was found to be extensively corroded in the area of the shell which is in contact with the sand cushion around the bottom of the drywell. Since then GPU Nuclear, the Licensee of OCNGS, has instituted a program of periodic inspection of the drywell shell sand cushion area through ultrasonic testing UT thickness measurements. The inspection has been extended to other areas of the drywell and some areas above the sand cushion have been found to be corroded also. From the UT thickness measurements, one can conclude that corrosion of the drywell shell in the sand cushion area is continuing. In an attempt to eliminate corrosion or reduce the corrosion rate, the licensee tried cathodic protection and found it to be of no avail. An examination of the results of consecutive UT measurements, confirmed that the corrosion is continuing. There is concern that the structural integrity of the drywell cannot be assured. Since the root cause of the corrosion in the sand cushion area is the presence of water in the sand, the licensee has considered sand removal to be an important element in its program to eliminate the corrosion threat to the drywell integrity.

In the program, the licensee first established the analysis criteria and then performed the analyses of the drywell for its structural adequacy with and without the presence of the sand. The licensee performed stress analyses and stability analyses for both with and without the sand cases and concluded the drywell with or without the sand to be in compliance with the criteria established for the reevaluation. It is to be noted that the original purpose of the sand cushion is to provide a smooth transition of stresses from the fixed portion to the free-standing portion of the steel drywell.

II. EVALUATION

The staff with the assistance of consultants from Brookhaven National Laboratory (BNL) has reviewed and evaluated the information (Refs. 1,2,3,4,5) provided by the licensee.

1. Re-Analysis Criteria

The drywell was originally designed and constructed to the requirements of ASME Section VIII code and applicable code cases, with a contract date of July 1, 1964. The section VIII code requirements for nuclear containment vessels at that time were less detailed than at any subsequent date. The evolution of the ASME Section III code for metal containments and its relation with ASME Section VIII code were reviewed and evaluated by Teledyne Engineering Services (TES). The evaluation criteria used are based on ASME Section III Subsection NE code through the 1977 summer addenda. The reason for the use of the code of this vintage is that it was used in the Mark I containment program to evaluate the steel torus for hydrodynamic loads and that the current ASME Section III Subsection NE Code is closely related to that version. The following are TES's findings relevant to Oyster Creek application:

a) The steel material for the drywell is A-212, grade B, Firebox Quality (Section VIII), but it is redesignated as SA-516 grade in Section III.

b) The relation between the allowable stress (S) in Section VIII and the stress intensity (Smc) in Section III for metal containment is 1.1S = Smc.

c) Categorization of stresses into general primary membrane, general bending and local primary membrane stresses and membrane plus bending stresses is adopted as in Subsection NE.

d) The effect of a locally stressed region on the containment shell is considered in accordance with NE-3213.10.

In addition to ASME Section III Subsection NE Code, the licensee has also invoked ASME Section XI IWE Code to demonstrate the adequacy of the Oyster Creek drywell. IWE-3519.3 and IWE-3122.4 state that it is acceptable if either the thickness of the base metal is reduced by no more than 10% of the normal plate thickness or the reduced thickness can be shown by analysis to satisfy the requirements of the design specification.

The staff has reviewed the licensee's adoption of ASME Section III Subsection NE and Section XI Subsection IWE in its evaluation of the structural adequacy of the corroded Oyster Creek drywell, and has found it to be generally reasonable and acceptable.

By adopting the Subsection NE criteria, the licensee has treated the corroded areas as discontinuities per NE-3213.10, which was originally meant for change in thicknesses, supports, and penetrations. These discontinuities are highly localized and should be designed so that their presence will have no effect on the overall behavior of the containment shell. NE-3213.10 defines clearly the level of stress intensity and the extent of the discontinuity to be considered localized. A stress intensity limit of 1.1 Smc is specified at the boundary of the region within which the membrane stress can be higher than 1.1 Smc. The region where the stress intensity varies from 1.1 Smc to 1.0 Smc is not defined in the code because of the fact that it varies with the loading. In view of this, the licensee rationalized that the 1.1 Smc can be applied beyond the region defined by NE-3213.10 for localized discontinuity without any restriction throughout the drywell. The staff disagreed with the licensee's interpretation of the code. The staff pointed out that for Oyster Creek drywell, stresses due to internal pressure should be used as the criterion to establish such a region. The interpretation of Section XI Subsections IWE-3519.3 and IWE-3122.4 can be made only in the same context. It is staff's position that the primary membrane stress limit of 1.1 Smc not be used indiscriminately throughout the drywell.

In order to use NE-3213.10 to consider the corroded area as a localized discontinuity, the extent of the reduction in thickness due to corrosion should be reasonably known. UT thickness measurements are highly localized; however, from the numerous measurements so far made on the Oyster Creek drywell, one can have a general idea of the overall corroded condition of the drywell shell and it is possible to judiciously apply the established re-analysis criteria.

2. Re-analyses

The re-analyses were made by General Electric Company for the licensee, one reanalysis considered the sand present and the other considered the drywell without the sand. Each re-analysis comprises a stress analysis and stability analysis. Two finite element models, one axisymmetric and another a 36° pie slice model were used for the stress analysis. The ANSYS computer program was used to perform the analyses. The axisymmetric model was used to determine the stresses for the seismic and the thermal gradient loads. The pie slice model was used for dead weight and pressure loads. The pie slice model includes the vent pipe and the reinforcing ring, and was also used for buckling analysis. The same models were used for the cases with

and without sand, except that in the former, the stiffness of sand in contact with the steel shell was considered. The shell thickness in the sand region was assumed to be 0.700" for the with-sand case and to be 0.736" for the without-sand case. The 0.70" was, as claimed by the licensee, used for conservatism and the 0.736" is the projected thickness at the start of fuel cycle 14R. The same thicknesses of the shell above the sand region were used for both cases. For the with-sand case, an analysis of the drywell with the original nominal wall thicknesses was made to check the shell stresses with the allowable values established for the re-analyses.

The licensee used the same load combinations as specified in Oyster Creek's final design safety analysis report (FDSAR) for the re-analyses. The licensee made a comparison of the load combinations and corresponding allowable stress limits using the SRP section 3.8.2 and concluded they are comparable.

The results of the re-analyses indicated that the governing thicknesses are in the upper sphere and the cylinder where the calculated primary membrane stresses are respectively 20,360 psi and 19,850 psi vs. the allowable stress value of 19,300 psi. There is basically no difference, in the calculated stresses at these levels, between the with and without sand cases. This should be expected, because in a steel shell structure the local effect or the edge effect is damped in a very short distance. The stresses calculated exceed the allowable by 3% to 6%, and such exceedance is actually limited to the corroded area as obtained from UT measurements. However, in order to perform the axisymmetric analysis and analysis of the pie slice model, uniform thicknesses were assumed for each section of the drywell. Therefore, the calculated over-stresses may represent only stresses at the corroded areas and the stresses for areas beyond the corroded areas are less and would most likely be within the allowable as indicated in results of the analyses for nominal thicknesses. The diagram in Ref. 6 indicated such a condition. It is to be noted that the stresses for the corroded areas were obtained by multiplying the stresses for nominal thicknesses by the ratios between the corroded and nominal thicknesses.

The buckling analyses of the drywell were performed in accordance with ASME Code Case N-284. The analyses were done on the 36° pie slice model for both with-sand and without-sand cases. Except in the sand cushion area where a shell thickness of 0.7" for the with-sand

case and a shell thickness of 0.736" for the without-sand case were used, nominal shell thicknesses were considered for other sections. The load combinations which are critical to buckling were identified as those involving refueling and post accident conditions. By applying a factor of safety of 2 and 1.67 for the load combinations involving refueling and the post-accident conditions respectively, the licensee established for both cases the allowable buckling stresses which are obtained after being modified by capacity and plasticity reduction factors. It is found that the without-sand, case for the post-accident condition is most limiting in terms of buckling with a margin of 14%. The staff and its BNL consultants concur with the licensee's conclusion that the Oyster Creek drywell has adequate margin against buckling with no sand support for an assumed sandbed region shell thickness of 0.736 inch.

A copy of BNL's technical evaluation report is attached to this SER.

III. CONCLUSION

With the assistance of consultants from BNL, the staff has reviewed and evaluated the responses to the staff's concerns and the detailed re-analyses of the drywell for the with-sand and without-sand cases. The reanalyses by the licensee indicated that the corroded drywell meets the requirements for containment vessels as contained in ASME Section III Subsection NE through summer 1977 addenda. This code was adopted in the Mark I containment program. The staff agrees with the licensee's justification of using the above mentioned code requirements with one exception, the use of 1.1 Smc throughout the drywell shell in the criteria for stress analyses. It is the staff's position that the primary membrane stress limit of 1.1 Smc not be used indiscriminately throughout the drywell. The staff accepted the licensee's reanalyses on the assumption that the corroded areas are highly localized as indicated by the licensee's UT measurements. The stresses obtained for the case of reduced thickness can only be interpreted to represent those in the corroded areas and their adjacent regions of the drywell shell. In view of these observations, it is essential that the licensee perform UT thickness measurements at refueling outages and at outages of opportunity for the life of the plant. The measurements should cover not only areas previously inspected but also areas which have never been inspected so as to confirm that the thicknesses of the corroded areas are as projected and

the corroded areas are localized. Both of these assumptions are the bases of the reanalyses and the staff acceptance of the reanalysis results.

References:

1. "An ASME Section VIII Evaluation of the Oyster Creek Drywell Part 1, Stress Analysis", GE Report No. 9-1 DRF #00664 November 1990, prepared for GPUN (with sand).

2. "Justification for use of Section III, Subsection NE, Guidance in Evaluating the Oyster Creek Drywell" TR-7377-1, Teledyne Engineering Services, November 1990 (Appendix A to Reference 1).

3. "An ASME Section VIII evaluation of the Oyster Creek Drywell, Part 2, Stability Analysis", GE Report No. 9-2 DRF #00664, Rev. O, & Rev. 1. November 1990, prepared for GPUN (with sand).

4. "An ASME Section VIII Evaluation of Oyster Creek Drywell for without sand case, Part I, stress analysis," GE Report No. 9-3 DRF #00664, Rev. O, February 1991. Prepared for GPUN.

5. "An ASME Section VIII Evaluation of Osyter Creek Drywell, for without sand case, Part 2 Stability Analysis", GE Report No. 9-4, DRF #00664 Rev. O, Rev. 1 November 1990, prepared for GPUN.

6. Diagram attached to a letter from J. C. Devine Jr. of GPUN to NRC dated January 17, 1992 (C321-92-2020, 5000-92-2094).

SALP INPUT

FACILITY NAME: Oyster Creek Nuclear Generating Station

LICENSEE: GPU Nuclear Corporation

SUMMARY OF REVIEW

Since the discovery of corrosion in the sand cushion area of the drywell, the licensee has performed UT thickness measurements at outage of opportunity and at refueling outages from the results of the UT measurements it can be concluded that corrosion is still continuing in view of this, the licensee has considered sand removal to be an important element in its program to eliminate the corrosion threat to the drywell integrity. Since removal of the sand may affect the behavior of the drywell, the licensee had General Electric performed stress and stability analyses of the drywell for both with and without sand conditions taking into consideration the reduction in thickness in the sand cushion region. The criteria for the re-analyses are based on ASME Section VI Code Subsection NE. The use of subsection NE was examined and justified by the licensee's consultant from Teledyne Engineering
Services. The staff with the assistance of consultants from Brookhaven National Laboratory reviewed the reanalyses and the criteria used and found them to be acceptable.

NARRATIVE DISCUSSION OF LICENSEE PERFORMANCE - FUNCTIONAL AREAS ENGINEERING/TECHNICAL SUPPORT

Since the discovery of the corrosion of the drywell, the licensee has been working diligently to monitor the state of the corrosion, to stop the source of leakage and to eliminate further aggravation. Even though in the review process differing opinion and disagreement with staff's position arose, the licensee has been co-operative and forthcoming in striving to resolve staff's concerns.

TECHNICAL EVALUATION REPORT

ON

STRUCTURAL ANALYSES OF THE CORRODED OYSTER CREEK STEEL DRYWELL

1. Introduction

An inspection of the steel drywell at the Oyster Creek Nuclear Generating Station in November 1986 revealed that some degradation due to corrosion had occurred in the sandbed region of the shell. Subsequent inspections also identified thickness degradations in the upper spherical and cylindrical sections of the drywell. The licensee, GPU Nuclear Corporation, has performed structural analyses to demonstrate the integrity of the drywell for projected corroded conditions that may exist at the start of the fourteenth refueling outage (14R). This outage is expected to start in October 1992. In an attempt to arrest the corrosion, the licensee plans to remove the sand from the sandbed region. Consequently, they have submitted structural analyses of the drywell both with and without sand for drywell wall thicknesses projected to exist at the start of 14R outage.

2. Summary of Licensee's Analyses

The analyses performed by the licensee utilized the drywell wall thicknesses summarized in Table 1.

Table 1
Drywell Wall Thicknesses

Drywell Region	As-Designed Thicknesses (in.)	Projected 95% Confidence 14R Thicknesses (in.)
Cylindrical Region	0.640	0.619
Knuckle	2.5625*	2.5625*
Upper Spherical Region	0.722	0.677
Middle Spherical Region	0.770	0.723
Lower Spherical Region Except Sand Bed Area	1.154	1.154
Sand Bed Region	1.154	0.736

*NOTE: Table 2-1 of both References 1 and 3 indicates that the knuckle thickness is 2.625". This appears to be a mistake since the knuckle thickness is shown to be 2-9/16" in Figure 1-1 of the same report.

The stress analysis for the "with sand" case is described in Reference 1. For this analysis the licensee utilized the as-designed thicknesses, except for the sandbed region where a thickness of 0.70" was used. The stress results were obtained from a finite element analysis which utilized axisymmetric solid elements and the ANSYS computer program. Later, the stress results were scaled to address the local thinning in areas other than the sandbed region (the projected 95% confidence 14R thicknesses in Table 1). The loads and load combinations considered in the analysis are based on the FSAR Primary Containment Design Report and the 1964 Technical Specification for the Containment. Appendix E of Reference 1 compares the load combinations considered in the analysis with those given in Section 3.8.2 of the NRC Standard Review Plan, Rev. 1, July 1981.

The stress analysis for the "without sand" case is described in Reference 3. For this analysis the licensee also utilized the as-designed thicknesses, except for the sandbed region where a thickness of 0.736" was used. In this case, two finite element models, an axisymmetric and a 36° pie slice model, were used. The axisymmetric model is essentially the same as that used in Reference 1; however, the elements representing the sand stiffness were removed. This model was used to determine the seismic and thermal stresses. The pie slice model was used to determine the dead weight and pressure stresses, as well as the stresses for load combinations. The pie slice model included the effects of the vent pipes and the reinforcing ring in the drywell shell in the vicinity of each vent pipe. The drywell and vent shell were modeled using 3-dimensional elastic-plastic quadrilateral shell elements. At a distance of 76 inches from the drywell shell, beam elements were used to model the remainder of the ventline. The loads and load combinations are the same as those considered in Reference 1.

The code of record for the Oyster Creek drywell is the 1962 Edition of the ASME Code, Section VIII with Addenda to Winter 1963, and Code Cases 1270N-5, 1271N and 1272N-5. The licensee utilized these criteria in evaluating the stresses in the drywell, but also utilized guidance from the NRC Standard Review Plan with regard to allowable stresses for service level C and the post-accident condition. The licensee also used guidance from Subsection NE of Section III of the ASME Code in order tc justify the use of a limit of $1.1S_{sc}$ in evaluating the general membrane stresses in areas of the drywell where reduced thicknesses are specified. Based on these criteria the licensee has concluded that the stresses in the drywell shell are within code allowable limits for both the "with sand" and "without sand" cases.

The licensee also performed stability analyses of the drywell for both the "with sand" case (Reference 2) and the "without sand" case (Reference 4). For the "with sand" case the licensee utilized the as-designed thicknesses shown in Table 1, except in the sandbed region where a thickness of 0.700 inch was used. For the "without

sand" case the same thicknesses were used , except in the sandbed region where a thickness of 0.736 inch was used. The buckling capability of the drywell for both the "with sand" and "without sand" cases was evaluated by using the 36° pie slice finite element model discussed above. For the "with sand" case spring elements were used in the sandbed region to model the sand support. For the "without sand" case these spring elements were removed. The most limiting load combinations which result in the highest compressive stresses in the sandbed region were considered for the buckling analysis. These are the refueling condition (Dead Weight + Live Load + Refueling Water Weight + External Pressure + Seismic) and the post-accident condition (Dead Weight + Live Load + Hydrostatic Pressure for Flooded Drywell + External Pressure + Seismic).

The buckling evaluations performed by the licensee follow the methodology described in ASME Code Case N-284, "Metal Containment Shell Buckling Design Methods, Section III, Class MC", Approved August 25, 1980. The theoretical elastic buckling stress is calculated by analyzing the three dimensional finite element model discussed above. Then the theoretical buckling stress is modified by capacity and plasticity reduction factors. The allowable compressive stress is obtained by dividing the calculated buckling stress by a factor of safety. In accordance with Code Case N-284 the licensee used a factor of safety of 2.0 for the refueling condition and 1.67 for the post-accident condition. The capacity reduction factors were also modified to take into account the effects of hoop stress. Originally the licensee based the hoop stress modification on data related to the axial compressive strength of cylinders (References 2 and 4). Later the licensee revised the approach based on a review of spherical shell buckling data and recalculated the drywell buckling capacities for both the "with sand" and "without sand" cases (Reference 8). For the "with sand" case, the licensee reports a margin above the allowable compressive stress of 47% for the refueling condition and 40% for the post-accident condition. For the "without sand" case, the licensee reports margins of 24.5% for the refueling condition and 14% for the post-accident condition.

3. Evaluation of Licensee's Approach

The analyses performed by the licensee as summarized in Section 2 and discussed more fully in References 1 through 4 have been reviewed and found to provide an acceptable approach for demonstrating the structural integrity of the corroded Oyster Creek drywell. The finite element analyses performed for both the stress and stability evaluations are consistent with industry practice. Except for the use of a limit of $1.1S_{ac}$ in evaluating the general membrane stress in areas of reduced drywell thickness, the loads, load combinations and acceptance criteria used by the licensee are consistent with the guidance given in Section 3.8.2 of the NRC Standard Review Plan, Rev. 1, July 1981. To further support their position, the licensee has provided two appendices to Reference 1.

Appendix A provides a detailed justification for the use of Section III, Subsection NE as guidance in evaluating the Oyster Creek drywell. Appendix E compares the load combinations given in the Final Design Safety Analysis Report (FDSAR) with the load combinations given in SRP 3.8.2 and demonstrates that the load combinations used in the analysis envelop those given in the SRP.

In the areas of the drywell where reduced thicknesses are specified, the licensee has used a limit of $1.1S_{ac}$ to evaluate the general membrane stresses. In support of this position the licensee has cited the provisions of NE-3213.1 of the ASME Code concerning local primary membrane stresses. In effect, the licensee's criteria would treat corroded or degraded areas as discontinuities. For such considerations the code places no limit on the extent of the region in which the membrane stress exceeds $1.0S_{ac}$ but is less than $1.1S_{ac}$. In support of this position the licensee has provided the opinion of Dr. W.E. Cooper, a well known expert on the development of the ASME Code. Dr. Cooper concluded that "given a design which satisfies the general Code intent, as the Oyster Creek drywell does as originally constructed, it is not a violation of Subsection NE requirements for the membrane stress to be between $1.0S_{ac}$ and $1.1S_{ac}$ over significant distances". The licensee has also cited the provisions of IWE-3519.3 which accepts up to a 10% reduction in the thickness of the original base metal.

The licensee's position has merit, but great caution must be exercised to assure that such a position is not applied indiscriminately. In the case of the Oyster Creek drywell the licensee has concluded that "there are very few locations where the calculated stress intensities for design basis conditions, would exceed $1.0S_{ac}$, and in these cases only slightly" (Reference 7). The licensee has provided additional information in Reference 9 to support this conclusion. Based on the information provided by the licensee which demonstrates that the use of the $1.1S_{ac}$ criteria is limited to localized areas, it is concluded that the Oyster Creek drywell meets the intent of the ASME Code.

As discussed in Section 2, the capacity reduction factors used in the buckling analysis are modified to take into account the beneficial effects of tensile hoop stress. As a result of a question raised during the review regarding this matter, the licensee submitted additional information in Reference 5 to support the approach. This information included a report prepared by C.D. Miller entitled "Effects of Internal Pressure on Axial Compression Strength of Cylinders" (CBI Technical Report No. 022891, February 1991). The report presented a design equation which was the lower bound of the test data included in the report. It also demonstrated that the equation used in References 2 and 4 was conservative relative to the proposed design equation. The report presented further arguments that the rules determined for axially compressed cylinders subjected to internal pressure can be applied to spheres. Subsequently the licensee has submitted Reference 8, which

indicates that the original approach was not conservative with regard to its application to spherical shapes and recommends a new equation. However, the documentation supporting the use of this equation is not included in Reference 8, but apparently is contained in a referenced report prepared by C.D. Miller entitled "Evaluation of Stability Analysis Methods Used for the Oyster Creek Drywell" (CBI Technical Report Prepared for GPU Nuclear Corporation, September 1991). This report was subsequently submitted and reviewed by the NRC staff. As discussed in Section 2, the use of the revised equation still results in calculated capacities in compliance with the ASME Code provisions; however, the margins beyond those capacities are reduced from those reported by References 2 and 4.

It is noted that the licensee may have "double-counted" the effects of hoop tension, since the theoretical elastic instability stress was calculated from the finite element model using the ANSYS Code. The elastic instability stress calculated by the ANSYS Code may have already taken into account the effects of hoop tensile stress. However, by comparing the theoretical elastic instability stress and the corresponding circumferential stress predicted by the licensee for the refueling and post-accident cases, it appears that the effect of hoop tension in the ANSYS calculations is small and there is sufficient margin in the results to compensate for the potential "double-counting". Furthermore, it is judged that there is sufficient capacity in the drywell to preclude a significant buckling failure under the postulated loading conditions since the licensee's calculations: (a) incorporate factors of safety of 1.67 to 2.0, depending upon the load condition, and (b) utilize a conservative assumption by considering the shell wall thickness to be severely reduced for the full circumference of the drywell throughout the sandbed region.

During the course of the review of the licensee's submittals, a number of other issues were raised regarding the approach. These included: (a) the basis and method of calculating the projected drywell thicknesses, (b) the scaling of the calculated stresses for the nominal thickness case by the thickness ratio, (c) the effect of stress concentrations due to the change of thickness, (d) monitoring of the drywell temperature, (e) sensitivity of stresses due to variations in the sand spring stiffness, (f) sensitivity of the plasticity reduction factor in the buckling analysis, (g) use of the 2 psi design basis external pressure in the buckling analysis, (h) effect of the large displacement method, (i) the treatment of the large concentrated loads considered in the analysis, and (j) the method of applying the seismic loads to the pie slice model. These issues were adequately addressed by the additional information provided by the licensee in References 5 and 6.

4. Conclusions

The licensee has demonstrated that the calculated stresses in the Oyster Creek drywell (both with and without the sandbed), as a result of the postulated loading conditions, meet the intent of the ASME Code for projected corroded conditions that may exist at the start of the fourteenth refueling outage. However, if the actual thickness in the sandbed region at 14R is close to the projected thickness of 0.736", there may not be adequate margin left for further corrosion through continued operation unless it is demonstrated that removal of sand will completely stop further thickness reductions. The licensee has also demonstrated that there is sufficient margin in the drywell design (both with and without the sandbed) to preclude a buckling failure under the postulated loading conditions.

It should be recognized that the conclusions reached by the licensee have been accepted for this particular application with due regard to all the assumptions made in the analysis and the available margins. The use of the $1.1S_m$ criteria for evaluating general membrane stress in corroded or degraded areas should be investigated further by the NRC staff and the ASME Code Committee and appropriate bounds established before it is accepted for general use. The licensee's buckling criteria regarding the modification of capacity reduction factors for tensile hoop stress and the determination of plasticity reduction factors should also be investigated in a similar manner.

5. References

1. GE Report Index No. 9-1, "An ASME Section VIII Evaluation of the Oyster Creek Drywell - Part 1 - Stress Analysis", November 1990.

2. GE Report Index No. 9-2, "An ASME Section VIII Evaluation of the Oyster Creek Drywell - Part 2 - Stability Analysis," November 1990.

3. GE Report Index No. 9-3, "An ASME Section VIII Evaluation of the Oyster Creek Drywell for Without Sand Case - Part 1 - Stress Analysis," February 1991.

4. GE Report Index No. 9-4, "An ASME Section VIII Evaluation of the Oyster Creek Drywell for Without Sand Case - Part 2 - Stability Analysis," February 1991.

5. GPU Nuclear letter dated March 20, 1991, "Oyster Creek Drywell Containment."

6. GPU Nuclear letter dated June 20, 1991, "Oyster Creek Drywell Containment".

7. GPU Nuclear letter dated October 9, 1991, "Oyster Creek Drywell Containment"

8. GPU Nuclear letter dated January 16, 1992, "Oyster Creek Drywell Containment".

9. GPU Nuclear letter dated January 17, 1992, "Oyster Creek Drywell Containment".

Exhibit 56

Letter from Alexander W. Dromerick to John J. Barton
(April 24, 1992)

April 24, 1992

Docket No. 50-219

Distribution:
Docket File
NRC & Local PDRs
PD I-4 Plant
SVarga
JCalvo
SNorris
ADromerick
OGC
CPTan
ACRS (10)
CWHehl, RI

Mr. John J. Barton
Vice President and Director
GPU Nuclear Corporation
Oyster Creek Nuclear Generating Station
Post Office Box 388
Forked River, New Jersey 08731

Dear Mr. Barton:

SUBJECT: EVALUATION REPORT ON STRUCTURAL INTEGRITY OF THE OYSTER CREEK DRYWELL (TAC NO. M79166)

The staff has completed the review and evaluation of the stress analyses and stability analyses reports of the corroded drywell with and without the sand bed. Our evaluation report is contained in the enclosure. GPUN used the analyses to justify the removal of the sand from the sand bed region. Even though the staff, with the assistance of consultants from Brookhaven National Laboratory (BNL), concurred with GPUN's conclusion that the drywell meets the ASME Section III Subsection NE requirements, it is essential that GPUN continue UT thickness measurements at refueling outages and at outages of opportunity for the life of the plant. The measurements should cover not only areas previously inspected but also accessible areas which have never been inspected so as to confirm that the thickness of the corroded areas are as projected and the corroded areas are localized.

We request that you respond within 30 days of receipt of this letter indicating your intent to comply with the above requirements as discussed in the Safety Evaluation.

The requirements of this letter affect fewer than 10 respondents, and therefore, are not subject to Office of Management and Budget review under P.L. 96-511.

Sincerely,

/s/

Alexander W. Dromerick, Sr. Project Manager
Project Directorate I-4
Division of Reactor Projects - I/II
Office of Nuclear Reactor Regulation

Enclosure:
As stated

cc w/enclosure:
See next page

OFFICIAL RECORD COPY Document Name: M79166

OFC	:LA:PDI-4	:PM:PDI-4	:D:PDI-4	:	:	:
NAME	:SNorris	:ADromerick:cn	:	:	:	:
DATE	:4/24/92	:4/24/92	:4/24/92	:	:	:

UNITED STATES
NUCLEAR REGULATORY COMMISSION
WASHINGTON, D. C. 20555

SAFETY EVALUATION BY THE OFFICE OF NUCLEAR REACTOR REGULATION

DRYWELL STRUCTURAL INTEGRITY

OYSTER CREEK NUCLEAR GENERATING STATION

GPU NUCLEAR CORPORATION

DOCKET NO. 50-219

I. INTRODUCTION

In 1986 the steel drywell at Oyster Creek Nuclear Generating Station (OCNGS) was found to be extensively corroded in the area of the shell which is in contact with the sand cushion around the bottom of the drywell. Since then GPU Nuclear Corporation, (GPUN, the licensee of OCNGS), has instituted a program of periodic inspection of the drywell shell sand cushion area through ultrasonic testing (UT) thickness measurements. The inspection has been extended to other areas of the drywell and some areas above the sand cushion have been found to be corroded also. From the UT thickness measurements, one can conclude that corrosion of the drywell shell in the sand cushion area is continuing. In an attempt to eliminate corrosion or reduce the corrosion rate, the licensee tried cathodic protection and found it to be of no avail. An examination of the results of consecutive UT measurements, confirmed that the corrosion is continuing. There is concern that the structural integrity of the drywell cannot be assured. Since the root cause of the corrosion in the sand cushion area is the presence of water in the sand, the licensee has considered sand removal to be an important element in its program to eliminate the corrosion threat to the drywell integrity.

In the program, the licensee first established the analysis criteria and then performed the analyses of the drywell for its structural adequacy with and without the presence of the sand. The licensee performed stress analyses and stability analyses for both with and without the sand cases and concluded the drywell with or without the sand to be in compliance with the criteria established for the reevaluation. It is to be noted that the original purpose of the sand cushion is to provide a smooth transition of stresses from the fixed portion to the free-standing portion of the steel drywell.

II. EVALUATION

The staff with the assistance of consultants from Brookhaven National Laboratory (BNL) has reviewed and evaluated the information (Refs. 1,2,3,4,5) provided by the licensee.

1. Re-Analysis Criteria

The drywell was originally designed and constructed to the requirements of ASME Section VIII code and applicable code cases, with a contract date of July 1, 1964. The Section VIII Code requirements for nuclear containment vessels at that time were less detailed than at any subsequent date. The evolution of the ASME Section III Code for metal containments and its relation with ASME Section VIII Code were reviewed and evaluated by Teledyne Engineering Services (TES). The evaluation criteria used are based on ASME Section III Subsection NE Code through the 1977 summer addenda. The reason for the use of the Code of this vintage is that it was used in the Mark I containment program to evaluate the steel torus for hydrodynamic loads and that the current ASME Section III Subsection NE Code is closely related to that version. The following are TES's findings relevant to Oyster Creek application:

a) The steel material for the drywell is A-212, grade B, Firebox Quality (Section VIII), but it is redesignated as SA-516 grade in Section III.

b) The relation between the allowable stress (S) in Section VIII and the stress intensity (Smc) in Section III for metal containment is 1.1S = Smc.

c) Categorization of stresses into general primary membrane, general bending and local primary membrane stresses and membrane plus bending stresses is adopted as in Subsection NF.

d) The effect of a locally stressed region on the containment shell is considered in accordance with NE-3213.10.

In addition to ASME Section III Subsection NE Code, the licensee has also invoked ASME Section XI IWE Code to demonstrate the adequacy of the Oyster Creek drywell. IWE-3519.3 and IWE-3122.4 state that it is acceptable if either the thickness of the base metal is reduced by no more than 10% of the normal plate thickness or the reduced thickness can be shown by analysis to satisfy the requirements of the design specification.

The staff has reviewed the licensee's adoption of ASME Section III Subsection NE and Section XI Subsection IWE in its evaluation of the structural adequacy of the corroded Oyster Creek drywell, and has found it to be generally reasonable and acceptable.

By adopting the Subsection NE criteria, the licensee has treated the corroded areas as discontinuities per NE-3213.10, which was originally meant for change in thicknesses, supports, and penetrations. These discontinuities are highly localized and should be designed so that their presence will have no effect on the overall behavior of the containment shell. NE-3213.10 defines clearly the

level of stress intensity and the extent of the discontinuity to be considered localized. A stress intensity limit of 1.1 Smc is specified at the boundary of the region within which the membrane stress can be higher than 1.1 Smc. The region where the stress intensity varies from 1.1 Smc to 1.0 Smc is not defined in the Code because of the fact that it varies with the loading. In view of this, the licensee rationalized that the 1.1 Smc can be applied beyond the region defined by NE-3213.10 for localized discontinuity without any restriction throughout the drywell. The staff disagreed with the licensee's interpretation of the Code. The staff pointed out that for Oyster Creek drywell, stresses due to internal pressure should be used as the criterion to establish such a region. The interpretation of Section XI Subsections IWE-3519.3 and IWE-3122.4 can be made only in the same context. It is staff's position that the primary membrane stress limit of 1.1 Smc not be used indiscriminately throughout the drywell.

In order to use NE-3213.10 to consider the corroded area as a localized discontinuity, the extent of the reduction in thickness due to corrosion should be reasonably known. UT thickness measurements are highly localized; however, from the numerous measurements so far made on the Oyster Creek drywell, one can have a general idea of the overall corroded condition of the drywell shell and it is possible to judiciously apply the established re-analysis criteria.

2. Re-analyses

The re-analyses were made by General Electric Company for the licensee, one reanalysis considered the sand present and the other considered the drywell without the sand. Each re-analysis comprises a stress analysis and stability analysis. Two finite element models, one axisymmetric and another a 36° pie slice model were used for the stress analysis. The ANSYS computer program was used to perform the analyses. The axisymmetric model was used to determine the stresses for the seismic and the thermal gradient loads. The pie slice model was used for dead weight and pressure loads. The pie slice model includes the vent pipe and the reinforcing ring, and was also used for buckling analysis. The same models were used for the cases with and without sand, except that in the former, the stiffness of sand in contact with the steel shell was considered. The shell thickness in the sand region was assumed to be 0.700" for the with-sand case and to be 0.736" for the without-sand case. The 0.70" was, as claimed by the licensee, used for conservatism and the 0.736" is the projected thickness at the start of fuel cycle 14R. The same thicknesses of the shell above the sand region were used for both cases. For the with-sand case, an analysis of the drywell with the original nominal wall thicknesses was made to check the shell stresses with the allowable values established for the re-analyses.

The licensee used the same load combinations as specified in Oyster Creek's final design safety analysis report (FDSAR) for the re-analyses. The licensee made a comparison of the load combinations and corresponding allowable stress

limits using the Standard Review Plan (SRP) section 3.8.2 and concluded they are comparable.

The results of the re-analyses indicated that the governing thicknesses are in the upper sphere and the cylinder where the calculated primary membrane stresses are respectively 20,360 psi and 19,850 psi vs. the allowable stress value of 19,300 psi. There is basically no difference, in the calculated stresses at these levels, between the with and without sand cases. This should be expected, because in a steel shell structure the local effect or the edge effect is damped in a very short distance. The stresses calculated exceed the allowable by 3% to 6%, and such exceedance is actually limited to the corroded area as obtained from UT measurements. However, in order to perform the axisymmetric analysis and analysis of the pie slice model, uniform thicknesses were assumed for each section of the drywell. Therefore, the calculated over-stresses may represent only stresses at the corroded areas and the stresses for areas beyond the corroded areas are less and would most likely be within the allowable as indicated in results of the analyses for nominal thicknesses. The diagram in Ref. 6 indicated such a condition. It is to be noted that the stresses for the corroded areas were obtained by multiplying the stresses for nominal thicknesses by the ratios between the corroded and nominal thicknesses.

The buckling analyses of the drywell were performed in accordance with ASME Code Case N-284. The analyses were done on the 36° pie slice model for both with-sand and without-sand cases. Except in the sand cushion area where a shell thickness of 0.7" for the with-sand case and a shell thickness of 0.736" for the without-sand case were used, nominal shell thicknesses were considered for other sections. The load combinations which are critical to buckling were identified as those involving refueling and post accident conditions. By applying a factor of safety of 2 and 1.67 for the load combinations involving refueling and the post-accident conditions respectively, the licensee established for both cases the allowable buckling stresses which are obtained after being modified by capacity and plasticity reduction factors. It is found that the without-sand, case for the post-accident condition is most limiting in terms of buckling with a margin of 14%. The staff and its Brookhaven National Laboratory (BNL) consultants concur with the licensee's conclusion that the Oyster Creek drywell has adequate margin against buckling with no sand support for an assumed sandbed region shell thickness of 0.736 inch.

A copy of BNL's technical evaluation report is attached to this safety evaluation.

III. CONCLUSION

With the assistance of consultants from BNL, the staff has reviewed and evaluated the responses to the staff's concerns and the detailed re-analyses of the drywell for the with-sand and without-sand cases. The reanalyses by the licensee indicated that the corroded drywell meets the requirements for

containment vessels as contained in ASME Section III Subsection NE through summer 1977 addenda. This Code was adopted in the Mark I containment program. The staff agrees with the licensee's justification of using the above mentioned Code requirements with one exception, the use of 1.1 Smc throughout the drywell shell in the criteria for stress analyses. It is the staff's position that the primary membrane stress limit of 1.1 Smc not be used indiscriminately throughout the drywell. The staff accepted the licensee's reanalyses on the assumption that the corroded areas are highly localized as indicated by the licensee's UT measurements. The stresses obtained for the case of reduced thickness can only be interpreted to represent those in the corroded areas and their adjacent regions of the drywell shell. In view of these observations, it is essential that the licensee perform UT thickness measurements at refueling outages and at outages of opportunity for the life of the plant. The measurements should cover not only areas previously inspected but also accessible areas which have never been inspected so as to confirm that the thicknesses of the corroded areas are as projected and the corroded areas are localized. Both of these assumptions are the bases of the reanalyses and the staff acceptance of the reanalysis results.

References:

1. "An ASME Section VIII Evaluation of the Oyster Creek Drywell Part I, Stress Analysis" GE Report No. 9-1 DRF #00664 November 1990, prepared for GPUN (with sand).

2. "Justification for use of Section III, Subsection NE, Guidance in Evaluating the Oyster Creek Drywell" TR-7377-1, Teledyne Engineering Services, November 1990 (Appendix A to Reference 1).

3. "An ASME Section VIII evaluation of the Oyster Creek Drywell, Part 2, Stability Analysis" GE Report No. 9-2 DRF #00664, Rev. 0, & Rev. 1. November 1990, prepared for GPUN (with sand).

4. "An ASME Section VIII Evaluation of Oyster Creek Drywell for without sand case, Part I, stress analysis" GE Report No. 9-3 DRF #00664, Rev. 0, February 1991. Prepared for GPUN.

5. "An ASME Section VIII Evaluation of Oyster Creek Drywell, for without sand case, Part 2 Stability Analysis" GE Report No. 9-4, DRF #00664 Rev. 0, Rev. 1 November 1990, prepared for GPUN.

6. Diagram attached to a letter from J. C. Devine Jr. of GPUN to NRC dated January 17, 1992 (C321-92-2020, 5000-92-2094).

Principal Contributor: C.P. Tan

Date: April 24, 1992

Attachment:
BNL Technical Evaluation Report

Exhibit 57

Letter from J.C. DeVine to NRC
(May 26, 1992)

GPU Nuclear Corporation
One Upper Pond Road
Parsippany, New Jersey 07054
201-316-7000
TELEX 136-482
Writer's Direct Dial Number:

May 26, 1992
5000-92-3026
C321-92-2163

U.S. Nuclear Regulatory Commission
Attn: Document Control Desk
Washington, DC 20555

Gentlemen:

Subject: Oyster Creek Nuclear Generating Station (OCNGS)
Docket No. 50-219
Facility Operating License No. DPR-16
Oyster Creek Drywell Containment

References: (1) NRC Letter dated April 24, 1992, "Evaluation Report on Structural Integrity of the Oyster Creek Drywell (TAC No. M79166)."

(2) GPUN Letter C320-92-264 dated November 26, 1990, "Oyster Creek Drywell Containment."

In response to the Reference 1 request, GPU Nuclear commits to continue taking UT drywell measurements at refueling outages and at other outages of opportunity. The measurements will be at areas previously inspected and also at other accessible areas not previously inspected. Drywell thickness measurements will continue for the life of the plant.

The following is our current plan for Oyster Creek drywell UT thickness measurements.

(1) During the 14R outage, GPU Nuclear will take UT thickness measurements in the drywell sandbed region, from the torus room side (outside the drywell), at shell locations not readily accessible from inside the drywell. These are areas not previously inspected. The specific locations selected for inspection will be identified once we have direct access to the sandbed region.

Assuming that these measurements confirm that we have bounded the corrosion problem with our current inspection locations, we currently do not plan to make repeat measurements at these specific locations.

(2) Now through the 15R outage, GPU Nuclear will continue taking UT thickness measurements in accordance with the priority method described in Reference 2, Attachment I, "GPUN Specification IS-328227-004, Functional Requirements for Drywell Containment Vessel Thickness Examination".

(3) After the 15R outage, GPU Nuclear will assess the condition of the drywell by evaluating the then current UT thickness measurements and will formulate an extended inspection plan. The plan will identify measurement locations including frequency of inspection for the remaining life of the plant.

If you have any questions or comments on this submittal or the overall drywell corrosion program, please contact Mr. Michael Laggart, Manager, Corporate Nuclear Licensing at (201) 316-7968.

Very truly yours,

G. P. Bond

for J. C. DeVine, Jr.
Vice President and Director
Technical Functions

JCD/RZ/amk

cc: Administrator, Region 1
Senior Resident Inspector
Oyster Creek NRC Project Manager

Exhibit 58

Letter from Alexander W. Dromerick to John J. Barton
(June 30, 1992)

Docket File

UNITED STATES
NUCLEAR REGULATORY COMMISSION
WASHINGTON, D.C. 20555

June 30, 1992

Docket No. 50-219

Mr. John J. Barton
Vice President and Director
GPU Nuclear Corporation
Oyster Creek Nuclear Generating Station
Post Office Box 388
Forked River, New Jersey 08731

Dear Mr. Barton:

SUBJECT: OYSTER CREEK DRYWELL CONTAINMENT (TAC NO. M79166)

In our letter of April 29, 1992, regarding Oyster Creek drywell containment, we requested that GPU Nuclear Corporation (GPUN), continue ultrasonic testing (UT) thickness measurements at refueling outages and at outages of opportunity for the life of the plant. The measurements should cover not only areas previously inspected but also accessible areas which have never been inspected so as to confirm that the thicknesses of the corroded areas are as projected and the corroded areas are localized. We also requested that you indicate your intent to comply with the above requirements as discussed in the Safety Evaluation.

In your letter of May 26, 1992, GPUN committed to continue taking UT drywell measurements at refueling outages and at other outages of opportunity. The measurements will be at areas previously inspected and also at other accessible areas not previously inspected. Drywell thickness measurements will continue for life.

You also indicated that the following is your current plan for Oyster Creek drywell UT thickness measurement.

(1) During the 14R outage, GPU Nuclear will take UT thickness measurements in the drywell sandbed region, from the torus room side (outside the drywell), at shell locations not readily accessible from inside the drywell. These are areas not previously inspected. The specific locations selected for inspection will be identified once GPU has direct access to the sandbed region.

Assuming that these measurements confirm that GPU has bounded the corrosion problem with current inspection locations, GPU does currently not plan to make repeat measurements at these specific locations.

(2) Now through the 15R outage, GPU Nuclear will continue taking UT thickness measurements in accordance with the priority method described in Reference 2, Attachment I, "GPUN Specification IS-328227-004, Functional Requirements for Drywell Containment Vessel Thickness Examination."

DFo1
1/

(3) After the 15R outage, GPU Nuclear will assess the condition of the drywell by evaluating the then current UT thickness measurements and will formulate an extended inspection plan. The plan will identify measurement locations including frequency of inspection for the remaining life of the plant.

We have reviewed the above information and find that your program commitments regarding UT inspection of the Oyster Creek drywell containment are acceptable. This closes TAC No. M79166.

Sincerely,

/s/

Alexander W. Dromerick, Sr. Project Manager
Project Directorate I-4
Division of Reactor Projects - I/II
Office of Nuclear Reactor Regulation

cc: See next page

Distribution:
Docket File
NRC & Local PDRs
PD I-4 Plant
SVarga
JCalvo
SNorris
ADromerick
OGC
GBagchi
RHermann
ACRS (10)
RBlough, RI

OFFICIAL RECORD COPY Document Name: M79166.INF

OFC	:LA:PDI-4	:PM:PDI-4	:BC:SGB	:BC:EMCB	:D:PDI-4	:	:
NAME	:SNorris	:ADromerick	:cn:GBagchi	:RHermann	:JStolz	:	:
DATE	:6/16/92	:6/16/92	:6/18/92	:6/21/92	:6/29/92	:	:

Exhibit 59

Letter from H.S. Mehta to Dr. Stephen Tumminelli
(December 11, 1992)

990-217

DEC 1 4 1992

December 11, 1992

To: Dr. Stephen Tumminelli
Manager, Engineering Mechanics
GPU Nuclear Corporation
1 Upper Pond Road
Parsippany, NJ 07054

Subject: Sandbed Local Thinning and Raising the Fixity Height Analyses (Line Items 1 and 2 in Contract # PC-0391407)

Dear Dr. Tumminelli:

The attached letter report documents the results of subject analyses. The original purchase order called for the analyses to be conducted on a spherical panel model rather than on the full pie slice model. However, the results are more useful when conducted on the full pie slice model since in that case no interpretation is required regarding the relationship between the spherical panel results and the pie slice model results. The pie slice model we have used in these studies has the refined mesh in the sandbed region.

A 3.5" PC Disk containing three ANSYS input files (0.636" case, 0.536" case and 1 foot wall case) is also enclosed with this letter. The detailed calculations have been filed in Chapter 10 of our Design Record File No. 00664.

This transmittal completes the scope of work identified in the subject PO. If you have any questions on the above item, please give me a call.

Sincerely,

H.S. Mehta, Principal Engineer
Materials Monitoring & Structural Analysis Services
Mail Code 747; Phone (408) 925-5029

Attachment: Letter Report

cc: D.K. Henrie (w/o Attach.)
J.M. Miller (w/o Attach.)
S. Ranganath (w/o Attach.)

HSMOC-57.wp

LETTER REPORT ON ADDITIONAL SANDBED REGION ANALYSES

1.0 SCOPE AND BACKGROUND

Structural Analyses of the Oyster Creek drywell assuming a degraded thickness of 0.736 inch in the sandbed region (and sand removed) were documented in GENE Report Numbers 9-3 and 9-4. A separate purchase order was issued (Contract # PC-0391407) to perform additional analyses. The PO listed the additional analyses under two categories: Line Item 001 and Line Item 002. This letter report documents the results of these analyses.

The additional analyses are the following:

(1) Investigate the effect on the buckling behavior of drywell from postulated local thinning in the sandbed region beyond the uniform projected thickness of 0.736" used in the above mentioned reports (Line Item 001).

(2) Determine the change in the drywell buckling margins when the fixity point at the bottom of the sandbed is moved upwards by $\approx$ 1 foot to simulate placement of concrete (Line Item 002).

The original PO called for the Line Item 001 analyses to be conducted on a spherical panel. The relative changes in the buckling load factors were to be assumed to be the same for the global pie slice model. However, the mesh refinement activity on the global pie slice model and the availability of work station, has given us the capability to conduct the same analyses on the global pie slice model itself, thus eliminating the uncertainties regarding the correlation between the panel model and the pie slice model.

All of the results reported in this report are based on the pie slice model with a refined mesh in the sandbed region.

2.0 LINE ITEM 001

Figure 1a shows the local thickness reductions modeled in the pie slice model. A locally thinned region of $\approx$ 6"x12" is modeled. The thickness of this region is 0.636" in one

case and 0.536" in the other case. The transition to the sandbed projected thickness of 0.736" occurs over a distance of 12" (4 elements).

The various thicknesses indicated in Figure 1a were incorporated in the pie slice model by defining new real constants for the elements involved. The buckling analyses conducted as a result of mesh refinement indicated that the refueling loading condition is the governing case from the point of view of ASME Code margins. Therefore, the stress and buckling analyses were conducted using the refueling condition loadings. The center of the thinned area was located close to the calculated maximum displacement point in the refueling condition buckling analyses with uniform thickness of 0.736 inch. Figure 1b shows the location of the thinned area in the pie slice model.

2.1 0.536 Inch Thickness Case

Figures 2 through 5 show the membrane meridional and circumferential stress distributions from the refueling condition loads. As expected, the tensile circumferential stress (Sx in element coordinate system) and the compressive meridional stress (Sy in element coordinate system) magnitudes in the thinned region are larger than those at the other edge of the model where the thickness is 0.736 inch. However, this is a local effect and the average meridional stress and the average circumferential stress is not expected to change significantly.

Figures 6 and 7 show the first buckling mode with the symmetric boundary conditions at both the edges of the model (sym-sym). This mode is clearly associated with the thinned region. The load factor value is 5.562. The second mode with the same boundary conditions is also associated with the thinned region. Figure 8 shows the buckled shape. The load factor value is 5.872.

Next, buckling analyses were conducted with the symmetric boundary conditions specified at the thinned edge and the asymmetric boundary conditions at the other edge (sym-asym). The load factor of the first mode for this case was 5.58. Figure 9 shows the buckling mode shape. It is clearly associated with the thinned region. Figure 10 shows the buckled mode shape with asymmetric boundary conditions at the both edges (asym-asym). As expected, the load factor for this case is considerably higher (7.037).

Thus, the load factor value of 5.562 is the lowest value obtained. The load factor for the same loading case (refueling condition) with a uniform thickness of 0.736" was 6.141. Thus, the load factor is predicted to change from 6.141 to 5.562 with the postulated thinning to 0.536".

2.2 0.636 Inch Thickness Case

Figures 11 through 14 show the membrane meridional and circumferential stress distributions from the refueling condition loads. As expected, the tensile circumferential stress (Sx in element coordinate system) and the compressive meridional stress (Sy in element coordinate system) magnitudes in the thinned region are larger than those at the other edge of the model where the thickness is 0.736 inch. However, this is a local effect and the average meridional stress and the average circumferential stress is not expected to change significantly.

Figures 15 and 16 show the first buckling mode with the symmetric boundary conditions at both the edges of the model (sym-sym). This mode is clearly associated with the thinned region. The load factor value is 5.91.

Next, buckling analysis was conducted with the symmetric boundary conditions specified at the thinned edge and the asymmetric boundary conditions at the other edge. The load factor of the first mode for this case was 5.945. Figure 17 shows the buckling mode shape. It is clearly associated with the thinned region. Based on the results of 0.536" case, the load factor for asym-asym case is expected to be considerably higher.

Thus, the load factor value of 5.91 is the lowest value obtained. The load factor for the same loading case (refueling condition) with a uniform thickness of 0.736" was 6.141. Thus, the load factor is predicted to change from 6.141 to 5.91 with the postulated thinning to 0.636".

2.3 Summary

The load factors for the postulated 0.536" and 0.636" thinning cases are 5.562 and 5.91, respectively. These values can be compared to 6.141 obtained for the case with a uniform sandbed thickness of 0.736 inch.

3.0 LINE ITEM 002

The objective of this task was to determine the change in the drywell buckling margins when the fixity point at the bottom of the sandbed is moved upwards by ≈ 1 foot to simulate placement of concrete. The elements in the sandbed region are approximately 3-inch square. Thus the nodes associated with the bottom four row of elements (nodes 1027 through 1271, Figure 18) were fixed in all directions.

The buckling analyses conducted as a result of mesh refinement indicated that the refueling loading condition is the governing case from the point of view of ASME Code margins. Therefore, the stress and buckling analyses were conducted using the refueling condition loadings. Figure 19 through 22 show the membrane meridional and circumferential stress distributions from the refueling condition loads. Figure 23 shows the calculated average values of meridional and circumferential stresses that are used in the buckling margin evaluation.

Figure 24 shows the first buckling mode with sym-sym boundary conditions. The load factor for this mode is 6.739. The load factor with asym-sym boundary conditions is 6.887 and the mode shape shown in Figure 25. It is clear that the sym-sym boundary condition gives the least load factor. Figure 26 shows the buckling margin calculation. It is seen that the buckling margin is 5.3% compared to 0% margin in the base case calculation.

To summarize, the load factor changes to 6.739 for the refueling condition when the fixity point at the bottom of the sandbed is moved upwards by ≈ 1 foot. This results in an excess margin of 5.3% above that required by the Code.

GPU Nuclear

Calculation Sheet

Subject	Calc No.	Rev. No.	Sheet No.
Oyster Creek Drywell			of

Originator	Date	Reviewed by	Date
M. Yekta	11/23/92		

Proposed Local Thining in the Refined Global Pie Slice

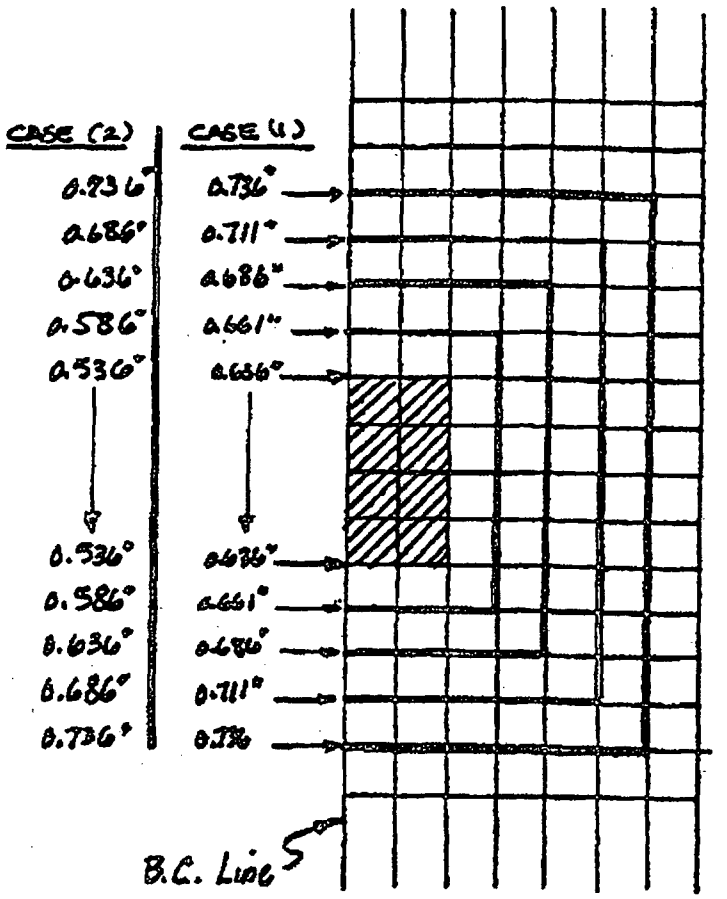

FIGURE 1a

FIGURE 1b

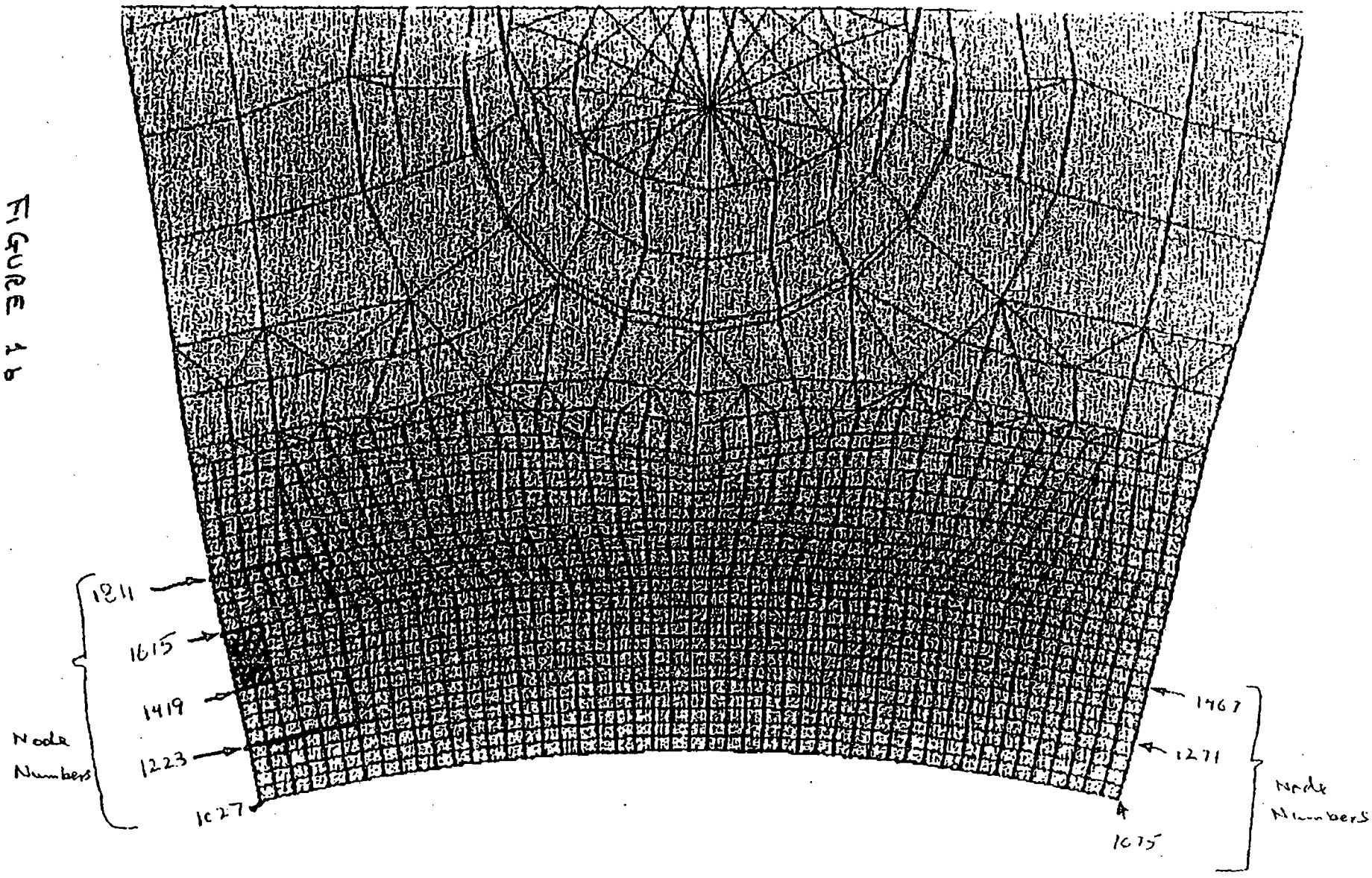

9726-3174

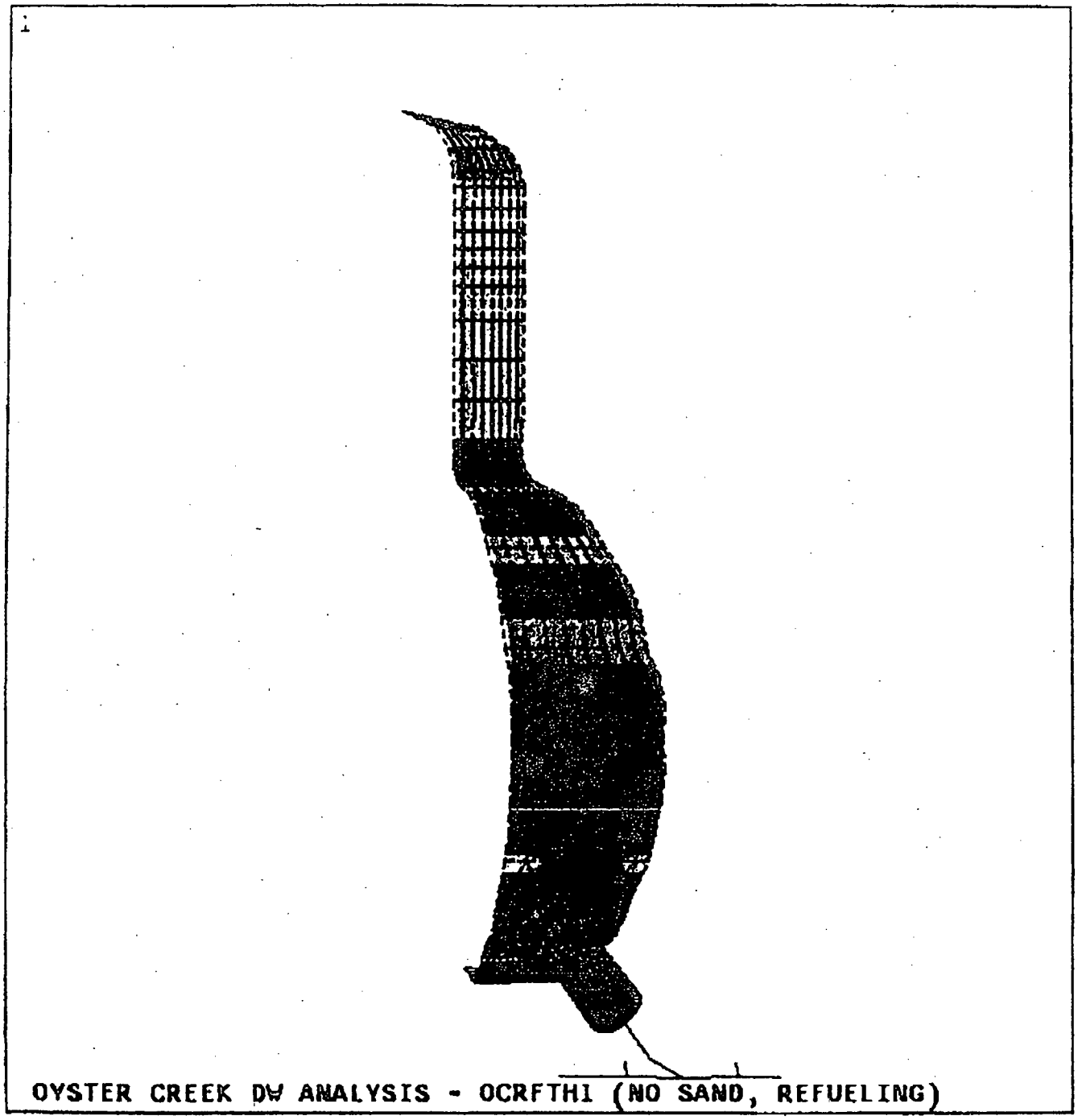
ANSYS 4.4A1
DEC 9 1992
17:41:51
POST1 STRESS
STEP=1
ITER=1
SX (AVG)
MIDDLE
ELEM CS
DMX =0.222715
SMN =-3561
SMX =7614
XV =1
YV =-0.8
DIST=718.786
XF =303.031
ZF =639.498
ANGZ=-90
CENTROID HIDDEN
-3561
-2319
-1078
163.887
1406
2647
3889
5131
6372
7614
OYSTER CREEK DW ANALYSIS - OCRFTH1 (NO SAND, REFUELING)

FIGURE 2

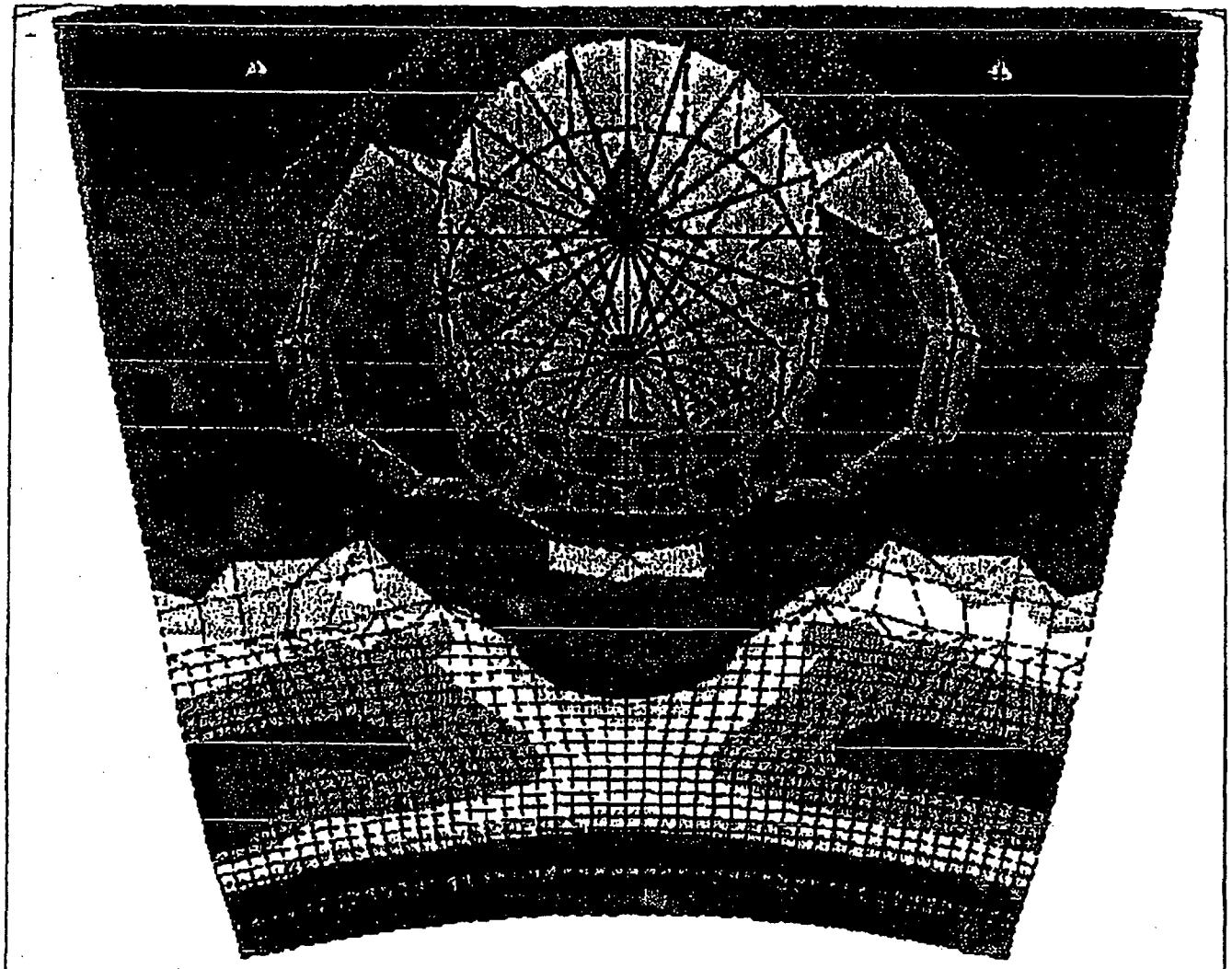

FIGURE 3

OYSTER CREEK DW ANALYSIS - OCRFTH1 (NO SAND, REFUELING)

FIGURE 4

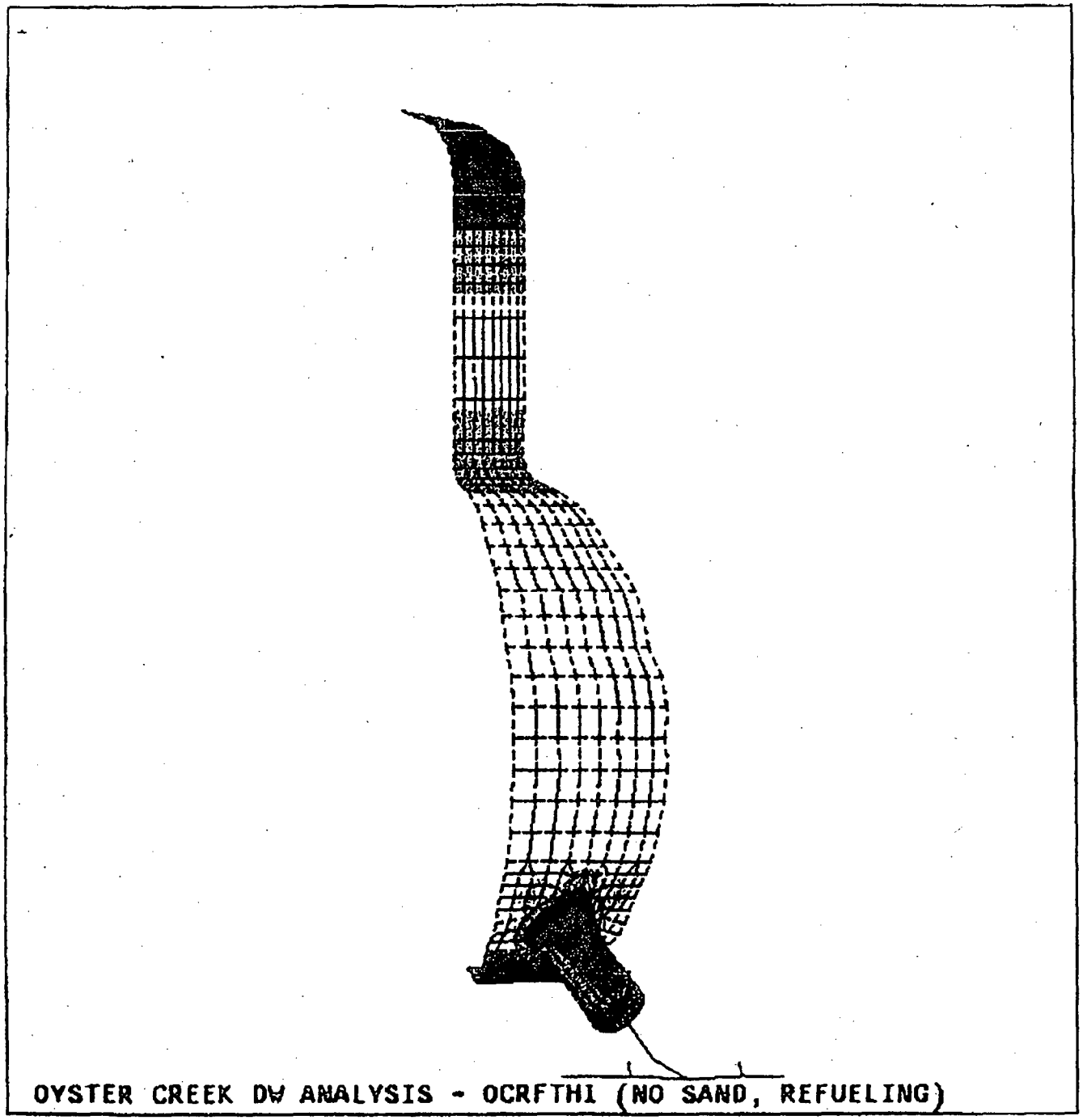

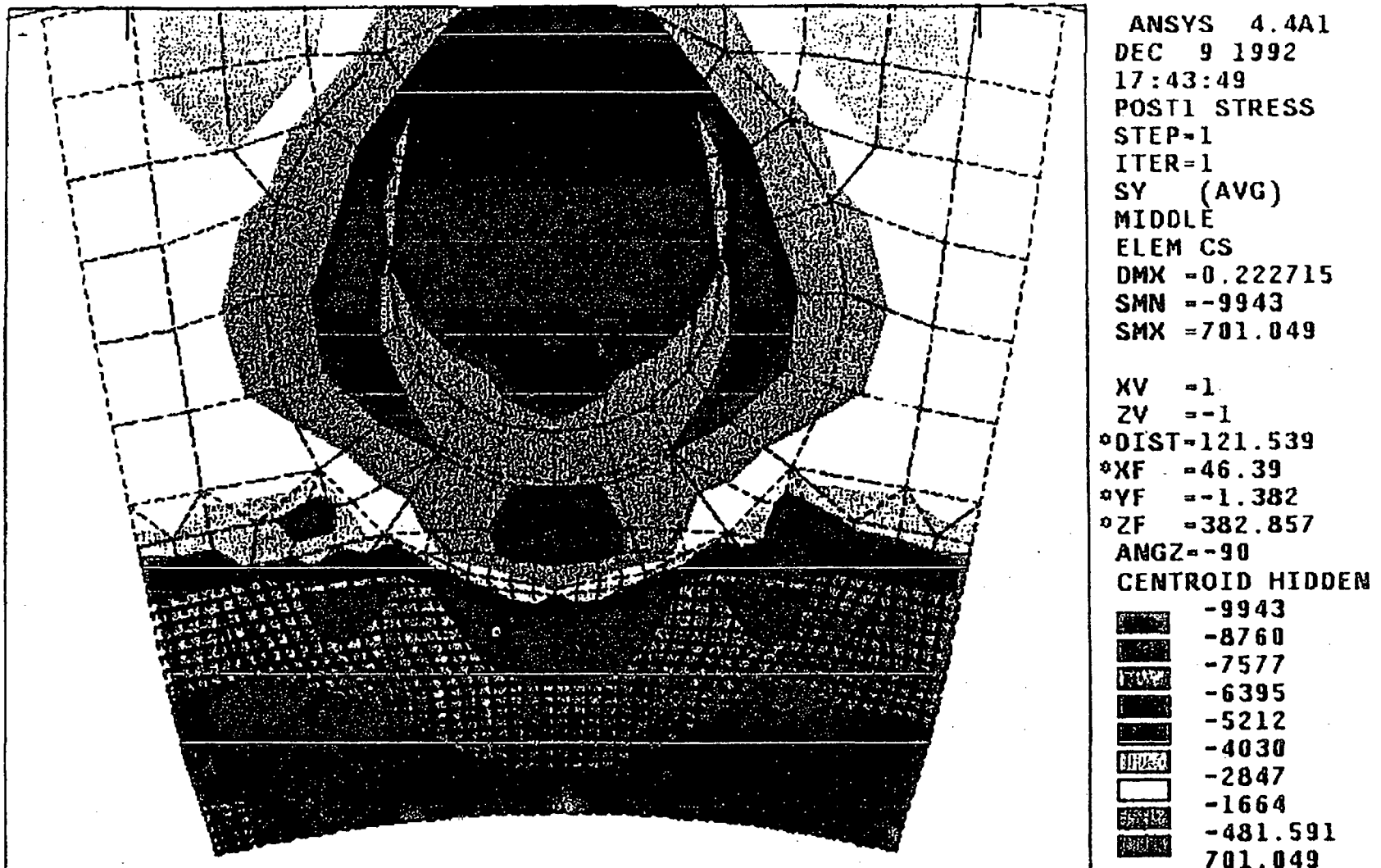

OYSTER CREEK DW ANALYSIS - OCRFTH1 (NO SAND, REFUELING)

FIGURE 5

FIGURE 6

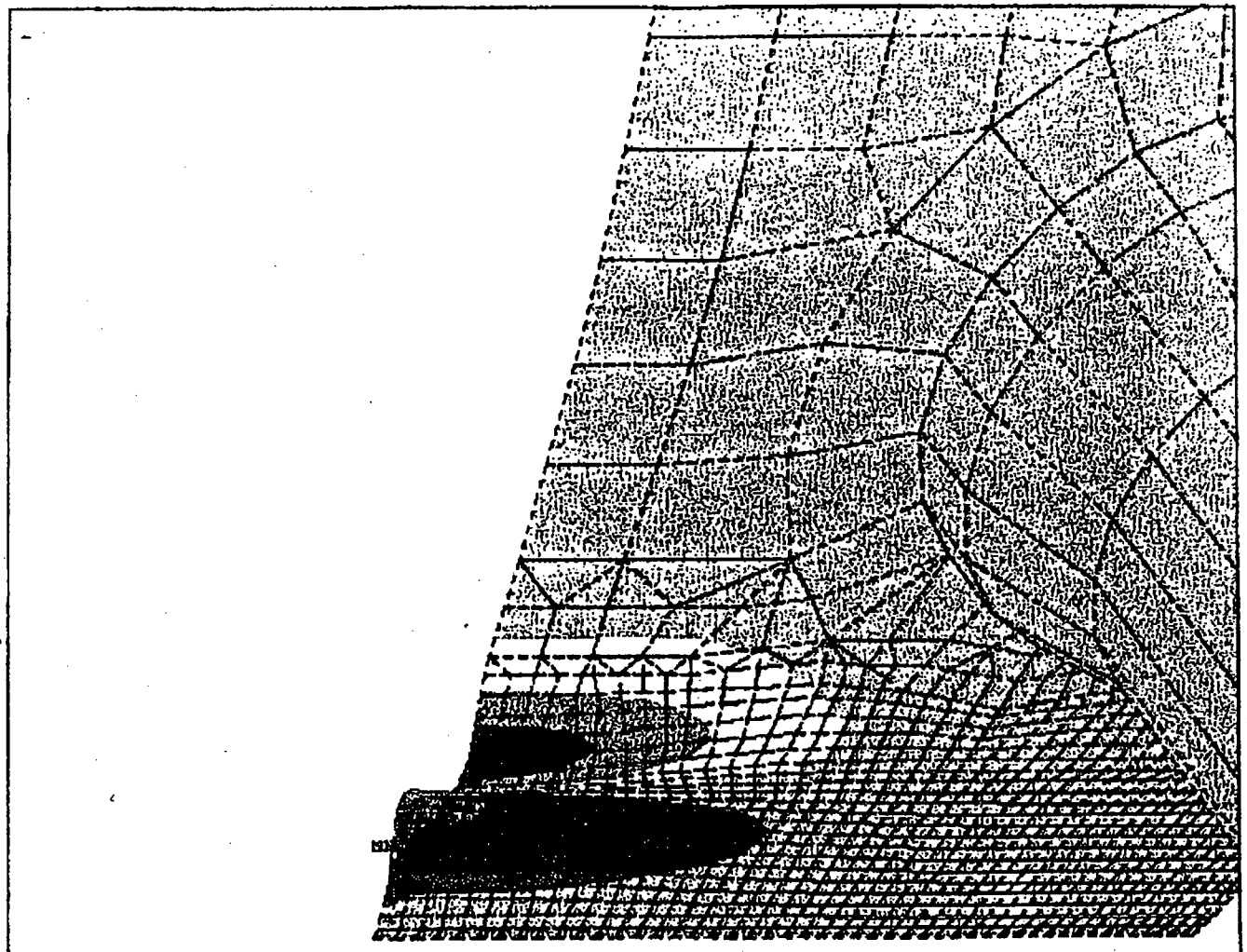

ANSYS 4.4A1
DEC 10 1992
6:55:43
POST1 STRESS
STEP=1
ITER=1
FACT=5.562
UX
D NODAL
DMX =0.006073
SMN =-0.006072
SMX =0.00345

XV =1
YV =-0.8
*DIST=89.401
*XF =262.142
*YF =-51.111
*ZF =148.214
ANGZ=-90
CENTROID HIDDEN

-0.006072
-0.005014
-0.003956
-0.002898
-0.00184
-0.782E-03
0.276E-03
0.001334
0.002392
0.00345

OYSTER CREEK DRYWELL ANALYSIS - OCRF05BSS (NO SAND, REFUELING)

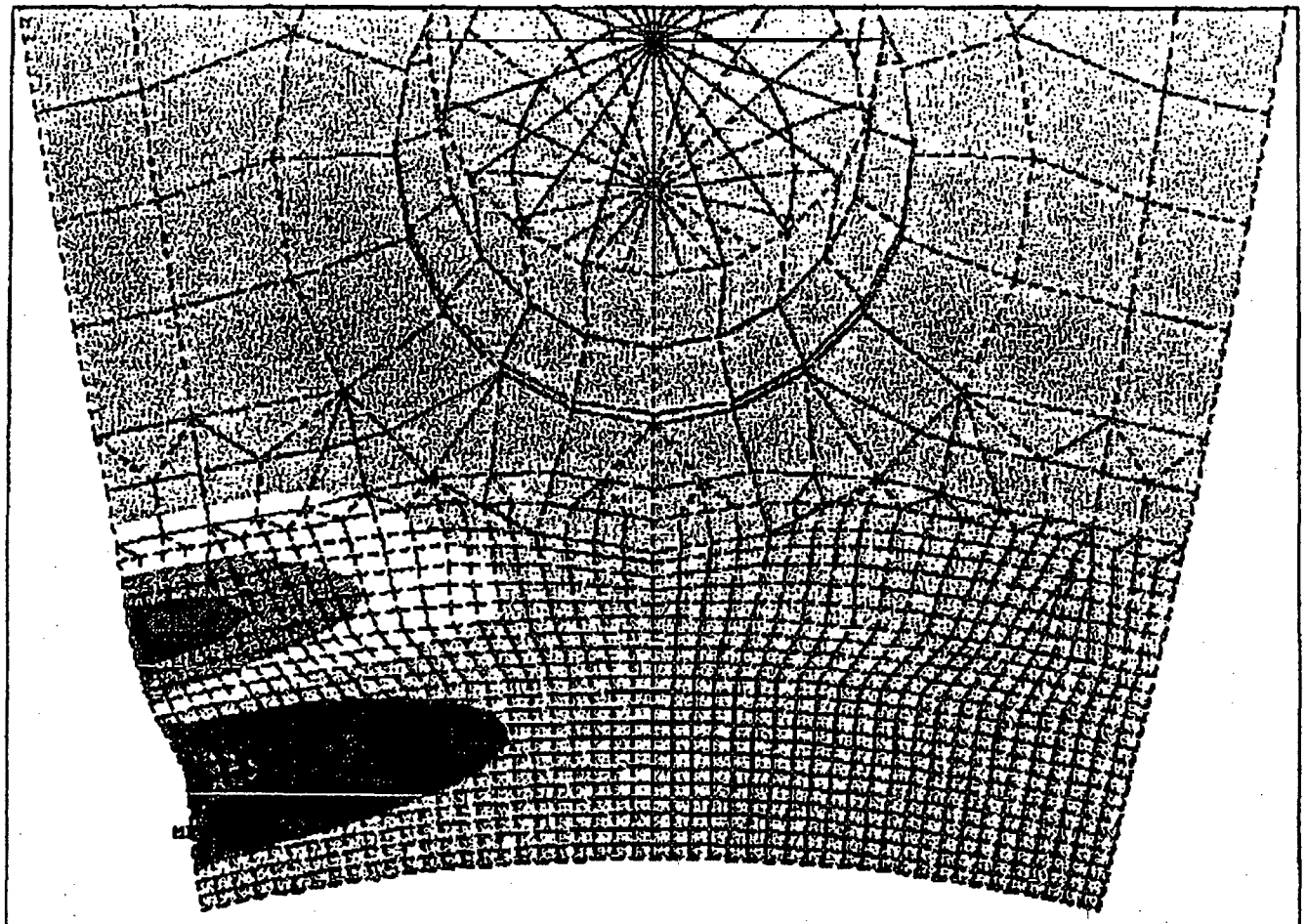

FIGURE 7

OYSTER CREEK DRYWELL ANALYSIS - OCRF05BSS (NO SAND, REFUELING)

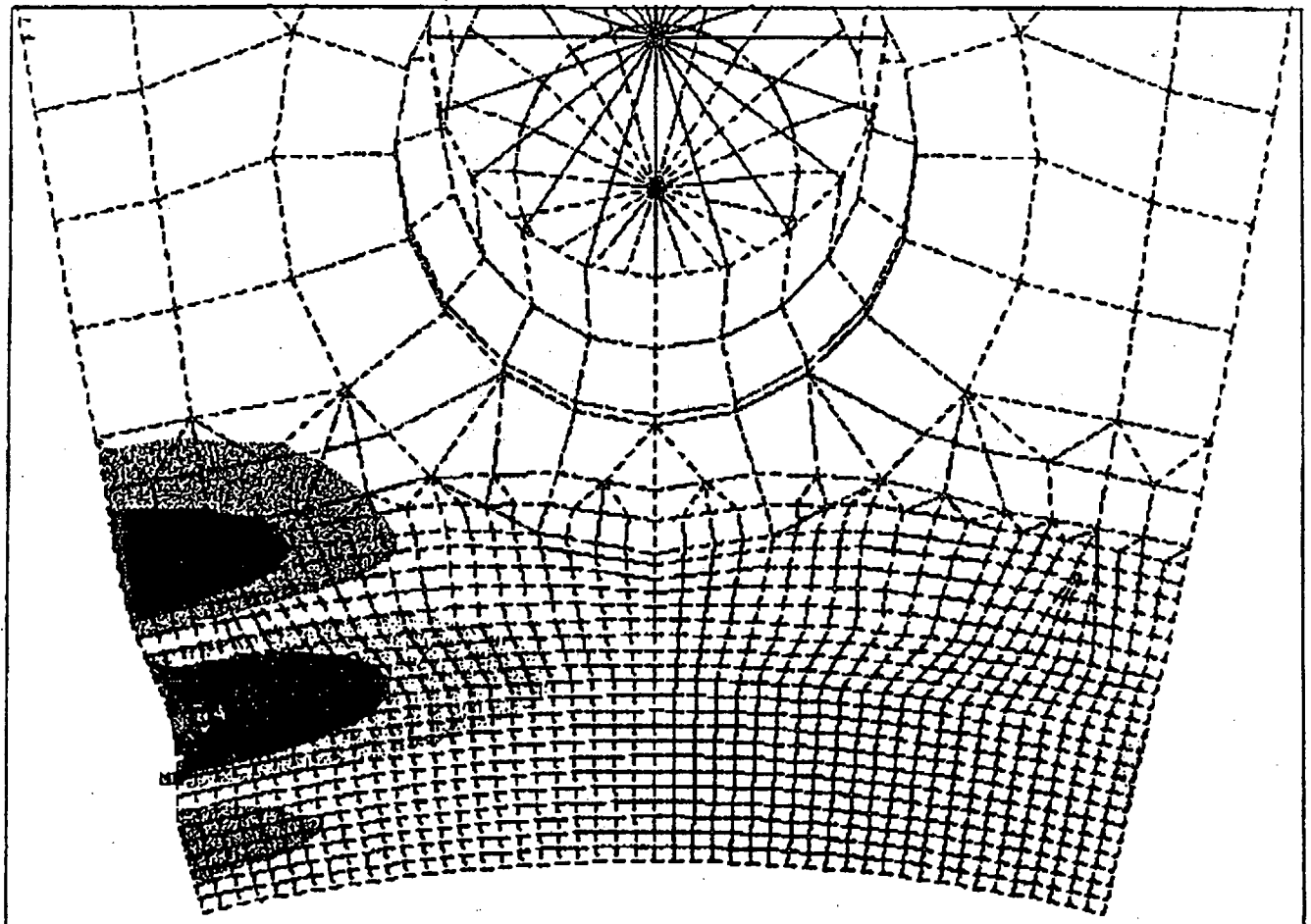

ANSYS 4.4A1
DEC 10 1992
8:10:04
POST1 STRESS
STEP=1
ITER=2
FACT=5.872
UX
D NODAL
DMX =0.006414
SMN =-0.006414
SMX =0.002261

XV =-1
ZV =-1
*DIST=110.004
*XF =29.455
*YF =0.460954
*ZF =365.922
ANGZ=-90
CENTROID HIDDEN

-0.006414
-0.00545
-0.004486
-0.003522
-0.002558
-0.001594
-0.630E-03
0.333E-03
0.001297
0.002261

FIGURE 8

ocRF05BSS

OYSTER CREEK DRYWELL ANALYSIS - [redacted] (NO SAND, REFUELING)

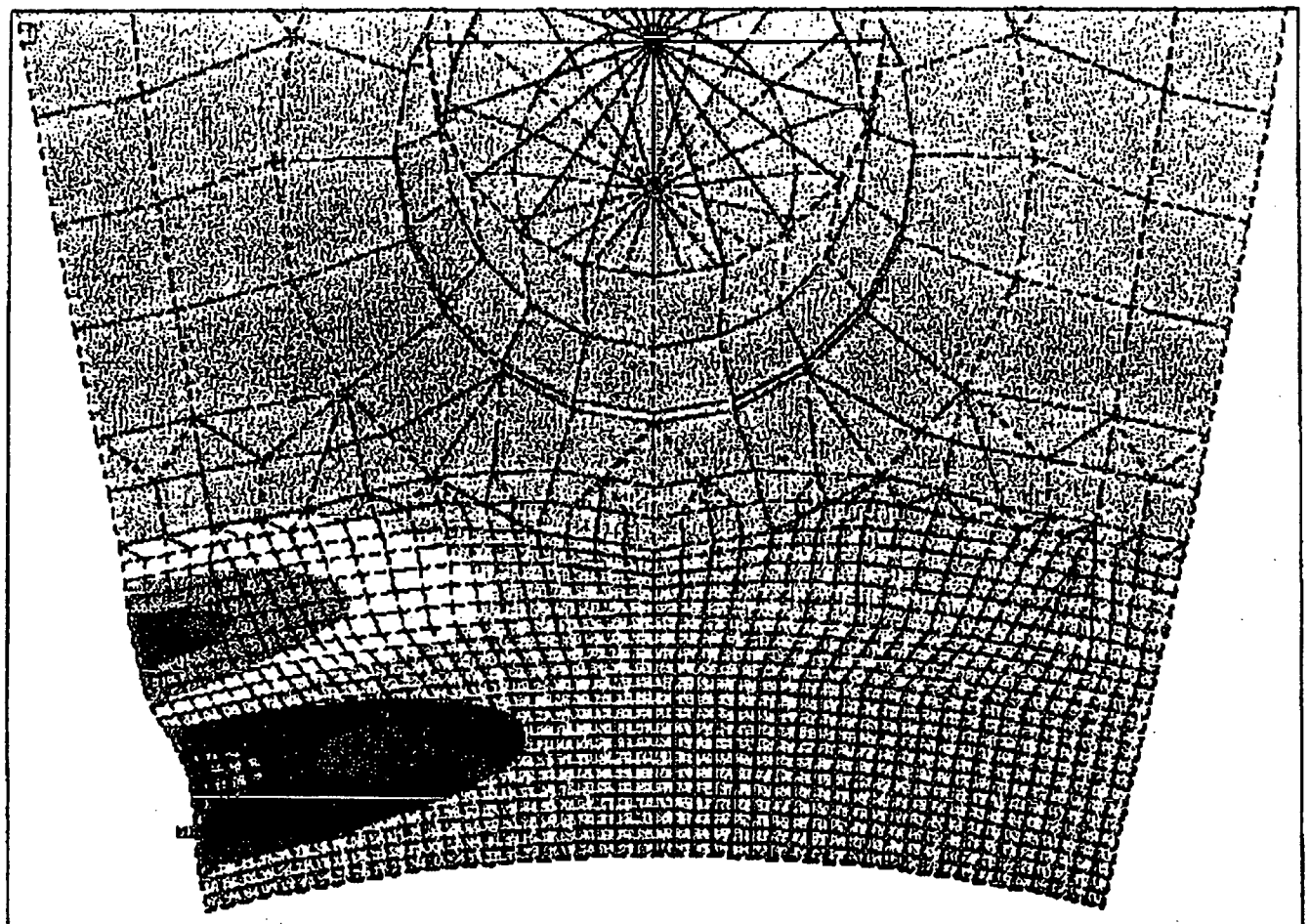

ANSYS 4.4A1
DEC 10 1992
7:29:08
POST1 STRESS
STEP=1
ITER=1
FACT=5.58
UX
D NODAL
DMX =0.005974
SMN =-0.005972
SMX =0.003682

XV =1
ZV =-1
*DIST=110.004
*XF =29.455
*YF =0.460954
*ZF =365.922
ANGZ=-90
CENTROID HIDDEN

-0.005972
-0.0049
-0.003827
-0.002754
-0.001681
-0.609E-03
0.464E-03
0.001537
0.00261
0.003682

FIGURE 9

OYSTER CREEK DW ANALYSIS - OCRF05AS (NO SAND, REFUELING)

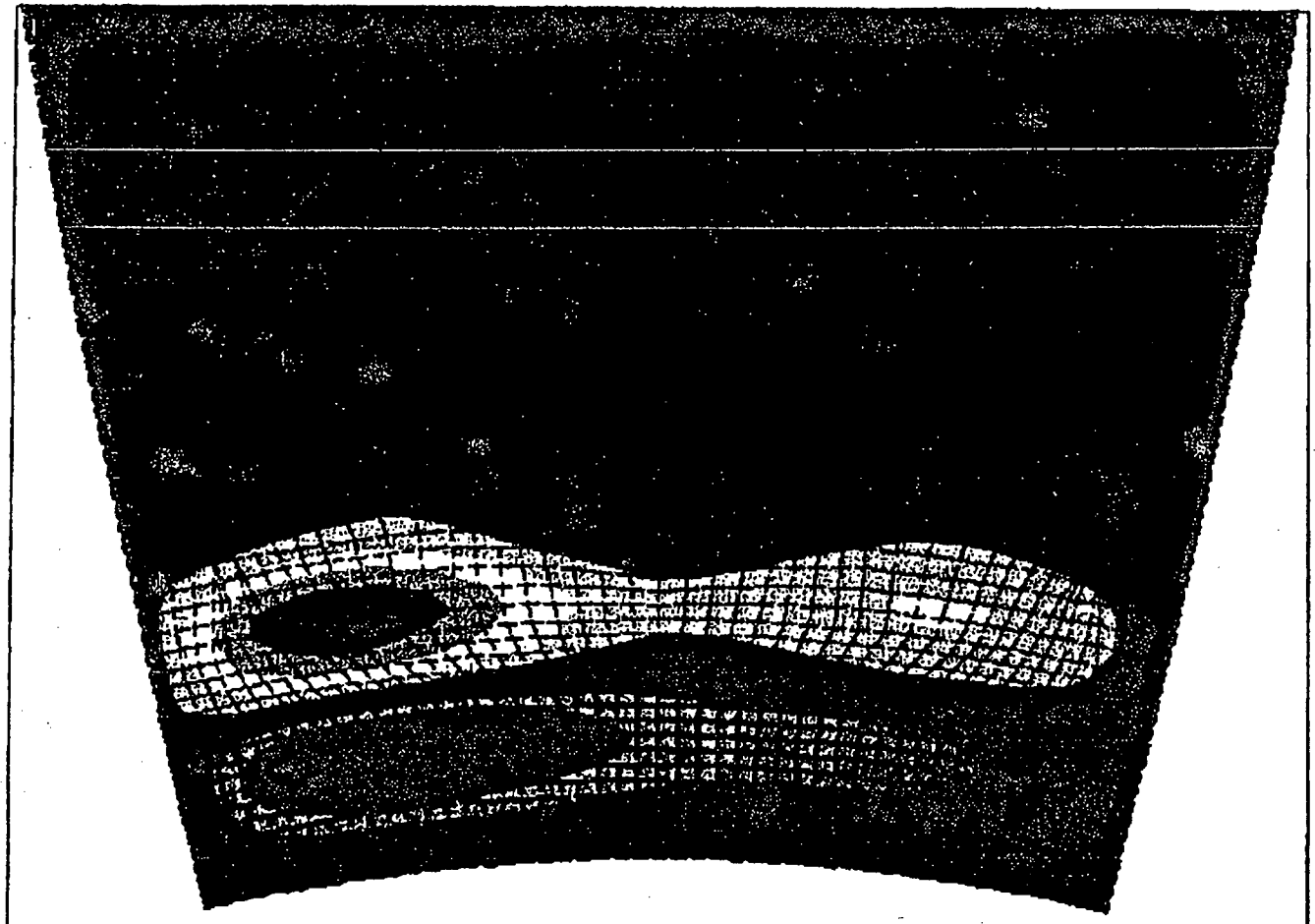

ANSYS 4.4A1
DEC 10 1992
10:12:22
POST1 STRESS
STEP=1
ITER=1
FACT=7.037
UX
D NODAL
DMX =0.003492
SMN =-0.002088
SMX =0.002164

XV =-1
ZV =-1
*DIST=110.004
*XF =29.455
*YF =0.460954
*ZF =365.922
ANGZ=-90
CENTROID HIDDEN

-0.002088
-0.001615
-0.001143
-0.670E-03
-0.198E-03
0.274E-03
0.747E-03
0.001219
0.001691
0.002164

FIGURE 10

OYSTER CREEK DW ANALYSIS - OCRF05AA (NO SAND, REFUELING)

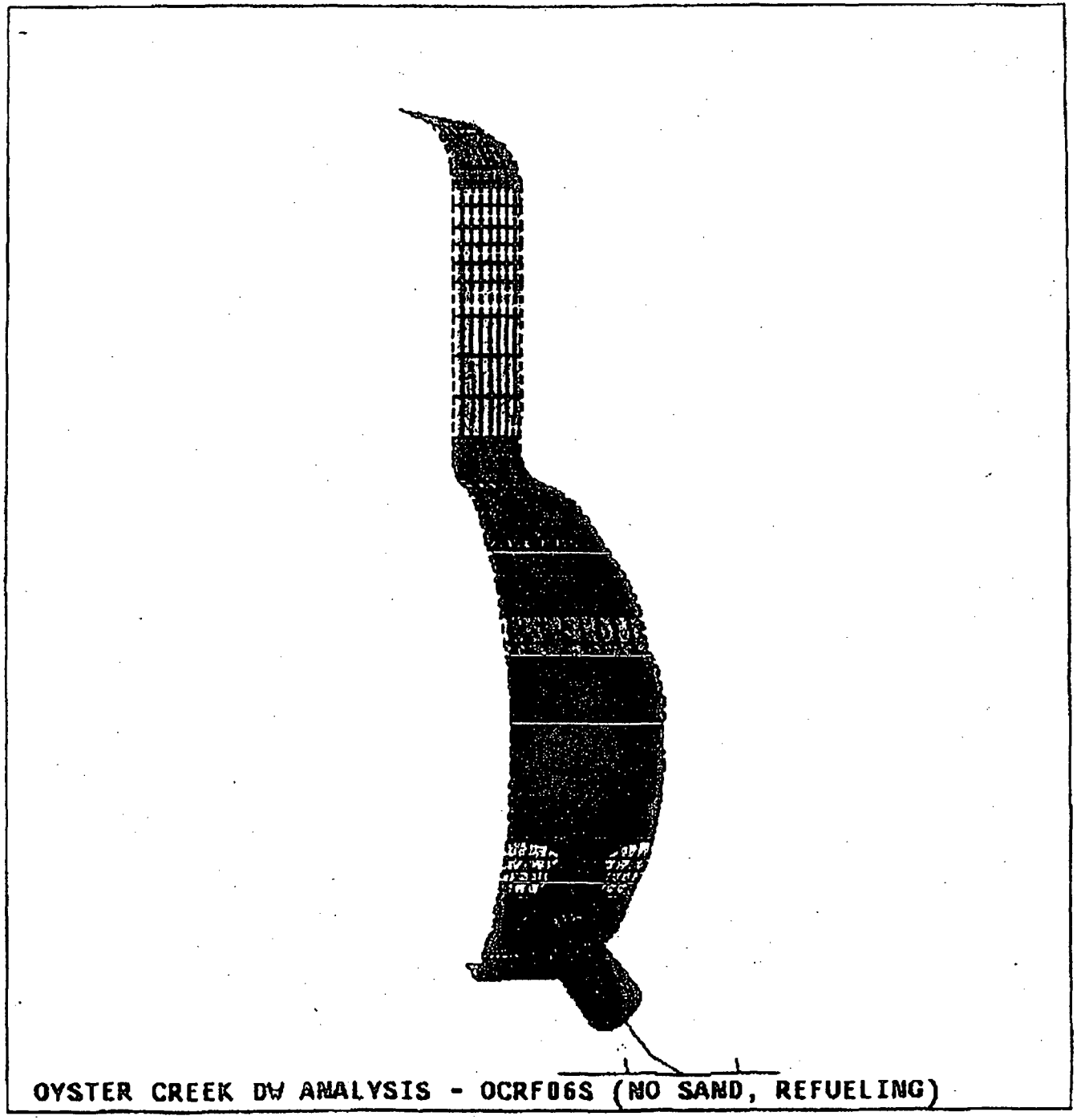
ANSYS 4.4A1
DEC 10 1992
8:18:30
POST1 STRESS
STEP=1
ITER=1
SX (AVG)
MIDDLE
ELEM CS
DMX =0.222456
SMN =-3554
SMX =6950
XV =1
YV =-0.8
DIST=718.786
XF =303.031
ZF =639.498
ANGZ=-90
CENTROID HIDDEN
-3554
-2387
-1220
-52.809
1114
2281
3448
4615
5783
6950
OYSTER CREEK DW ANALYSIS - OCRF06S (NO SAND, REFUELING)

FIGURE 11

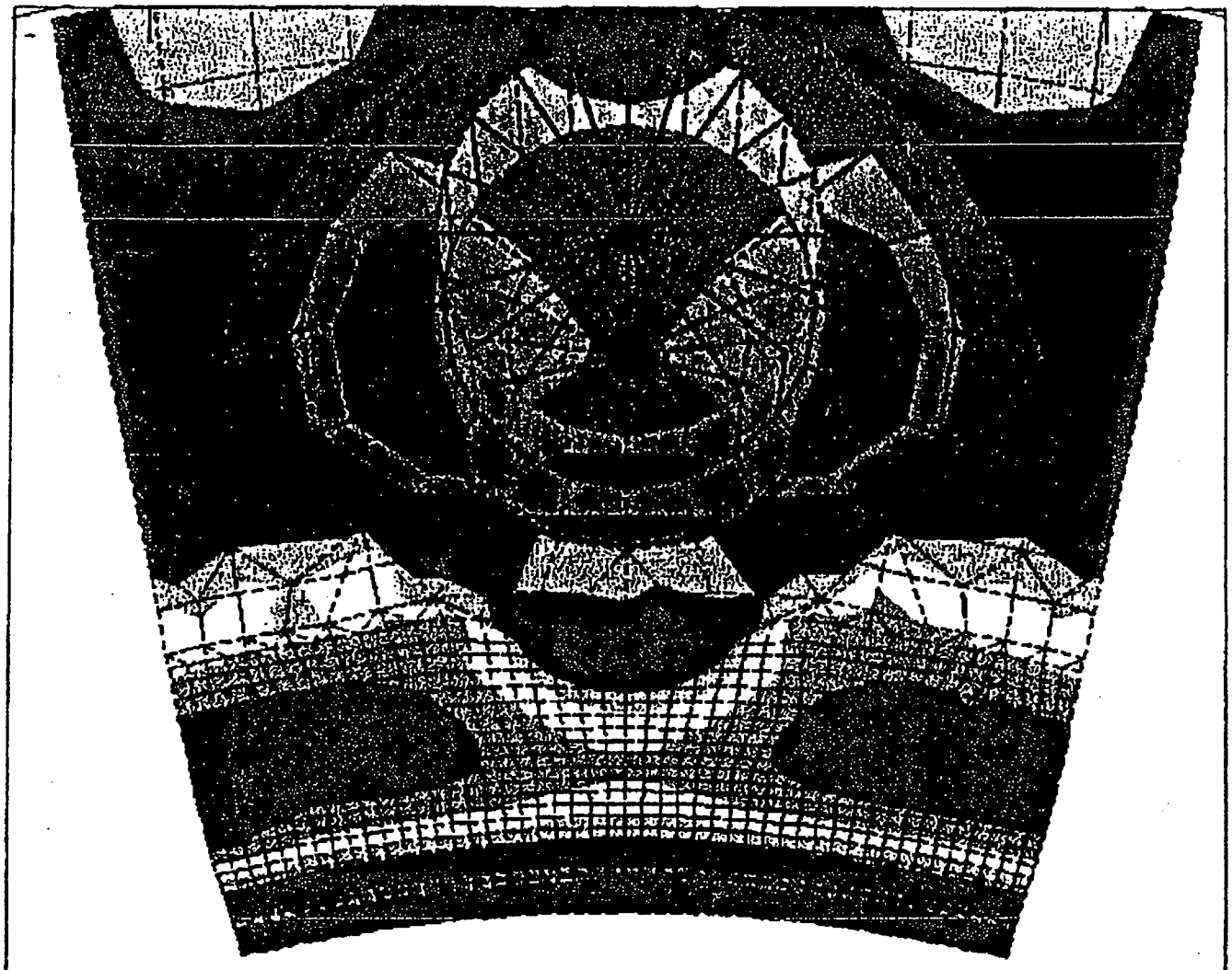

ANSYS 4.4A1
DEC 10 1992
8:21:15
POST1 STRESS
STEP=1
ITER=1
SX (AVG)
MIDDLE
ELEM CS
DMX =0.222456
SMN =-3554
SMX =6950

XV =1
ZV =-1
*DIST=121.539
*XF =46.39
*YF =-1.382
*ZF =-382.857
ANGZ=-90
CENTROID HIDDEN

-3554
-2387
-1220
-52.809
1114
2281
3448
4615
5783
6950

OYSTER CREEK DW ANALYSIS - OCRF06S (NO SAND, REFUELING)

FIGURE 12

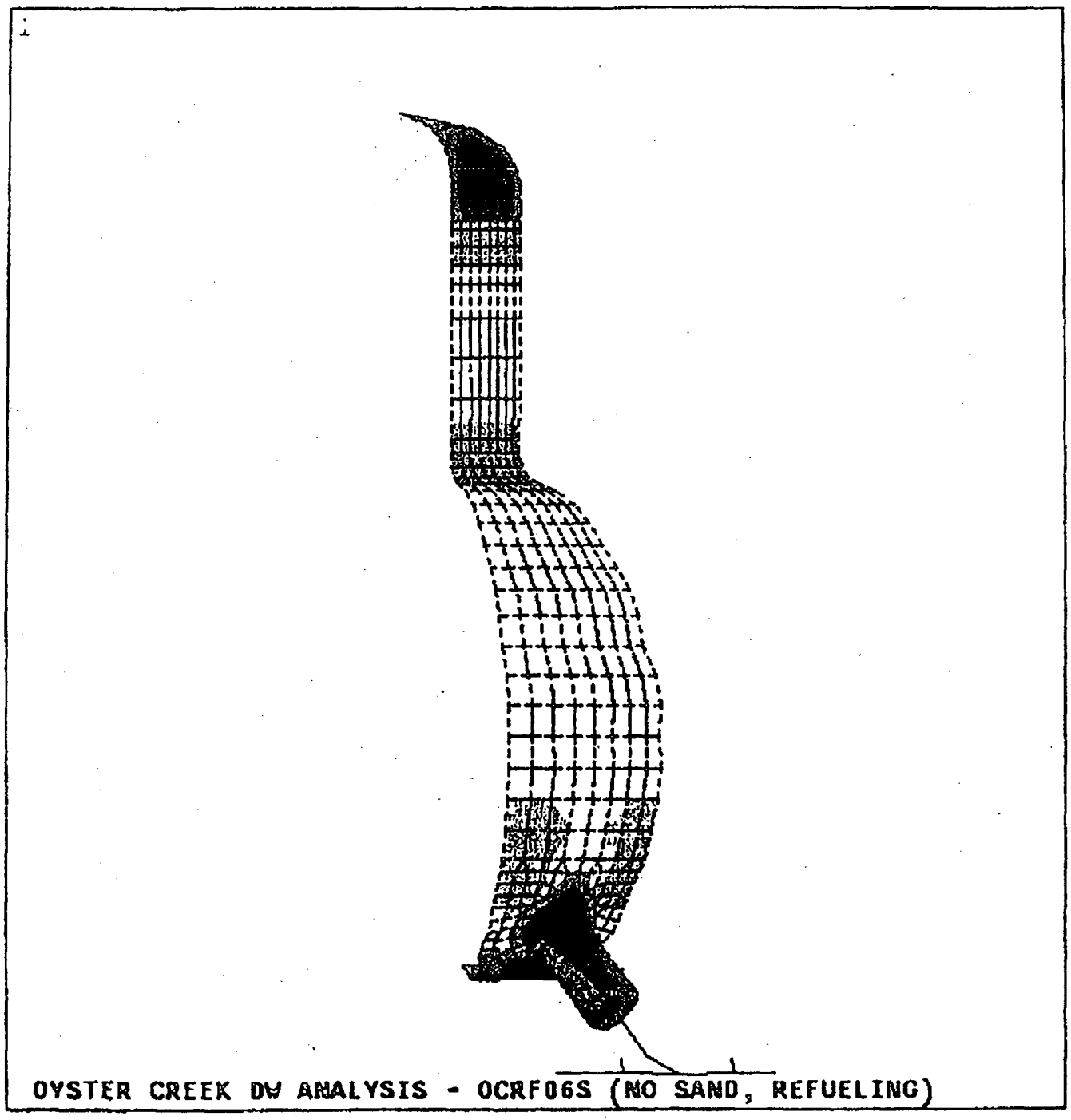

OYSTER CREEK DW ANALYSIS - OCRF06S (NO SAND, REFUELING)

FIGURE 13

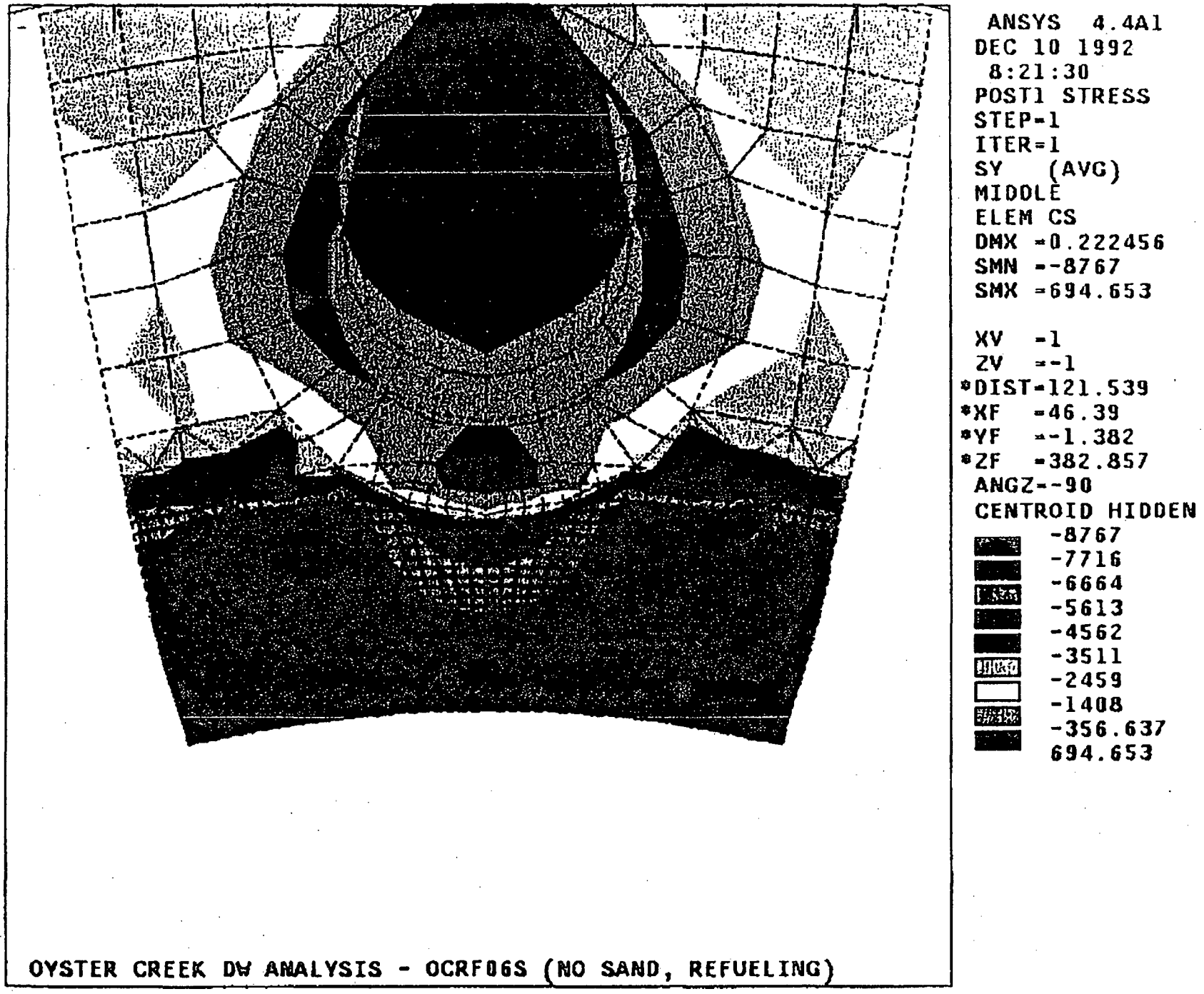

FIGURE 14

OYSTER CREEK DW ANALYSIS - OCRF06S (NO SAND, REFUELING)

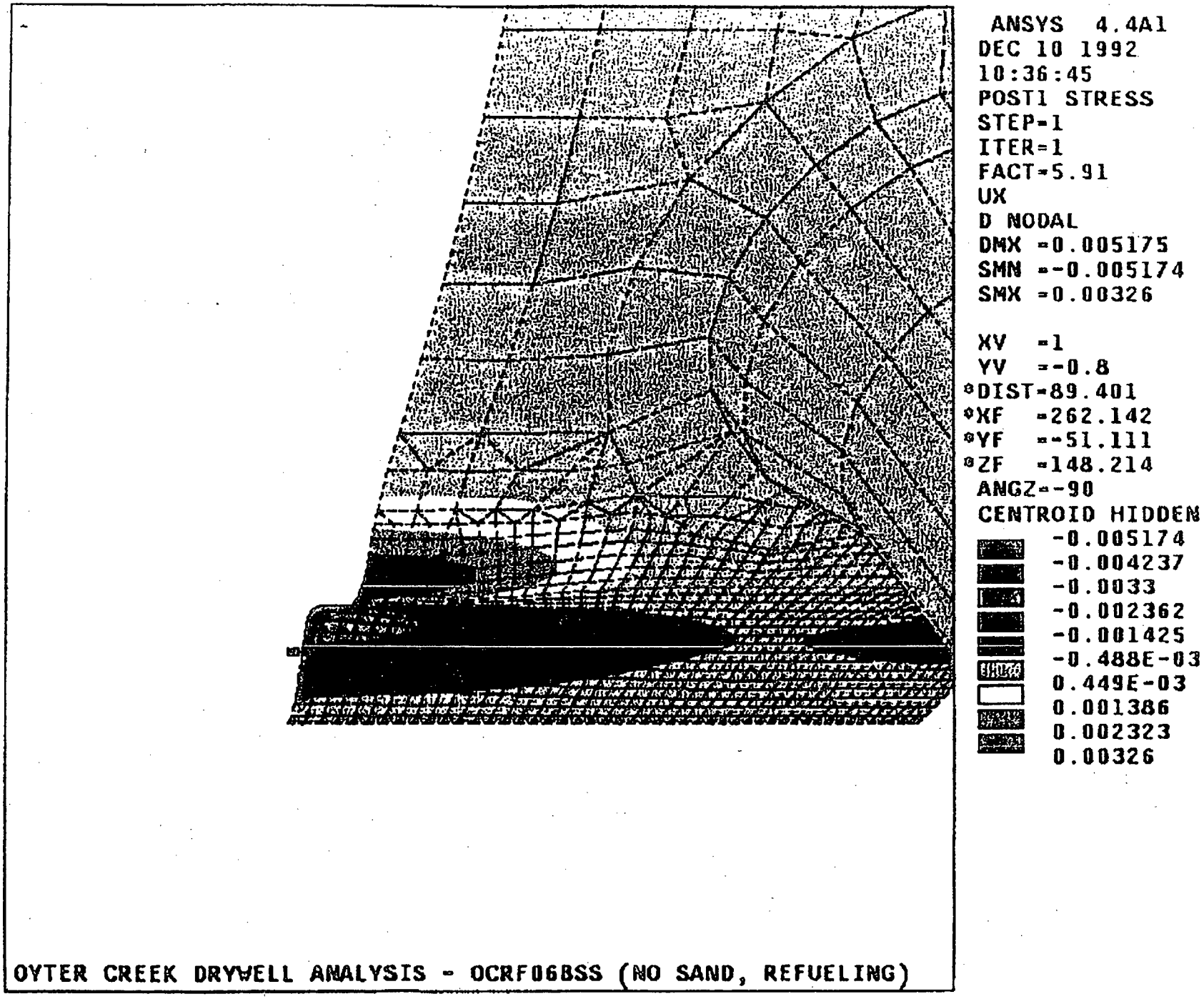

FIGURE 15

OYTER CREEK DRYWELL ANALYSIS - OCRF06BSS (NO SAND, REFUELING)

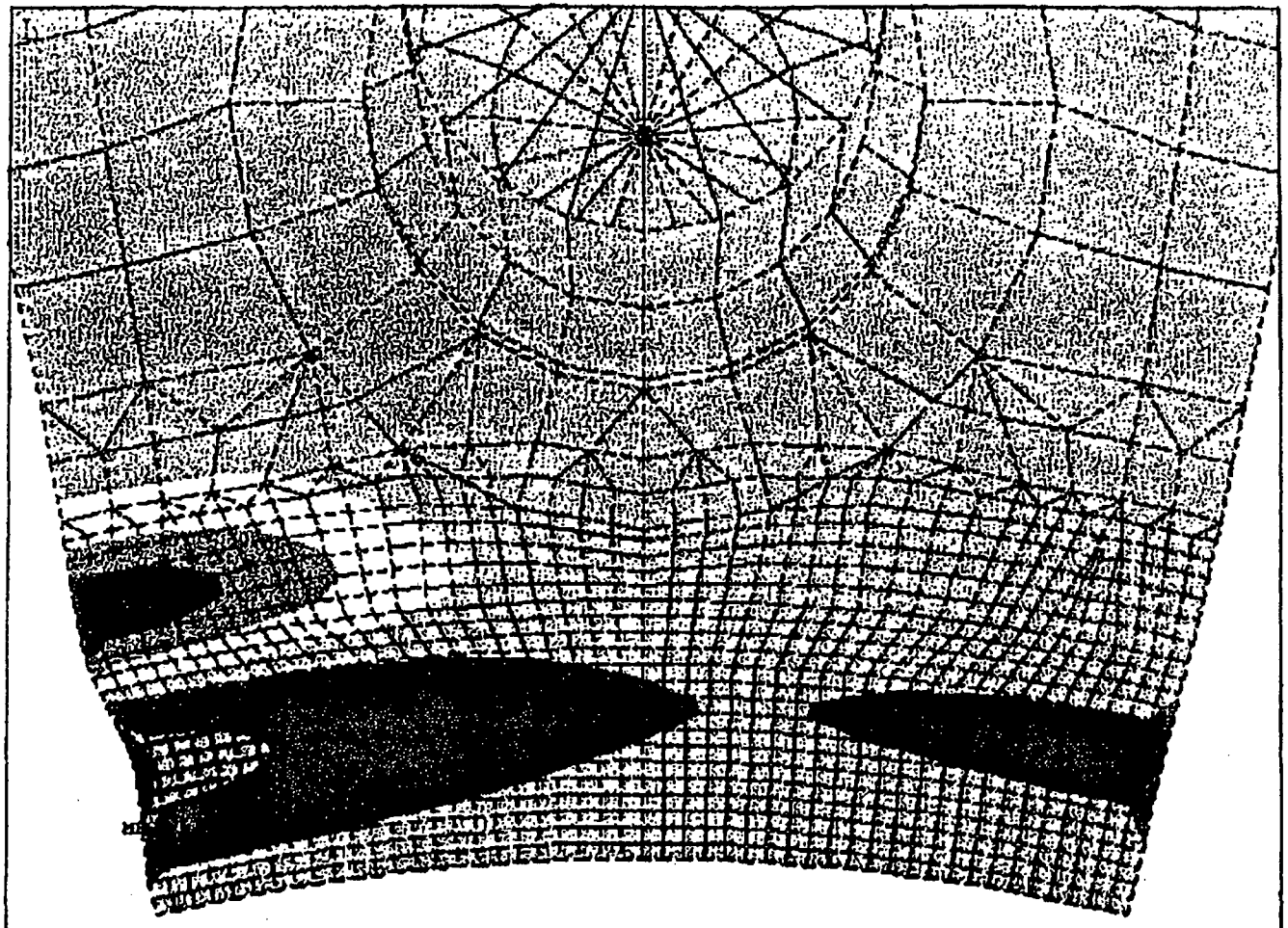

FIGURE 16

OYTER CREEK DRYWELL ANALYSIS - OCRF068SS (NO SAND, REFUELING)

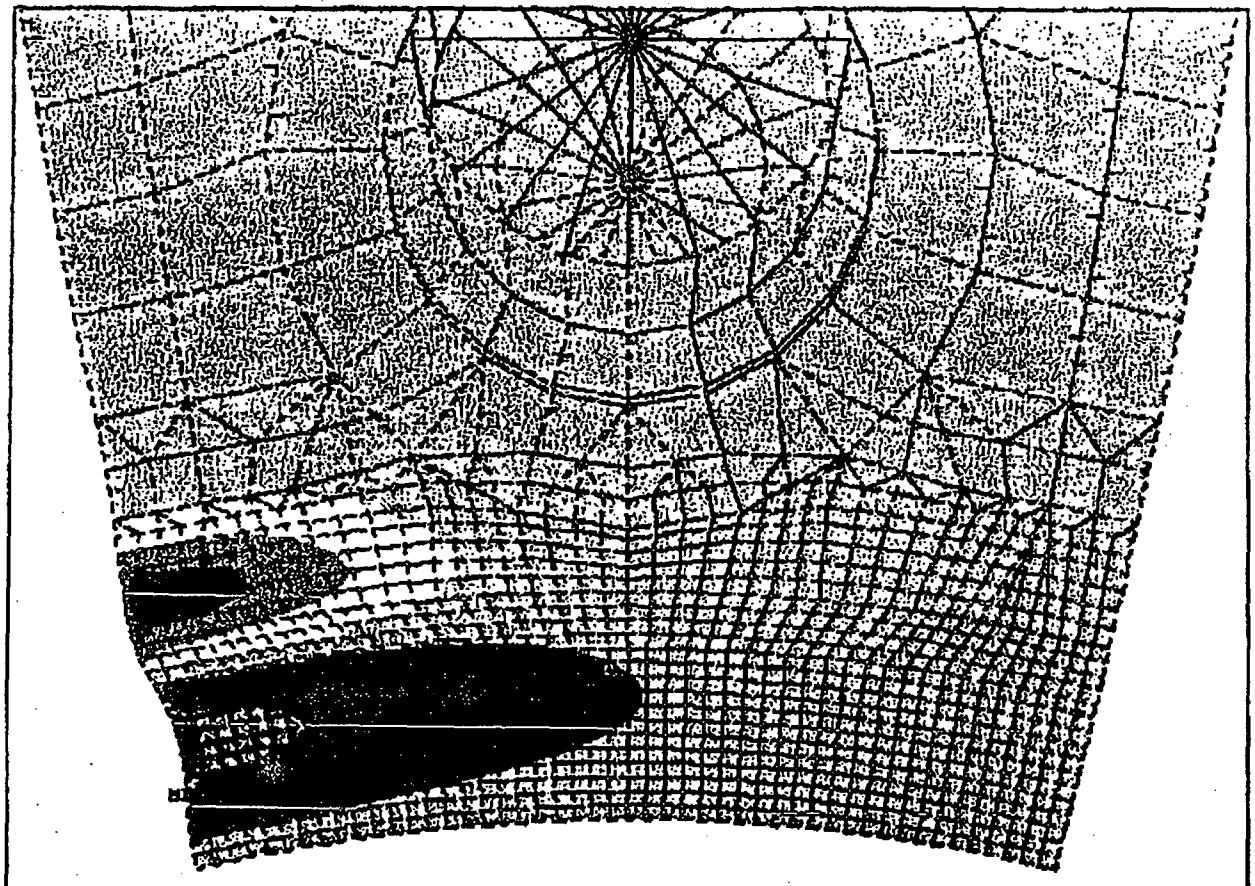

FIGURE 17

OYSTER CREEK DW ANALYSIS - OCRF06AS (NO SAND, REFUELING)

990 - 2174

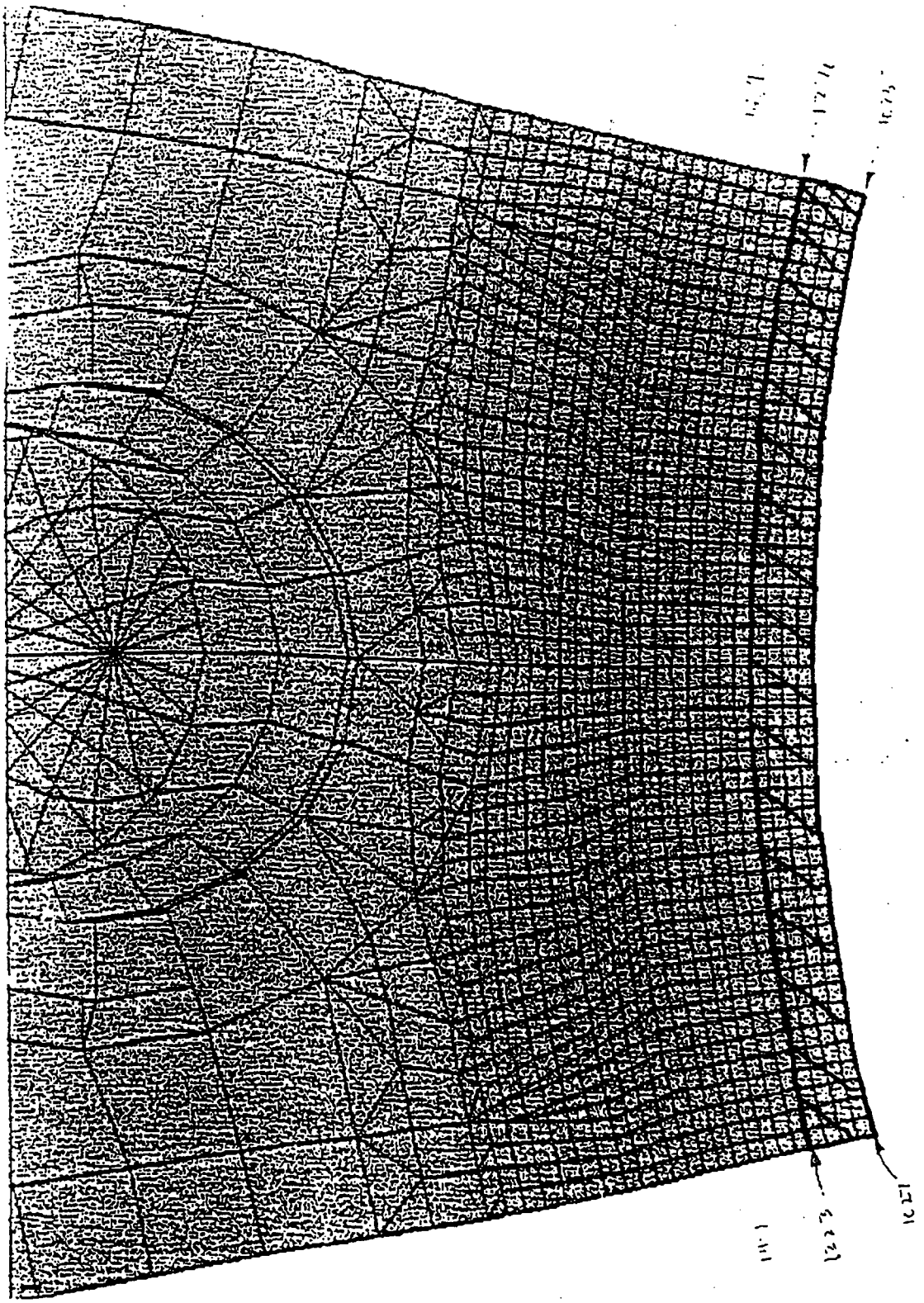

FIGURE 18

FIGURE 19

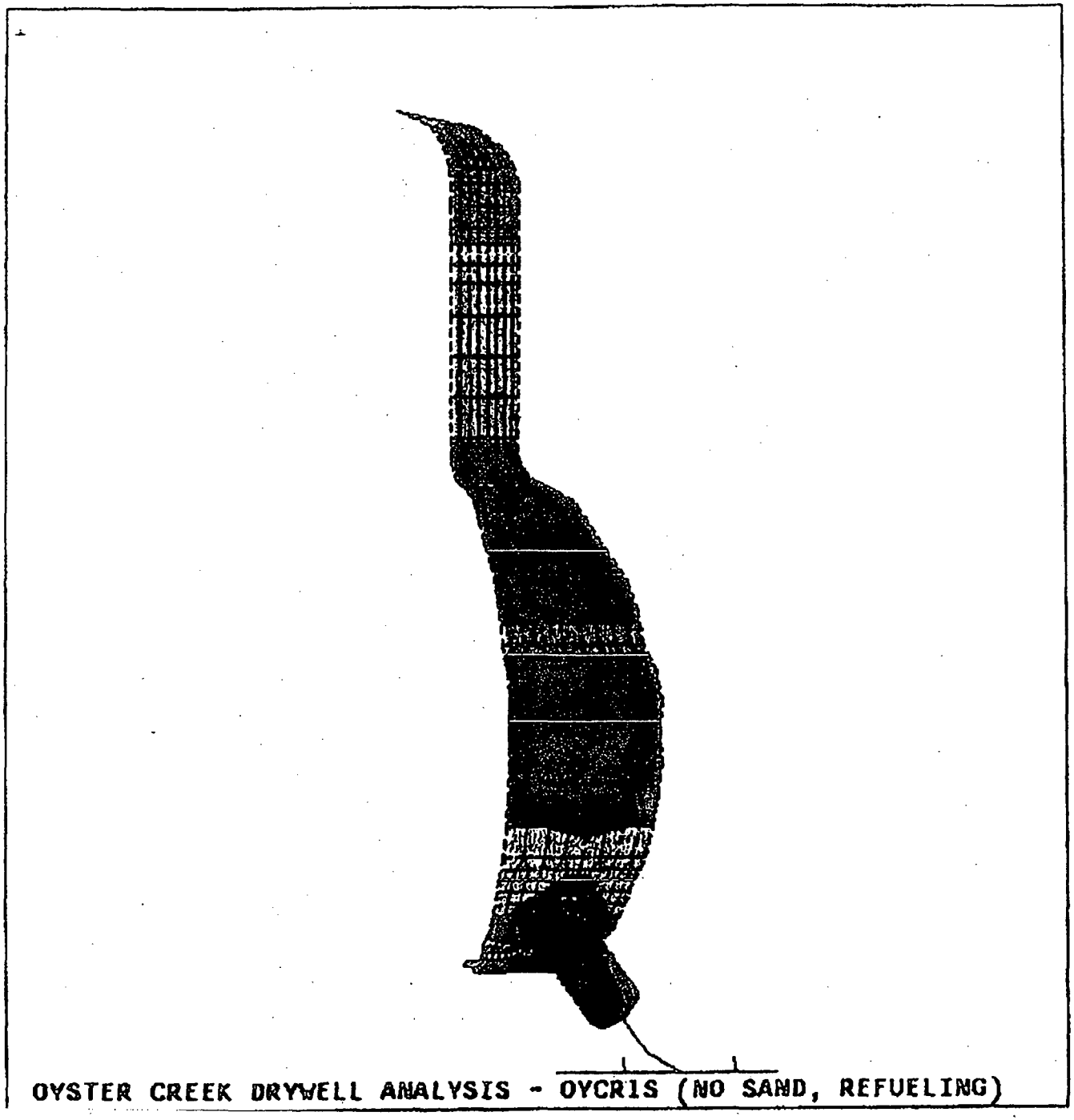

OYSTER CREEK DRYWELL ANALYSIS - OYCR1S (NO SAND, REFUELING)

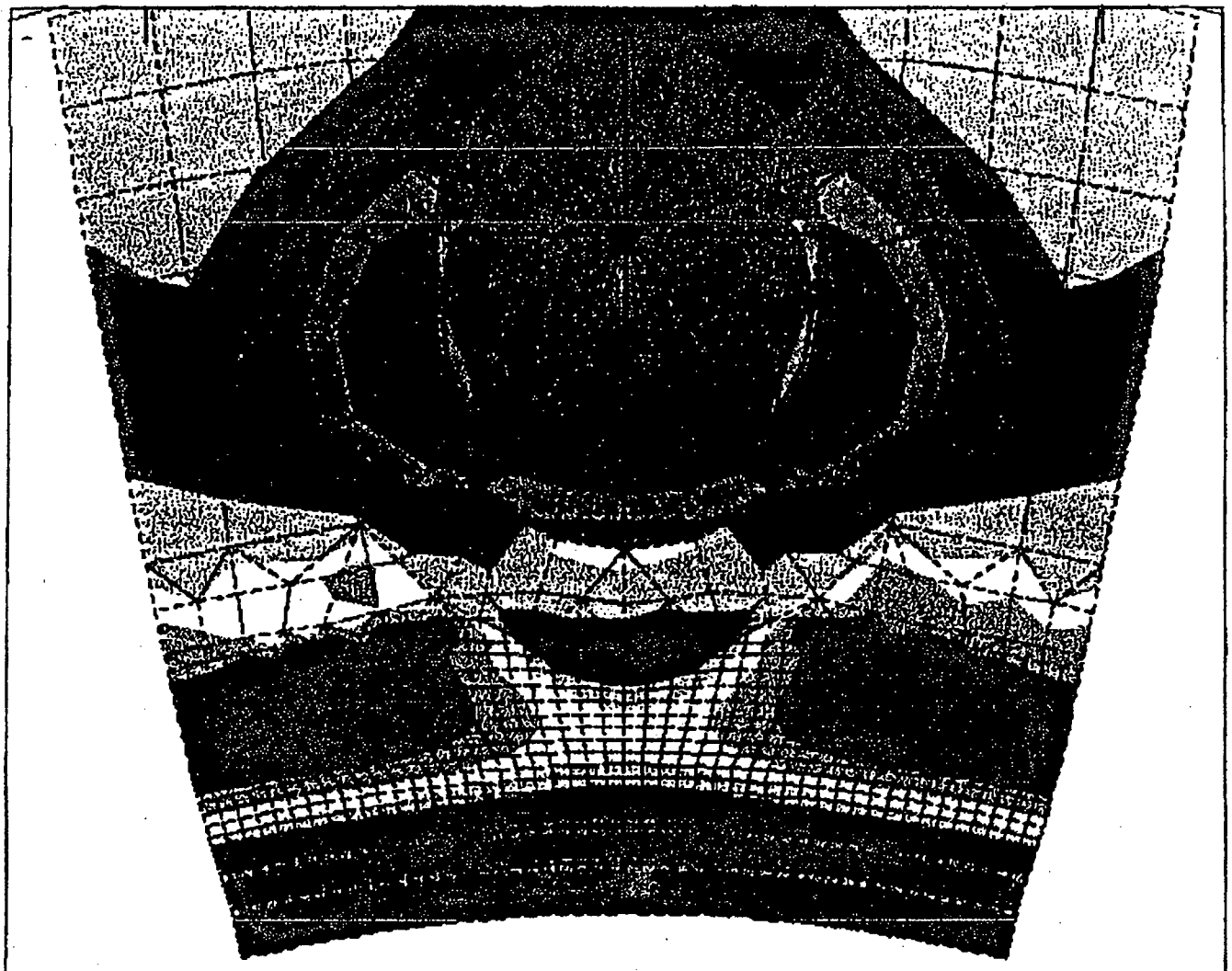

FIGURE 20

OYSTER CREEK DRYWELL ANALYSIS - OYCRIS (NO SAND, REFUELING)

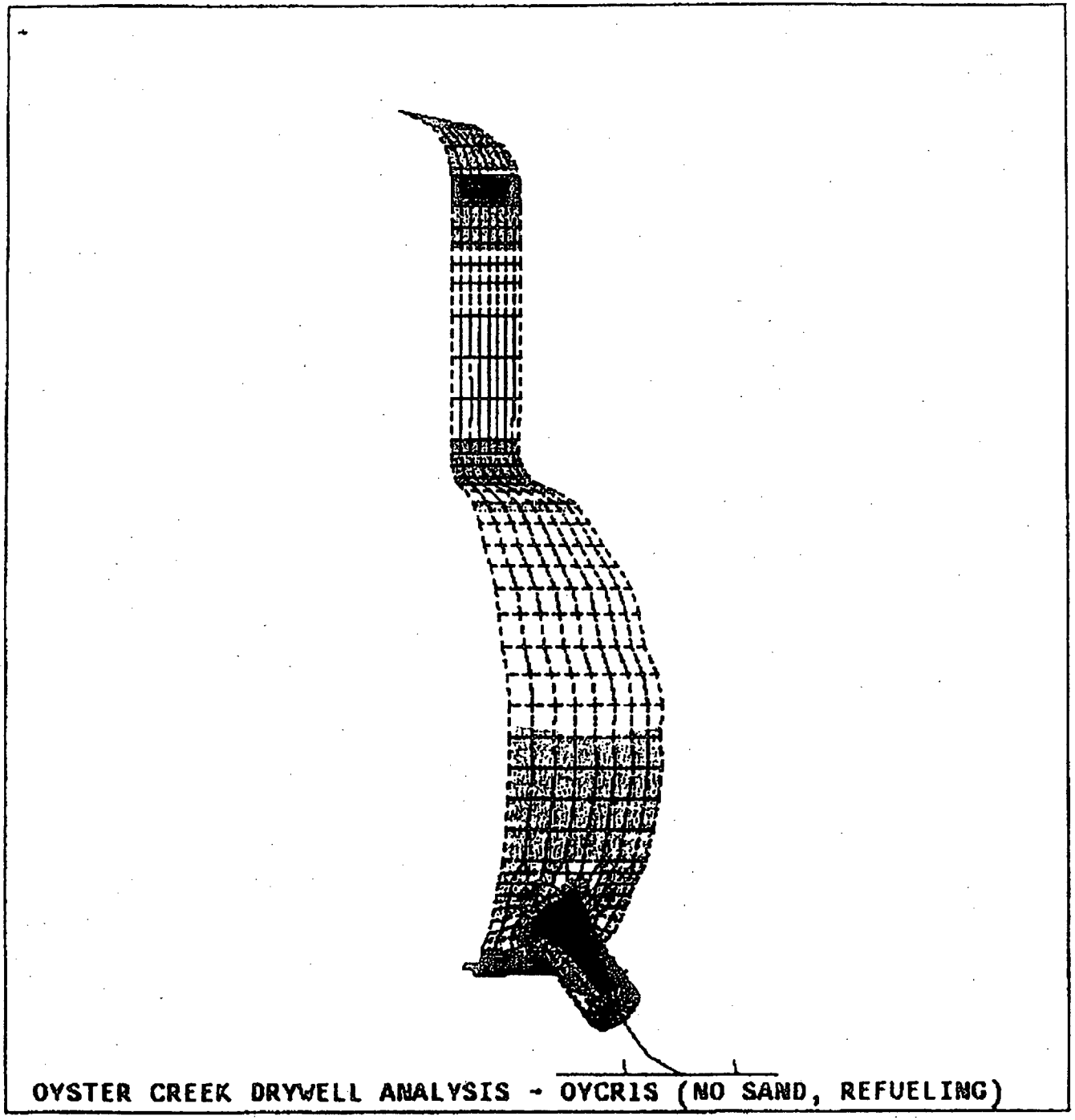
ANSYS 4.4A1
DEC 7 1992
12:44:44
POST1 STRESS
STEP=1
ITER=1
SY (AVG)
MIDDLE
ELEM CS
DMX =0.211959
SMN =-7956
SMX =766.953
XV =1
YV =-0.8
DIST=718.786
XF =303.031
ZF =639.498
ANGZ=-90
CENTROID HIDDEN
-7956
-6987
-6018
-5049
-4079
-3110
-2141
-1172
-202.301
766.953
OYSTER CREEK DRYWELL ANALYSIS - OYCR1S (NO SAND, REFUELING)

FIGURE 21

FIGURE 22

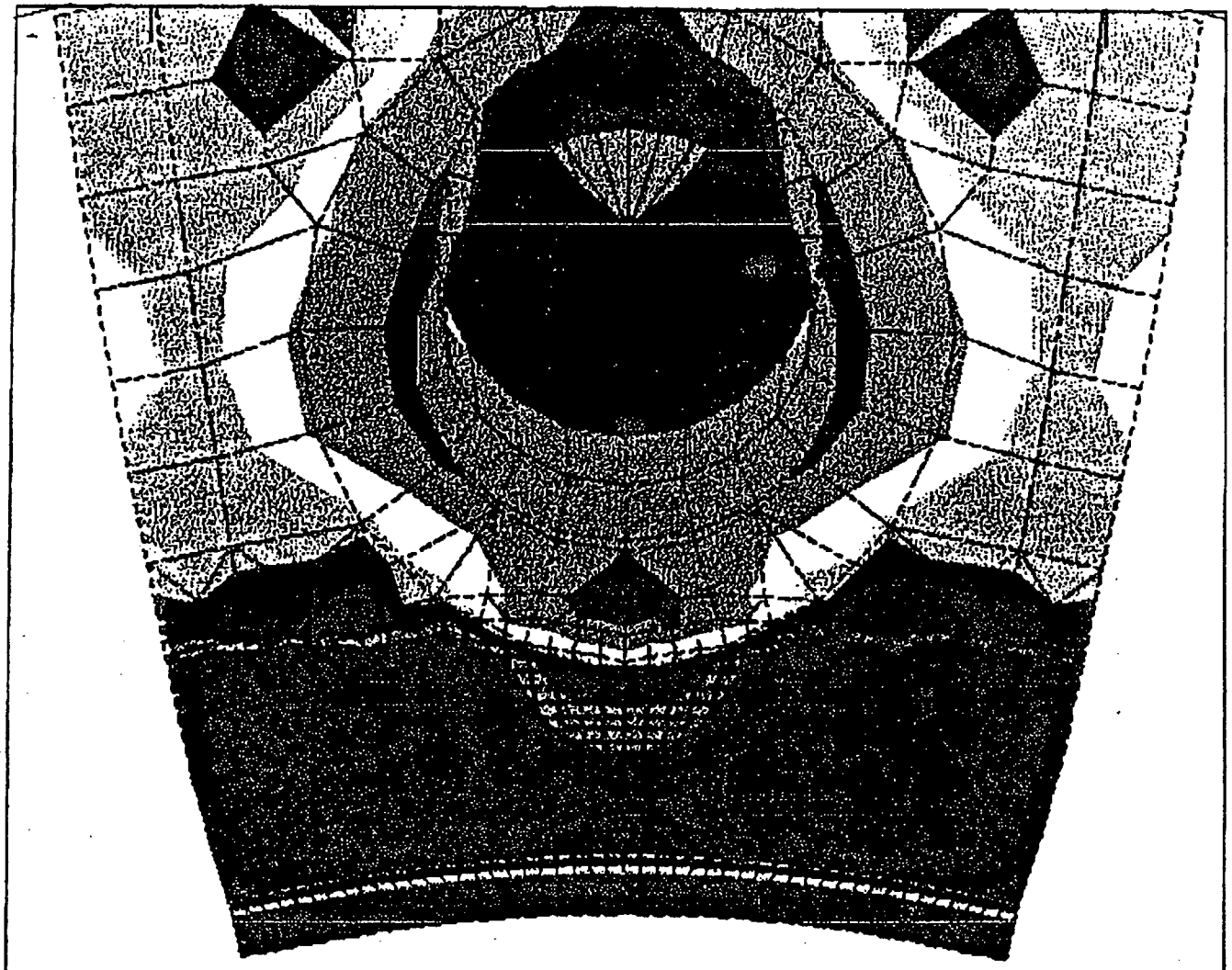

ANSYS 4.4A1
DEC 7 1992
12:34:18
POSTI STRESS
STEP=1
ITER=1
SY (AVG)
MIDDLE
ELEM CS
DMX =0.211959
SMN =-7956
SMX =766.953

XV =1
ZV =-1
*DIST=121.539
*XF =46.39
*YF =-1.382
*ZF =-382.857
ANGZ=-90
CENTROID HIDDEN

-7956
-6987
-6018
-5049
-4079
-3110
-2141
-1172
-202.301
766.953

OYSTER CREEK DRYWELL ANALYSIS - OYCRIS (NO SAND, REFUELING)

APPLIED MERIDIONAL AND CIRCUMFERENTIAL STRESSES - REFUELING CONDITION
ONE FOOT INCREASE IN FIXITY CASE; STRESS RUN: OCRFRLSB.OUT

AVERAGE APPLIED MERIDIONAL STRESS:

The average meridional stress is defined as the average stress across the elevation including nodes 1419 through 1467. Stresses at nodes 1419 and 1467 are weighted only one half as much as the other nodes because they lie on the edge of the modeled 1/10th section of the drywell and thus represent only 1/2 of the area represented by the other nodes.

Nodes	# of Nodes	Meridional Stress (ksi)	# of Nodes x Meridional Stress (ksi)
1419-1467	1	-7.726	-7.726
1423-1463	2	-7.738	-15.476
1427-1459	2	-7.760	-15.520
1431-1455	2	-7.682	-15.364
1435-1451	2	-7.394	-14.788
1439-1447	2	-7.014	-14.028
1443	1	-6.834	-6.834
Total:	12		-89.736
			12
Average Meridional Stress:			-7.478 (ksi)

AVERAGE APPLIED CIRCUMFERENTIAL STRESS:

The circumferential stress is averaged along the vertical line from node 1223 to node 2058.

Nodes	# of Nodes	Circumferential Stress (ksi)	# of Nodes x Circumferential Stress (ksi)
1223	0	-1.175	0.000
1419	1	0.505	0.505
1615	1	4.165	4.165
1811	1	5.846	5.846
2058	1	5.024	5.024
Total:	4		15.54
			4
Average Circumferential Stress:			3.885 (ksi)

OCRFST06.WK1

FIGURE 23

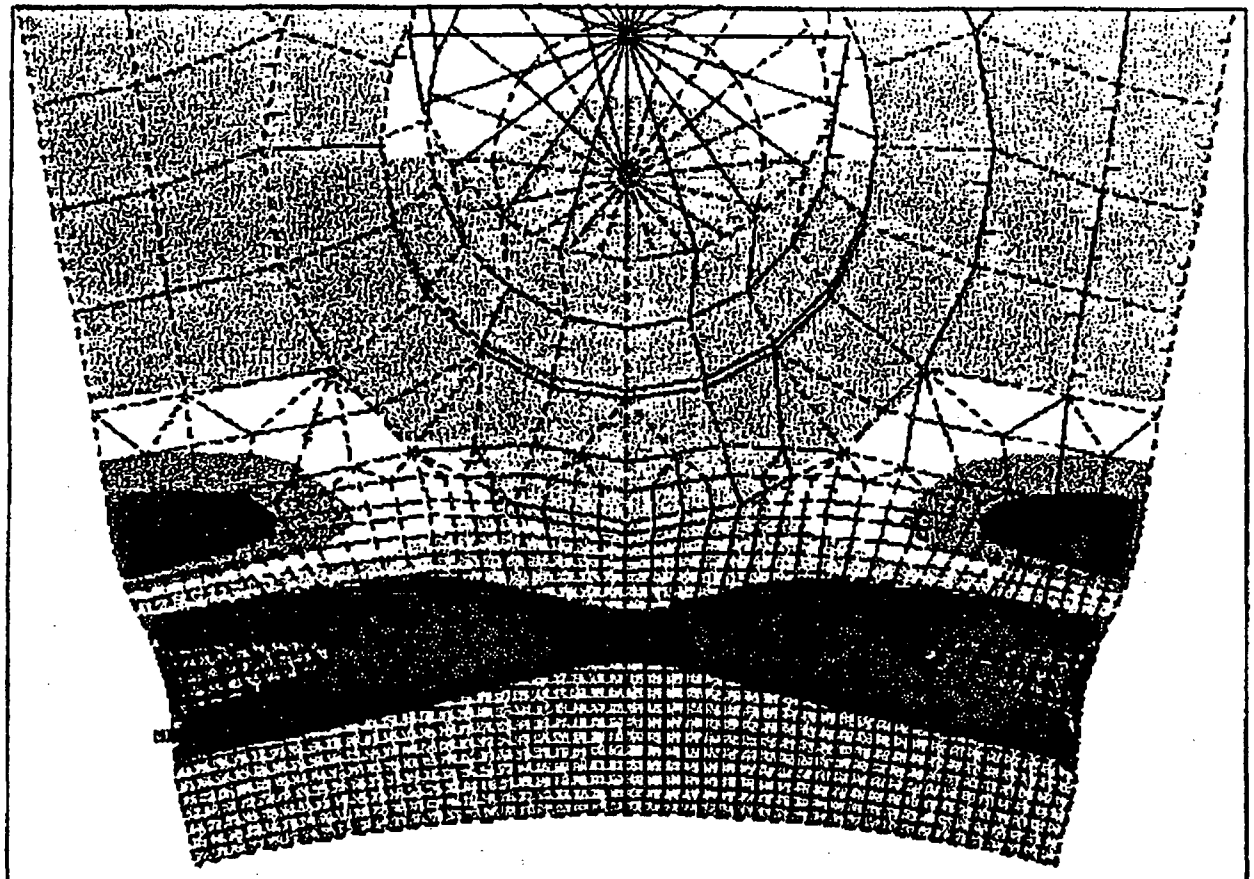

ANSYS 4.4A1
DEC 8 1992
6:15:38
POST1 STRESS
STEP=1
ITER=1
FACT=6.739
UX
D NODAL
DMX =0.003681
SMN =-0.00368
SMX =0.001848

XV =1
ZV =-1
*DIST=110.004
*XF =29.455
*YF =0.460954
*ZF =365.922
ANGZ=-90
CENTROID HIDDEN

-0.00368
-0.003065
-0.002451
-0.001837
-0.001223
-0.609E-03
0.567E-05
0.620E-03
0.001234
0.001848

OYSTER CREEK DRYWELL ANALYSIS - ocrfs-s (NO SAND, REFUELING)

FIGURE 24

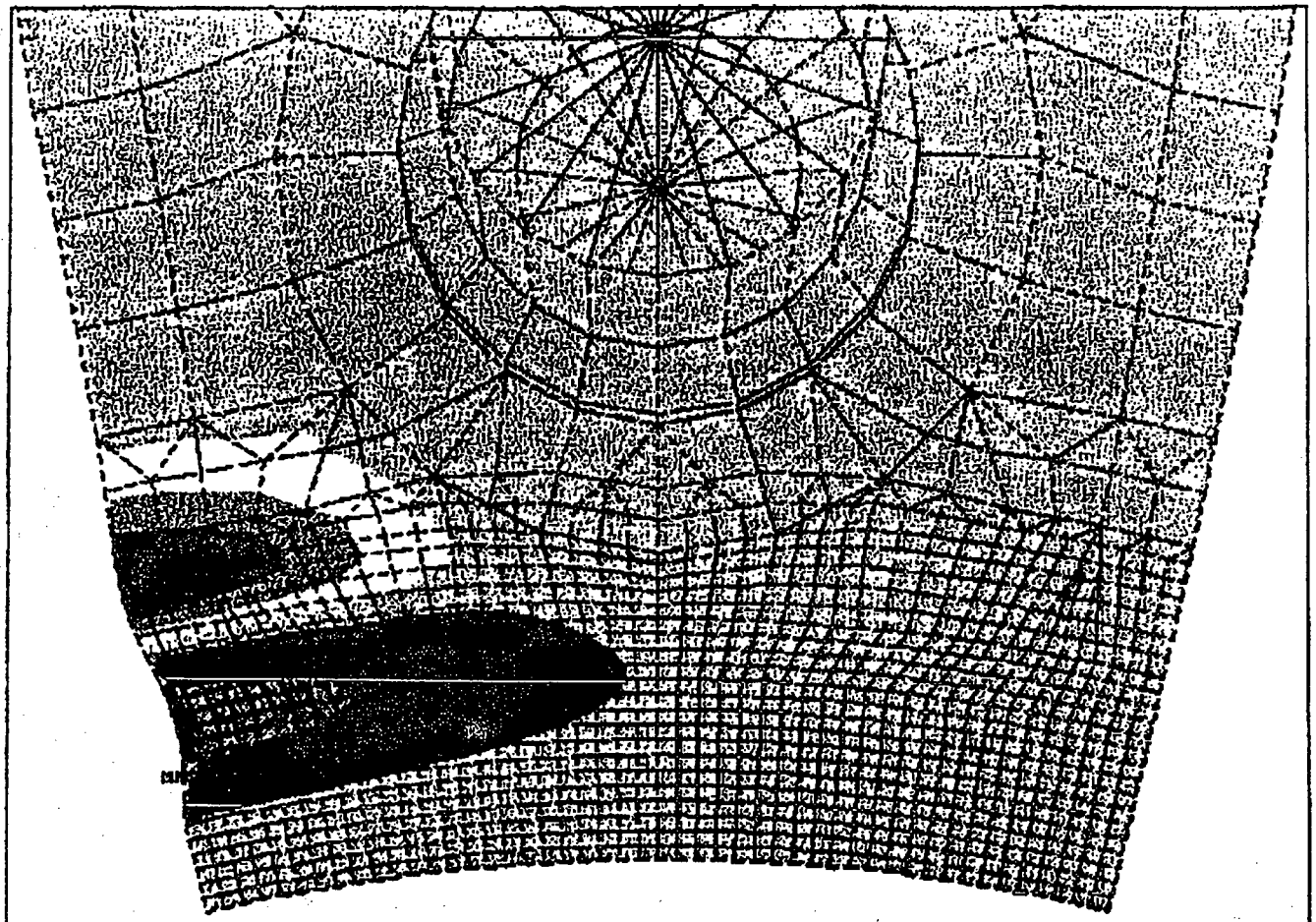

ANSYS 4.4A1
DEC 9 1992
11:35:17
POST1 STRESS
STEP=1
ITER=1
FACT=6.887
UX
D NODAL
DMX =0.005136
SMN =-0.005134
SMX =0.003244

XV =1
ZV =-1
*DIST=110.004
*XF =29.455
*YF =0.460954
*ZF =365.922
ANGZ=-90
CENTROID HIDDEN

-0.005134
-0.004203
-0.003273
-0.002342
-0.001411
-0.480E-03
0.451E-03
0.001382
0.002313
0.003244

OYSTER CREEK DRYWELL ANALYSIS (ASYM-SYMM) - (NO SAND, REFUELING)

FIGURE 25

990-2174

CALCULATION OF ALLOWABLE BUCKLING STRESSES - REFUELING CASE, NO SAND
ONE FOOT INCREASE IN FIXITY CASE; STRESS RUN OCRFRLSB.OUT,
BUCKLING RUN OYCRSBBK.OUT

ITEM	PARAMETER	UNITS	VALUE	LOAD FACTOR
	*** DRYWELL GEOMETRY AND MATERIALS			
1	Sphere Radius, R	(in.)	420	
2	Sphere Thickness, t	(in.)	0.736	
3	Material Yield Strength, Sy	(ksi)	38	
4	Material Modulus of Elasticity, E	(ksi)	29600	
5	Factor of Safety, FS	-	2	
	*** BUCKLING ANALYSIS RESULTS			
6	Theoretical Elastic Instability Stress, Ste	(ksi)	50.394	6.739
	*** STRESS ANALYSIS RESULTS			
7	Applied Meridional Compressive Stress, Sm	(ksi)	7.478	
8	Applied Circumferential Tensile Stress, Sc	(ksi)	3.885	
	*** CAPACITY REDUCTION FACTOR CALCULATION			
9	Capacity Reduction Factor, ALPHAi	-	0.207	
10	Circumferential Stress Equivalent Pressure, Peq	(psi)	13.616	
11	'X' Parameter, X= (Peq/4E) (d/t)^2	-	0.075	
12	Delta C (From Figure -)	-	0.064	
13	Modified Capacity Reduction Factor, ALPHA,i,mod	-	0.313	
14	Reduced Elastic Instability Stress, Se	(ksi)	15.753	2.107
	*** PLASTICITY REDUCTION FACTOR CALCULATION			
15	Yield Stress Ratio, DELTA=Se/Sy	-	0.415	
16	Plasticity Reduction Factor, NUi	-	1.000	
17	Inelastic Instability Stress, Si = NUi x Se	(ksi)	15.753	2.107
	*** ALLOWABLE COMPRESSIVE STRESS CALCULATION			
18	Allowable Compressive Stress, Sall = Si/FS	(ksi)	7.877	1.053
19	Compressive Stress Margin, M=(Sall/Sm -1) x 100%	(%)	5.3	

FIGURE 26

Final

REFNSND2.WK1

9 6 0 - 2 1 7

Exhibit 60

Sandia Report on Structural Integrity Analysis of the Degraded Drywell Containment of Oyster Creek Nuclear Generating Station.

SANDIA REPORT

SAND2007-0055
Unlimited Release
Printed January 2007

Structural Integrity Analysis of the Degraded Drywell Containment at the Oyster Creek Nuclear Generating Station

Jason P. Petti

Prepared by
Sandia National Laboratories
Albuquerque, New Mexico 87185

Sandia is a multiprogram laboratory operated by Sandia Corporation,
a Lockheed Martin Company, for the United States Department of Energy's
National Nuclear Security Administration under Contract DE-AC04-94AL85000.

Sandia National Laboratories

Issued by Sandia National Laboratories, operated for the United States Department of Energy by Sandia Corporation.

Available to DOE and DOE contractors from
U.S. Department of Energy
Office of Scientific and Technical Information
P.O. Box 62
Oak Ridge, TN 37831

Telephone: (865)576-8401
Facsimile: (865)576-5728
E-Mail: reports@adonis.osti.gov
Online ordering: http://www.osti.gov/bridge

Available to the public from
U.S. Department of Commerce
National Technical Information Service
5285 Port Royal Rd
Springfield, VA 22161

Telephone: (800)553-6847
Facsimile: (703)605-6900
E-Mail: orders@ntis.fedworld.gov
Online order: http://www.ntis.gov/help/ordermethods.asp?loc=7-4-0#online

SAND2007-0055
Unlimited Release
Printed January 2007

Structural Integrity Analysis of the Degraded Drywell Containment at the Oyster Creek Nuclear Generating Station

Jason P. Petti
Systems & Structures Department
Sandia National Laboratories
P.O. Box 5800
Albuquerque, NM 87185-0744

Abstract

This study examines the effects of the degradation experienced in the steel drywell containment at the Oyster Creek Nuclear Generating Station. Specifically, the structural integrity of the containment shell is examined in terms of the stress limits using the ASME Boiler and Pressure Vessel (B&PV) Code, Section III, Division I, Subsection NE, and examined in terms of buckling (stability) using the ASME B&PV Code Case N-284. Degradation of the steel containment shell (drywell) at Oyster Creek was first observed during an outage in the mid-1980s. Subsequent inspections discovered reductions in the shell thickness due to corrosion throughout the containment. Specifically, significant corrosion occurred in the sandbed region of the lower sphere. Since the presence of the wet sand provided an environment which supported corrosion, a series of analyses were conducted by GE Nuclear Energy in the early 1990s. These analyses examined the effects of the degradation on the structural integrity. The current study adopts many of the same assumptions and data used in the previous GE study. However, the additional computational recourses available today enable the construction of a larger and more sophisticated structural model.

Acknowledgment

The U.S. Nuclear Regulatory Commission's (NRC) Office of Nuclear Reactor Regulation (NRR) sponsored this analysis program under NRC Project J3312. The author would like to acknowledge Hansraj Ashar, Noel Dudley, Sujit Samaddar, Samir Chakrabarti, Donnie Ashley and Sally Adams of NRC for their technical and administrative oversight of this project. In addition, the author would like to thank Sandia management and colleagues, Michael Hessheimer, Matt Turgeon, and Jeff Smith, for their helpful discussions and advice.

Contents

Abstract 3
Acknowledgment 4
Contents 5
Figures 6
Tables 8
Executive Summary 11
1. Introduction 15
2. Oyster Creek Drywell Finite Element Model 17
2.1 Finite Element Program and Modeling Procedures 17
2.2 Geometry 18
2.2.1 Drywell Head, Cylinder, Stiffeners, and Knuckle 20
2.2.2 Drywell Sphere & Personnel Lock/Equipment Door 24
2.2.3 Ventline and Ventline Jet Deflector 27
2.3 Boundary Conditions 29
2.4 Loading 34
2.4.1 General Loads: Gravity, Dead, Penetration, and Compressible Material Loads 35
2.4.2 Seismic Load 42
2.4.3 Refueling Condition Specific Loads: Live, External Pressure, and Refueling Loads 43
2.4.4 Accident Condition Specific Loads: Internal Pressure and Thermal Loads 45
2.4.5 Post-Accident Condition Specific Load: Hydrostatic Load 45
2.5 Material Properties 46
2.6 Degraded Model 46
2.7 Mesh Size 50
3. Stress Analysis 55
3.1 Refueling Condition 56
3.2 Accident Condition 58
3.3 Post-Accident Condition 64
3.4 Conclusion 66
4. Stability Analysis 67
4.1 Refueling Condition 68
4.2 Post-Accident Condition 72
4.3 Conclusion 76
5. Sandbed Region Minimum Thickness Study 77
6. Summary of Assumptions 81
7. Conclusions 83
8. References 85
9. Appendix A – Natural Frequency Extraction 86
10. Appendix B – Sandbed UT Measurement Data and Shell Thickness Development 91

Figures

Figure 2-1. Oyster Creek Reactor Building and Containment 19
Figure 2-2. Extent of Drywell and Ventlines Including the Current Model (Approximate Elevations) 20
Figure 2-3. Head and Cylinder Shell Thickness and Dimensions 21
Figure 2-4. Model with Head Removed for Refueling 21
Figure 2-5. Cylinder Stiffener Layout 22
Figure 2-6. Knuckle Region Shell Thickness 23
Figure 2-7. Upper and Middle Sphere Shell Geometry 24
Figure 2-8. Thickened Middle Sphere Geometry 25
Figure 2-9. Personnel Lock and Equipment Hatch Geometry 26
Figure 2-10. Lower and Bottom Sphere Geometry 27
Figure 2-11. Drywell Geometry near Ventline Penetration 27
Figure 2-12. Ventline Geometry 28
Figure 2-13. Ventline Deflector Geometry 29
Figure 2-14. Boundary Condition at the Bottom of the Drywell with Cross-section View of Embedded Drywell Shell 30
Figure 2-15. Boundary Condition at the Ends of the Ventlines 31
Figure 2-16. Ventline Header Submodel 32
Figure 2-17. Ventline Spring Locations 32
Figure 2-18. Boundary Condition at the End of the Hatch Penetration 33
Figure 2-19. Boundary Condition at the Stabilizers 33
Figure 2-20. Upper and Lower Spray Header Locations 36
Figure 2-21. Weld Pad Locations 36
Figure 2-22. Flange and Stabilizer Locations 37
Figure 2-23. Upper and Lower Beam Seat Locations 38
Figure 2-24. Personnel Lock and Equipment Door Loads Application Region 38
Figure 2-25. Penetration Load Application Regions in the Drywell Sphere 40
Figure 2-26. Penetration Load Application Regions in the Drywell Cylinder 41
Figure 2-27. Elevation 16' Penetration Load Application Region Between the Ventlines 41
Figure 2-28. Refueling Load on Drywell Cylinder 44
Figure 2-29. Bay 1 UT Measurement Locations Taken from Outside of the Containment (Image Extracted from GPU Nuclear Calculation Sheet, 1993) 48
Figure 2-30. Lower Sphere Bay Combination Regions (Ventlines Removed for Clarity) 48
Figure 2-31. Detailed View of Local Bay 1 Region (Ventline Removed for Clarity) 49
Figure 2-32. Degraded Thicknesses in the Lower Sphere (inches) 50
Figure 2-33. Finite Element Mesh for the Refueling Load Case 51
Figure 2-34. Finite Element Mesh in the Drywell Cylinder for the Refueling Load Case 52
Figure 2-35. Finite Element Mesh for the Accident and Post-Accident Load Cases 52
Figure 2-36. Finite Element Mesh in the Drywell Cylinder and Head for the Accident and Post-Accident Load Cases 53
Figure 2-37. Finite Element Mesh in the Upper and Middle Sphere 53
Figure 2-38. Finite Element Mesh in the Lower Sphere, Bottom Sphere, and Ventlines 54
Figure 2-39. Finite Element Mesh for the Local Thin Regions under the Ventlines in Bay 1 and 13 54

Figure 3-1. Meridional Membrane Stress Distribution in the Lower Sphere for the Refueling Load Case with No Degradation (ksi) 57
Figure 3-2. Meridional Membrane Stress Distribution in the Lower Sphere for the Refueling Load Case with Degradation (ksi) 57
Figure 3-3. Meridional Membrane Stress Distribution in Local Bay 13 Region for the Refueling Load Case with Degradation (ksi) 58
Figure 3-4. Circumferential Membrane Stress Distribution in Sandbed for the Accident Load Case with No Degradation (Internal Pressure without Thermal Load) (ksi) 61
Figure 3-5. Circumferential Membrane Stress Distribution in Sandbed for the Accident Load Case with No Degradation (Internal Pressure with Thermal Load) (ksi) 62
Figure 3-6. Circumferential Membrane Stress Distribution in Sandbed and Local Thin Region Under the Ventline in Bay 13 for the Accident Load Case with Degradation (Internal Pressure without Thermal Load) (ksi) 62
Figure 3-7. Circumferential Membrane Stress Distribution in Sandbed for the Accident Load Case with Degradation (Internal Pressure with Thermal Load) (ksi) 63
Figure 3-8. Meridional Membrane Plus Bending Stress Distribution (Tension on the Inside Surface of the Drywell Shell) in Sandbed for the Accident Load Case with No Degradation (Internal Pressure with Thermal Load) (ksi) 63
Figure 3-9. Circumferential Membrane Stress Distribution in Sandbed for the Post-Accident Load Case with No Degradation (ksi) 65
Figure 3-10. Circumferential Membrane Stress Distribution in Sandbed and Local Thin Region Under the Ventline in Bay 13 for the Post-Accident Load Case with Degradation (ksi) 65
Figure 4-1. Buckling at the Upper Beam Seat for the Refueling Case with No Degradation 68
Figure 4-2. Buckling in the Sandbed Region for the Refueling Case with No Degradation 69
Figure 4-3. Buckling at the Upper Beam Seat for the Refueling Case with Best Estimate Degradation 70
Figure 4-4. Buckling in the Sandbed Region for the Refueling Case with Best Estimate Degradation 71
Figure 4-5. Buckling in the Cylinder for the Post-Accident Load Case with No Degradation 73
Figure 4-6. Buckling in the Sandbed Region for the Post-Accident Load Case with No Degradation 74
Figure 4-7. Buckling in the Sandbed Region for the Post-Accident Load Case with Best Estimate Degradation 75
Figure 5-1. Drywell Lower Sphere for Establishing a Minimum Thickness in the Sandbed Region (Ventlines and Hatch Removed for Clarity) 78
Figure 5-2. Effective Factor of Safety Values Computed for Various Thicknesses in the Sandbed Region for the Refueling Load Combination 79
Figure 5-3. Buckling in the Sandbed Region with a Thickness of 0.844" for the Refueling Load Combination 80
Figure 9-1. Modified Model for Natural Frequency Extraction 87
Figure 9-2. Lower Sphere Region (Highlighted in Red) Set to a Thickness of 0.835" for the Degraded Natural Frequency Extraction 88
Figure 9-3. Base State and the First 5 Frequencies and Mode Shapes for the Drywell Containment with No Degradation 89

Figure 9-4. Base State and the First 5 Frequencies and Mode Shapes for the Drywell Containment with Degradation 90
Figure 10-1. Bay 1 and Bay 3 UT Measurement Locations Taken from Outside of the Containment (Images Extracted from GPU Nuclear Calculation Sheet, 1993) 91
Figure 10-2. Bay 1 UT Measurement Locations Taken from Outside of the Containment (Image Extracted from GPU Nuclear Calculation Sheet, 1993) 96
Figure 10-3. Bay 3 UT Measurement Locations Taken from Outside of the Containment (Image Extracted from GPU Nuclear Calculation Sheet, 1993) 96
Figure 10-4. Bay 5 UT Measurement Locations Taken from Outside of the Containment (Image Extracted from GPU Nuclear Calculation Sheet, 1993) 97
Figure 10-5. Bay 7 UT Measurement Locations Taken from Outside of the Containment (Image Extracted from GPU Nuclear Calculation Sheet, 1993) 97
Figure 10-6. Bay 9 UT Measurement Locations Taken from Outside of the Containment (Image Extracted from GPU Nuclear Calculation Sheet, 1993) 98
Figure 10-7. Bay 11 UT Measurement Locations Taken from Outside of the Containment (Image Extracted from GPU Nuclear Calculation Sheet, 1993) 98
Figure 10-8. Bay 13 UT Measurement Locations Taken from Outside of the Containment (Image Extracted from GPU Nuclear Calculation Sheet, 1993) 99
Figure 10-9. Bay 15 UT Measurement Locations Taken from Outside of the Containment (Image Extracted from GPU Nuclear Calculation Sheet, 1993) 99
Figure 10-10. Bay 17 UT Measurement Locations Taken from Outside of the Containment (Image Extracted from GPU Nuclear Calculation Sheet, 1993) 100
Figure 10-11. Bay 19 UT Measurement Locations Taken from Outside of the Containment (Image Extracted from GPU Nuclear Calculation Sheet, 1993) 100

Tables

Table 2-1. Cylinder Stiffeners 22
Table 2-2. Load Combination Components 34
Table 2-3. Dead Load Tractions 39
Table 2-4. Penetration Load Tractions 42
Table 2-5. Live Load Tractions 44
Table 2-6. Main Drywell Shell Model Thicknesses, Original and Degraded 47
Table 2-7. Degraded Lower Sphere Shell Model Thicknesses 49
Table 3-1. Refueling Load Case Peak Stresses with No Degradation, Primary Stresses (Percentage of ASME Limit in Parenthesis) 56
Table 3-2. Refueling Load Case Peak Stresses with Degradation, Primary Stresses (Percentage of ASME Limit in Parenthesis) 56
Table 3-3. Accident Load Case Peak Stresses with No Degradation, Primary Stresses (Percentage of ASME Limit in Parenthesis) 59
Table 3-4. Accident Load Case Peak Stresses with No Degradation, Primary + Secondary Stresses (Percentage of ASME Limit in Parenthesis) 60
Table 3-5. Accident Load Case Peak Stresses with Degradation, Primary Stresses (Percentage of ASME Limit in Parenthesis) 60
Table 3-6. Accident Load Case Peak Stresses with Degradation, Primary + Secondary Stresses (Percentage of ASME Limit in Parenthesis) 60

Table 3-7. Post-Accident Load Case Peak Stresses with No Degradation, Primary Stresses (Percentage of ASME Limit in Parenthesis) 64
Table 3-8. Post-Accident Load Case Peak Stresses with Best Estimate Degradation, Primary Stresses (Percentage of ASME Limit in Parenthesis) 64
Table 4-1. Buckling Evaluation at the Upper Beam Seat for the Refueling Load Case with No Degradation 69
Table 4-2. Buckling Evaluation in the Sandbed Region for the Refueling Load Case with No Degradation 70
Table 4-3. Buckling Evaluation at the Upper Beam Seat for the Refueling Load Case with Best Estimate Degradation 71
Table 4-4. Buckling Evaluation in the Sandbed Region for the Refueling Load Case with Best Estimate Degradation 72
Table 4-5. Buckling Evaluation in the Cylinder for the Post-Accident Load Case with No Degradation 73
Table 4-6. Buckling Evaluation in the Sandbed Region for the Post-Accident Load Case with No Degradation 75
Table 4-7. Buckling Evaluation in the Sandbed Region for the Post-Accident Load Case with Best Estimate Degradation 76
Table 5-1. Main Drywell Shell Model Thicknesses Outside of Sandbed Region 78
Table 5-2. Buckling Evaluation for the Refueling Load Case with a Thickness of 0.844" in the Sandbed 80
Table 7-1. Comparison of Conclusion Between GE Study (GE, 1991a and b) and the Current Study 83
Table 9-1. Drywell Shell Thicknesses for Natural Frequency Extraction Analyses 87
Table 9-2. Summary of the First 5 Natural Frequencies for Drywell with and without Degradation 90
Table 10-1. UT Measurement Data for Bay Combinations 1-3, 3-5, 5-7, and 7-9. 92
Table 10-2. UT Measurement Data for Bay Combinations 9-11, 11-13, and 13-15. 93
Table 10-3. UT Measurement Data for Bay Combinations 15-17, 17-19, and 19-1. 94
Table 10-4. UT Measurement Data for Local Bay 1 and 13 Regions. 95

(Page Intentionally Left Blank)

Executive Summary

The Oyster Creek Nuclear Generating Station is a GE Mark I BWR which began operation in 1969. It is located in New Jersey and is operated by AmerGen/Exelon. The drywell portion of the containment vessel consists of a free-standing welded steel shell with an upper cylindrical section atop a lower spherical section. The steel containment rests on a reinforced concrete base mat and is surrounded by a reinforced concrete reactor building.

Corrosion of the steel drywell containment shell at Oyster Creek was first observed during an outage in November 1986 (GE, 1991a). Subsequent inspections discovered reductions in the shell thickness due to general corrosion in many regions of the drywell containment. Significant corrosion occurred in the sandbed region of the lower sphere. The sandbed is located below the ventlines that lead down to the torus section of the containment and just above the concrete base mat. A small pocket of sand was originally placed adjacent to the steel shell at the base to provide a transition, or "cushion", as the shell emerges from being embedded in concrete. Inspections concluded that water leakage occurred through the gap between the reactor building and the drywell shell and collected in the sandbed region. Since the wet sand provided an environment which supported corrosion, the Licensee embarked on a series of corrective actions including removing the sand from the sandbed region, cleaning and coating the affected surfaces, and sealing the gap between the containment vessel and the concrete to prevent further penetration by water. The Licensee also implemented periodic re-inspections of selected areas of the vessel to monitor the progression, if any, of the corrosion damage.

Prior to the removal of the sand from the sandbed region, the Licensee tasked GE Nuclear with assessing the vessel in its degraded state to determine whether or not the degradation prevented the vessel from performing its intended design function. They concluded that the degraded drywell shell, with the sand removed, still satisfied the ASME Boiler & Pressure Vessel (B&PV) Code stress and stability limits, albeit with a reduced design pressure. The sand was removed and based on subsequent inspections, the Licensee has claimed that there is no on-going corrosion in the sandbed region of the drywell shell. Inspections have, however, discovered ongoing corrosion in the portions of the drywell above the sandbed region (sphere and cylinder).

In July of 2005, the Licensee submitted an application to the U.S. Nuclear Regulatory Commission (NRC) to extend the operating life of the plant from 40 to 60 years (extend from 2009 to 2029). The NRC Office of Reactor Regulation (NRR) commissioned Sandia National Laboratories (SNL) to perform an evaluation of the degraded containment vessel to determine if the Licensee's contention, that the current known condition of the vessel and the progressive damage expected over the extended service life did not compromise the design function or licensing basis, was reasonable. The scope of the analyses performed by Sandia was defined by NRC staff and the procedures employed were discussed with NRC staff throughout the project.

In this evaluation, Sandia developed a detailed three-dimensional (3D) finite element model of the drywell containment vessel using information provided by the NRC and the Licensee. Analyses for the governing load combinations were performed for the vessel in its' original, as-designed state and for a representation of the vessel in an approximation of the current degraded state. Based on previous work performed at Sandia (Cherry and Smith, 2001, Spencer et. al,

2006), modeling of the corrosion damage was represented by uniform shell thinning. The degraded condition of the sandbed region in the model is based on the measurements performed in 1993 (GPU Nuclear, 1993). These measurements were taken prior to the application of the protective coating. The shell thicknesses of the model in the sandbed region are based on averages of the available measurements. Assuming these measurements made in the accessible portions of the sandbed are representative of the entire region, the average of the measurements should be conservatively biased since the thickness measurements were only made at the thinnest points (by visual inspection). No statistical analysis of the Licensee's in-situ thickness measurements was performed. Rather, the averaging procedure used to develop thicknesses was based on engineering judgment. No additional reduction in thickness due to ongoing corrosion during the 20-year plant life extension was considered in the sandbed region, accepting the Licensee's contention that corrosion processes have been arrested. The thicknesses in the upper portions of the degraded drywell model were based on the additional thickness measurements performed by the Licensee over the past 20 years and included an estimate of future corrosion by linear extrapolation of past corrosion rates.

The models were then used to evaluate the structural integrity of the vessel in terms of the stress limits specified in the ASME Boiler and Pressure Vessel (B&PV) Code, Section III, Division I, Subsection NE, and in terms of buckling (stability) limits specified in ASME B&PV Code Case N-284. The analyses performed in this study aim only to independently confirm the general conclusions reached in a previous study performed by GE Nuclear Energy in the early 1990s. Two important points regarding the current analysis are important to recognize:

- The original design of the containment based on the analyses by the Licensee and GE and subsequent analyses of the degraded vessel have been accepted by the NRC and are part of the current licensing basis.

- The current analysis by Sandia cannot, and is not intended to, reproduce the results of the original licensing basis analyses. As such, the baseline (i.e. un-degraded) analysis was performed so that the effects of the degradation could be clearly isolated. The results of the current analysis should, therefore, focus more on the relative reduction in design margin due to the corrosion modeled, than the absolute stresses or stability limits which are calculated. This relative reduction in margin, examined together with the current licensing basis and additional relevant information, should be considered by the NRC staff in the development of the basis to accept or reject the Licensee's application for an extended license. By itself, the analysis performed by Sandia cannot be used for this decision.

A significant amount of data, primarily regarding the external loads on the drywell shell, was extracted directly from the GE analyses due to insufficient plant information to allow independent calculation of these loads. Every effort was made to use the best available information for the current models and analyses. However, since the GE analyses and the current analyses use a different modeling approach, the data taken directly from the GE analysis was of necessity modified to fit the current approach.

The purpose of the Sandia analyses was to assess the effects of degradation on the stress and buckling behavior for the drywell containment. In this context, the results of the analyses show that the degradation does not result in a definitive violation of the stresses or buckling criterion in the ASME code given the modeling procedures and assumptions outlined in this report.

(Page Intentionally Left Blank)

1. Introduction

This study examines the effects of the degradation experienced in the steel drywell containment at the Oyster Creek Nuclear Power Plant. Specifically, the structural integrity of the containment shell is examined in terms of the stress limits using the ASME Boiler and Pressure Vessel (B&PV) Code, Section III, Division I, Subsection NE, and examined in terms of buckling (stability) using the ASME B&PV Code Case N-284.

The analyses performed in this study aim to independently confirm the general conclusions reached in a previous study performed by GE Nuclear Energy in the early 1990s. Since the GE analyses and the analyses performed here use different models, and in some cases, different assumptions, a direct comparison to the previous GE analysis is not the intent of this effort. In addition, a significant amount of data was taken directly from the GE analysis and applied or modified as required for the current study. This was necessary when information was not available, or was not made available, to be independently verified. Within the project schedule, all efforts were made to use the best available information for the models and analysis used in the current study. All stress and buckling analyses were performed for both a representation of the containment in its degraded condition and in its original, as-built, condition. The study of the as-built conditions provides base-line analyses to assess the effects of degradation on the stress and buckling behavior for the containment.

Degradation of the steel drywell containment shell at Oyster Creek was first observed during an outage in November 1986 (GE, 1991a). Subsequent inspections discovered reductions in the shell thickness due to corrosion throughout the containment. Specifically, significant corrosion occurred in the sandbed region of the lower sphere. The sandbed is located below the ventlines that lead down to the torus section of the containment. The small pocket of sand was originally placed adjacent to the steel shell at the base to provide a transition as the shell emerges from being embedded in concrete. Water leakage through the gap between the reactor building and the drywell shell collected in the sandbed region. Since the presence of the wet sand provided an environment which supported corrosion, a series of analyses were conducted by GE Nuclear Energy to examine the effects of removing the sand. GE determined that the degraded drywell shell with removal of the sand was acceptable based on ASME B&PV stress and stability limits. Therefore, the sand was removed and the surface of the drywell shell epoxy coated to protect the surface from additional degradation. Subsequent inspections have supported the claim that there is no on-going corrosion in the sandbed region of the drywell shell. However, inspections have shown the existence of ongoing corrosion in the upper portions of the drywell (sphere and cylinder).

Thickness measurements have been performed during refueling outages at the plant over the last 20 years. The UT measurement data used to estimate the thickness of the containment shell was limited to a few selected regions in the sandbed and throughout the remaining containment. Since only a very small percentage of the total shell surface has been measured, a number of assumptions were made in this study to assign appropriate shell thicknesses throughout the drywell model. These are described in more detail in subsequent sections.

The degraded Oyster Creek drywell shell was analyzed in this study using a full three-dimensional (3D) finite element model. The previous analyses by GE employed both an axi-symmetric and a 36° slice model of the drywell. These analyses were conducted in the 1990-91 timeframe and were constrained by the computational limits of the day. Due to a significant increase in computational power relative to the time of the GE analysis, a full 3D model was created here and is described in detail in this report.

2. Oyster Creek Drywell Finite Element Model

A full three-dimensional (3D) finite element model of the Oyster Creek drywell was developed for this study. A full 3D, 360°, model enables a more sophisticated analysis which includes structural detail that account for the asymmetries of the containment vessel. It also provides for a more realistic representation of the boundary conditions, thicknesses transitions, and the spatial variation of the degradation.

Two reports summarizing the work performed by GE (GE, 1991a and 1991b) along with a partial set of drywell structural drawings (CB&I, 1980) were the two resources used to develop the model geometry. Unfortunately, many of the resources available to the GE analysts were not available, or were not made available in time for use in this study. In a number of instances, this has led to the need to assume information required to complete this program. For example, many items related to the structural loads documented by GE could not be confirmed or recreated. In these cases, the information that was available from the GE study and/or other sources was used, combined, or adapted for use in the current analysis. These assumptions and procedures are documents throughout this report, and are summarized in a section at the end of this report.

2.1 Finite Element Program and Modeling Procedures

The finite element modeling conducted in this study uses the ABAQUS (ABAQUS, 2004) suite of analysis software. Specifically, Version 6.5-6 of the ABAQUS/Standard general-purpose finite element program and the ABAQUS/CAE interactive environment are used to perform the analyses and to create the solid models and finite element meshes, respectively. ABAQUS/Standard is employed since all of the analyses performed here are static. The CAE component of ABAQUS provides an interface for defining the model geometry, material properties, shell thicknesses, boundary conditions, loadings, and meshing. After the analysis is completed using ABAQUS/Standard, the Visualization module within CAE (also identified as ABAQUS/Viewer) is used to examine the analysis results.

The analyses performed here include geometric nonlinearities, also known as large-displacement or finite strain analyses. When applying geometric nonlinearities to the analysis, the element formulation at each load step is performed using the current configuration (e.g. deformed shape).

A combination of standard, "S4R", 4-noded, and "S3R, 3-noded, reduced integration shell elements are used here to model the drywell. The meshing technique used is identified as "quad-dominated" in ABAQUS/CAE. The method meshes the geometry using quad (4-noded) elements, but does introduce tri (3-noded) elements in regions where introducing a quad element would result in a severely distorted element.

Shell elements are used in modeling when the thickness dimension is significantly less than the in-plane dimensions. Typically, the reference surface of the shell element is set at the mid-section, or centerline, of the structure being modeled. The thickness of the shell is set in the

"Section" definitions within ABAQUS. Each nodes in a given shell elements have six degrees-of-freedom, three translational and three rotational.

The use of shell elements introduces discontinuities at the interface between plates of differing thickness. The actual structure also included discontinuities at these locations due to the interface of plates of differing thickness. These interfaces often include a small tapered region. Here, the thicker plate is gradually reduced in thickness over a length on the order of the plate thickness, and welded to the thinner plate. In the models developed in this study, a small region is included at the interface of plates of differing thickness to represent the transition region in the actual structure. This "transition" region is set to a thickness equal to the average of the plates on either side. The length of the model transition is based on the actual, or estimated, transition length given in the structural drawings (CB&I, 1980).

2.2 Geometry

The Oyster Creek reactor building contains a GE BWR Nuclear Steam Supply System with a steel Mark I containment vessel. Figure 2-1 illustrates the pressure suppression system which includes the pressure suppression chamber (torus) and the drywell (containment vessel) connected with a series of ventlines. Figure 2-1 also shows the positioning of the containment vessel within the reactor building (one half of the reactor building has been removed to view the containment vessel) and a detailed view of the sandbed region below the ventlines. Since the drywell is not exactly a symmetric structure, it is modeled in full for this study. The series of ventlines which connect the drywell with the torus includes a flexible bellow (not shown) at the interface between the ventline and the torus. Since these bellows prevent significant structural interaction, the torus shell was not included in the model and is shown in Figure 2-1 for illustrative purposes only. As stated previously, the ventlines are modeled down past the interface with the torus, ending at the intersection with the ventline header.

Figure 2-2 shows the extent of the structure modeled for the current analysis. As stated above, the torus is not included in the model. The drywell is modeled from an elevation of 2'-3" (2 feet, 3 inches) to an elevation of 107'-9". At the top of the drywell, the head region is a 2:1 ellipse. Below the head, the drywell cylinder has an inside diameter of 33 feet (33') and the drywell sphere has an inside diameter of 70 feet (70'). The cylindrical and spherical regions are joined by a thickened knuckle. The equator of the drywell sphere is located at elevation 37'-3". The largest drywell penetration is the personnel lock/equipment hatch located at an elevation of 27'-6". The centerline of the ventlines extends down to an elevation of 0'-6". The sandbed region is located in the lower sphere of the drywell shell just below the ventlines. Below the sandbed, part of the lower sphere and the entire bottom sphere are completely contained within concrete on both sides below elevation 8'-11.25" (lower sphere extends down to elevation 6'-10.25"). Additional details related to the geometry, shell thickness, boundary conditions, and loadings are provided throughout the next several subsections. The plate thicknesses given in these sections are for the drywell in its as-built state. The thinning due to the corrosion that exists in the shell is described in Section 2.6

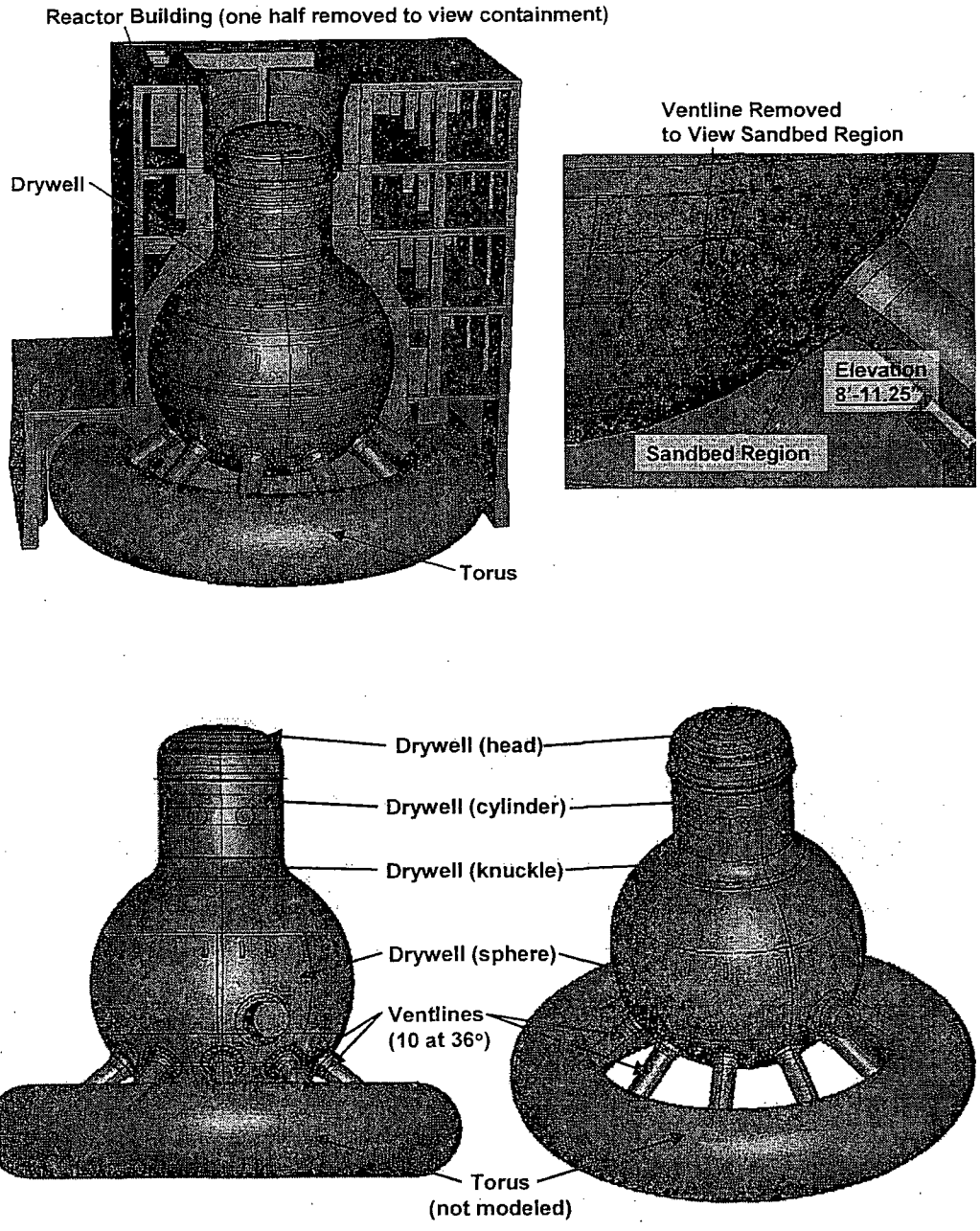

Figure 2-1. Oyster Creek Reactor Building and Containment

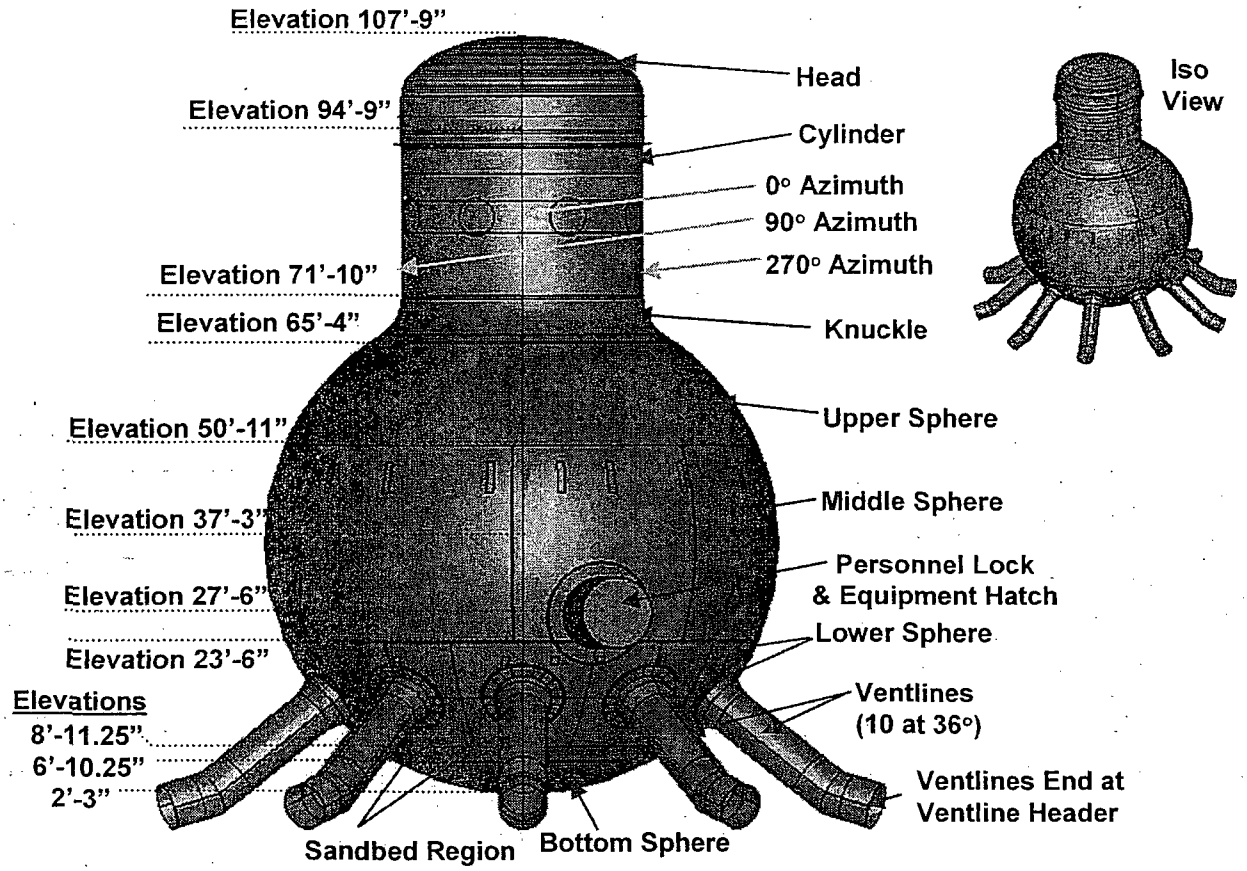

Figure 2-2. Extent of Drywell and Ventlines Including the Current Model (Approximate Elevations)

2.2.1 Drywell Head, Cylinder, Stiffeners, and Knuckle

Figure 2-3 shows the drywell head residing at the top of the structure up to an elevation of 107'-9". The 2:1 ellipse that defines the geometry of the head region extends down to an elevation of 99'-6". The head region has a shell thickness of 1.1875". In the region below the head, the flange assembly includes a double tongue-and-groove seal at an elevation of 94'-9". At this elevation, the head separates from the drywell during refueling as shown in Figure 2-4. For the analyses of the refueling load case, a separate model was created that has an identical geometry to the full model with the exception of the head being removed. In the full model, the flange assembly region is assigned the same thickness at the head, 1.1875". The geometry of the flange assembly is complex with the actual thickness varying from 1.25" to 1.5".

Since the thickness dimension is not represented when using shell elements, the location of the shell in the model is defined in space at the mid-section of the actual shell. This leads to the radius of the flange assembly to be 16'-6.59375". This number is computed by adding the actual inside radius in this region, 16'-6", to one half of the shell thickness, or 1.1875"/2.

Underneath the flange assembly, the shell thickness is reduced to 0.64" below elevation 92'-2.75". The model also includes a thin "transition" region between the flange assembly region

and the lower cylinder. In the actual structure, the steel plate is tapered from one thickness to the next over a short distance. The transition region represents this tapered region and is assigned a thickness equal to the average, 0.91375", of the two surrounding plates (e.g. 1.1875" and 0.64"). Since the inside radius of the cylinder remains constant and the thickness of the lower cylinder is less than the flange assembly region, the centerline of the shell is shifted inward producing a radius of 16'-6.32".

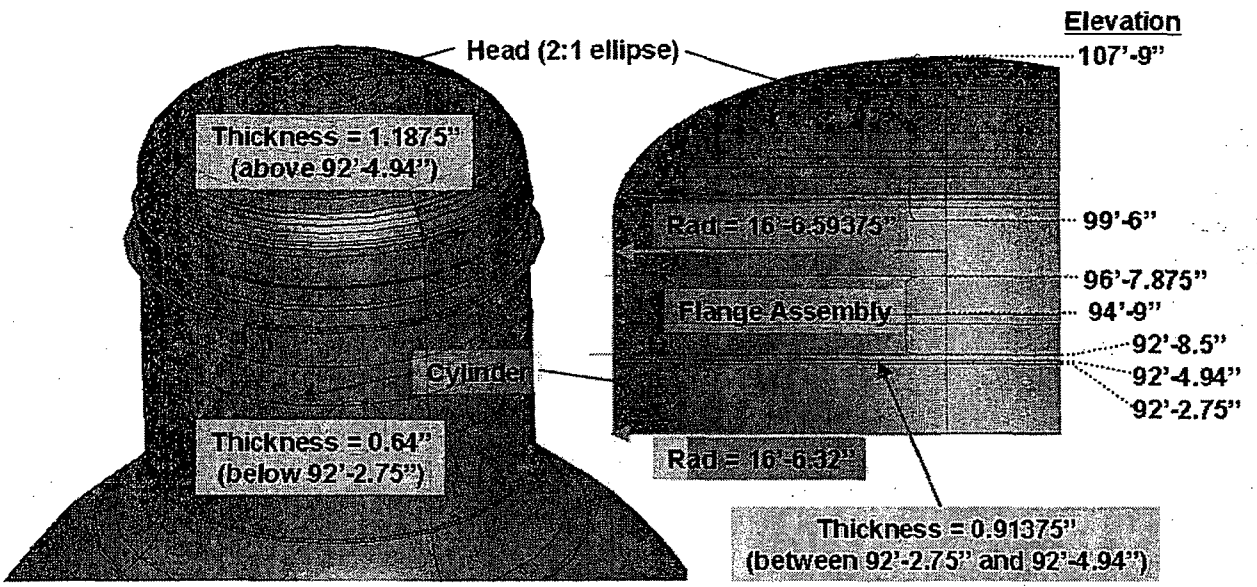

Figure 2-3. Head and Cylinder Shell Thickness and Dimensions

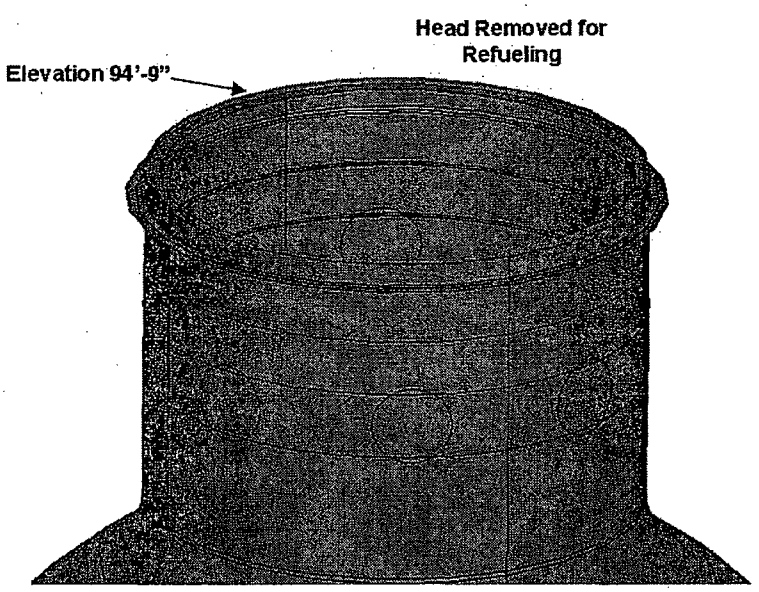

Figure 2-4. Model with Head Removed for Refueling

The cylinder region of the drywell also contains several stiffeners. Figure 2-5 and Table 2-1 summarizes the stiffener's dimensions and positions. Figure 2-5 gives an inside "cut" view of the cylinder. Half of Stiffener-0 resides within the cylinder and half resides outside the cylinder. Stiffeners 1, 3, 4, and 5 are positioned completely within the cylinder. Only Stiffener-2 and 2a are attached completely to the outside of the cylinder. Stiffener-2 is connected directly to the outside surface of the cylinder shell. Stiffener-2a is thinner than Stiffener-2 and is attached to the outer extent of Stiffener-2.

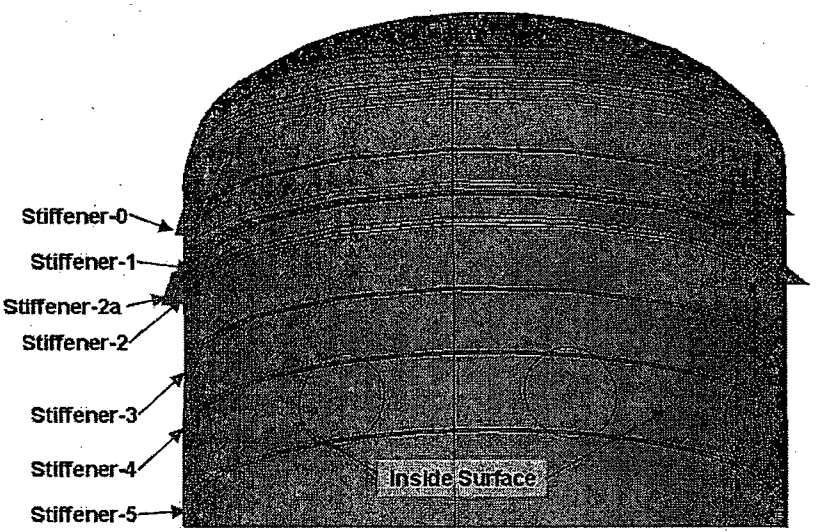

Figure 2-5. Cylinder Stiffener Layout

Table 2-1. Cylinder Stiffeners

Stiffener	Elevation	Length (inches)	Thickness (inches)	Orientation
Stiffener-0	96'-7.875"	12.5	2.25	half & half
Stiffener-1	94'-3"	12	1.0	inside
Stiffener-2	92'-8.5"	7	2.75	outside
Stiffener-2a	92'-8.5"	7.38	1.0	outside
Stiffener-3	88'-8.5"	6	0.5	inside
Stiffener-4	84'-11.8"	6	0.75	inside
Stiffener-5	80'-6.3"	6	0.75	inside

The knuckle illustrated in Figure 2-6 connects the drywell's cylindrical region to the upper sphere. A thin transition region is introduced between the cylinder and knuckle and between the knuckle and upper sphere. The upper fillet portion of the knuckle has a 72" radius. Below an elevation of 66'-5.77", the knuckle fillet is joined to the upper sphere with a linear section of the knuckle. The thickness of the entire knuckle (elevation 65'-4.27" to 71'-6.28") is set at 2.5625". This is the minimum specified thickness in this region as stated in the previous GE study (GE, 1991a). However, the structural drawings (CB&I, 1980) and other sections of the GE study indicate a knuckle thickness of 2.625". The lower value of 2.5625" is adopted for the undegraded thickness of the knuckle since that value was confirmed[1] and is more conservative.

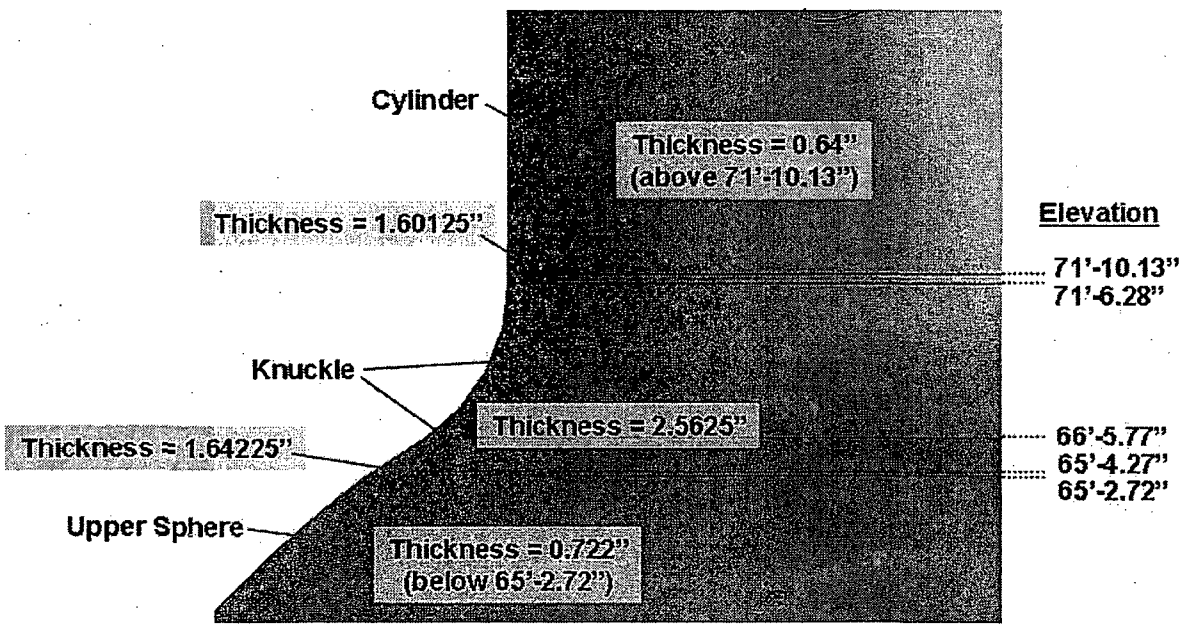

Figure 2-6. Knuckle Region Shell Thickness

[1] June 21, 2006, conference call between Sandia National Laboratories, NRC, and Exelon.

2.2.2 Drywell Sphere & Personnel Lock/Equipment Door

The largest section of the drywell is the spherical region which lies below the cylinder. The sphere has an inside radius of 35' and is composed of four main regions of different thickness. Figure 2-7 shows the upper and middle sphere regions. The upper sphere has a thickness of 0.722" and the middle sphere was constructed with a thickness of 0.77". As mentioned previously, the position of the shell in the model created here is set at the mid-section of the shell in the actual structure. Therefore, the radii of the upper and middle sphere are 35'-0.361" and 35'-0.385", respectively. The 0.746" thick transition region between the upper and middle sphere lies between elevations 50'-11.25" and 50'-10.8". At the lower extent of the middle sphere, a 0.962" transition region connects the middle sphere with the 1.154" thick lower sphere between elevations 23'-6.74" and 23'-4.82".

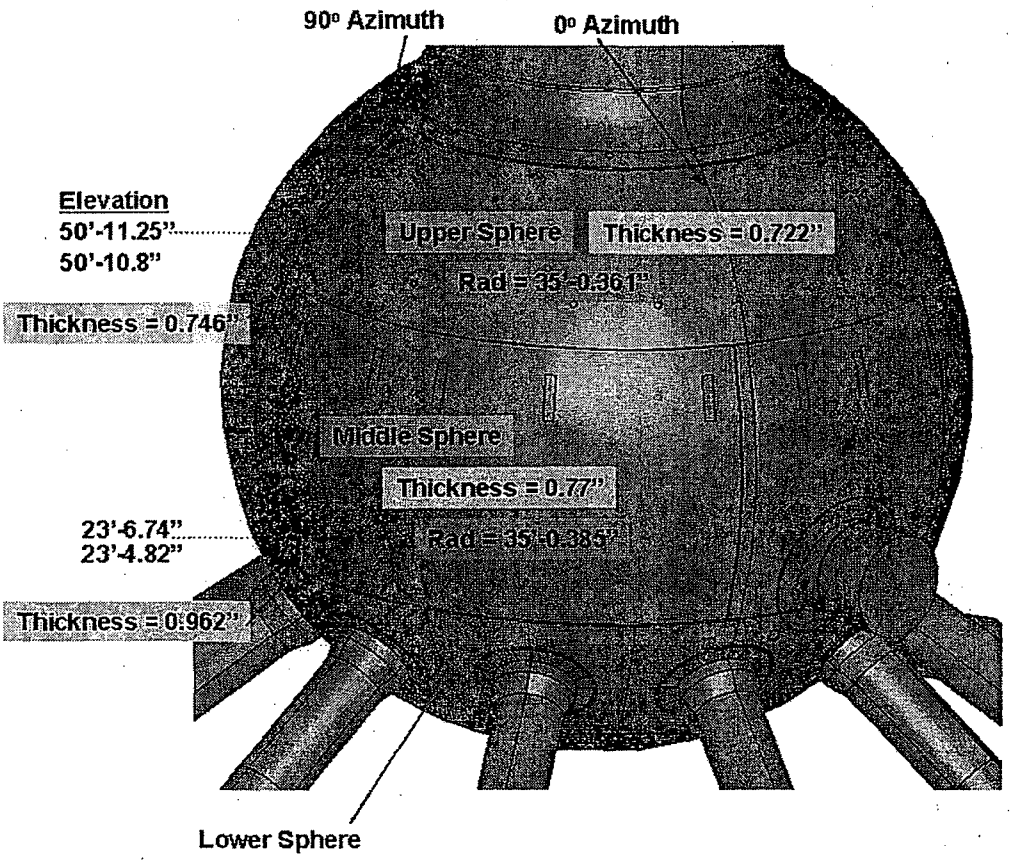

Figure 2-7. Upper and Middle Sphere Shell Geometry

A section of the middle sphere is thickened between azimuths 2.5° and 317.5 ° due to the presence of the personnel lock and equipment hatch penetration as shown in Figure 2-8. (The values for the azimuths were assumed from an examination of the structural drawings (CB&I, 1980).) This thickened region is 1.0625" and extends from the lower sphere to the upper sphere (23'-6.74" to 50'-10.8"). Transition regions surround the thickened middle sphere on all sides. The transition along the top is 0.89225", along the vertical sides is 0.91625", and along the bottom (outside of the hatch) is 1.10825". There are also two small transition regions at the top corners (0.819125") and two small transition regions at the bottom corners (1.035125") of the thickened middle sphere. The thickness of these corner regions are weighted averages of the surrounding plates.

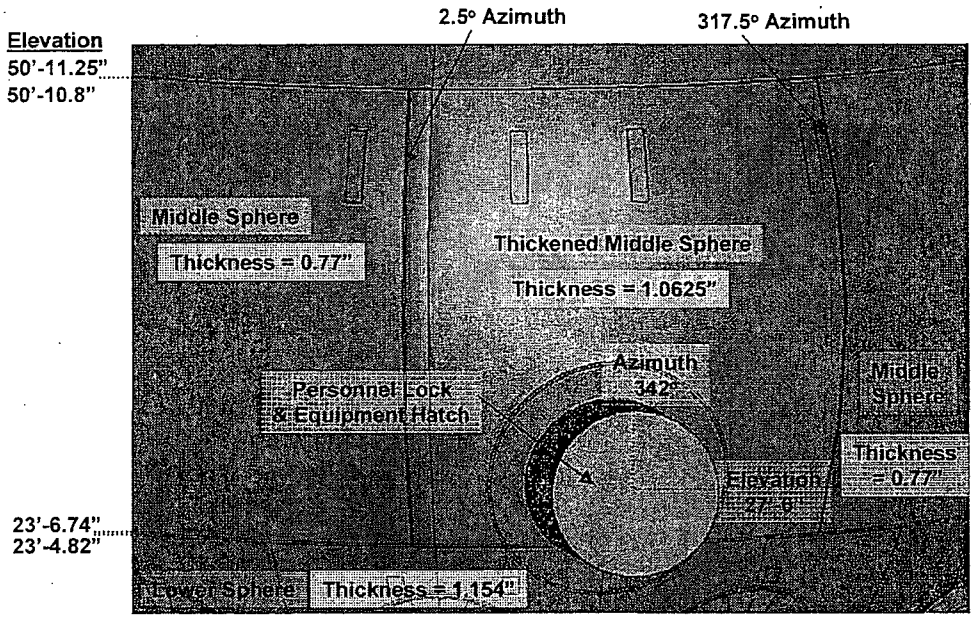

Figure 2-8. Thickened Middle Sphere Geometry

Figure 2-9 illustrates the personnel lock and equipment hatch penetration. The penetration is 10' in diameter and extends from the thickened middle sphere down into the lower sphere. The center of the penetration is located at an elevation of 27'6" and an azimuth of 342°. Embedded within the drywell shell and surrounding the penetration is a 2.625" thick plate. The outer diameter of this thickened region is approximately 14'-1.5". A thin transition region lies between this thickened plate surrounding the penetration and the surrounding thickened middle sphere (t = 1.84375") and lower sphere (t = 1.8895").

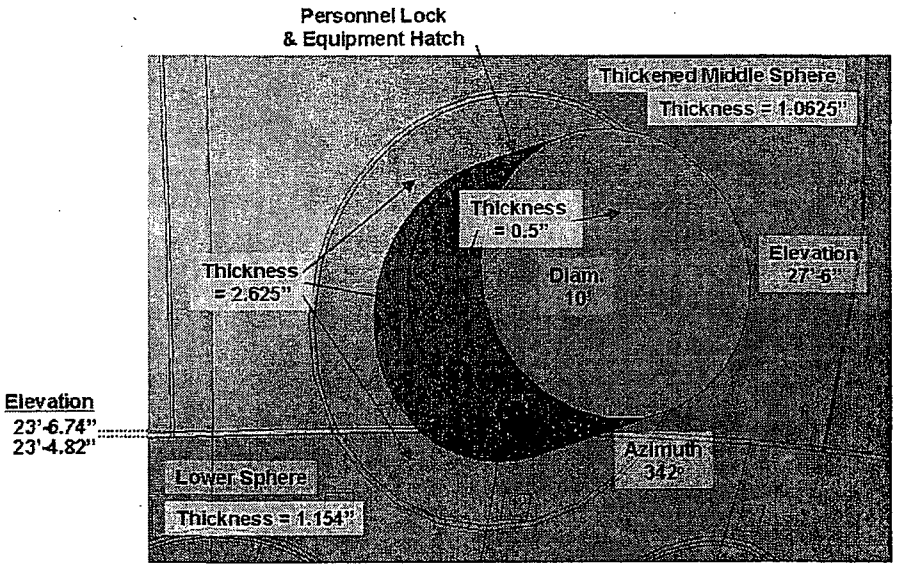

Figure 2-9. Personnel Lock and Equipment Hatch Geometry

The penetration extends away from the drywell shell to a distance of 41'-6" from the centerline of the drywell. This is the location of a vertical support within the reactor building. This is discussed in additional detail in the following section on boundary conditions. The penetration has a thickness of 2.625" at the connection with the drywell shell. The outer 5'-9" length of the penetration has been set to a thickness of 0.5". In the actual structure, the thickness of this outer region varies and has been set to 0.5" to simplify the model. Only this outer shell of the penetration is modeled here. The internals of the personnel lock and equipment hatch are included through applied loads and are described in the loading section.

Below the middle sphere and the hatch penetration is the 1.154" thick lower sphere region of the drywell as shown in Figure 2-10. The lower sphere extends from an elevation of 23'-4.82" down to 6'-10.25" and has a radius of 35'-0.577". The section of the lower sphere below an elevation of 8'-11.25" is embedded within concrete on both sides. The lowest extent of the drywell is the bottom sphere with a thickness of 0.676" and a radius of 35'-0.338". The entire bottom sphere is also embedded within concrete. The sandbed region is located at the bottom of the lower sphere, from elevation 8'-11.25" up to 12'-3".

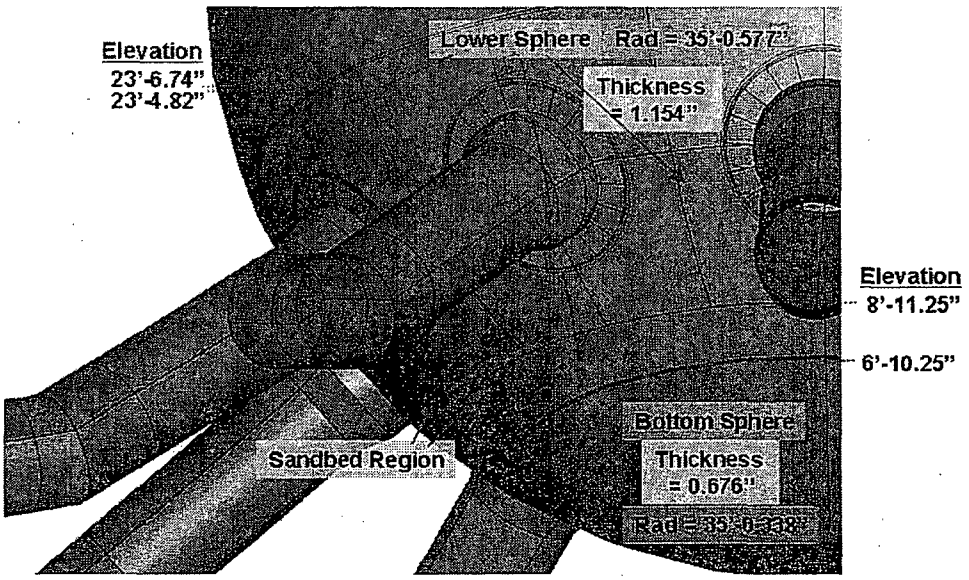

Figure 2-10. Lower and Bottom Sphere Geometry

2.2.3 Ventline and Ventline Jet Deflector

Within the lower sphere of the drywell, 10 ventlines spaced at 36° connect the torus to the drywell. As shown in Figure 2-11, the elevation of the center of the ventline penetration into the drywell shell is 15-6.8". (The actual elevation is 15'-7.25". The difference is due to round-off error in constructing the geometry). The ventline is 7'-10" in diameter at the intersection with the drywell shell and transitions down to a diameter of 6'-6.25". As with the personnel lock and equipment hatch penetration, the thickness of the drywell shell surrounding the ventline penetration is thickened. Here the thickened region is 2.875" with a thin transition zone of 2.0145".

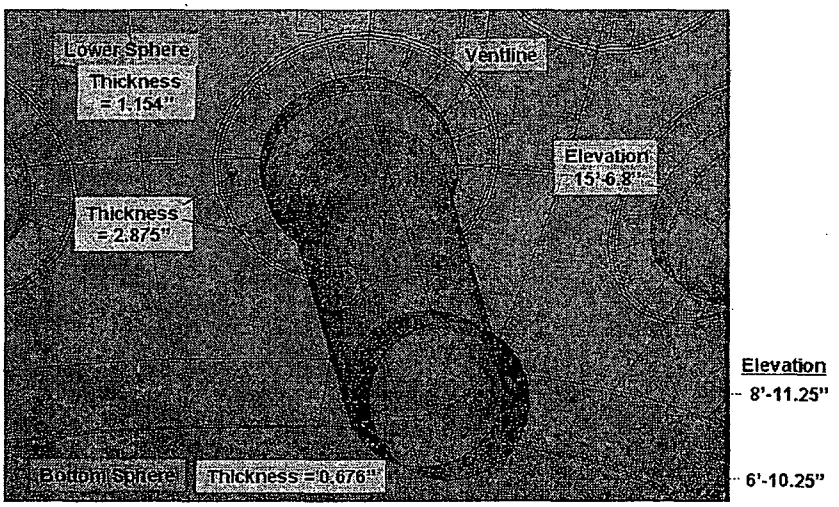

Figure 2-11. Drywell Geometry near Ventline Penetration

Figure 2-12 illustrates the extent of the ventline modeled in this study. At the intersection with the drywell, a 2.5" thick section of the ventline at a diameter of 7'-10" extends approximately 1'-3.2" away from the drywell shell. The diameter of the ventline then transitions down to 6'-6.25" with a 0.4375" thick region which extends approximately 1'-11.8". A 0.25" thick region then extends another 14'-0.7" to a 0.3125" thick section. This section extends approximately 4'-2.3" to a point where the angle of the ventline changes from 38°21' to 17° from horizontal. The next section of 0.3125" thick ventline is approximately 2'-5.2" in length with a 0.25" thick section extending the final 4'-1". The center of the end of the ventline is at an elevation of 0'-6". The ventline ends at the connection with the ventline header. Springs are attached to the end of the ventline to account for the additional stiffness provided by the ventline header. This is discussed in detail in the next section. Part of the lower section of ventline modeled here is actually contained within the torus and connected with a bellow. It is assumed that the bellows prevent any meaningful structural interaction, and therefore the torus and bellow are not modeled here.

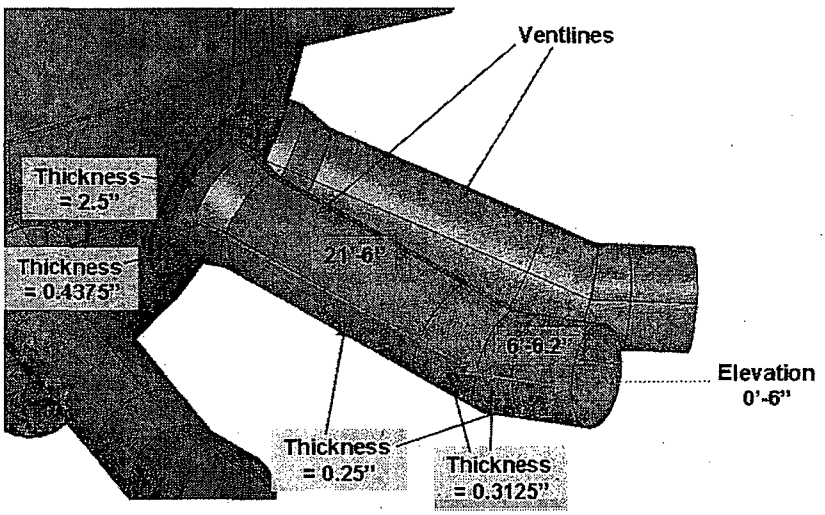

Figure 2-12. Ventline Geometry

Figure 2-13 shows the ventline jet deflector included in the current model. The deflector includes 20 - 0.875" thick gusset plates that connect the inside of the drywell shell to the 2.31" thick deflector plate. The thickness of the gusset plate could not be identified on the structural drawings (CB&I, 1980), and was taken from the value given in the GE report (GE, 1991b). The actual deflector plate is 2.5" thick and includes 189 holes through the thickness of the plate. Since including the holes explicitly is beyond the fidelity of this model, the plate was modeled as solid with a reduced thickness to maintain a constant volume with the actual plate. This reduced thickness solid plate approximates the membrane stiffness exhibited by the perforated plate due to the consistent cross-sectional area (on average).

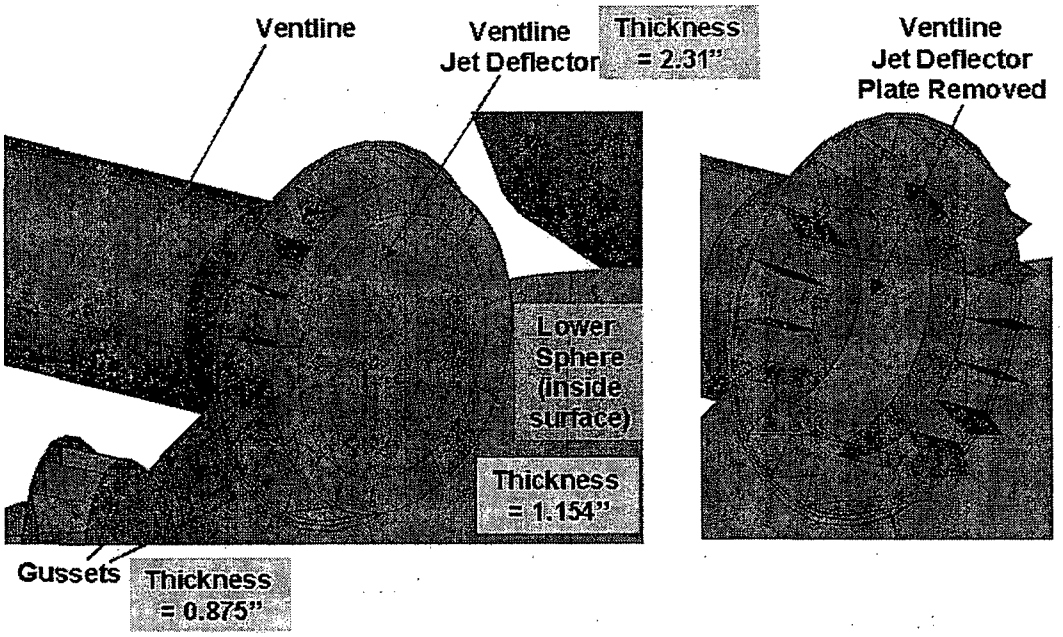

Figure 2-13. Ventline Deflector Geometry

The only penetrations explicitly modeled here are the ventlines and the personnel lock and equipment hatch. Other penetrations are included through loads applied to the structure and are discussed in the subsequent loading section.

2.3 Boundary Conditions

The boundary conditions applied to the current model attempt to approximate the conditions within the actual structure. At the same time, it must be acknowledged that all finite element models are idealizations. The boundary conditions that can be applied to a given model, while increasingly realistic and complex, will never exactly represent the complexities in an actual structure.

Here, four boundary condition regions have been created and applied to the model. Figure 2-14 shows the fixed region of the drywell shell below elevation 8'-11.25". This region is fixed since the drywell shell is surrounded by concrete on both sides. Outside of the drywell, concrete rises up to an elevation of 8'-11.25". Above the concrete, the sandbed region extends up to an elevation of 12'-3". The sand has been removed from this region and is currently open space. Within the interior of the drywell shell, a concrete floor extends up to an elevation of 10'-3" with curbs extending up to 11'-0" below the ventlines and up to 12'3" between the ventlines. Since the current state of the bond between the drywell shell and the concrete inside of the drywell is not know to the analyst and because of the absence of concrete outside of the drywell shell, the concrete inside of the drywell above an elevation of 8'-11.25" is not accounted for in the model. This is believed to be a realistic assumption since the shell deforms outward, away from the interior concrete, for the load cases examined in this study.

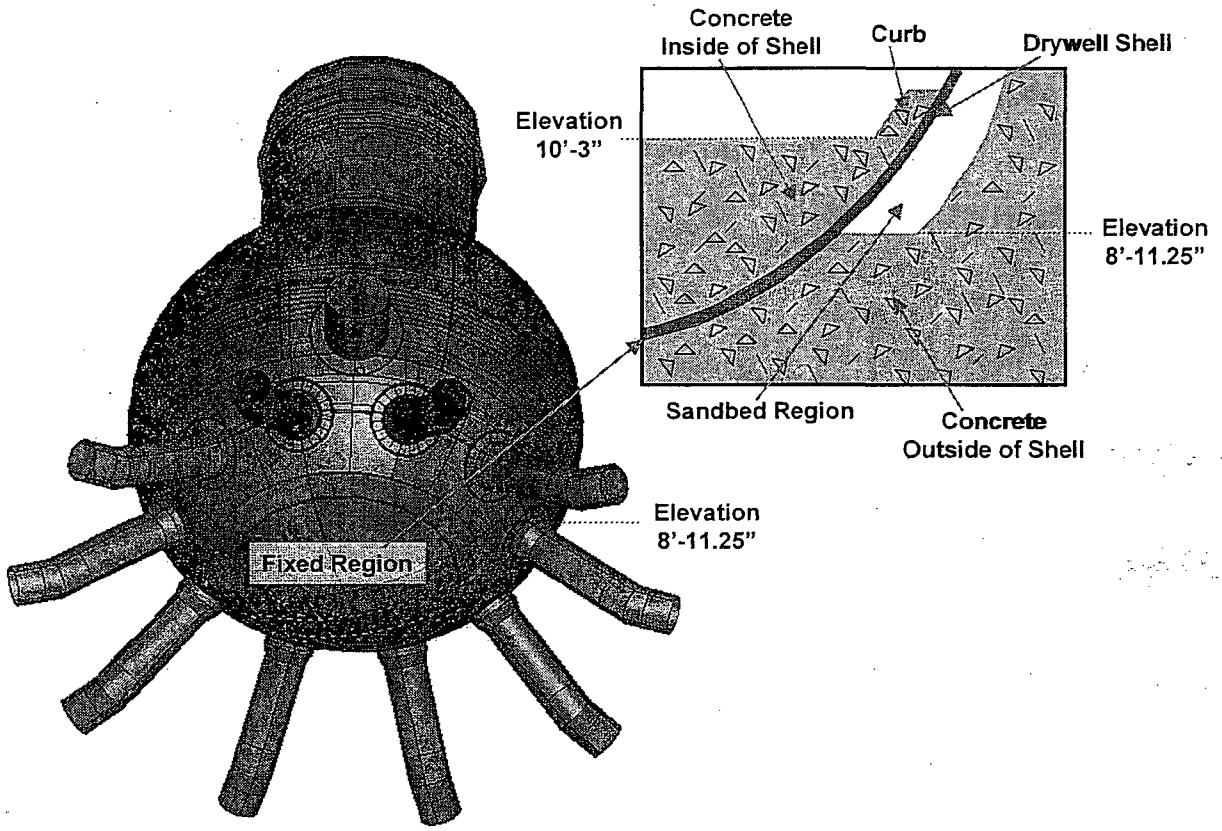

Figure 2-14. Boundary Condition at the Bottom of the Drywell with Cross-section View of Embedded Drywell Shell

Figure 2-15 shows the highlighted ends of the ventlines where the degrees of freedom are fixed against rotation and lateral displacement. Springs are attached to the ends of the ventlines in the vertical and radial directions. Since the spring constant used by GE at the ends of the ventlines to represent the compliance of the ventline header connection were not documented, a sub-analysis of the ventline header was performed for this study to estimate the stiffness provided to the ends of the ventlines. Figure 2-16 shows the ventline header and the submodel used to determine the spring constants to be applied to the ends of the ventlines in the main model. A section of the ventline header was extracted and analyzed with symmetry boundary conditions at one end and fixed displacement at the location of the ventline header columns. The end of the ventline header submodel that intersects with the ventline is fixed laterally and unit displacements are imposed in the radial and vertical directions. The reactions along this edge are summed and multiplied by two to account for the section of the ventline header on the other side of the ventline. The summed reactions in the radial and vertical directions are the resistance that would be applied to the ventline from the ventline header. The springs acting vertically are applied at two points with magnitudes of 2332 kips/in. The vertical springs are located on each

side of the end of the ventline as shown in Figure 2-17. Figure 2-17 also shows the springs that act radially at the top and bottom of the end of the ventline. These springs have a magnitude of 519.9 kips/in. These points of application were selected since the largest reactions resisting the imposed displacements are the located near these locations.

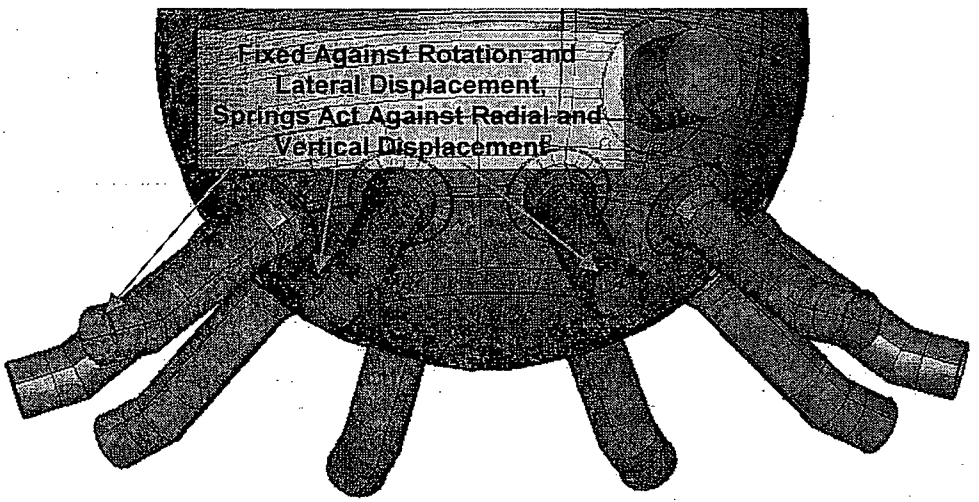

Figure 2-15. Boundary Condition at the Ends of the Ventlines

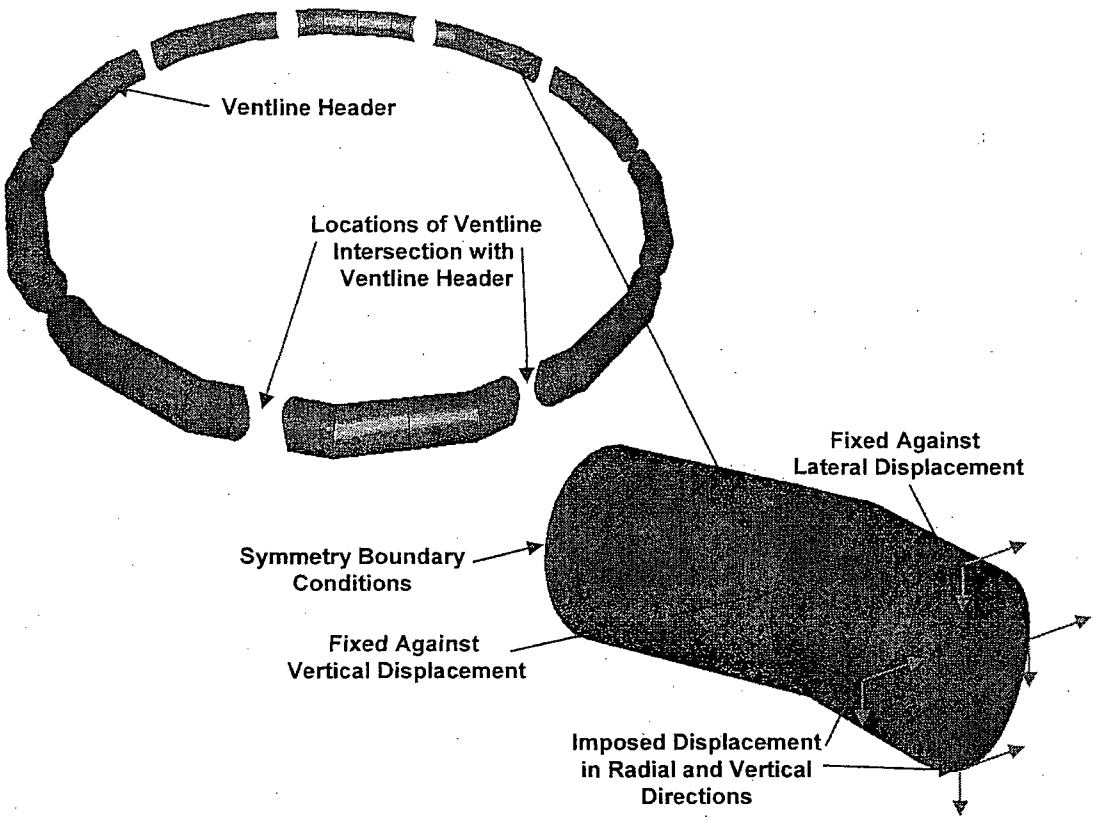

Figure 2-16. Ventline Header Submodel

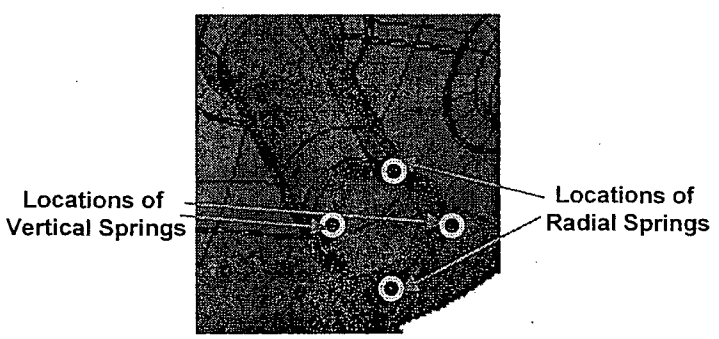

Figure 2-17. Ventline Spring Locations

The outer extend of the personnel lock and equipment hatch is shown in Figure 2-18. The end of the penetration included in the model extends 41'-6" from the centerline of the drywell. At this point, the penetration reaches a roller support within the reactor building. The end of the hatch is constrained against vertical displacement at this point.

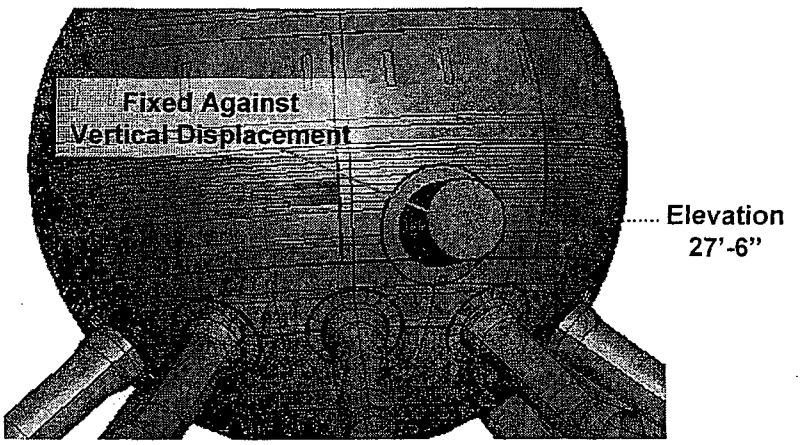

Figure 2-18. Boundary Condition at the End of the Hatch Penetration

Finally, Figure 2-19 illustrates the boundary condition at the seismic lateral stabilizers. These stabilizers are centered at an elevation of 82'-9" and have a diameter of 5'-3". There are 8 stabilizers spaced at 45° around the circumference of the drywell cylinder. The structural details in these regions allow the steel shell to move radially and vertically, but constrain the shell against lateral displacement. Lateral motion for a cylindrical shell can be described as a twisting or rotation in the azimuth direction (see CB&I, 1980, for structural detail).

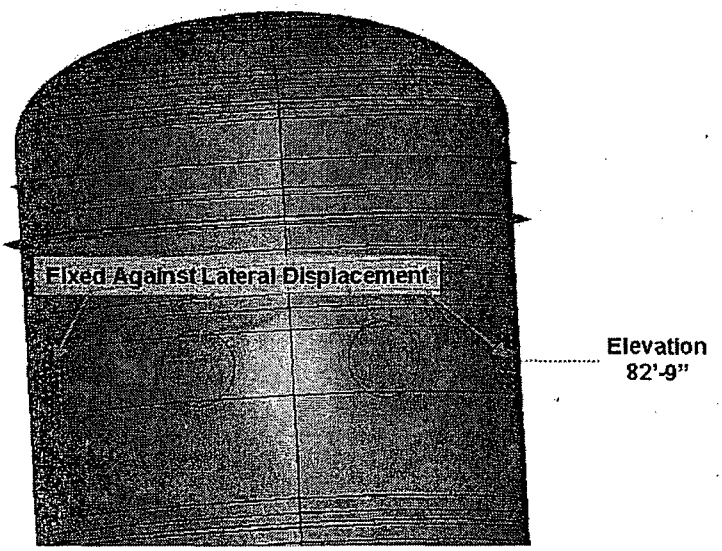

Figure 2-19. Boundary Condition at the Stabilizers

2.4 Loading

The load combinations for the Oyster Creek drywell stress and stability analyses are provided in the "Technical Specification for Primary Containment Analysis – Oyster Creek Nuclear Generating Station" (Reference 1-4 of GE, 1991a) and summarized in the previous GE analyses (GE 1991a and b). Based on the detailed discussion of the different load combinations in the GE reports and the previous acceptance of their calculations, the following three load combinations are explored in this study:

- Case IV – Refueling Condition,
- Case V – Accident Condition,
- Case VI – Post-Accident Condition.

GE determined that these three load combinations essentially envelope all other scenarios, and therefore, define the governing set of load combinations. Stress analyses are performed for all three of the above load combinations. In addition, only Case IV – Refueling Condition, and Case VI – Post-Accident Condition, are examined for the stability (buckling) analysis. The current analysis assumes that these two conditions govern the potential buckling in the sandbed region since the accident condition does not produce significant compressive stresses in the containment.

Each of the above load combinations includes a specific set of load types. Among these, the dead, live, and equipment loads were applied in the GE analysis using calculated loads from an earlier study by Chicago Bridge & Iron (Reference 2.4.3 of Reference 1-4 of GE, 1991a). This reference was not made available for the current study, and therefore, the loads documented by GE (Tables 2-5a through 2-5c of GE, 1991a) were adapted and applied to the current model.

In addition, to the loads mentioned above, several other load types are required to complete the load combinations of interest. These include seismic, water loads, and internal pressure, among others. The set of loads applied for each load combination was extracted from the previous GE analysis (GE, 1991a) and the FSAR (FSAR, 2003) and is summarized in Table 2-2. A description of each load type is given in following subsections.

Table 2-2. Load Combination Components

Load Type	Load Combinations			Load Source
	Refueling Condition	Accident	Post-Accident	
Dead Load – Gravity of Shell	×	×	×	General
Dead Loads – Shell Attachments	×	×	×	GE Report
Penetration Loads	×	×	×	GE Report
Compressible Material	×	×	×	GE Report
Live Loads	×			GE Report
Internal Pressure		×		FSAR
External Pressure	×			GE Report
Hydrostatic Internal Pressure			×	GE Report
Seismic Loads	×	×	× (flooded)	FSAR
Refueling Loads	×			GE Report
Thermal Load at 292°F		×		FSAR

2.4.1 General Loads: Gravity, Dead, Penetration, and Compressible Material Loads

This section describes the general loads that are applied in each of the load combinations considered in this study. The first of these loads employs a distributed body force to apply gravitation forces to the model. In ABAQUS, the user must define the material density, the model geometry, and the value for the acceleration of gravity to enable the simulation of gravity. Since the current model is defined in units of inches, the gravity constant is defined as 386.4 in/s^2. In addition to the gravity load, a 0.0694 psi (10 psf) vertical load is applied to the exterior of the entire drywell shell. This represents the weight of the compressible material that lies in the approximately 3" gap between the drywell shell and the surrounding concrete shield wall.

The dead load for components attached to the drywell shell, but not explicitly modeled, are included through the application of a series of surface traction loads. The current study uses the loads defined in Table 2.5a of the previous GE analysis (GE, 1991a). As mentioned earlier, these loads were compiled by an even earlier study by Chicago Bridge & Iron. In the GE analysis, these dead loads were applied by "smearing" the load from a specific item attached to the drywell shell along the circumference of the shell at the elevation the item is located. In other words, the total load from an item or series of items was summed together and distributed along the entire 360° of the drywell. Since the GE model was only a 36° slice of the drywell, 10% of the total load was then distributed along the slice as nodal loads applied at the appropriate elevation. Here, the current model contains the entire 360° extent of the drywell shell. Therefore, the location of these applied loads can be as specific as the information available. Here, the region of application was defined on the drywell shell by "imprinting" the shape of the attachment. This imprinting creates surfaces within ABAQUS that can be used to define where a specific load is applied. The load is applied by "smearing" it along the defined surface as a surface traction. This smearing is similar to the method used in the GE analysis, but the load is smeared over the actual location on the shell where a piece of equipment or other items are attached in the real structure. This method provides a more realistic loading condition in the model.

In applying the surface tractions for the dead loads given in the GE analysis report (Table 2.5a of GE, 1991a), the drywell surface was imprinted with the locations of each item listed. These locations were determined from a set of structural drawings of the drywell (CB&I, 1980). Figure 2-20 through Figure 2-24 illustrate the regions of application for each of the loads defined in the GE analysis report (GE, 1991a). Figure 2-20 shows the region of application for the upper and lower spray headers. The center of the application region is located at elevation 64'-6" and 37'-3" for the upper and lower headers, respectively[2]. Since the drawing or schematic showing the exact regions of attachment to the drywell shell was not provided, it was assumed that the region of attachment spans 3" in elevation both above and below the center points given above. Therefore, the total width of the regions of load application is 6" in elevation. The actual width of the region depends on the curvature of the drywell shell at each location. The load is also assumed to extend around the entire circumference.

[2] August 3, 2006, conference call between Sandia National Laboratories, NRC, and Exelon.

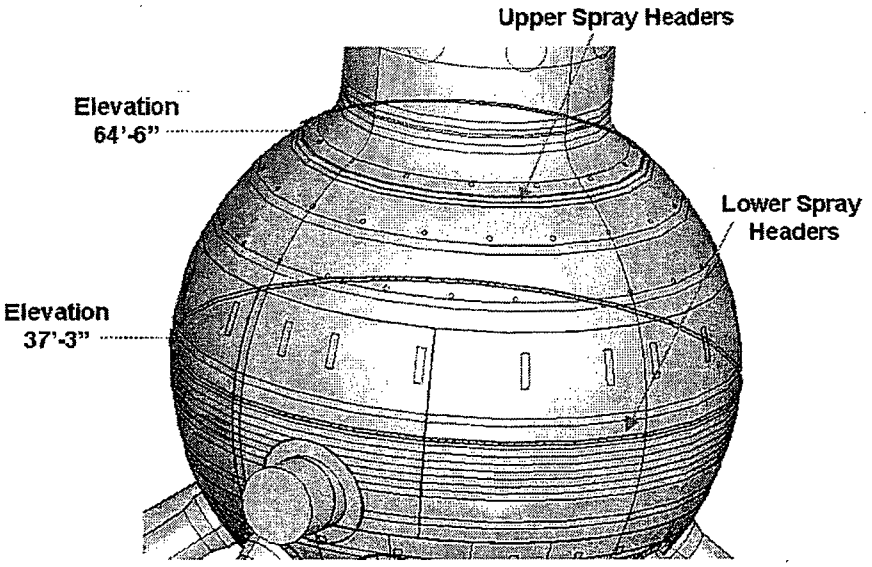

Figure 2-20. Upper and Lower Spray Header Locations

Figure 2-21 illustrates the regions of load application for the upper, middle, and lower weld pads (CB&I, 1980). Each of the weld pads covers a 8" diameter region imprinted onto the drywell shell. In the actual structure, the weld pads are attached to interior surface of the drywell. Based on the structural drawings of the weld pad layout, the center of the upper, middle, and lower weld pads are located at elevations 66'-3.2", 61'-2", and 54'-9", respectively. The number of weld pads and spacing along the drywell circumference also varies: 15 pads at 24°, 20 pads at 18°, and 24 pads at 15°, respectively.

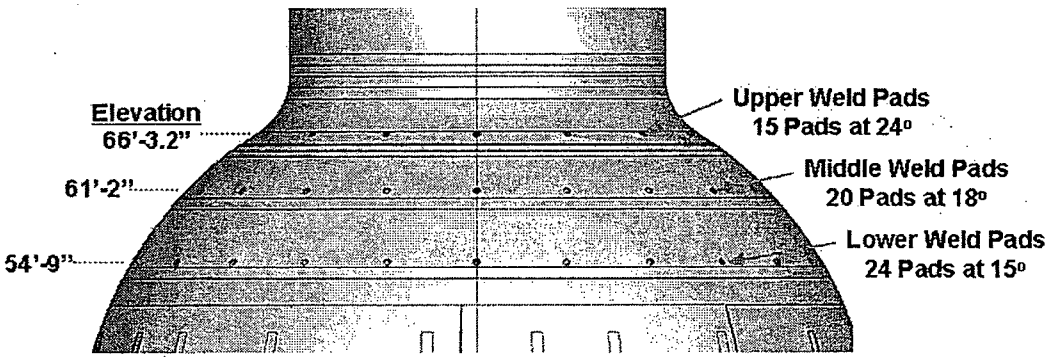

Figure 2-21. Weld Pad Locations

Figure 2-22 shows the regions of load application for the top and bottom flanges, as well as the stabilizers (CB&I, 1980). Each of these items is located in the cylinder region of the drywell. The top flange spans from and elevation of 96'-7.878" down to 94'-9". The bottom flange extends from 94'-9" down to 92'-8.5". Both of these loads are applied along the entire circumfer-

ence of the cylinder. The stabilizer load is applied at 8 circular regions spaced at 45° and centered at elevation 82'-9". Each of the stabilizer regions is 5'-3" in diameter.

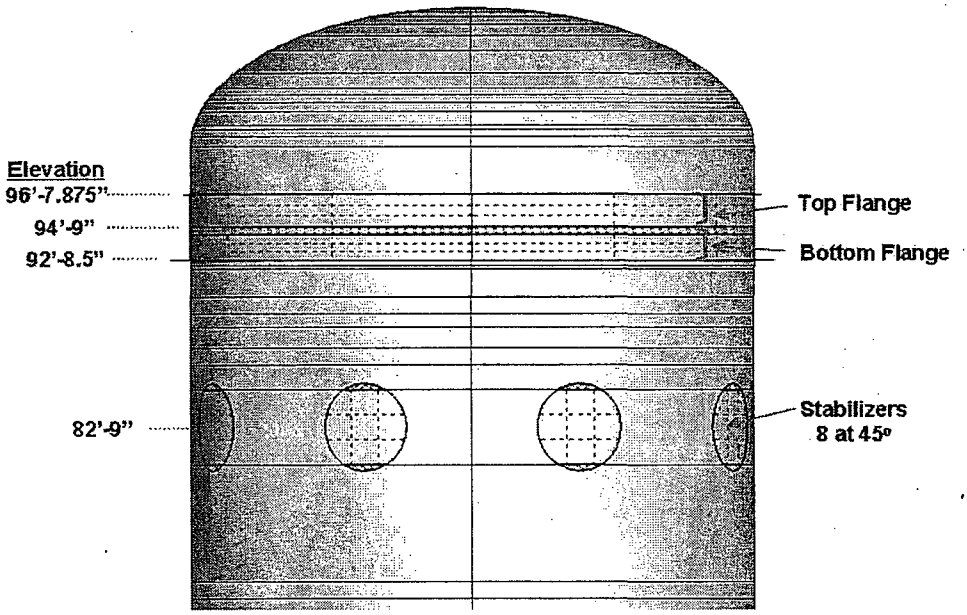

Figure 2-22. Flange and Stabilizer Locations

Figure 2-23 illustrates the load application regions for the upper and lower beam seats (CB&I, 1980). These are the attachment points of beam within the drywell sphere. The imprinted region for the upper beam seats is approximately 12" wide and 51" high and centered at an elevation of 46'-4.5". The spacing of the 20 seats around the circumference varies from seat to seat, and range from 12° to 25°30'. These dimensions and spacings were derived using the structural drawings. The imprinted region for the lower beam seats is approximately 12" wide and 13.5" high and centered at an elevation of 20'-11.125". The spacing of the 20 seats around the circumference varies from seat to seat, and range from 11°45' to 29°40'. Since the surface imprints for 6 of the lower beam seats overlapped other surface partitions for the thickened regions around the personnel lock and several ventlines, the height of the region of application was reduced in slightly to 10". This modification was introduced to avoid oddly shaped surfaces which can be problematic during the meshing of the geometry. In addition, the load for the beam seats was distributed evenly among the 20 seats for both the upper and lower seats. Due to the varying spacing of the beam seats, the load could have been distributed using tributary areas. Since the exact makeup and details of the total load are unknown here, a simple even distribution was applied.

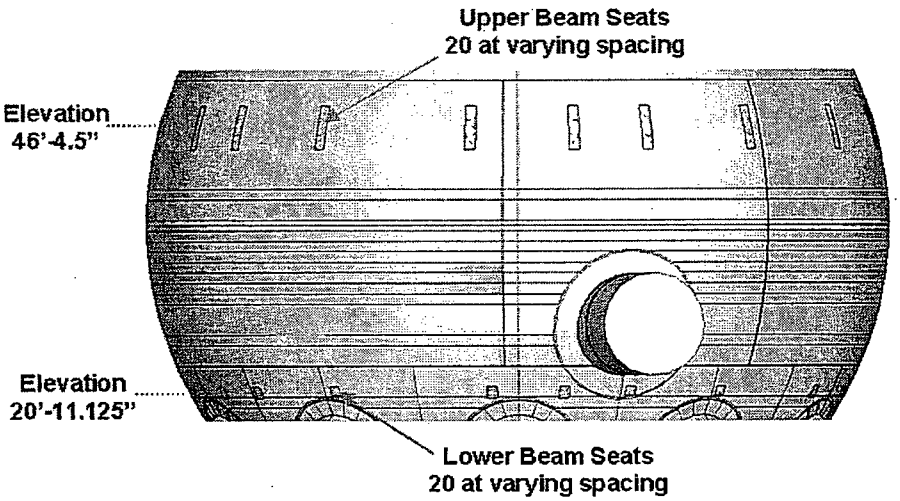

Figure 2-23. Upper and Lower Beam Seat Locations

Figure 2-24 shows the load application region for the personnel lock and equipment doors. This area is essentially the thickened region of the drywell shell surrounding the penetration. The penetration is centered at an elevation of 27'-3".

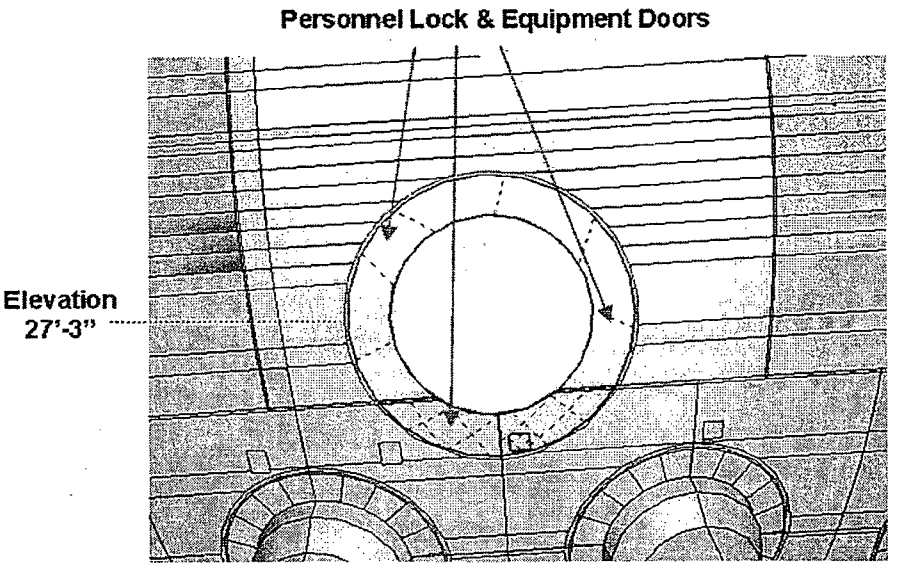

Figure 2-24. Personnel Lock and Equipment Door Loads Application Region

The final load listed in the GE dead load Table 2-5a (GE, 1991a) is for the vents. It is assumed that this additional load accounts for the portion of the ventline that was not modeled explicitly in the GE model. Since the entire ventline is modeled in the current model, no additional load was applied to the structure.

Table 2-3 summarizes the dead loads described above. The total load given in Table 2-5a of the GE report (GE, 1991a), the total surface area from the current ABAQUS model, and the resulting applied traction are all provided. The ABAQUS total area is the summed surface area for all of the regions of application for a given dead load case. The traction is simply the total load divided by the area. These tractions are applied to the appropriate regions on the drywell shell in the vertical direction.

Table 2-3. Dead Load Tractions

Dead Load Case	GE Total Load* kips	ABAQUS Total Area** in^2	Traction*** ksi
Upper Header	36	15847.2	0.00227
Lower Header	41	15848.1	0.00259
Upper Weld Pads	52****	754	0.06897
Middle Weld Pads	59.2****	1005.3	0.05889
Lower Weld Pads	56.2****	1206.4	0.04675
Top Flange	20.1	28543.4	0.00070
Bottom Flange	20.7	30571.1	0.00068
Stabilizers	21.65	12508.7	0.00173
Upper Beam Seats	1102	12688.3	0.08685
Lower Beam Seats	556	---	---
- Standard Size	389.2	2563.3	0.15184
- Reduced Size	166.8	811.7	0.20549
Equipment Doors, Lock	169.1	11938.3	0.01416

*** GE Total Load – This is the total load reported in the Table 2-5a of the GE analysis report (GE, 1991a).**
**** ABAQUS Total Area – This is the total summed surface area from the current ABAQUS model for each of the dead load items listed in the GE report.**
***** Traction – This is the GE Total Load divided by the ABAQUS Total Area. These tractions are applied to the appropriate regions for each dead load case. The tractions are applied in the downward or vertical direction.**
****** The GE Total Loads for the three weld pad loads given in Table 2-3 are the sum of two separate loads for each set of weld pads in GE Table 2-5a.**

In addition to the above dead loads, the Oyster Creek has numerous penetrations that were not modeled explicitly in the current model. These penetration loads are listed in Table 2-5b of the GE report (GE, 1991a). Unfortunately, the penetration identification numbers provided in this table do not correspond to the penetration identification numbers given in the structural drawing's penetration schedule (CB&I, 1980). Since the correlation between these two numbering systems could not be readily provided to the analyst, the loads from each penetration in the GE Table 2-5b (GE, 1991a) were summed to give a total load at each elevation and distributed along

the entire drywell circumference. GE Table 2-5b documents penetration loads at 17 different elevations: 16', 20', 26', 30', 31', 32', 33', 34', 35', 36', 40', 54', 60', 70', 73', 87', and 90'. These elevations were assumed to be the centerline of the application region and extend 6" in elevation in each direction. For example, the region of application for the penetration load at 33' is from 32'-6" to 33'-6". The regions of application for each of the penetration elevations are shown in Figure 2-25 and Figure 2-26. Typically, the total penetration load for a given elevation is distributed along the entire circumference of the drywell. Gaps in the application regions do exist near the personnel lock and equipment hatch. These regions are excluded from the application region since the hatch is an explicitly modeled penetration and other penetrations do not pass through that region. Figure 2-27 shows the application region for the penetration load at the 16' elevation. The load is distributed in the drywell shell between the ventlines including within a portion of the thickened region around the ventlines. The 16' elevation penetration load is distributed along this identical region between each of the ventlines.

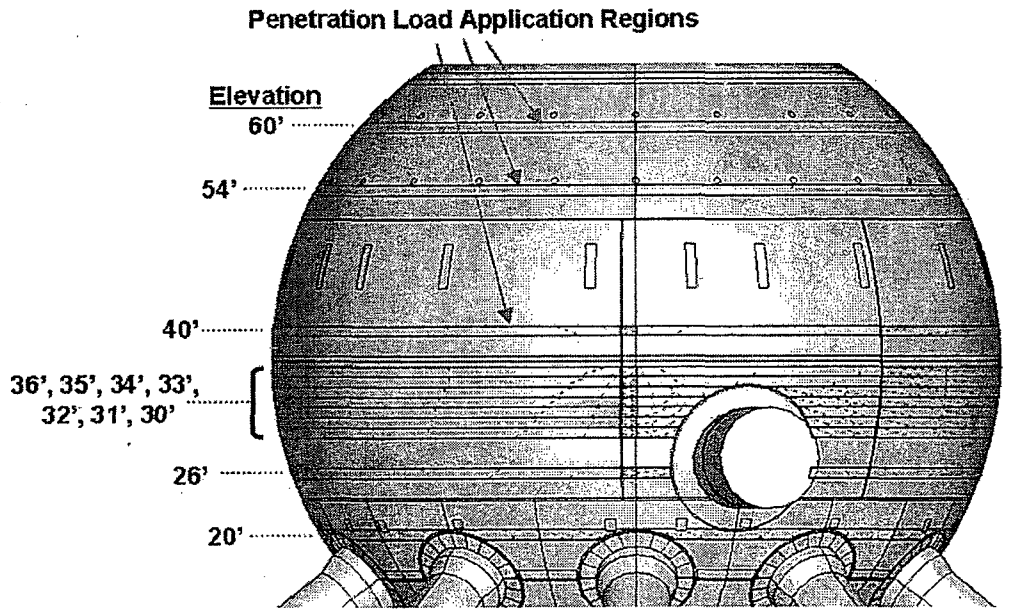

Figure 2-25. Penetration Load Application Regions in the Drywell Sphere

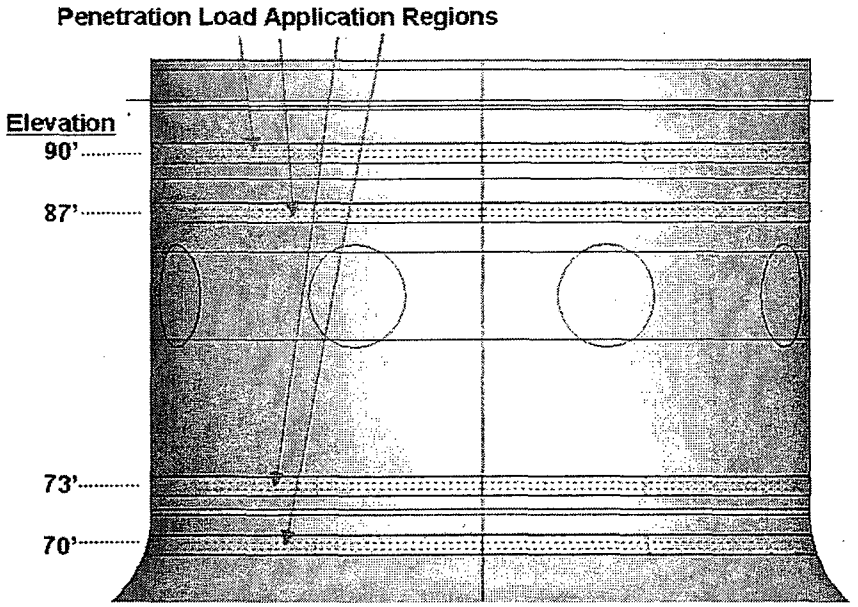

Figure 2-26. Penetration Load Application Regions in the Drywell Cylinder

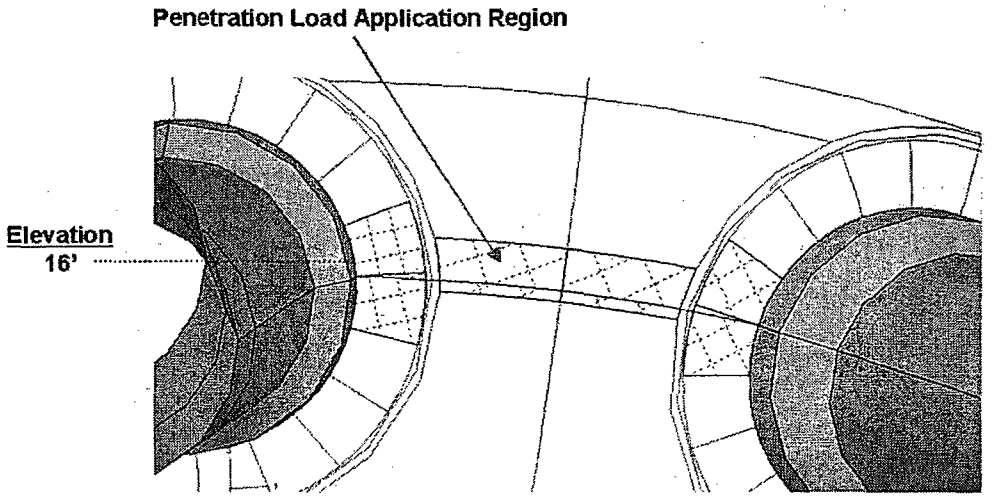

Figure 2-27. Elevation 16' Penetration Load Application Region Between the Ventlines

Table 2-4 provides a summary of the penetration load tractions applied to the current ABAQUS model. The total load given in Table 2-5b of the GE report (GE, 1991a) is provides along with the total surface area from the current ABAQUS model and the resulting applied traction. The ABAQUS total area is the total surface area for the region of application for a given penetration elevation. The traction is simply the total load divided by the area. These tractions are applied to the appropriate regions on the drywell shell in the vertical direction.

Table 2-4. Penetration Load Tractions

Penetration Load Elevation	GE Total Load* kips	ABAQUS Total Area** in^2	Traction*** ksi
16'	168.1	24169.7	0.006955
20'	11.2	23809.4	0.000470
26'	11.1	29530.9	0.000376
30'	50.5	29688.2	0.001701
31'	16.5	29836.7	0.000553
32'	0.75	30044.2	0.000025
33'	15.45	30342.4	0.000509
34'	28.05	30805.2	0.000911
35'	1.5	31616.3	0.000047
36'	1.55	31696.3	0.000049
40'	43.35	31702	0.001367
54' ****	7.85	31694.5	0.000248
60'	0.7	31694.5	0.000022
70'	5.75	15651.8	0.000367
73'	8.85	14953	0.000592
87'	1.0	14953	0.000067
90'	15.0	14953	0.001003

*** GE Total Load – This is the total load reported in the Table 2-5b of the GE analysis report (GE, 1991a).**
**** ABAQUS Total Area – This is the total summed surface area from the current ABAQUS model for each of the penetration load elevation listed in the GE report.**
***** Traction – This is the GE Total Load divided by the ABAQUS Total Area. These tractions are applied to the appropriate regions for each penetration load elevations, and act in the downward or vertical direction.**
****** 54' Elevation Loads – The loads for this elevation are centered at 53'-10" to avoid creating oddly shaped surfaces at the intersection with the lower weld pads.**

2.4.2 Seismic Load

A full dynamic simulation of the governing seismic loading would be ideal in determining the resulting stresses. GE applied this method by performing a dynamic using an appropriate time history. In addition, the Oyster Creek FSAR (FSAR, 2003) states that a dynamic seismic analysis was also performed by John A. Blume & Associates. Neither this report nor the seismic ground motions were available for the current study. Although, the FSAR states that this dynamic analysis by John A. Blume & Associates confirmed that the original static coefficients used by Chicago Bridge & Iron in the design of the structure were acceptable. These static coefficients are 22% laterally and 10% vertically (acting simultaneously) of the permanent gravity load. The use of the static coefficients to simulate the seismic loading is justified due to the confirmatory nature of this study.

Since the degraded drywell containment (degradation described in Section 2.6) may potentially exhibit a different dynamic behavior than the original, as-designed containment, the suitability of using the static coefficients to approximate the seismic loading is uncertain. In order to address this issue, a short study was conducted which compares the natural frequencies and associated mode shapes for the drywell in its original and degraded conditions. The details of this study are included in the Appendix A (Section 9) of this document. Since the frequencies and mode shapes proved relatively insensitive to the levels of degradation experienced in the Oyster Creek drywell, the use of the static seismic coefficients to simulate the seismic loading for the degraded structure is assumed to be acceptable.

The static coefficients are applied to the current ABAQUS model using body forces. The gravity loading in ABAQUS was utilized for this purpose. In addition to the standard 1g gravity load, an additional 0.1g was applied downward and 0.22g was applied in one lateral direction, as performed in the original design by CB&I. Several orientations of the seismic lateral load were examined to determine the case that produced the highest stresses in the sandbed region. The direction for the 0.22g lateral load that extends from the 180° azimuth to the 90° azimuth was determined to produce the highest stresses, in general, throughout the sandbed region.

The 0.22g lateral seismic load was applied in the Accident and Refueling load cases. For the Post-Accident load case, the drywell is flooded with water up to an elevation of 74'-6". The additional seismic load from the mass of the water is introduced into the analysis by increasing the value of the acceleration of gravity for the lateral seismic load and applying it to the drywell shell model that does not include the water explicitly. To determine the appropriate increase in the acceleration of gravity, the total mass of the drywell shell (degraded and undegraded) was computed within ABAQUS. The total weight of the water flooding the drywell (20% removed for the reactor vessel, GE, 1991a) was computed and added to the weight of the drywell shell. The weight of the combined drywell shell and water for the degraded containment was determined to be 10.6 times the weight of the drywell shell allow, and 10.0 times for the undegraded shell. Therefore, the lateral seismic load for the degraded analysis uses 2.3g, and the undegraded shell uses 2.2g. These loads are applied to the entire drywell shell. This method is extremely approximate, but judged appropriate based on the limited seismic information available. It is assumed that the vertical seismic loads are unaffected by the presence of the water during the Post-Accident load condition.

2.4.3 Refueling Condition Specific Loads: Live, External Pressure, and Refueling Loads

For the refueling load condition, the head of the drywell is removed as illustrated in Figure 2-4. The additional weight on the cylindrical portion of the drywell is given as 561 lbs/in along the circumference (Ref. 2.4.3 of Ref. 1-4 of GE, 1991a). This load is applied in the current model as a shell edge traction as shown in Figure 2-28.

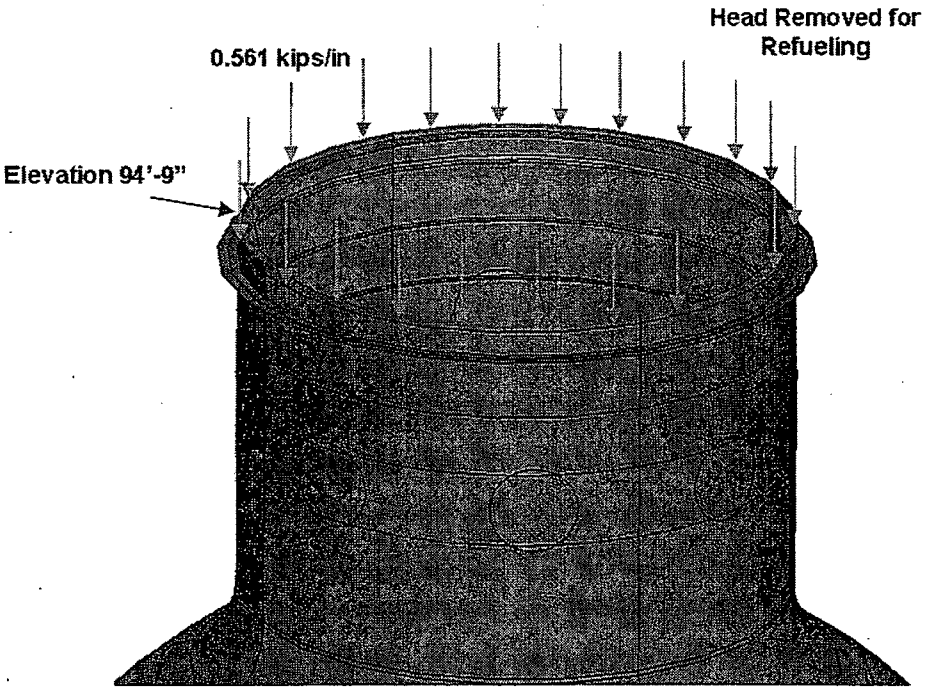

Figure 2-28. Refueling Load on Drywell Cylinder

In addition to the refueling cylinder load, the refueling load combination includes a 2 psi external load. This load was applied to the entire exposed exterior surface of the drywell shell.

The final refueling load combination specific item is the live loading. The live loads for the drywell are provides in Table 2-5c of the GE report (GE, 1991a). Table 2-5 summarizes the live loads and the applied tractions. The region of live load application for each item is identical to the region of application for the dead load.

Table 2-5. Live Load Tractions

Live Load	GE Total Load* kips	ABAQUS Total Area** in^2	Traction*** ksi
Upper Header	4.2	15847.2	0.000265
Lower Header	7.15	15848.1	0.000451
Upper Weld Pads	20	754	0.026525
Middle Weld Pads	20	1005.3	0.019895
Lower Weld Pads	24	1206.4	0.019894
Equipment Doors, Lock	115	11938.3	0.009633

*** GE Total Load – This is the total load reported in the Table 2-5c of the GE analysis report (GE, 1991a).**
**** ABAQUS Total Area – This is the total summed surface area from the current ABAQUS model for each of the live load items listed in the GE report.**
***** Traction – This is the GE Total Load divided by the ABAQUS Total Area. These tractions are applied to the appropriate regions for each live load case. The tractions are applied in the downward or vertical direction.**

2.4.4 Accident Condition Specific Loads: Internal Pressure and Thermal Loads

The accident condition includes an internal pressure within the drywell of 44 psi at a temperature of 292°F (FSAR, 2003) due to the design basis accident (LOCA, loss of coolant accident). This pressure is applied to the interior surface of the drywell shell above elevation 8'-11.25", or the bottom of the sandbed. However, the concrete floor within the drywell does extend up to an elevation of 10'-3" with curbs extending between the ventlines up to an elevation of 12'-3". In the previous discussion of the boundary conditions, the interior concrete above the bottom of the sandbed is ignored and only the shell below elevation 8'-11.25" is fixed since it is surrounded by concrete on both sides. The actual condition of the bond between the drywell shell and the concrete floor inside the drywell is not known. If a small gap exists, it would be likely that gas could enter and pressurize the shell below the level of the concrete floor.

In the previous GE accident condition analysis, the thermal stresses in the sandbed region were determined using a heat transfer analysis. Specifically, this region is below the concrete floor at an elevation of 10'-3" and extends down to the bottom of the sandbed at 8'-11.25". Since there is not sufficient information and/or explanation provided in the GE report to reproduce the heat transfer analysis or apply the temperatures given in this region, the entire shell in the current analysis is set to 292°F down to an elevation of 8'-11.25". As stated above, the condition of the bond between the drywell shell interior and the concrete below 10'-3" is not known to the analyst. A small gap would allow the temperature of the shell below 10'-3" to be heated uniformly. The internal pressurization and heating of the shell down to the fixed boundary condition at elevation 8'-11.25" produces a severe discontinuity in the drywell shell. At the point in the shell just above 8'-11.25", the increase in the temperature causes the steel shell to expand and the internal pressure forces the steel shell outward. The high bending stresses in this region were originally designed to be tempered by the sand outside of the shell above elevation 8'-11.25". Based in part on the previous reviewed and approved study be GE (GE, 1991a and b), the shell was determined to resist the potential accident condition without the sand present. The sand in the sandbed region was subsequently. Since the focus of this study was not to assess the decision to remove the sand, potentially conservative boundary conditions and applied loads (pressure and thermal) were used here.

2.4.5 Post-Accident Condition Specific Load: Hydrostatic Load

The only post-accident condition specific loading is the hydrostatic load from the flooding of the drywell interior. In this condition, the water fills the drywell from the top of the concrete floor at 10'-3" up to the 74'-6" elevation. Assuming a density of water at 62.3 lbs/ft^3, the hydrostatic pressure in the drywell interior at 10'-3" is 4003 psf (0.02780 ksi). This load reduces linearly to zero at the 74'-6" elevation. Since the elevation that the water reaches in the ventlines extends below the 10'-3" elevation, the hydrostatic load in the ventlines increases appropriately with the distance from the top of the water at 74'-6".

2.5 Material Properties

The drywell shell was constructed out of A-212-61T Grade B pressure vessel steel. The modulus of elasticity, E, has been reported as 29,500 ksi at temperatures from 70°F to 100°F, 28,800 ksi at 200°F, and 28,300 ksi at 300°F (IPE, 1992). The yield stress for the material is 50.7 ksi from 70°F to 100°F, 46.1 ksi at 200°F, and 45.1 ksi at 300°F (IPE, 1992). The coefficient of thermal expansion is assumed to be 6.5E-6°F^{-1}. The density of the steel is 0.283 lb/in3 (GE, 1991b), which is equivalent to its value in the required ABAQUS density units, 7.324E-7 kips-sec^2/in^4.

2.6 Degraded Model

Section 2.2 provides the steel plate thicknesses throughout the drywell in Oyster Creek's as-build state. For over 20 years, the drywell has experienced extensive thinning due to corrosion. Since UT measurements have only been taken at a limit number of locations throughout the shell, the current analysis adopts average measured thickness values for different regions of the drywell reported by AmerGen. Average values have been adopted to establish a "realistic" model that reflects the current conditions.

Since uniform thinning was used in this analysis, any additional stress concentration that might occur at the location of a crack-like pit or a highly non-uniform region was not captured in this analysis. While some pit data has been documented, it is not detailed enough to make any assessment of these types of local defects.

The cylinder, upper sphere, and middle sphere degraded thicknesses are based on the minimum average thickness values from recent documentation on the condition of the drywell shell up to 2004 (AmerGen, April 7, 2006). The minimum average values reported at any location within each of the cylinder, upper sphere, and middle sphere are 0.604", 0.676", and 0.678", respectively. Due to ongoing corrosion, the thicknesses of the cylinder and middle sphere were further reduced. A location in the cylinder shows a corrosion rate of 0.0003"/yr. Based on 25 years of additional corrosion (2004 to 2029), the cylinder was modeled at a thickness of 0.585" (0.604" – 0.00075"/yr x 25yr = 0.585"). One location in the middle sphere shows an ongoing corrosion rate of 0.00075"/yr. This leads to a thickness of the middle sphere of 0.670" (0.678" - 0.0003"/yr x 25yr = 0.670"). The knuckle is reduced slightly in thickness from 2.5625" to 2.54" (AmerGen, April 4, 2006). These thicknesses are taken as uniform throughout the entire region and are summarized in Table 2-6.

The middle sphere and thickened regions around penetrations are decreased in thickness by the same magnitude as the surrounding regions. For example, the thickened middle sphere is reduced in thickness by 0.1" since the middle sphere is reduced by 0.1". The thin transition regions that fall between the main regions are set typically to a thickness equal to the average of the surrounding plates, as described previously for the geometry without degradation. Thicknesses in the cylinder stiffeners, hatch, and ventlines do not include any degradation and are equal to their as-built values.

Table 2-6. Main Drywell Shell Model Thicknesses, Original and Degraded

Section	Original Thickness, in	Degraded Thickness, in	Section	Original Thickness, in	Degraded Thickness, in
Head	1.1875	N/C	Reinforcing Around Ventlines	2.875	2.618
Upper Cylinder	1.1875	N/C	Lower Sphere Below Sandbed	1.154	N/C
Main Cylinder	0.640	0.585	Bottom Sphere	0.676	N/C
Knuckle	2.5625	2.54	Middle Sphere Thickened	1.0625	0.9625
Upper Sphere	0.722	0.676	Reinforcing Around Hatch	2.625	2.525
Middle Sphere	0.770	0.670	Lower Sphere	1.154	See below

N/C – No Change

For modeling the degradation in the sandbed region, the lower sphere was divided into 10 regions to be assigned uniform thicknesses. These regions extend from the centerline of one ventline to the centerline of the adjacent ventline. Each of these newly defined regions contains one-half of the two different, but adjacent, bays. This was done in order to avoid placing the thickness discontinuity at the centerline between the ventlines, since this is typically the location of the highest stresses. If the thickness jump was placed at this location, the stresses of interest would be difficult to interpret.

The thickness values used in these 10 regions were defined based on a set of UT measurements from a study performed in 1993 (GPU Nuclear, 1993). In these calculations, a selected set of thickness measurements were taken from the outside of the containment before the application of the epoxy coating. Measurements are provided for each bay of the sandbed as shown in Figure 2-29 for Bay 1. The image in Figure 2-29 was extracted from the 1993 GPU Nuclear Calculation Sheet. Since the set of thickness values are reported to be the thinnest areas (by visual inspection) in each bay, the averages used here are still biased conservative. As stated above, the 10 regions used in the analysis combine one-half of two adjacent bays. For example, the thicknesses for points in the right half of Bay 3 are combined with the thicknesses for points in the left half of Bay 1 (Points 8, 9, 15, 18, and 19 in Figure 2-29). This is continued around the circumference of the sandbed as shown in Figure 2-30. In addition, the effects of locally thinner regions were explored by introducing two 30" by 18" regions under the ventlines of Bay 1 and Bay 13 as shown in Figure 2-31 for Bay 1 (labeled as the "Bathtub" in Figure 2-29). These two Bays showed a concentration of thin points within a local region. The GPU Nuclear Calculation sheet provided the approximate dimensions of the local thin region in Bay 1, but not for Bay 13. Due to a lack of information for Bay 13, the dimensions and placement of the local region in Bay 13 were assumed to be identical to the region shown for Bay 1.

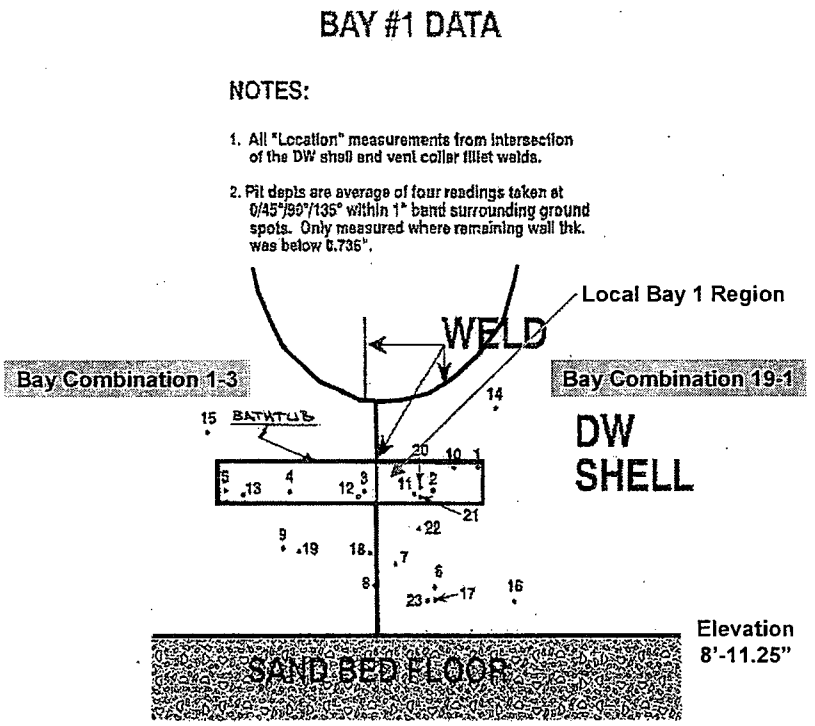

Figure 2-29. Bay 1 UT Measurement Locations Taken from Outside of the Containment (Image Extracted from GPU Nuclear Calculation Sheet, 1993)

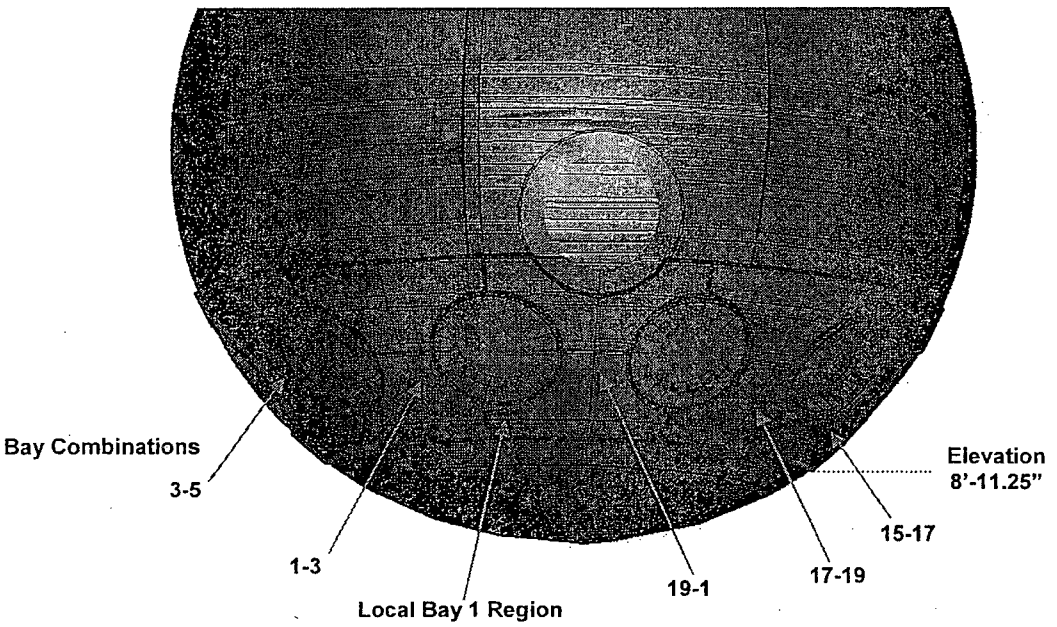

Figure 2-30. Lower Sphere Bay Combination Regions (Ventlines Removed for Clarity)

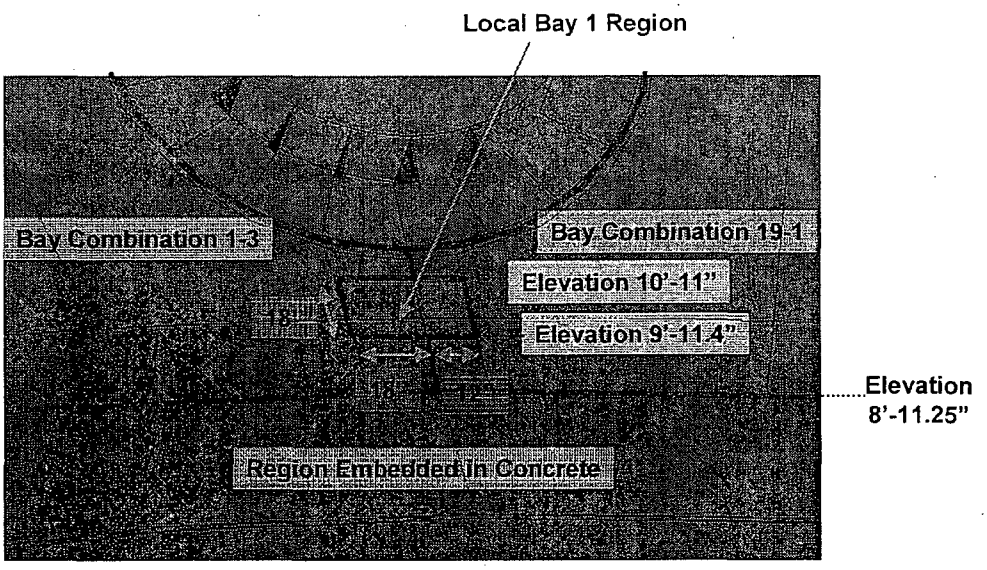

Figure 2-31. Detailed View of Local Bay 1 Region (Ventline Removed for Clarity)

The average of the datapoints that fall within each bay combination (e.g. Bay 1-3) was computed and assigned to the thickness in that defined region of the model.
Table 2-7 summarizes the thicknesses throughout the lower sphere based on the average UT measurements. Figure 2-32 illustrates the layout of the thicknesses prescribed to the bay combinations in the lower sphere. To explore the effects of significant local thinning, the lowest measured value at any point within the two local regions (Bay 1 and 13) was assigned as the uniform thickness throughout the entire 30" by 18" section. The measurement values that fall within each of these local regions were not used in the averaging to define the uniform thickness assigned to the surrounding bay combinations. A detailed description of the computation of these thicknesses is provided in Appendix B (Section 10).

Table 2-7. Degraded Lower Sphere Shell Model Thicknesses

Bay Combination	Thickness, Degraded, inches
Bay 1-3	0.894
Bay 3-5	0.922
Bay 5-7	0.998
Bay 7-9	0.998
Bay 9-11	0.835
Bay 11-13	0.859
Bay 13-15	0.842
Bay 15-17	0.857
Bay 17-19	0.904
Bay 19-1	0.858
Local Bay 1 Region	0.705
Local Bay 13 Region	0.618

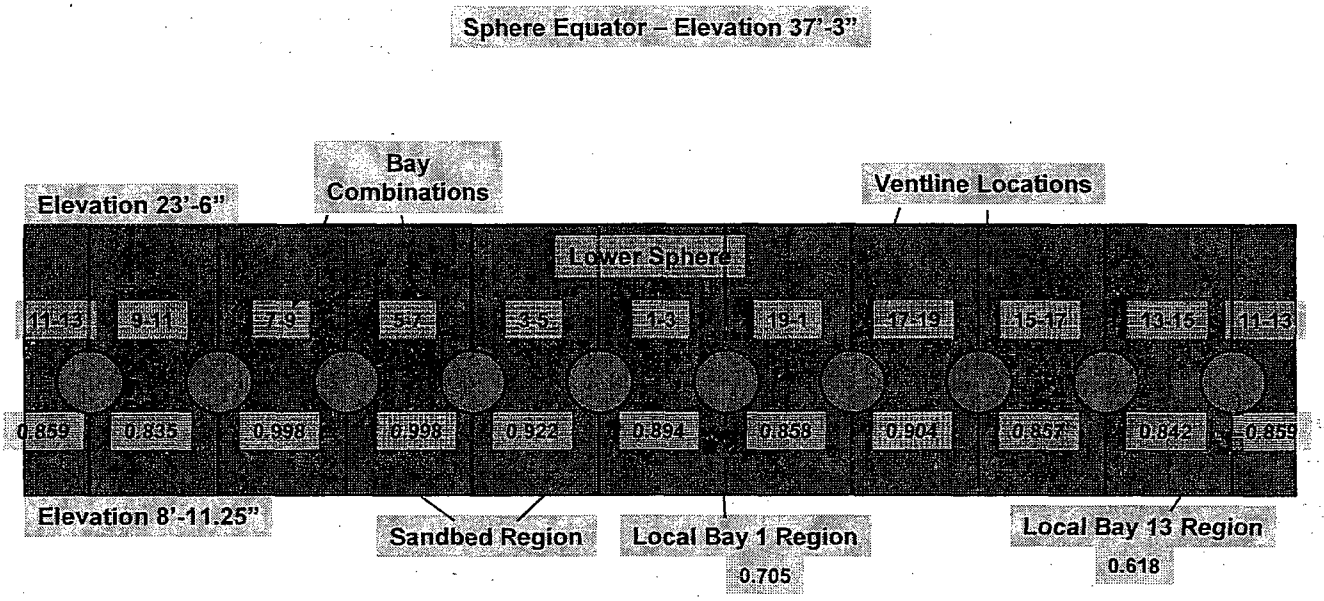

Figure 2-32. Degraded Thicknesses in the Lower Sphere (inches)

2.7 Mesh Size

The solid geometry describes in Section 2.2 was meshed within the ABAQUS/CAE utility. A nominal mesh seed size of 4" was applied to the geometry. Typically, this leads to elements sizes that have a 4" by 4" square dimension. Due to the unique shape of the model and the surface partitions introduced for application of the boundary conditions, loadings, and to divide the shell sections of different thickness, some elements contain edges slightly larger that 4" with some edges much smaller that 4". In the two local regions where the effects of more extensive degradation is explored, smaller elements (1" by 1") are employed to better capture the potentially high stresses. As stated previously, the mesh used throughout the model adopts a quad-dominated scheme. This enables the meshing utility to insert 3-noded, or tri, elements when needed to avoid creating a poorly shaped quad element.

A 4" element size was employed based on a limited mesh convergence study. Models with nominal element sizes of 3", 4", and 5" were constructed using the accident load conditions. For each of these meshes, the hoop stresses at the same location in the sandbed were compared at one point. In addition, the meridional stresses at the same location in the sandbed were compared at one point. The meridional stresses at the point examined were not sensitive to the mesh size. For the hoop stresses at the point examined, the percentage of area reduction for a typical element was compared to the percentage of hoop stress increase as the element size was reduced. The area reduction percentage when going from a 5" nominal mesh to 4" nominal mesh was in excess of one order of magnitude larger than the percentage increase in the hoop stress. In other

words, a significant reduction in the element size only lead to a slight increase in the stress. The reduction of the element size from 4" to 3" produced a percentage ratio that was nearly two orders of magnitude. The percentage ratio of one order of magnitude was judged to be acceptable, and therefore, the 4" nominal element size mesh was adopted for all analyses in this study.

Figure 2-33 illustrates the finite element mesh for the refueling load case. This mesh contains 245,192 shell elements. Figure 2-34 shows a detailed view of the drywell cylinder mesh with the head removed. The same identical mesh is used for perform the stress analyses of the containment in its original and degraded states, as well as for the eigenvalue buckling analyses.

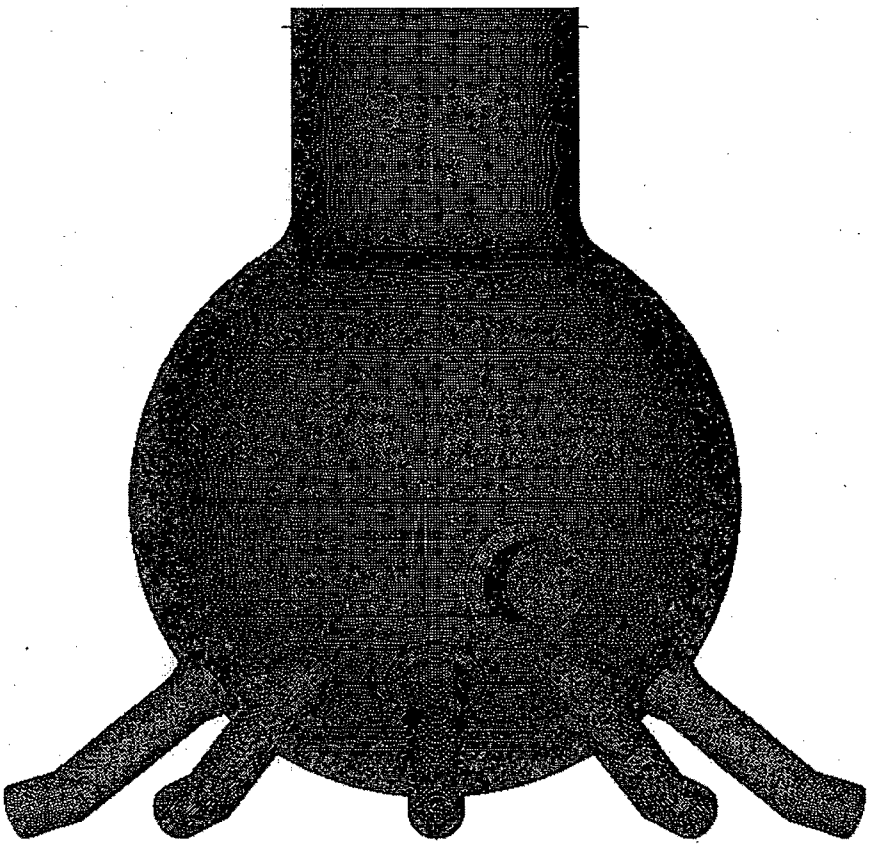

Figure 2-33. Finite Element Mesh for the Refueling Load Case

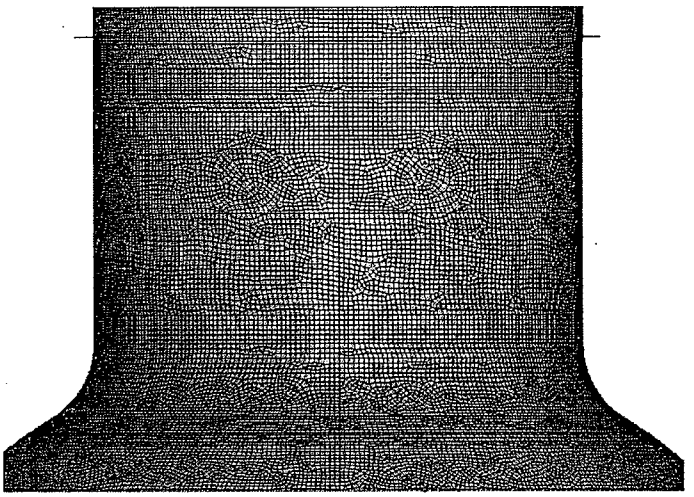

Figure 2-34. Finite Element Mesh in the Drywell Cylinder for the Refueling Load Case

Figure 2-35 illustrates the finite element mesh used for the accident and post-accident load cases. The mesh contains more elements than the refueling mesh with 263,446. The additional elements are required due to the including of the head as shown in Figure 2-36. As with the refueling mesh, this mesh is used for all accident and post-accident analyses.

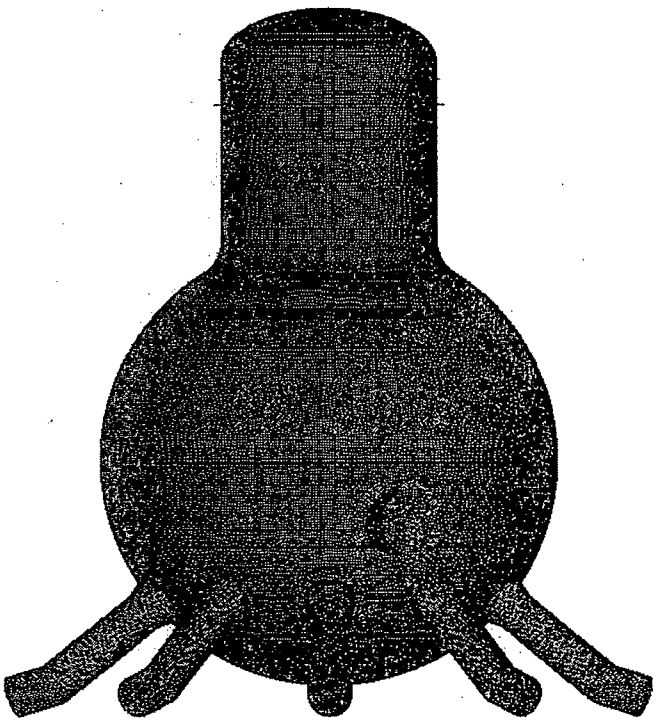

Figure 2-35. Finite Element Mesh for the Accident and Post-Accident Load Cases

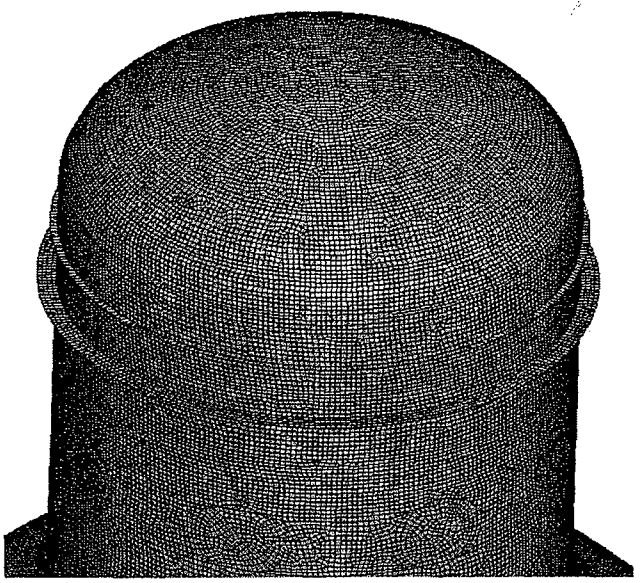

Figure 2-36. Finite Element Mesh in the Drywell Cylinder and Head for the Accident and Post-Accident Load Cases

Figure 2-37 illustrates the mesh in the upper and middle sphere regions of the drywell. The portion of the personnel lock/equipment hatch modeled is also visible as well as the upper portion of the lower sphere and ventlines. The mesh for the refueling case and the mesh for the accident and post-accident analyses are similar in these regions.

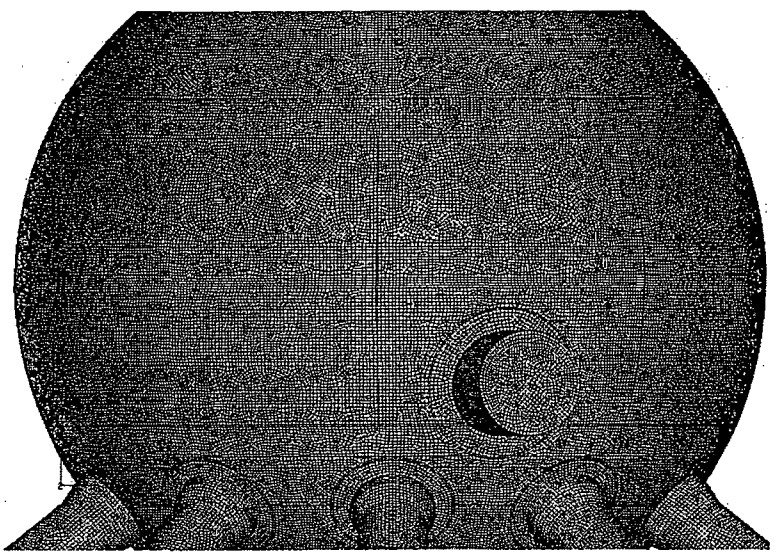

Figure 2-37. Finite Element Mesh in the Upper and Middle Sphere

Figure 2-38 shows the finite element mesh in the lower sphere, bottom sphere, and ventlines. As stated for the upper and middle sphere, the meshes in these lower drywell regions are similar for the refueling and accident/post-accident models.

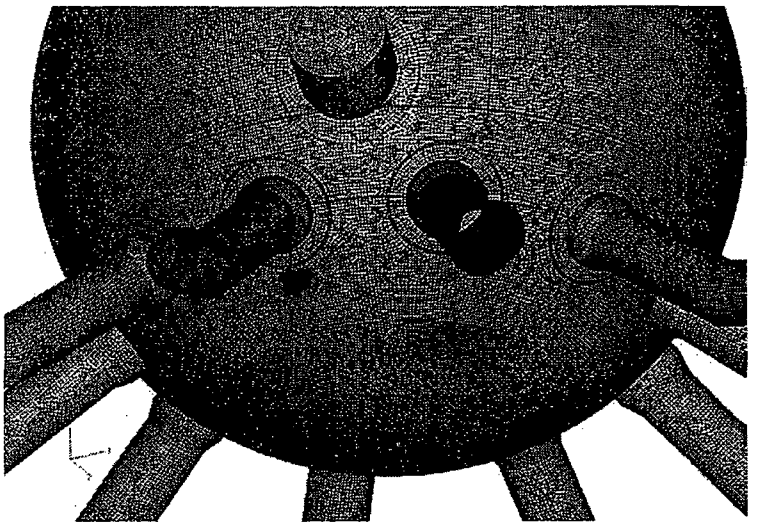

Figure 2-38. Finite Element Mesh in the Lower Sphere, Bottom Sphere, and Ventlines

The mesh in the local thinned regions is shown in Figure 2-39. While the meshes for the local thinned regions under the ventline for Bay 1 and 13 are not identical, they are similar with a typical element size equal to 1" x 1". The elements in these local thinned regions have been reduced in size compared to the surrounding mesh to better capture any potential stress concentrations. No detailed mesh convergence study was performed to determine the optimum element size in these regions.

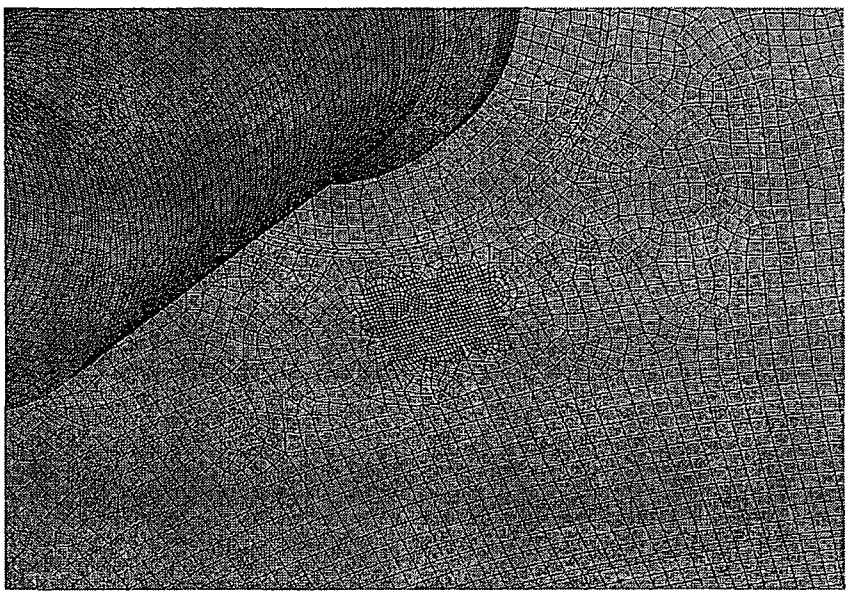

Figure 2-39. Finite Element Mesh for the Local Thin Regions under the Ventlines in Bay 1 and 13

3. Stress Analysis

In this analysis, the structural integrity of the drywell shell is examined in terms of the stress limits using a combination of the values used in the previous analysis by GE (GE, 1991a) and the current ASME code. The GE analysis provided a description of the allowable stresses per the original design code (1962 ASME Code, Section VIII). Using this code, the appropriate code case (1272-N-5) was used to define the allowable primary and secondary stresses for the different loading conditions. Since the original pressure vessel steel used to construct the drywell shell has been designated, it was determined to be appropriate to adopt the original stress criterion while also considering the current code. The allowable stress based on the re-designated steel in the current 2004 ASME B&PV Code, Section III, Division 1, Subsection NE (ASME, 2004) is slightly higher that the original value used by GE. The use of the original value is therefore a conservative assumption.

As reported in the GE report (GE, 1991a), the allowable stress, S, for the SA-212 Grade B steel used for the drywell is defined at 17.5 ksi. The primary stresses include the general membrane stress and the general membrane plus bending stress. For the refueling load case (Service Level B) and the accident load case (Service Level C), the allowable general membrane stress, S_{mc}, were set equal to 1.1 times the allowable stress, or 1.1 x 17.5 = 19.3 ksi. The general membrane plus bending stress is set equal to 1.5 times the general membrane allowable stress, or 1.5 x 19.3 = 29 ksi. The primary plus secondary stress is set equal to 3 times the allowable stress, or 3 x 17.5 = 52.5 ksi. Secondary stresses include thermal stresses and bending stresses at gross structural discontinuities (e.g. the intersection of two plates of different thickness). For the post-accident (Service Level D) load case, the general membrane, general membrane plus bending, and the primary plus secondary stress allowables are 38 ksi, 57 ksi, and 70 ksi.

In the FSAR (FSAR, 2003), it is stated the steel designated SA-212 Gr. B has been superseded in the ASME code by SA-516 Gr. 70. In the 2004 ASME code, Section II, Part D, Subpart 1, Table 1A, the allowable stress at room temperature is given as 20 ksi. Since this value is slightly larger than the 17.5 ksi used previously, the lower value of 17.5 ksi is used here. When using this value for the allowable stress, S, the 2004 ASME Section III, Division I, Subsection NE, Class MC, Article NE-3000 (ASME, 2004), as well as the Standard Review Plan (SRP, 1996) produces similar values as compared to the allowables defined above by GE. The allowables in the current code for "not integral and continuous" structures are slightly more conservative than those for "integral and continuous" structures, and produce the same allowables as describes above. Therefore, these values are conservatively adopted here. In addition, the allowables for primary plus secondary stresses for Level C and Level D do not need to be evaluated per the ASME Code. For consistency with the previous GE analysis, these stresses are evaluated using the limits of 52.5 ksi and 70 ksi for Level C and D, respectively.

The stress analyses comparison with the code allowables treats the peak surface stresses for the shell elements used in this analysis as membrane plus bending stresses. If a case was encountered where the surface stress exceeded the membrane plus bending stress allowable, the stress value was explored further to determine if the surface stress resided at a gross structural discontinuity. In these cases, the stress values were considered to be primary plus secondary values and assessed using the higher stress limits defined in the ASME code. The results of the elastic

ABAQUS stress analyses for the Refueling, Accident, and Post-accident load cases are summarized below.

3.1 Refueling Condition

The analyses of the refueling load condition employed the model and loadings described in Section 2. Two stress analyses were performed for the refueling load case. These included the containment with and without degradation. The thicknesses used for the upper portions of the degraded drywell are outlined in Table 2-6. In the lower sphere of the drywell, the average UT measurement data was used to assign shell thicknesses as outlined in Table 2-7. Table 3-1 and Table 3-2 summarize the peak stresses for each of the analyses. In each case and for each region of the containment, the peak membrane stresses are reported as well as the peak membrane plus bending stresses. The membrane plus bending stresses are the surface stresses provided in the analysis output for each shell element. The membrane stresses are taken at the midsection output value for each shell element. The peak stresses in both the meridional and circumferential directions are provided. Values given as positive represent tensile stresses, and values given as negative are compressive stresses. The percentage of the ASME limit for each stress value is provided in parenthesis. For each analysis, the stresses remain within ASME code allowables (Service Level B).

Table 3-1. Refueling Load Case Peak Stresses with No Degradation, Primary Stresses (Percentage of ASME Limit in Parenthesis)

Drywell Region	Membrane Stresses, ksi			Membrane + Bending Stresses, ksi		
	Meridional	Circumferential	ASME Limit	Meridional	Circumferential	ASME Limit
Cylinder	-1.31 (6.8)	-1.33 (6.9)	19.3	-1.59 (5.5)	-1.53 (5.3)	29
Knuckle	-0.59 (3.1)	-2.06 (10.7)	19.3	-2.33 (8.0)	-2.45 (8.4)	29
Upper Sphere	-2.49 (12.9)	-0.88 (4.6)	19.3	-6.27 (21.6)	-4.62 (15.9)	29
Middle Sphere	-4.45 (23.1)	-2.08 (10.8)	19.3	-7.94 (27.4)	-8.65 (29.8)	29
Thickened Middle Sphere	-2.71 (14.0)	3.89 (20.2)	19.3	-5.05 (17.4)	-5.66 (19.5)	29
Lower Sphere	-5.02 (26.0)	6.05 (31.3)	19.3	-12.14 (41.9)	9.64 (33.2)	29

Positive values are tension, negative values are compression. ASME Limits based on stress magnitude.

Table 3-2. Refueling Load Case Peak Stresses with Degradation, Primary Stresses (Percentage of ASME Limit in Parenthesis)

Drywell Region	Membrane Stresses, ksi			Membrane + Bending Stresses, ksi		
	Meridional	Circumferential	ASME Limit	Meridional	Circumferential	ASME Limit
Cylinder	-1.43 (7.4)	-1.44 (7.5)	19.3	-1.72 (5.9)	-1.64 (5.7)	29
Knuckle	-0.60 (3.1)	-2.08 (7.2)	19.3	-2.38 (12.3)	-2.48 (8.6)	29
Upper Sphere	-2.71 (14.0)	-1.01 (3.5)	19.3	-6.94 (36.0)	-5.18 (17.9)	29
Middle Sphere	-5.51 (28.5)	-2.58 (13.4)	19.3	-9.72 (33.5)	-10.65 (36.7)	29
Thickened Middle Sphere	-3.15 (16.3)	4.99 (25.9)	19.3	-5.78 (19.9)	7.06 (24.3)	29
Lower Sphere	-6.37 (33.0)	8.00 (41.5)	19.3	-14.70 (50.7)	14.32 (49.4)	29
Local Region 1	-5.01 (26.0)	3.94 (20.4)	19.3	-7.25 (25.0)	4.42 (15.2)	29
Local Region 13	-5.02 (26.0)	3.91 (20.3)	19.3	-7.31 (25.2)	4.39 (15.1)	29

Figure 3-1, Figure 3-2, and Figure 3-3 show the meridional membrane stress distributions in the lower sphere regions for the refueling case without degradation, and with degradation. Figure 3-3 shows a detailed view of the local thin region in under the ventline in Bay 13. Note that the scales for the color stress contours are not the same for the no degradation case and for the degradation case. The regions in light gray have tensile meridional stresses which are typically much lower in magnitude than the compressive stresses for this loading condition. The meridional membrane stress distribution is similar for each case, with the highest stresses near the bottom of the sandbed and between the ventlines. The local thin area in Figure 3-3 does not experience significantly higher stresses since the compressive load is typically lower beneath the ventlines and the load in that region is easily redistributed around the thin region.

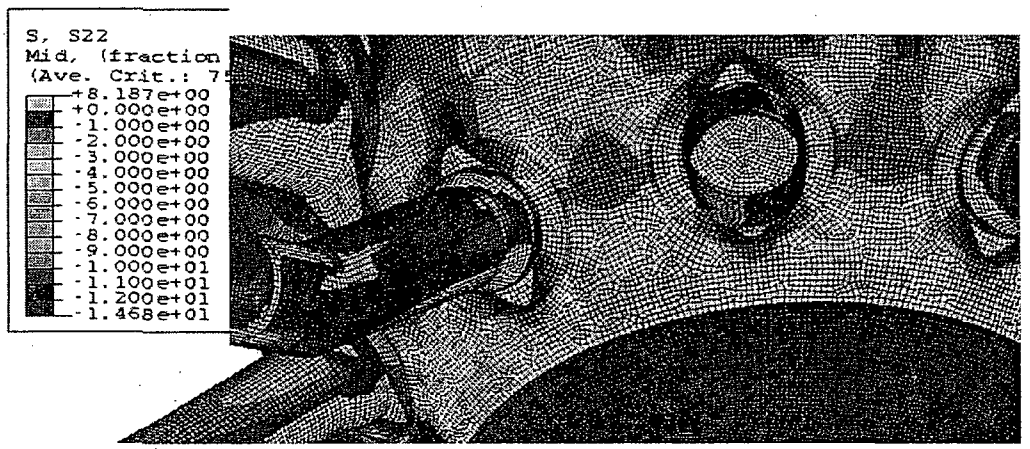

Figure 3-1. *Meridional Membrane Stress Distribution in the Lower Sphere for the Refueling Load Case with No Degradation (ksi)*

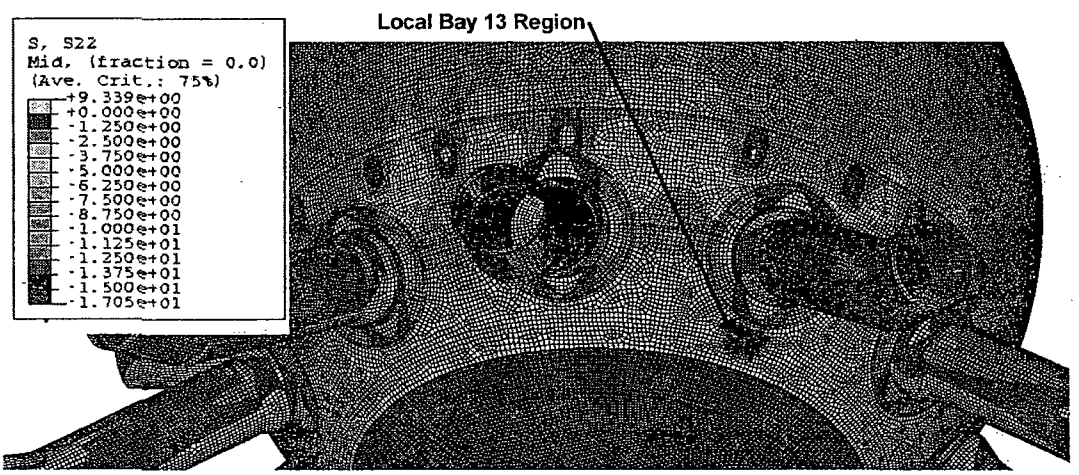

Figure 3-2. Meridional Membrane Stress Distribution in the Lower Sphere for the Refueling Load Case with Degradation (ksi)

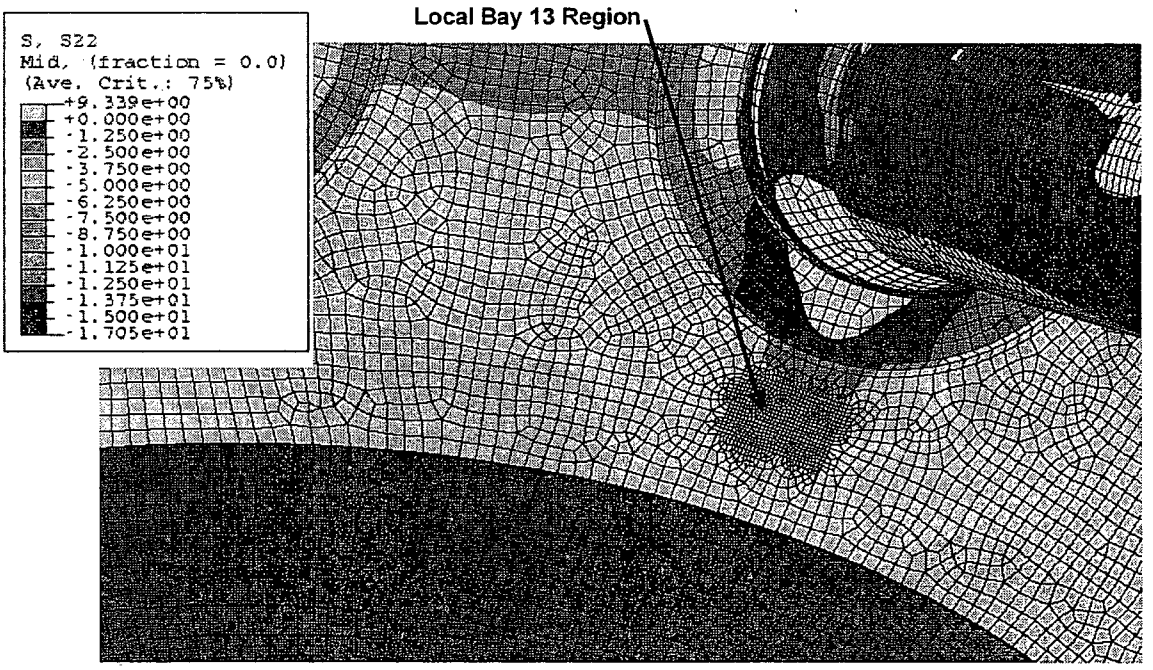

Figure 3-3. Meridional Membrane Stress Distribution in Local Bay 13 Region for the Refueling Load Case with Degradation (ksi)

3.2 Accident Condition

The analyses of the accident load condition employed the model and loadings described in Section 2. Two analyses were performed for the stress analysis of the accident load case. These included the containment with and without degradation. The thicknesses used for the upper portions of the degraded drywell are outlined in Table 2-6. The degraded shell thicknesses for the lower sphere are outlined in
Table 2-7. Table 3-3 through Table 3-6 summarize the peak stresses for each analysis. Table 3-3 and Table 3-5 include the peak membrane stresses and the peak membrane plus bending stresses. In addition, the peak primary plus secondary stresses are provided in Table 3-4 and Table 3-6. These values are typically surface stresses that include the thermal stress component from the increase of the drywell shell from 70°F to the accident temperature of 292°F. As for the refueling case, the peak stresses in both the meridional and circumferential directions are provided. Values given as positive represent tensile stresses, and values given as negative are compressive stresses.
For each analysis, the stresses remain within ASME code allowables (Service Level C) with a few potential exceptions which required additional discussion. The meridional membrane plus

bending allowable stress for the degraded analysis was exceeded in the upper sphere at the intersection with the knuckle. This was then determined to be a gross structural discontinuity, and therefore, the stress in this region was well below the primary plus secondary stress allowable.

The only remaining stress potentially exceeding the allowable is for the meridional and circumferential primary plus secondary stresses at the bottom of the lower sphere. These values are extremely large, exceeding the assumed allowable even for the case with no degradation. The high stresses in this region are caused by a combination of the bending due to the internal pressure and the thermal expansion due to the increase in the temperature from 70°F to the accident temperature of 292°F. While the introduction of degradation does increase these stresses, it appears to be a secondary effect. The model constructed in this study uses several approximations of the geometry and loading in this region. These include the assumption that beginning the increase in temperature from 70°F while the service temperature is closer to 150°F. Any potential stress relaxation due to the higher service temperature has been neglected. In addition, the temperature in the entire sandbed region is raised to 292 °F and the internal pressure is applied to the inside of the drywell shell down to an elevation of 8'-11.25". The previous GE analysis included a heat transfer analysis to determine the thermal gradient in the drywell shell in the sandbed region due to the concrete slab within the drywell extending up to an elevation of 10'-3". Since the present condition of the bond between the drywell shell and the concrete between the elevations of 10'-3" and 8'-11.25" is not currently know, the temperature and internal pressure were conservatively extended down to 8'-11.25". These assumptions, especially the extension of the temperature down to the point of fixity (elevation 8'-11.25"), imposes a severe discontinuity in the shell as discussed in Section 2.4.4. The potential conservativeness of the assumptions adopted here should be considered when interpreting the analysis results. It should be noted that the sand that originally filled the sandbed was included in the original design to mitigate the bending stresses in this location. The sand was removed based in part by the previous analysis by GE (GE, 1991a). In addition, the intent of this study was not to reinvestigate the acceptability of removing the sand since this was performed in the approved analyses by GE. Finally, the ASME code does not require an evaluation for primary plus secondary stresses (stresses including thermal effects) for Level C loading. The evaluation is performed here to remain consistent with the stress evaluation in the previous GE analysis.

Table 3-3. Accident Load Case Peak Stresses with No Degradation, Primary Stresses (Percentage of ASME Limit in Parenthesis)

Drywell Region	Membrane Stresses, ksi			Membrane + Bending Stresses, ksi		
	Meridional	Circumferential	ASME Limit	Meridional	Circumferential	ASME Limit
Cylinder	6.80 (35.2)	14.02 (72.6)	19.3	12.15 (41.9)	14.90 (51.4)	29
Knuckle	3.59 (18.6)	13.79 (71.5)	19.3	10.33 (35.6)	15.83 (54.6)	29
Upper Sphere	12.73 (66.0)	13.68 (70.9)	19.3	28.86 (99.5)	16.43 (56.7)	29
Middle Sphere	12.57 (65.1)	13.98 (72.4)	19.3	16.35 (56.4)	16.01 (55.2)	29
Thickened Middle Sphere	10.61 (55.0)	11.13 (57.7)	19.3	13.68 (47.2)	12.27 (42.3)	29
Lower Sphere	9.44 (48.9)	10.95 (56.7)	19.3	14.42 (49.7)	17.39 (60.0)	29

Positive values are tension, negative values are compression. ASME Limits based on stress magnitude.

Table 3-4. Accident Load Case Peak Stresses with No Degradation, Primary + Secondary Stresses (Percentage of ASME Limit in Parenthesis)

Drywell Region	Primary + Secondary Stresses, ksi		
	Meridional	Circumferential	ASME Limit
Cylinder	12.19 (23.2)	15.01 (28.6)	52.5
Knuckle	10.37 (19.8)	15.89 (30.3)	52.5
Upper Sphere	28.97 (55.2)	16.46 (31.4)	52.5
Middle Sphere	17.34 (33.0)	15.99 (30.5)	52.5
Thickened Middle Sphere	13.00 (24.8)	12.28 (23.4)	52.5
Lower Sphere	82.51 (157.2)	-62.71 (119.4)	52.5

Table 3-5. Accident Load Case Peak Stresses with Degradation, Primary Stresses (Percentage of ASME Limit in Parenthesis)

Drywell Region	Membrane Stresses, ksi			Membrane + Bending Stresses, ksi		
	Meridional	Circumferential	ASME Limit	Meridional	Circumferential	ASME Limit
Cylinder	7.46 (38.7)	15.36 (79.6)	19.3	13.59 (46.9)	16.28 (56.1)	29
Knuckle	3.63 (18.8)	13.96 (72.3)	19.3	10.47 (36.1)	16.02 (55.2)	29
Upper Sphere	13.61 (70.5)	14.70 (76.2)	19.3	30.77 (58.6)	17.61 (60.7)	52.5 / 29
Middle Sphere	14.45 (74.9)	16.59 (86.0)	19.3	20.12 (69.4)	18.29 (63.1)	29
Thickened Middle Sphere	11.83 (61.3)	12.31 (63.8)	19.3	16.07 (55.4)	13.63 (47.0)	29
Lower Sphere	13.24 (68.6)	14.73 (76.3)	19.3	27.11 (93.5)	24.62 (84.9)	29
Local Region 1	8.91 (46.2)	13.46 (69.7)	19.3	15.46 (53.3)	15.36 (53.0)	29
Local Region 13	10.13 (52.5)	14.41 (74.7)	19.3	17.29 (59.6)	16.45 (56.7)	29

Positive values are tension, negative values are compression. ASME Limits based on stress magnitude.

Table 3-6. Accident Load Case Peak Stresses with Degradation, Primary + Secondary Stresses (Percentage of ASME Limit in Parenthesis)

Drywell Region	Primary + Secondary Stresses, ksi		
	Meridional	Circumferential	ASME Limit
Cylinder	13.60 (25.9)	16.31 (31.1)	52.5
Knuckle	10.48 (20.0)	16.04 (30.6)	52.5
Upper Sphere	30.80 (58.7)	17.61 (33.5)	52.5
Middle Sphere	21.50 (41.0)	19.52 (37.2)	52.5
Thickened Middle Sphere	14.79 (28.2)	14.21 (27.1)	52.5
Lower Sphere	88.55 (168.7)	-63.13 (120.2)	52.5
Local Region 1	32.59 (62.1)	12.52 (23.8)	52.5
Local Region 13	34.59 (65.9)	13.54 (25.8)	52.5

Figure 3-4 through Figure 3-7 illustrate the circumferential membrane stresses in the sandbed region of the cases without and with degradation. Both cases are show with and without the application of the thermal loading. With dead loads and the internal pressure load, the sandbed region is in tension circumferentially. The addition of the thermal loading causes sections of the sandbed region to go into compression due to the constraint at the point the drywell shell is embedded within concrete below elevation 8'-11.25" and below the ventlines. The sections of the sandbed and lower sphere that remain in tension are at significantly lower values due to the constraint provided by the ventlines. For the degraded case prior to the application of the thermal load, the local thinned region in Bay 13 does experience higher stresses than the surrounding area as shown in Figure 3-6. The thermal loads cause a significant reduction in the tensile stresses in this region. As discussed previously, the meridional membrane plus bending stresses also experience significantly higher stresses. Figure 3-8 illustrates the meridional membrane plus bending stresses, or the tensile stresses on the inside surface of the drywell shell, for the case without degradation after application of the internal pressure and thermal loads. The thermal expansion below the ventlines causes the sandbed region of the drywell shell to extend outward. This produces a significant stress concentration at the point the drywell shell becomes fixed within the concrete below elevation 8'-11.25". This bending stress concentration is highlighted in Figure 3-8 by the ring of red, orange, and yellow elements. The bending at this location is so severe the outside surface of the drywell shell is in significant compression, exceeding 60 ksi in some regions. It should be noted that the analyses performed here are elastic, and therefore, the stress reported do not include the effects of material yielding and plastic deformation. As mentioned previously, the addition of degradation does increase the bending stresses in this region, but the degradation appears to be secondary to the basic geometry and the modeling assumptions in this location.

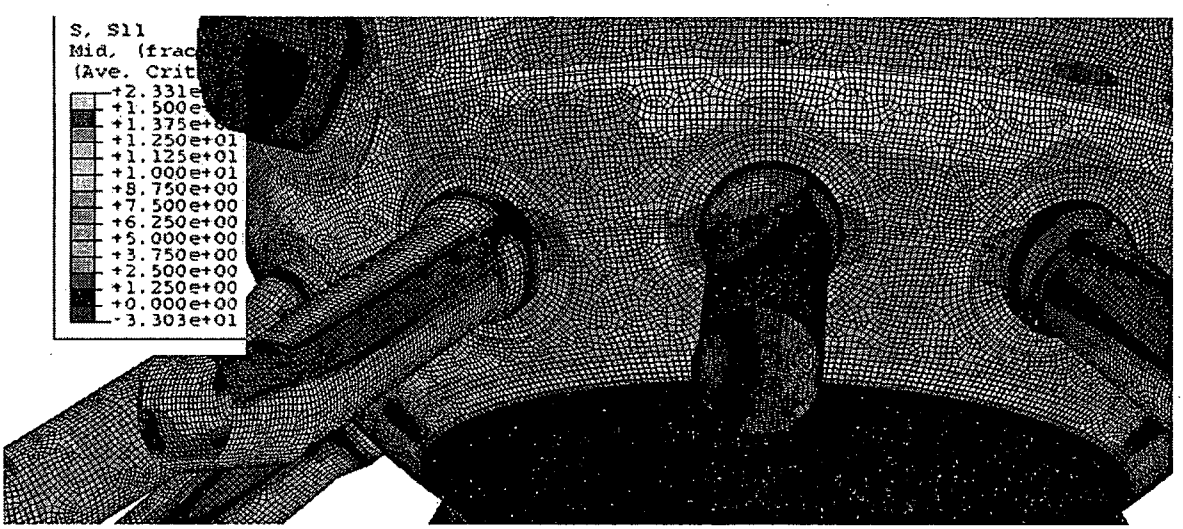

Figure 3-4. Circumferential Membrane Stress Distribution in Sandbed for the Accident Load Case with No Degradation (Internal Pressure without Thermal Load) (ksi)

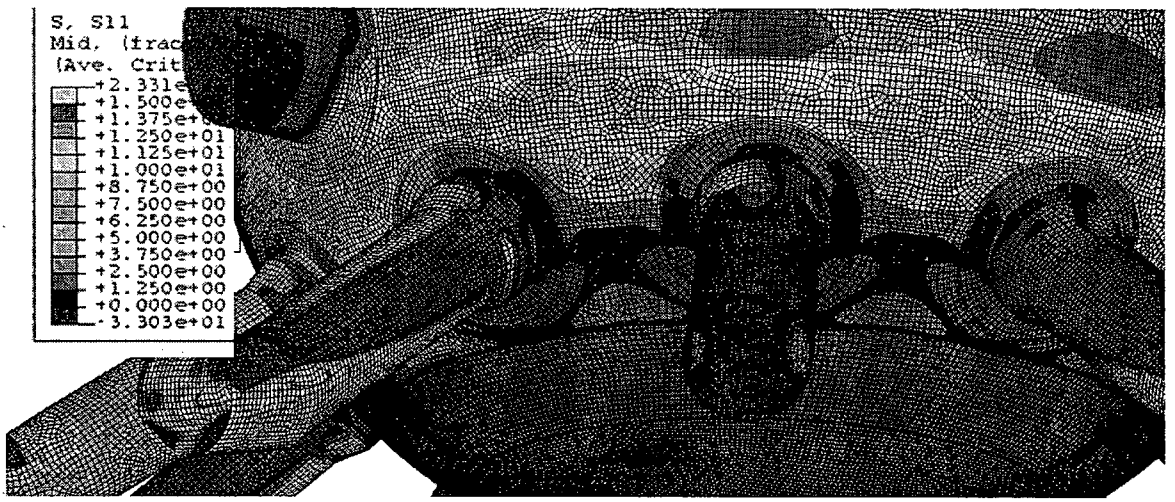

Figure 3-5. Circumferential Membrane Stress Distribution in Sandbed for the Accident Load Case with No Degradation (Internal Pressure with Thermal Load) (ksi)

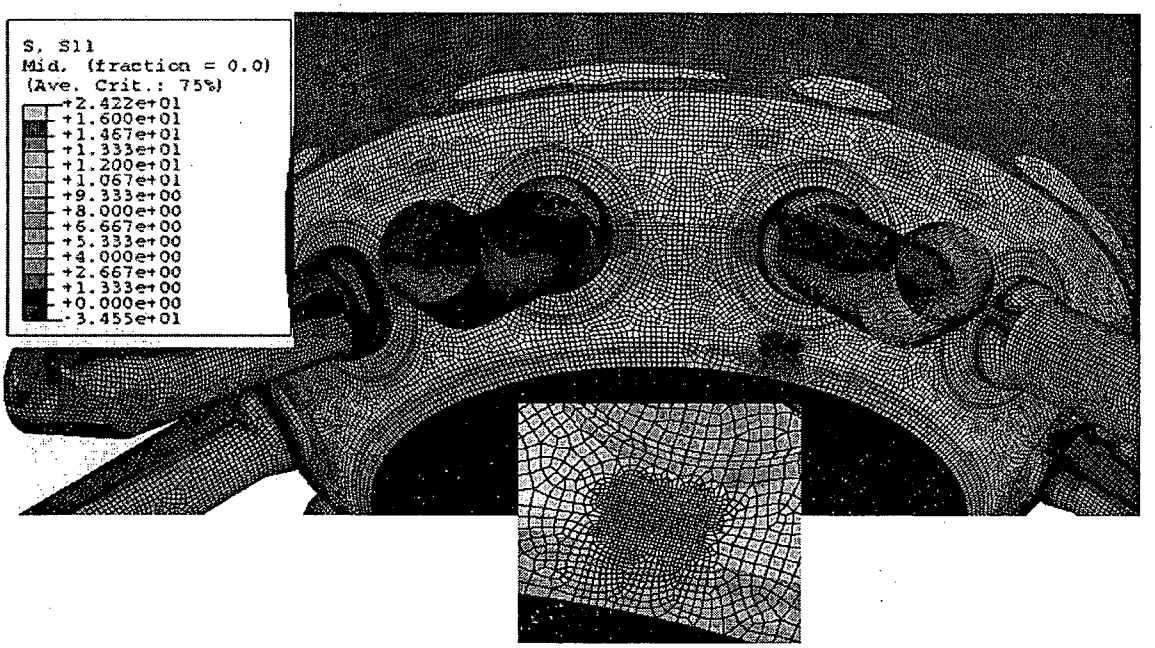

Figure 3-6. Circumferential Membrane Stress Distribution in Sandbed and Local Thin Region Under the Ventline in Bay 13 for the Accident Load Case with Degradation (Internal Pressure without Thermal Load) (ksi)

Figure 3-7. Circumferential Membrane Stress Distribution in Sandbed for the Accident Load Case with Degradation (Internal Pressure with Thermal Load) (ksi)

Figure 3-8. Meridional Membrane Plus Bending Stress Distribution (Tension on the Inside Surface of the Drywell Shell) in Sandbed for the Accident Load Case with No Degradation (Internal Pressure with Thermal Load) (ksi)

3.3 Post-Accident Condition

The analyses of the post-accident load condition employed the model and loadings that are described in the previous section. Two analyses were performed for the stress analysis of the post-accident load case. These included the containment with and without degradation. The thicknesses for the upper portions of the degraded drywell are outlined in Table 2-6. The thicknesses in the lower sphere of the drywell are outlined in Table 2-7.

For the Post-Accident condition, Table 3-7 and Table 3-8 summarize the peak stresses for each analysis. In each case and for each region of the containment, the peak membrane stresses are reported as well as the peak membrane plus bending stresses. The membrane plus bending stresses are the surface stresses provided in the analysis output for each shell element. The membrane stresses are taken in the midsection output value for each shell element. The peak stresses in both the meridional and circumferential directions are provided. Values given as positive represent tensile stresses, and values given as negative are compressive stresses. For each analysis, the stresses remain within ASME code allowables (Service Level D).

Table 3-7. Post-Accident Load Case Peak Stresses with No Degradation, Primary Stresses (Percentage of ASME Limit in Parenthesis)

Drywell Region	Membrane Stresses, ksi			Membrane + Bending Stresses, ksi		
	Meridional	Circumferential	ASME Limit	Meridional	Circumferential	ASME Limit
Cylinder	-1.68 (4.4)	-4.76 (12.5)	38	-4.25 (7.5)	-6.96 (12.2)	57
Knuckle	-0.43 (1.1)	-1.29 (3.4)	38	-1.99 (3.5)	-1.58 (2.8)	57
Upper Sphere	1.41 (3.7)	5.37 (14.1)	38	-4.65 (8.2)	6.39 (11.2)	57
Middle Sphere	2.75 (7.2)	12.27 (32.3)	38	-5.44 (9.5)	12.61 (22.1)	57
Thickened Middle Sphere	-5.03 (13.2)	13.43 (35.3)	38	-10.22 (17.9)	15.90 (27.9)	57
Lower Sphere	-10.10 (26.6)	18.34 (48.3)	38	-25.00 (43.9)	21.36 (37.5)	57

Table 3-8. Post-Accident Load Case Peak Stresses with Best Estimate Degradation, Primary Stresses (Percentage of ASME Limit in Parenthesis)

Drywell Region	Membrane Stresses, ksi			Membrane + Bending Stresses, ksi		
	Meridional	Circumferential	ASME Limit	Meridional	Circumferential	ASME Limit
Cylinder	-1.80 (4.7)	-4.87 (12.8)	38	-4.49 (7.9)	-6.94 (12.2)	57
Knuckle	-0.40 (1.1)	-1.19 (3.1)	38	-1.91 (3.4)	1.58 (2.8)	57
Upper Sphere	1.44 (3.8)	5.92 (15.6)	38	-5.12 (9.0)	6.93 (12.2)	57
Middle Sphere	3.19 (8.4)	14.13 (37.2)	38	-6.49 (11.4)	14.48 (25.4)	57
Thickened Middle Sphere	-5.58 (14.7)	17.25 (45.4)	38	-13.05 (22.9)	19.35 (33.9)	57
Lower Sphere	-13.21 (34.8)	24.04 (63.3)	38	-28.60 (50.2)	29.51 (51.8)	57
Local Region 1	-7.24 (19.1)	17.31 (45.6)	38	-15.93 (27.9)	20.20 (35.4)	57
Local Region 13	-8.87 (23.3)	20.31 (53.4)	38	-18.75 (32.9)	23.67 (41.5)	57

Figure 3-9 and Figure 3-10 illustrate the circumferential membrane stresses in the sandbed region for the post-accident load case, without degradation and with degradation, respectively. Note that the color stress contours used in these two figures are not set at the same scale. The stresses in the degraded analysis are much larger than the case with no degradation. The local thin region under the ventline in Bay 13 experiences higher stresses, but do not approach the allowables.

Figure 3-9. Circumferential Membrane Stress Distribution in Sandbed for the Post-Accident Load Case with No Degradation (ksi)

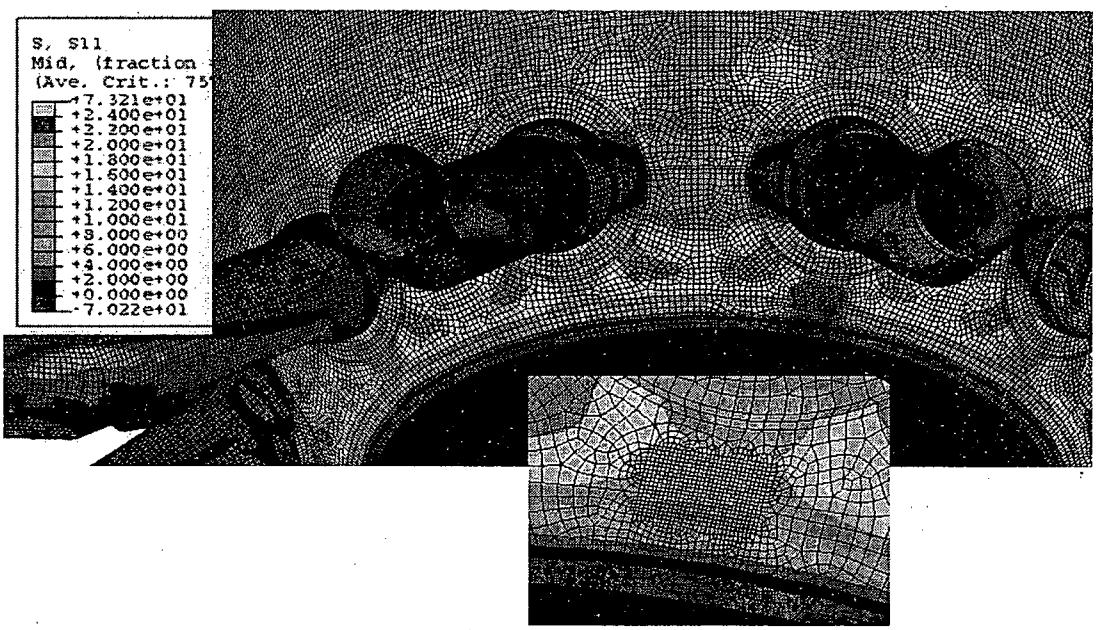

Figure 3-10. Circumferential Membrane Stress Distribution in Sandbed and Local Thin Region Under the Ventline in Bay 13 for the Post-Accident Load Case with Degradation (ksi)

3.4 Conclusion

The ASME allowable stresses are met for all three load cases examined here given the modeling and loading procedures outlined in Section 2. The only potential exception is for the primary plus secondary stresses located at the base of the sandbed region of the accident condition due to the thermal expansion of the shell. The primary cause of these high stresses is the number of modeling and loading assumptions in this region, with the introduction of degradation producing only a secondary effect. In addition, the primary plus secondary stresses (includes thermal stresses) were compared to the allowables use in the previous GE analysis (GE, 1991a). The current code does not require an evaluation of the primary plus secondary stresses for Service Level C, but were performed here for consistency with the previous study and since some evaluation of the shell was judged to be appropriate. Beyond the stresses at the base of the sand-bed region for the accident condition, the introduction of the degradation does cause a noticeable increase in the stress levels throughout the drywell shell for each load condition. In general, the accident condition causes the largest stress increases throughout the containment when degradation is introduced.

4. Stability Analysis

In this analysis, the structural integrity of the drywell shell is examined in terms of stability using the ASME Code Case N-284, "Metal Containment Shell Buckling Design Methods, Section III, Division 1, Class MC." This stability analysis used the stresses computed through the stress analysis outlined in the previous section. The refueling and post-accident load cases were assumed to be the governing load combinations for potential buckling in the drywell. The effective factors of safety against buckling were computed and compared to the required ASME code allowables.

Here, the theoretical elastic buckling stress, σ_{ie}, is computed using a combination of the stress analyses described in the previous section and a separate eigenvalue extraction analysis in ABAQUS. The eigenvalue buckling analysis provides the load factors, λ, that cause buckling given the applied loads. For each eigenvalue, or load factor, the analysis provides the resulting buckling mode or displaced shape. Each load factor defines the multiplier on the applied loads that would cause the given buckling mode. For example, a load factor of 4 indicates that the applied loads would need to be increased by a factor of 4 to cause that buckling mode to occur. The load factor can also be applied to the compressive stress value, σ_c, located in the buckling region to compute the buckling stress. Therefore, the stress determined from the stress analysis of a specific load case and level of degradation is multiplied by the load factor computed in the eigenvalue buckling analysis to produce the theoretical elastic buckling stress, $\sigma_{ie} = \lambda\sigma_c$. The same models used for the stress analyses in the previous section are used in the eigenvalue buckling analyses.

Since the theoretical elastic buckling stress does not take into account the imperfections that exist within any fabricated shell structure, σ_{ie} is modified in N-284 by capacity and plasticity reduction factors. This is necessary due to the buckling phenomenon being highly sensitive to imperfections.

The capacity reduction factor, α, for an unstiffened sphere in uniaxial compression equals 0.207. In the previous analysis by GE (GE, 1991b), they employed an increased capacity reduction factor due to the tensile stresses in the circumferential direction. Article 1500 of N-284 and a reference by Johnson (Johnson, 1976), among others, were used to justify the use of an increased capacity reduction factor. Article 1500 and the Johnson reference explain that an increase in buckling capacity have been observed in cases where circumferential tensile stresses are produced due to internal pressure. This internal pressure has the effect of smoothing out the initial imperfections that are often the site of buckling initiation. GE applied the method provided in the Johnson reference to increase the capacity reduction factor for examining buckling for both the post-accident and refueling load cases. While the post-accident case includes an internal pressure from the flooded drywell, the refueling case has no internal pressure. The circumferential tensile stresses in the sandbed region for the refueling case stem from the geometry of the structure. Article 1500 of N-284 states clearly that an increased capacity reduction factor may be justified due to internal pressure. Since no further justification was provided in the previous GE analysis to use this increased factor for cases with circumferential tensile stresses not due to internal pressure, this method was not adopted for the refueling load case. However, since the

post-accident load case includes internal pressure, a modified version of the method used by GE is applied and described in a section describing the post-accident buckling results.

The plasticity reduction factor, η, for spheres under uniaxial compression is provided in N-284. For values of $\Delta < 0.55$, $\eta = 1.0$, and for values of $0.55 < \Delta < 1.6$, $\eta = 0.45/\Delta = 0.18$, where $\Delta = \alpha\sigma_{ie}/\sigma_y$ and σ_y is the material yield strength.

The compressive buckling stress, σ_c, can be evaluated using the reduced theoretical elastic buckling stress that equal $\alpha\ \eta\ \sigma_{ie}/FS$, where FS equals the factor of safety. The factor of safety equal 2.0 for Service Level B (refueling) and 1.67 for Service Level D (post-accident).

4.1 Refueling Condition

For the refueling load case with no degradation, the fist buckling mode occurs at the upper beam seats in the middle sphere. These locations are shown in Figure 2-23. The load that the beam applies to the drywell shell is applied to these locations with surface tractions. The original thickness of the middle sphere was 0.77 inches. Figure 4-1 illustrates the buckled displaced shape for this mode with a load factor of 13.36. The drywell shell buckles inward and down due to the load of the attached beam. In the previous GE analysis, the load for the beam seats was smeared along the entire circumference of the drywell, and therefore did not predict this type of buckling mode. Buckling modes are extremely dependent on the constraint conditions. This model does not account for the possible constraint by the beam attached to the interior surface of the shell. Without further study, it is not know if the attached beam would prevent the buckling in this region. Even so, the N-284 buckling evaluation in Table 4-1 indicates that the compressive stress in this region does not exceed the allowable stress for the case with no degradation. The effective factor of safety (inelastic instability stress divided by the applied compressive stress) equals 2.77 which is larger that the factor of 2 required for Service Level B loadings. Here, the compressive stress used in the buckling evaluation was taken at the element that shows the maximum buckled displacement (red region in Figure 4-1). Subsequent buckling modes occur in other locations throughout the middle sphere, the cylinder, and then in the sandbed region of the lower sphere.

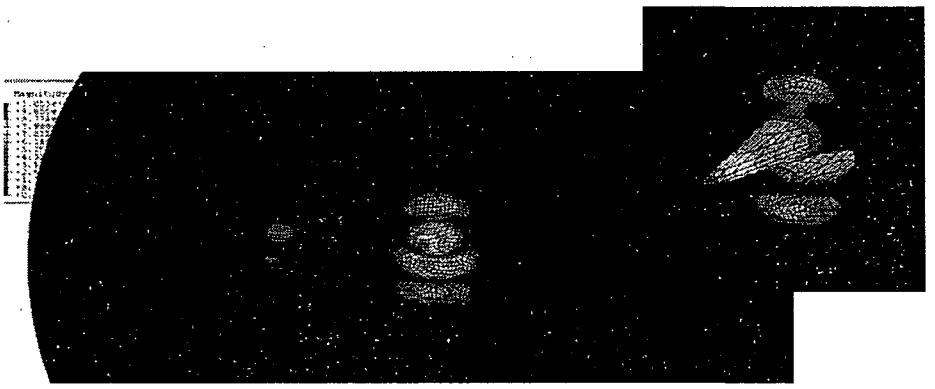

Figure 4-1. Buckling at the Upper Beam Seat for the Refueling Case with No Degradation

Table 4-1. Buckling Evaluation at the Upper Beam Seat for the Refueling Load Case with No Degradation

Sphere Radius, in	420
Sphere Thickness, in	0.77
Material Yield Stress, ksi	38
Elastic Modulus, ksi	29500
Factor of Safety, FS	2
Applied Meridional Compressive Stress from Analysis, σ_c, ksi	4.45
Load Factor from Bucking Analysis, λ	13.36
Theoretical Elastic Buckling Stress, $\sigma_{ie} = \lambda\sigma_c$, ksi	59.452
Capacity Reduction Factor, α	0.207
Reduced Elastic Instability Stress, $\sigma_e = \alpha\sigma_{ie}$, ksi	12.307
Yield Stress Ration, $\Delta = \sigma_e/\sigma_y$	0.324
Plasticity Reduction Factor, η	1.0
Inelastic Instability Stress, $\sigma_i = \eta\sigma_e$, ksi	12.307
Allowable Compressive Stress, $\sigma_{all} = \sigma_i/FS$, ksi	6.153
Applied Compressive Stress Percentage of Allowable, $\sigma_c/\sigma_{all} * 100$	72.3%
Effective Factor of Safety, $FS_E = \sigma_i/\sigma_c$	2.77

For the refueling load case with no degradation, buckling is eventually predicted in the sandbed region as shown in Figure 4-2 with the evaluation outlined in Table 4-2. The buckling occurs in two different regions of the sandbed, between the ventlines in Bays 1 and 3, and between the ventlines in Bays 17 and 19. The largest displacements occur in the 1.154 inch thick shell between Bays 1 and 3. Therefore, this location is used to evaluate the compressive buckling stresses. Table 4-2 shows that the effective factor of safety is 3.85 which exceeds 2.

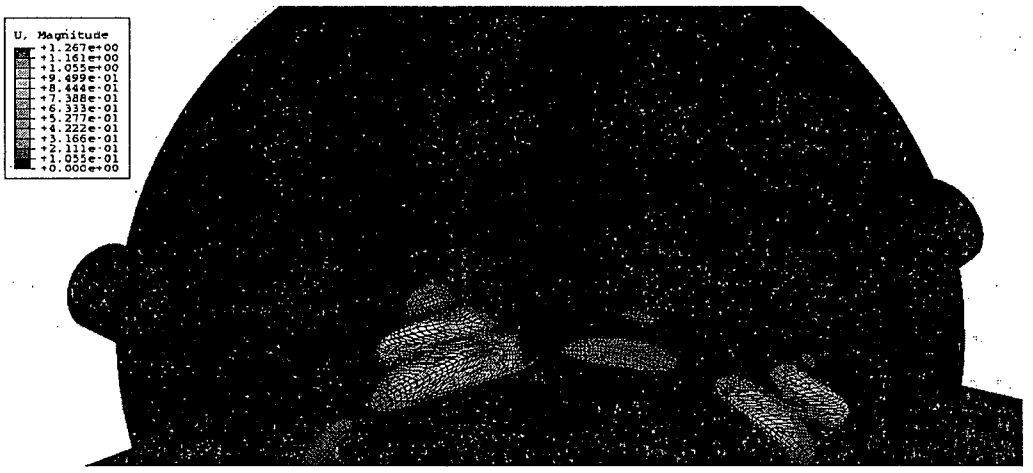

Figure 4-2. Buckling in the Sandbed Region for the Refueling Case with No Degradation

Table 4-2. Buckling Evaluation in the Sandbed Region for the Refueling Load Case with No Degradation

Sphere Radius, in	420
Sphere Thickness, in	1.154
Material Yield Stress, ksi	38
Elastic Modulus, ksi	29500
Factor of Safety, FS	2
Applied Meridional Compressive Stress from Analysis, σ_c, ksi	4.32
Load Factor from Bucking Analysis, λ	18.61
Theoretical Elastic Buckling Stress, $\sigma_{ie} = \lambda\sigma_c$, ksi	80.374
Capacity Reduction Factor, α	0.207
Reduced Elastic Instability Stress, $\sigma_e = \alpha\sigma_{ie}$, ksi	16.637
Yield Stress Ration, $\Delta = \sigma_e/\sigma_y$	0.438
Plasticity Reduction Factor, η	1.0
Inelastic Instability Stress, $\sigma_i = \eta\sigma_e$, ksi	16.637
Allowable Compressive Stress, $\sigma_{all} = \sigma_i/FS$, ksi	8.319
Applied Compressive Stress Percentage of Allowable, $\sigma_c/\sigma_{all} * 100$	51.9%
Effective Factor of Safety, $FS_E = \sigma_i/\sigma_c$	3.85

Figure 4-3 and Table 4-3 illustrate the buckling in the upper beam seat for the refueling load case with degradation. In this case, the thickness of the middle sphere has been reduced to 0.67". Therefore, the stresses in this region increase leading to a decrease in the load factor (9.49). This indicates that the applied loads are closer to causing the shell to buckle. The N-284 evaluation produces an effective factor of safety equal to 1.96 which is just under the require value of 2. As discussed previously, the constraint provided by the beam may affect the buckling predicted here.

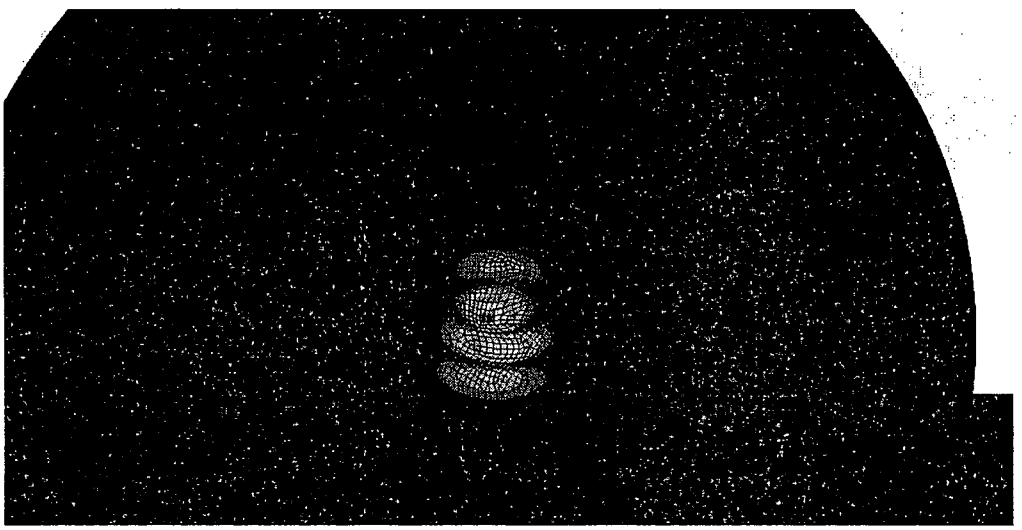

Figure 4-3. Buckling at the Upper Beam Seat for the Refueling Case with Best Estimate Degradation

Table 4-3. Buckling Evaluation at the Upper Beam Seat for the Refueling Load Case with Best Estimate Degradation

Sphere Radius, in	420
Sphere Thickness, in	0.67
Material Yield Stress, ksi	38
Elastic Modulus, ksi	29500
Factor of Safety, FS	2
Applied Meridional Compressive Stress from Analysis, σ_c, ksi	5.39
Load Factor from Bucking Analysis, λ	9.49
Theoretical Elastic Buckling Stress, $\sigma_{ie} = \lambda\sigma_c$, ksi	51.15
Capacity Reduction Factor, α	0.207
Reduced Elastic Instability Stress, $\sigma_e = \alpha\sigma_{ie}$, ksi	10.59
Yield Stress Ration, $\Delta = \sigma_e/\sigma_y$	0.279
Plasticity Reduction Factor, η	1.0
Inelastic Instability Stress, $\sigma_i = \eta\sigma_e$, ksi	10.59
Allowable Compressive Stress, $\sigma_{all} = \sigma_i/FS$, ksi	5.29
Applied Compressive Stress Percentage of Allowable, $\sigma_c/\sigma_{all} * 100$	101.8%
Effective Factor of Safety, $FS_E = \sigma_i/\sigma_c$	1.96

Figure 4-4 and Table 4-4 predict buckling in the sandbed region for the refueling load case with degradation. In this analysis, sandbed Bay Combination 13-15 was the first to buckle at a thickness of 0.842 inches. This region is just adjacent to the local thin region (t = 0.618 inches) under the ventline in Bay 13. Since Bay Combination 9-11 (t = 0.835 in) is thinner than 13-15, it is possible the local thin region adjacent to Bay Combination 13-15 aids in the initiation of the buckling of the entire region. The effective factor of safety for this buckling mode is 2.15 which just exceeds the required value of 2.

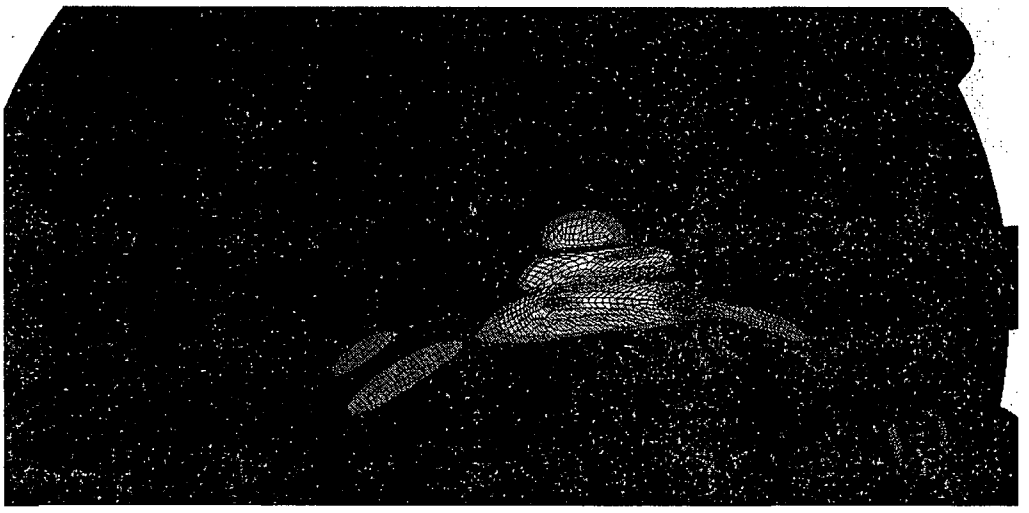

Figure 4-4. Buckling in the Sandbed Region for the Refueling Case with Best Estimate Degradation

Table 4-4. Buckling Evaluation in the Sandbed Region for the Refueling Load Case with Best Estimate Degradation

Sphere Radius, in	420
Sphere Thickness, in	0.842
Material Yield Stress, ksi	38
Elastic Modulus, ksi	29500
Factor of Safety, FS	2
Applied Meridional Compressive Stress from Analysis, σ_c, ksi	4.47
Load Factor from Bucking Analysis, λ	10.40
Theoretical Elastic Buckling Stress, $\sigma_{ie} = \lambda\sigma_c$, ksi	46.49
Capacity Reduction Factor, α	0.207
Reduced Elastic Instability Stress, $\sigma_e = \alpha\sigma_{ie}$, ksi	9.62
Yield Stress Ration, $\Delta = \sigma_e/\sigma_y$	0.253
Plasticity Reduction Factor, η	1.0
Inelastic Instability Stress, $\sigma_i = \eta\sigma_e$, ksi	9.62
Allowable Compressive Stress, $\sigma_{all} = \sigma_i/FS$, ksi	4.81
Applied Compressive Stress Percentage of Allowable, $\sigma_c/\sigma_{all} * 100$	92.9%
Effective Factor of Safety, $FS_E = \sigma_i/\sigma_c$	2.15

4.2 Post-Accident Condition

The analysis of the post-accident load case with no degradation produces numerous spurious buckling modes prior to those determined to be realistic in nature. These spurious modes occur at the ends of the ventlines and equipment hatch and are judged to be caused by the approximate boundary conditions used in those regions. The first realistic buckling mode for the no degradation case occurs in the cylinder. From the displaced shape for this buckling mode in Figure 4-5, it appears that it is caused by a combination of the additional lateral seismic load used for the flooded condition and the lateral constraints applied to the stabilizers.

Table 4-5 summarizes the buckling evaluation. Here the applied meridional compressive stress is actually taken as the minimum principal stress since the maximum compressive stresses in this region are slightly rotated from the meridional axis. The effective factor of safety for this mode is 2.85 which exceeds the required 2. When degradation is introduced, buckling first occurs in the critical sandbed region and not in the cylinder. Therefore, an evaluation of buckling in the degraded cylinder has not been included here.

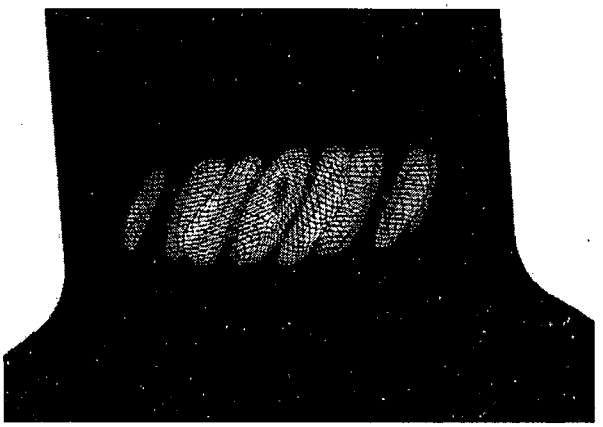

Figure 4-5. Buckling in the Cylinder for the Post-Accident Load Case with No Degradation

Table 4-5. Buckling Evaluation in the Cylinder for the Post-Accident Load Case with No Degradation

Sphere Radius, in	198
Sphere Thickness, in	0.640
Material Yield Stress, ksi	38
Elastic Modulus, ksi	29500
Factor of Safety, FS	1.67
Applied Meridional Compressive Stress from Analysis, σ_c, ksi	2.3
Load Factor from Bucking Analysis, λ	13.75
Theoretical Elastic Buckling Stress, $\sigma_{ie} = \lambda\sigma_c$, ksi	31.625
Capacity Reduction Factor, α	0.207
Reduced Elastic Instability Stress, $\sigma_e = \alpha\sigma_{ie}$, ksi	6.546
Yield Stress Ration, $\Delta = \sigma_e/\sigma_y$	0.172
Plasticity Reduction Factor, η	1.0
Inelastic Instability Stress, $\sigma_i = \eta\sigma_e$, ksi	6.546
Allowable Compressive Stress, $\sigma_{all} = \sigma_i/FS$, ksi	3.920
Applied Compressive Stress Percentage of Allowable, $\sigma_c/\sigma_{all} * 100$	58.7%
Effective Factor of Safety, $FS_E = \sigma_i/\sigma_c$	2.85

For buckling in the sandbed for the post-accident case, the allowable compressive stress is increased to account for the additional buckling capacity due to the internal pressure. A modified version of the procedure used by GE (GE, 1991b) is applied here. The only difference in the standard N-284 procedure is in the computation of the reduced elastic instability stress, σ_e. Based on the method outlined by Johnson (Johnson, 1976), $\sigma_e = \alpha\sigma_{ie} + \Delta C(Et/r)$, where α and σ_{ie} are computed the same as in N-284 with ΔC determined from a chart provided in Johnson (Johnson) and reprinted by GE (GE, 1991b). The chart of ΔC requires the computation of the 'X' parameter, where $X = (P/4E)(2r/t)^2$. Here, P is the internal pressure within the vessel and is taken as the maximum hydrostatic pressure near the bottom of the sandbed, 0.0278 ksi. GE applied a slightly modified version of this procedure by using the computed tensile stress in the buckled region to "back-out" an equivalent internal pressure. They then used the ΔC chart to compute a modified capacity reduction factor. The method used in the current study produces slightly lower allowable compressive stresses, and is therefore more conservative.

Table 4-6 shows the buckling calculations in the sandbed region for the post-accident case with no degradation and is illustrated in Figure 4-6. The largest displacement magnitudes for this buckling mode occur between the ventlines in Bays 17 and 19. After adjusting for the circumferential tensile stresses caused by the internal water pressure, the effective factor of safety is 3.47 which exceeds the required 1.67 for Service Level D loading.

Figure 4-6. Buckling in the Sandbed Region for the Post-Accident Load Case with No Degradation

Table 4-6. Buckling Evaluation in the Sandbed Region for the Post-Accident Load Case with No Degradation

Sphere Radius, r, in	420
Sphere Thickness, t, in	1.154
Material Yield Stress, ksi	38
Elastic Modulus, E, ksi	29500
Factor of Safety, FS	1.67
Applied Meridional Compressive Stress from Analysis, σ_c, ksi	6.25
Load Factor from Bucking Analysis, λ	13.94
Theoretical Elastic Buckling Stress, $\sigma_{ie} = \lambda\sigma_c$, ksi	87.12
Capacity Reduction Factor, α	0.207
Internal Pressure, P, ksi	0.0278
'X' Parameter, $X = (P/4E)(2r/t)^2$	0.125
ΔC (from Johnson, 1976)	0.095
Reduced Elastic Instability Stress, $\sigma_e = \alpha\sigma_{ie}+\Delta C(Et/r)$, ksi	25.73
Yield Stress Ration, $\Delta = \sigma_e/\sigma_y$	0.677
Plasticity Reduction Factor, η	0.844
Inelastic Instability Stress, $\sigma_i = \eta\sigma_e$, ksi	21.73
Allowable Compressive Stress, $\sigma_{all} = \sigma_i/FS$, ksi	13.01
Applied Compressive Stress Percentage of Allowable, $\sigma_c/\sigma_{all} * 100$	48.0%
Effective Factor of Safety, $FS_E = \sigma_i/\sigma_c$	3.47

Figure 4-7 and Table 4-7 illustrate buckling in the sandbed for the post-accident load case with degradation. Buckling first occurs in Bay Combination 13-15 at a thickness of 0.842 inches. This is just adjacent to the local thin region (t = 0.618 inches) under the ventline in Bay 13. After adjusting for the internal pressure effects, the effective factor of safety is 2.6 which exceeds the required 1.67.

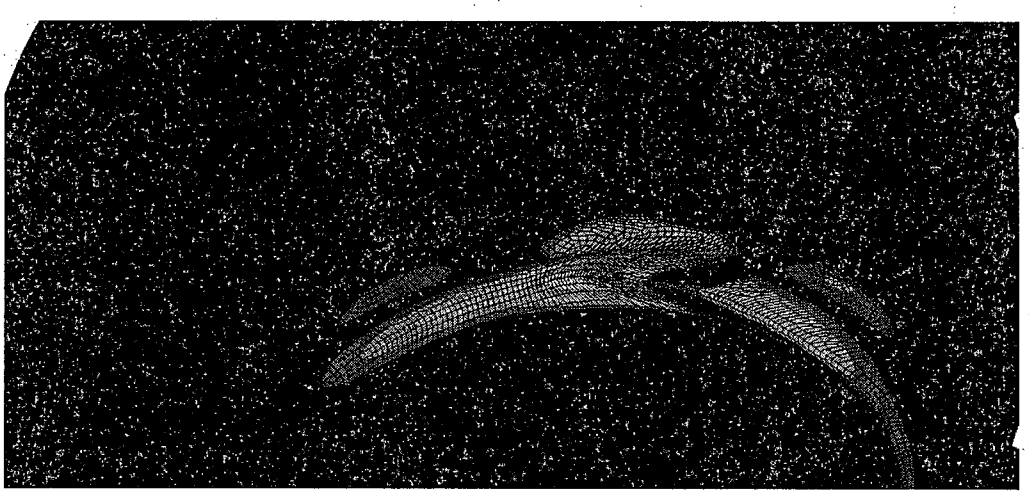

Figure 4-7. Buckling in the Sandbed Region for the Post-Accident Load Case with Best Estimate Degradation

Table 4-7. Buckling Evaluation in the Sandbed Region for the Post-Accident Load Case with Best Estimate Degradation

Sphere Radius, r, in	420
Sphere Thickness, t, in	0.842
Material Yield Stress, ksi	38
Elastic Modulus, E, ksi	29500
Factor of Safety, FS	1.67
Applied Meridional Compressive Stress from Analysis, σ_c, ksi	7.99
Load Factor from Bucking Analysis, λ	7.58
Theoretical Elastic Buckling Stress, $\sigma_{ie} = \lambda\sigma_c$, ksi	60.53
Capacity Reduction Factor, α	0.207
Internal Pressure, P, ksi	0.0278
'X' Parameter, $X = (P/4E)(2r/t)^2$	0.234
ΔC (from Johnson, 1976)	0.14
Reduced Elastic Instability Stress, $\sigma_e = \alpha\sigma_{ie}+\Delta C(Et/r)$, ksi	20.81
Yield Stress Ration, $\Delta = \sigma_e/\sigma_y$	0.547
Plasticity Reduction Factor, η	1.0
Inelastic Instability Stress, $\sigma_i = \eta\sigma_e$, ksi	20.81
Allowable Compressive Stress, $\sigma_{all} = \sigma_i/FS$, ksi	12.46
Applied Compressive Stress Percentage of Allowable, $\sigma_c/\sigma_{all} * 100$	64.1%
Effective Factor of Safety, $FS_E = \sigma_i/\sigma_c$	2.60

4.3 Conclusion

The buckling evaluation performed here using ASME N-284 show that based on the loadings and the model described in Section 2, both the refueling and post-accident load combinations met buckling requirements with a one exception. The buckling at the upper beam seat for the refueling load case with degradation does not met the required factor of safety of 2. As described earlier, the potential constraint provided by the attached beam has not been included in this analysis. In all cases, the introduction of degradation causes a significant decrease in the effective factor of safety against buckling. In the sandbed region, the degraded state analyzed in this study predicts an effective factor of safety of 2.15. This model includes spatial variation in the degradation and two local areas with increased thinning. In order to establish a minimum acceptable uniform thickness, an additional study was performed and is described in the next section.

5. Sandbed Region Minimum Thickness Study

In addition to the stress and stability analysis of the drywell shell using the average UT measurements in the sandbed region (thicknesses described in Section 2.6, and analyses outlined in Sections 3 and 4), a minimum sandbed thickness study was also performed. These analyses aim to establish the minimum uniform thickness in the sandbed region that maintains compliance with the ASME B&PV code. The minimum acceptable shell thickness established here is based on a buckling (stability) analysis for the refueling load case. The refueling load case appears to govern the potential for instability since a relatively low effective factor of safety was produced in the average UT measurement analysis at 2.15. For Service Level B (refueling condition), a factor of safety of 2.0 is required by ASME N-284.

The previous GE analysis (GE, 1991b) assumed a uniform sandbed shell thickness of 0.736". Their analyses produced an applied compressive stress of 7.58 ksi in the sandbed region and an inelastic buckling stress of 21.30 ksi (per ASME N-284). This produces an effective factor of safety of 2.81. A subsequent calculation documented in a 1993 GPU Nuclear Calculation Sheet (GPU Nuclear, 1993) shows an applied compressive stress of 7.58 ksi in the sandbed region for a shell thickness of 0.736", but with a lower value for the inelastic buckling stress at 15.18 ksi. This produces an effective factor of safety of 2.0, or at the required ASME N-284 value.

The inconsistency between the two calculations appears to stem from a difference in the application of the increased capacity reduction factor due to the tensile stresses in the circumferential (hoop) direction. This issue was discussed in detail in the previous stability analysis section. Article 1500 of ASME N-284 states clearly that an increased capacity reduction factor may be justified if an internal pressure loading is present and causes tensile stresses in the circumferential direction. This internal pressure aids in "smoothing" the initial imperfections and increased the buckling capacity under compressive meridional stresses. The lack of an internal pressure load for the refueling load case prevents the justified use of an increased capacity reduction factor. As with the buckling calculations for the refueling load case in the previous section, the minimum thickness study does not employ any increase in the capacity reduction factor.

The shell thicknesses used in the minimum thickness study are summarized in Table 5-1 for regions outside of the sandbed region. The degraded thickness values for the majority of the drywell are equivalent to the values used in the average UT measurement analysis. The only exception being the thickness assigned to the lower sphere above an elevation of 15'-6.8", or the center of the ventlines. In this region of the lower sphere (see Figure 5-1), the thickness is set to 1.154", or the nominal as-built value. This remains consistent with inspections of the upper portions of the lower sphere. In the average UT measurement analysis, additional conservatism was introduced by degrading the entire lower sphere uniformly in each bay combination. However, several confirmatory analyses performed during this study showed that the thickness assigned to the lower sphere above elevation 15'-6.8" has only a negligible effect since the buckling occurs in the sandbed below 15'-6.8".

In the lower sphere below elevation 15'-6.8" (sandbed region), the drywell shell is set to a uniform thickness. This region is shown in Figure 5-1. While the same finite element mesh was used as for the average UT measurement analyses, the local thinned regions under the ventlines

for Bays 1 and 13 are uniformly thinned consistent with the surrounding shell. In addition, this study only examined the minimum thickness required in the sandbed region and not in the upper portions of the sphere or in the cylinder.

Table 5-1. Main Drywell Shell Model Thicknesses Outside of Sandbed Region

Section	Original Thickness, in	Degraded Thickness, in	Section	Original Thickness, in	Degraded Thickness, in
Head	1.1875	N/C	Reinforcing Around Ventlines	2.875	2.618
Upper Cylinder	1.1875	N/C	Lower Sphere (below Sandbed)	1.154	N/C
Main Cylinder	0.640	0.585	Bottom Sphere	0.676	N/C
Knuckle	2.5625	2.54	Middle Sphere Thickened	1.0625	0.9625
Upper Sphere	0.722	0.676	Reinforcing Around Hatch	2.625	2.525
Middle Sphere	0.770	0.670	Lower Sphere (above El. 15'-6.8")	1.154	N/C

N/C – No Change

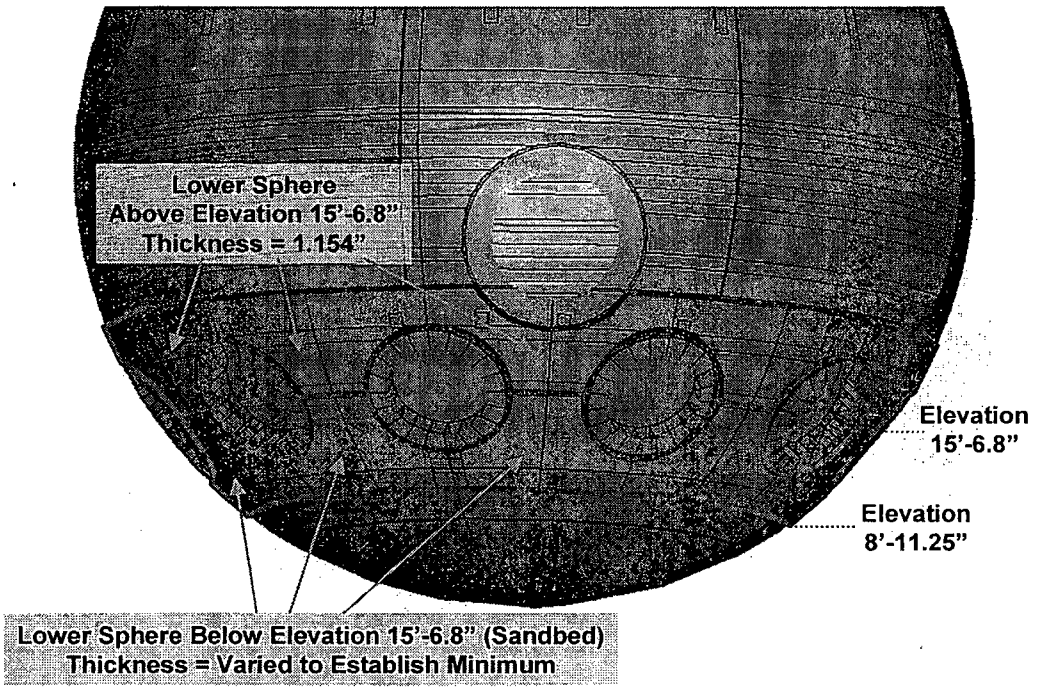

Figure 5-1. Drywell Lower Sphere for Establishing a Minimum Thickness in the Sandbed Region (Ventlines and Hatch Removed for Clarity)

The thickness values assigned to the sandbed region were varied from 0.800" up to 1.050" with a concentration of analyses performed between 0.800" and 0.860". In the previous buckling analysis section, a buckling analysis was also performed for the undegraded drywell containment which included a uniform thickness of 1.154" throughout the sandbed region. The results of each of these analyses are summarized in Figure 5-2. Here, the effective factor of safety is plotted against the associated shell thickness in the sandbed region. This study shows that a thickness of 0.844" is required in the sandbed region to produce an effective factor of safety equal to the ASME N-284 value of 2.0.

Figure 5-2 also plots the datapoint established in the previous buckling analysis section using average UT measurement data. In that analysis, the bay combination that buckled first was set to a thickness of 0.842" and resulted in an effective factor of safety equal to 2.15. Although the thicknesses used in the minimum thickness analysis and the average UT measurement analysis are essential equivalent, there are several important factors that produce the difference in safety factors. First, the average UT measurement analysis included two locally thinned regions that, in general, cause lower effective factors of safety for buckling in the adjacent bays than without the locally thinned regions. However, the effect of the locally thinned is outweighed by the existence of bay combinations with thickness far exceeding 0.842" (see Figure 2-32). For the average UT measurement analyses, 5 out of the 10 bay combinations were assigned thicknesses near or above 0.9". The existence of thicker bays enables a redistribution of the compressive loads leading to buckling. Therefore, the average UT measurement analysis produced an effective factor of safety of 2.15 with a thickness of 0.842", while the minimum thickness study produced an effective factor of safety of 2.0 with a thickness of 0.844". In the minimum thickness study, the entire sandbed region was uniformly thinned which prevents any redistribution of the load through thicker shell regions. The effect of the locally thinned regions was not rigorously explored in the average UT measurement analyses, but it is likely that the effective factor of safety of 2.15 would increase without the presence of the locally thinned region.

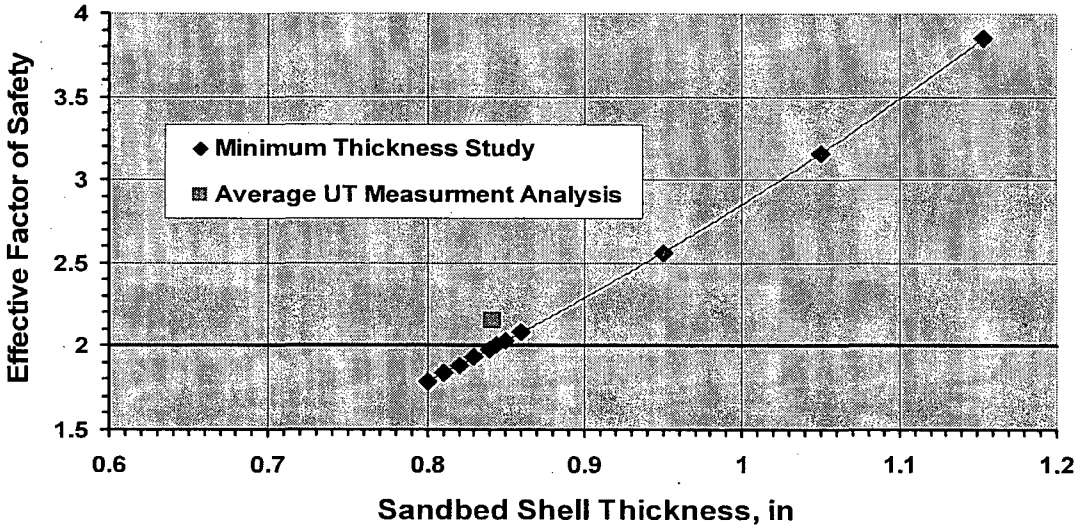

Figure 5-2. Effective Factor of Safety Values Computed for Various Thicknesses in the Sandbed Region for the Refueling Load Combination

Figure 5-3 and Table 5-2 illustrate the buckling location and ASME N-284 calculations for the sandbed with a thickness of 0.844". The major displacements for the first buckling mode in the sandbed are located between the ventline in Bays 1 and 3.

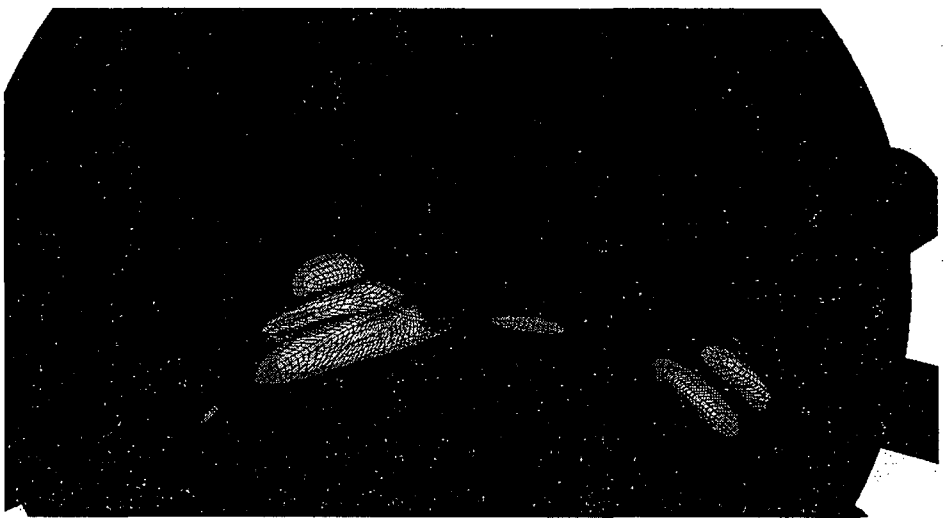

Figure 5-3. Buckling in the Sandbed Region with a Thickness of 0.844" for the Refueling Load Combination

Table 5-2. Buckling Evaluation for the Refueling Load Case with a Thickness of 0.844" in the Sandbed

Sphere Radius, in	420
Sphere Thickness, in	0.844
Material Yield Stress, ksi	38
Elastic Modulus, ksi	29500
Factor of Safety, FS	2
Applied Meridional Compressive Stress from Analysis, σ_c, ksi	4.78
Load Factor from Bucking Analysis, λ	9.67
Theoretical Elastic Buckling Stress, $\sigma_{ie} = \lambda\sigma_c$, ksi	46.19
Capacity Reduction Factor, α	0.207
Reduced Elastic Instability Stress, $\sigma_e = \alpha\sigma_{ie}$, ksi	9.56
Yield Stress Ration, $\Delta = \sigma_e/\sigma_y$	0.252
Plasticity Reduction Factor, η	1.0
Inelastic Instability Stress, $\sigma_i = \eta\sigma_e$, ksi	9.56
Allowable Compressive Stress, $\sigma_{all} = \sigma_i/FS$, ksi	4.78
Applied Compressive Stress Percentage of Allowable, $\sigma_c/\sigma_{all} * 100$	100.0%
Effective Factor of Safety, $FS_E = \sigma_i/\sigma_c$	2.00

6. Summary of Assumptions

The study performed for this program required a number of assumptions. A summary of the most significant assumptions is provided below.

- The Accident and Post-Accident load combinations are assumed to govern the stress analysis.

- The Refueling and Post-Accident load combinations are assumed to govern the buckling (stability) analysis.

- Information of the loads applied to the finite element model was taken from the previous study by GE. These loads were not independently verified.

- The seismic loading was applied using static coefficients provided in the Final Safety Analysis Report (FSAR, 2003). The static coefficients were applied using body forces in both the vertical and lateral directions. The displacement time histories (ground motions) were not made available for this study. The body forces used for the seismic loads were increased in the post-accident load combination to account for the mass of the water flooding the drywell.

- The ventlines were modeled down to the intersection with the ventline header. Here, springs acting in the radial and vertical directions were added to approximate the compliance of the ventline header. The spring constants were based on a simple submodel analysis of the ventline header. Since the ventline is connected to the torus with a flexible bellow, all interaction between the ventline and torus was neglected.

- The ventline jet deflector was modeled as a solid plate. In reality, the deflector has multiple holes throughout the plate. The thickness of the solid plate in the current model was reduced to account for the holes.

- In a number of cases, the exact location that a specific load acts upon the drywell shell was not known. The magnitude and elevation of these loads were provided in the GE report, but the azimuth locations remained unknown. In these cases (mainly in the case of the penetration loads), the loads were distributed along the entire circumference of the drywell as a surface traction.

- The loads applied to the drywell shell were "smeared" along a region defined on the shell surface. Typically, the region of application was taken as the area where an item is actually attached to the shell in the real structure. As mentioned above, the penetration loads were smeared along the entire circumference since loads for individual penetrations were not provided.

- The spacing of the upper and lower beam seats around the circumference is not constant, but the appropriate load distribution at each seat was not known. The loads for the upper

and lower beam seats were distributed equally at each point of attachment to the drywell shell.

- The concrete that fills the drywell shell interior from an elevation of 8'-11.25" to 10'-3", and the additional curbs, have not been accounted for in this model. The drywell shell is assumed encased in concrete below elevation 8'-11.25" (bottom of sandbed).

- For the accident load combination, the internal 44 psi pressure and the thermal load of 292°F (starting at 70°F) were applied to the entire drywell shell down to an elevation of 8'-11.25". The concrete within the interior of the drywell shell extends up to 10'-3" with curbs extending up to 12'-3". Since the bond between the steel shell and the concrete is not known, it was assumed that a gap could exist which would enable gas to pressurize and heat the shell down to 8'-11.25", or the bottom of the sandbed region on the exterior of the shell. Even if no gap exists initially, it is likely that the initial pressurization (pressure << 44 psi) acting on the shell above elevation 10'-3" would cause a gap to open. This would allow heated gas to flow between the shell and concrete.

- The Personnel Lock & Equipment Hatch penetration geometry (extent modeled and thicknesses assigned) was approximated and the outer surface fixed against vertical displacement.

- The coefficient of thermal expansion for the A-212-61T Grade B pressure vessel steel used for the drywell was assumed to be 6.5E-6°F^{-1}.

- A number of assumptions were made to develop the thicknesses assigned to the model in its degraded state. Section 2.6 provides a detailed discussion of these items.

- A very limited mesh convergence study was performed which led to the use of a 4" nominal element size. It was assumed that this mesh size was acceptable even though all load combinations were not examined in the convergence study and no checks on buckling were performed using different mesh sizes. In addition, a 1" nominal mesh size was used in the two local regions under the ventlines in Bay 1 and 13. No checks were performed to assess the mesh size in these regions.

- Several assumptions were made in developing the ASME stress limits. These are discussed in Section 3. .

- ASME Code Case N-284 was used to assess the stability of the degraded drywell shell. It was assumed that since the refueling case does not include any internal pressure, that the increase in buckling capacity used by GE for cases with circumferential (hoop) tension was not appropriate. Since the post-accident load case includes internal pressure, an increase in the capacity was applied.

7. Conclusions

The structural integrity of the degraded Oyster Creek drywell shell has been analyzed in this study. The allowable stresses and the buckling stability were both examined in accordance with the ASME B&PV code. The ASME allowable stresses are met for all three load cases examined here given the modeling and loading procedures outlined in Section 2. The only potential exception is for the primary plus secondary stresses located at the base of the sandbed region of the accident condition due to the thermal expansion of the shell. There are a number of modeling and loading assumptions in this region that may contribute to the stress magnitudes recorded in the current analysis. In addition, the primary plus secondary stresses were compared to the allowables use in the previous GE analysis (GE, 1991a). The current code does not require an evaluation of the primary plus secondary stresses for Service Level C. However, these stresses were assessed in this report to be consistent with the previous evaluation by GE. The buckling evaluation performed here using ASME N-284 show that based on the loadings and the model described in Section 2 both the refueling and post-accident load combinations met buckling requirements with a one exception. The buckling at the upper beam seat for the refueling load case with degradation does not meet the required factor of safety of 2. As described in Section 4, the potential constraint provided by the attached beam has not been included in this analysis. Table 7-1 summarizes the major conclusions for this study and for the previous GE analyses.

Table 7-1. Comparison of Conclusion Between GE Study (GE, 1991a and b) and the Current Study

Current Study Conclusion	GE Study Conclusion
The ASME B&PV stress analysis of the degraded Oyster Creek drywell shows all values within code limits. The current study uses average UT measurement data to assign thicknesses in the sandbed region. (Note that some primary plus secondary stresses for the accident condition are of concern as discussed in Section 3.)	**The ASME B&PV stress analysis of the degraded Oyster Creek drywell shows all values within code limits. The GE study assumed a conservative uniform thickness of 0.736" in the sandbed region.**
ASME B&PV Code Case N-284 stability analysis of the degraded Oyster Creek drywell shows that acceptable factors of safety are met. The current study uses average UT measurement data to assign thicknesses in the sandbed region. (Note that the buckling at the upper beam seats produces an effective factor of safety slightly less than 2 for the refueling load case, but this may be affected by the modeling of that specific detail.)	**ASME B&PV Code Case N-284 stability analysis of the degraded Oyster Creek drywell shows that acceptable factors of safety are met. The GE study assumed a conservative uniform thickness of 0.736" in the sandbed region.**
The minimum uniform shell thickness required to meet the ASME N-284 buckling safety factor was determined to be 0.844" in the sandbed region. This thickness was established using the buckling analysis for the refueling load case.	**The minimum uniform shell thickness required to meet the ASME N-284 buckling safety factor was determined to be 0.736". This thickness was established using the refueling load case. (The thickness of 0.736" was established in a calculation by GPU Nuclear, 1993. This calculation included an increase in the capacity reduction factor not used in the current study.)**

The assessments performed here employ a uniform thinning of the drywell shell over large sections of the surface. The thicknesses assigned in each region were based on limited measurement data since a very small percentage of the shell has been examined. In many cases, the raw data was not available. This led to the use of averages provided by AmerGen throughout the relevant documentation.

8. References

ABAQUS Analysis User's Manual, Version 6.5. 2004. Pawtucket, RI: Hibbit, Karlsson & Sorenson, Inc.

AmerGen April 4, 2006, Letter to U.S. NRC, 2130-06-20284, NRC Docket No. 50-219.

AmerGen April 7, 2006, Letter to U.S. NRC, 2130-06-20289, NRC Docket No. 50-219.

ASME (American Society of Mechanical Engineers). 2004. *Boiler and Pressure Vessel Code.* Sections III and VIII. New York, NY: American Society of Mechanical Engineers.

Cherry, J.L., and Smith, J.A., Capacity of Steel and Concrete Containment Vessels with Corrosion Damage, NUREG/CR-6707, SAND2000-1735, U.S. Nuclear Regulatory Commission, 2000.

Chicago Bridge & Iron (CB&I, 1980) Structural Drawings of the Oyster Creek Drywell, Torus, and Ventlines, attached to AmerGen letter to NRC, July 7, 2006, NRC Docket No. 50-219.

Final Safety Analysis Report (Updated), Oyster Creek Nuclear Generating Station (FSAR), AmerGen, Exelon, Revision 13, April 2003.

GE Stress Analysis Report, "An ASME Section VIII Evaluation of the Oyster Creek Drywell for Without Sand Case – Part I – Stress Analysis", GE Index #9-3, DRF #00664, February 1991a.

GE Stability Analysis Report, "An ASME Section VIII Evaluation of the Oyster Creek Drywell for Without Sand Case – Part II– Stability Analysis", GE Index #9-4, DRF #00664, February 1991b.

GPU Nuclear, Calculation Sheet, Oyster Creek Drywell External UT Evaluation, C-1302-187-5320-024, 1993.

Individual Plant Examination Submittal Report, Oyster Creek, (IPE), June 1992.

Johnson, B,G. editor, Guide to Stability of Design Criteria for Metal Structures, Third Edition, John Wiley & Sons, 1976.

Spencer, B.W., Petti, J.P., and Kunsman, D.M., Risk-Informed Assessment of Degraded Containment Vessels, NUREG/CR-6920, SAND2006-3772P, U.S. Nuclear Regulatory Commission, 2006.

Standard Review Plan for the Review of Safety Analysis Reports for Nuclear Power Plants (SRP), NUREG-0800, U.S. Nuclear Regulatory Commission, 1996.

9. Appendix A – Natural Frequency Extraction

An eigenvalue extraction was performed to calculate the natural frequencies for the degraded drywell shell in addition to the drywell shell in its original condition. This analysis was performed to assess the potential effects of degradation on the dynamic behavior of the drywell containment during a seismic event. The change in the natural frequencies when introducing degradation can provide justification for using a simplified static seismic analysis. The FSAR (FSAR, 2003) for Oyster Creek include the static seismic coefficients used in the original design of the drywell. If only minor differences exist between the natural frequencies for the containment in its original condition (the condition used to establish the static coefficients) and the containment in its degraded state, the dynamic behavior of the containment would not be significantly altered by the degradation. Therefore, the same static seismic coefficients could be applied when simulating the seismic loading for the degraded containment as for the as-built containment.

The model used previously for the stress and buckling analyses was modified and used to perform a natural frequency extraction in ABAQUS. Initial attempts to extract the natural frequencies for the drywell structure used the same model described in Section 2. That model included a section of the personnel lock/equipment hatch and the 10 ventlines down to the intersection with the ventline header. The natural frequency extraction analyses that included these penetrations resulted in spurious modes where the displacements of each mode concentrated at the ends of the penetrations. At these locations, the boundary conditions are approximated and applied to the structure as described in Section 2. These applied boundary conditions and approximated geometry cause these spurious, or unrealistic, mode shapes. In order to avoid these spurious modes, the geometry of the drywell was simplified by removing the hatch and ventline penetrations. The resulting "holes" in the drywell shell were subsequently "filled-in" with solid material to avoid spurious mode shapes with deformation concentrated around the holes. This results in the geometry illustrated in Figure 9-1. The nodes along the bottom of the sphere below elevation 8'-11.25" are fixed in all directions and the seismic stabilizers are fixed against lateral displacement as described for the full model in Section 2.

The thicknesses for the drywell with and without degradation are summarized in Table 9-1. The degraded thicknesses in the cylinder and upper sections of the sphere are the same as in the average UT measurement analysis. The thickness of the entire lower sphere is set to a uniform value of 0.835" for the natural frequency extraction of the degraded drywell. This region is highlighted in Figure 9-2. The thickened reinforcing plates surrounding the hatch and ventlines in the actual structure are not thickened in the frequency extraction performed here. These simplifications in the geometry enable a general assessment of the effects of degradation on the natural frequencies. This analysis was not intended to provide the exact frequencies for the drywell structure, but only to justify the use of the static seismic coefficients for the seismic loading component of the stress and buckling analyses. Therefore, the assumptions (e.g. the use of 0.835" for the thickness in the lower sphere and the simplified geometry) are judged to be acceptable in order to study the general effect of degradation on the natural frequencies.

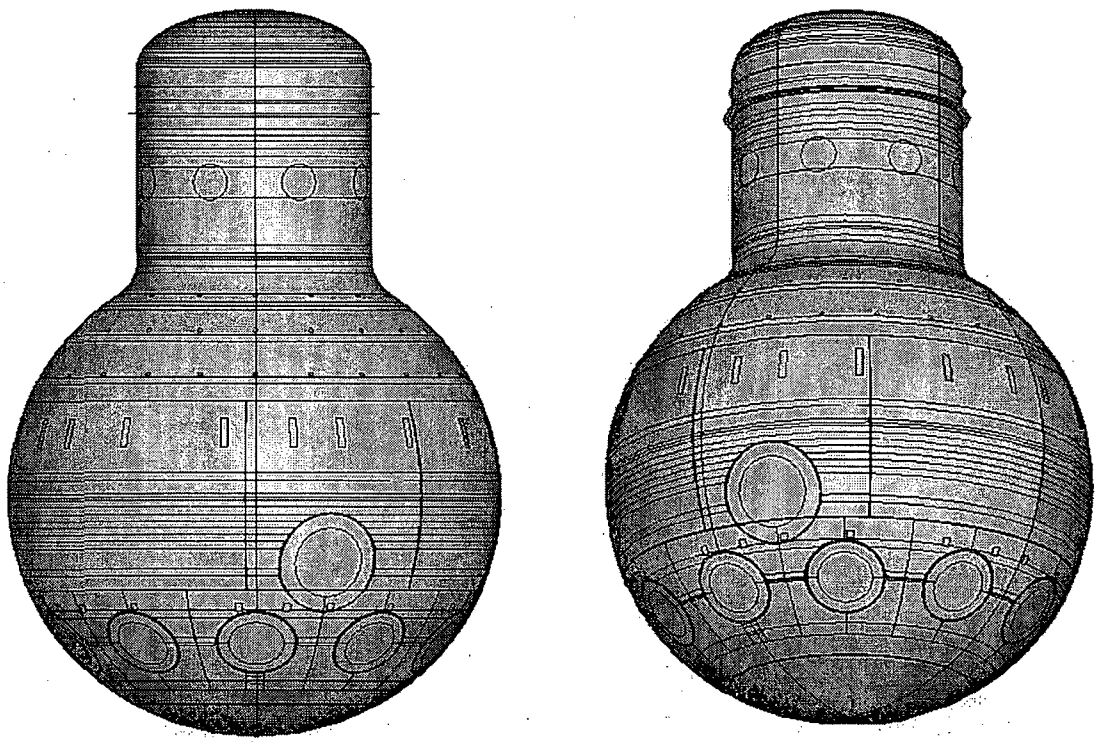

Figure 9-1. Modified Model for Natural Frequency Extraction

Table 9-1. Drywell Shell Thicknesses for Natural Frequency Extraction Analyses

Section	Original Thickness, in	Degraded Thickness, in	Section	Original Thickness, in	Degraded Thickness, in
Head	1.1875	N/C	Middle Sphere	0.770	0.670
Upper Cylinder	1.1875	N/C	Bottom Sphere	0.676	N/C
Main Cylinder	0.640	0.585	Middle Sphere Thickened	1.0625	0.9625
Knuckle	2.5625	2.54	Lower Sphere Below Sandbed	1.154	N/C
Upper Sphere	0.722	0.676	Lower Sphere in Sandbed and Above	1.154	0.835

N/C – No Change

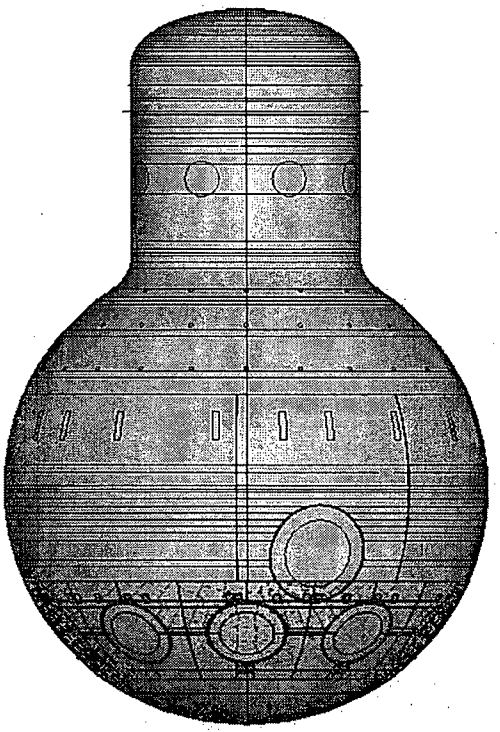

Figure 9-2. Lower Sphere Region (Highlighted in Red) Set to a Thickness of 0.835" for the Degraded Natural Frequency Extraction

The lowest 5 frequencies and mode shapes from the ABAQUS eigenvalue extraction are illustrated in Figure 9-3 and Figure 9-4 for the containment without and with degradation, respectively. The frequencies show only minimal decreases with the introduction of degradation with the lowest frequency dropping from 20.46Hz to 19.12Hz. The differences are smaller at the higher frequencies (modes 2 through 5). The displacements for each of the mode shapes are nearly identical. The first mode is a vertical extension of the drywell, or stretching mode. The second and third modes are overturning modes where the drywell is "bent" between the cylindrical and spherical sections of the structure. The forth and fifth modes are compressive modes where the cylinder is compressed down vertically toward the drywell sphere. These shapes are generally consistent between the analyses with and without degradation. Table 9-2 summarizes the comparison of the frequencies for the two analyses. Since the effects of the degradation on the frequencies and associated mode shapes are minimal, the use of the original design static seismic coefficients is judged to be acceptable.

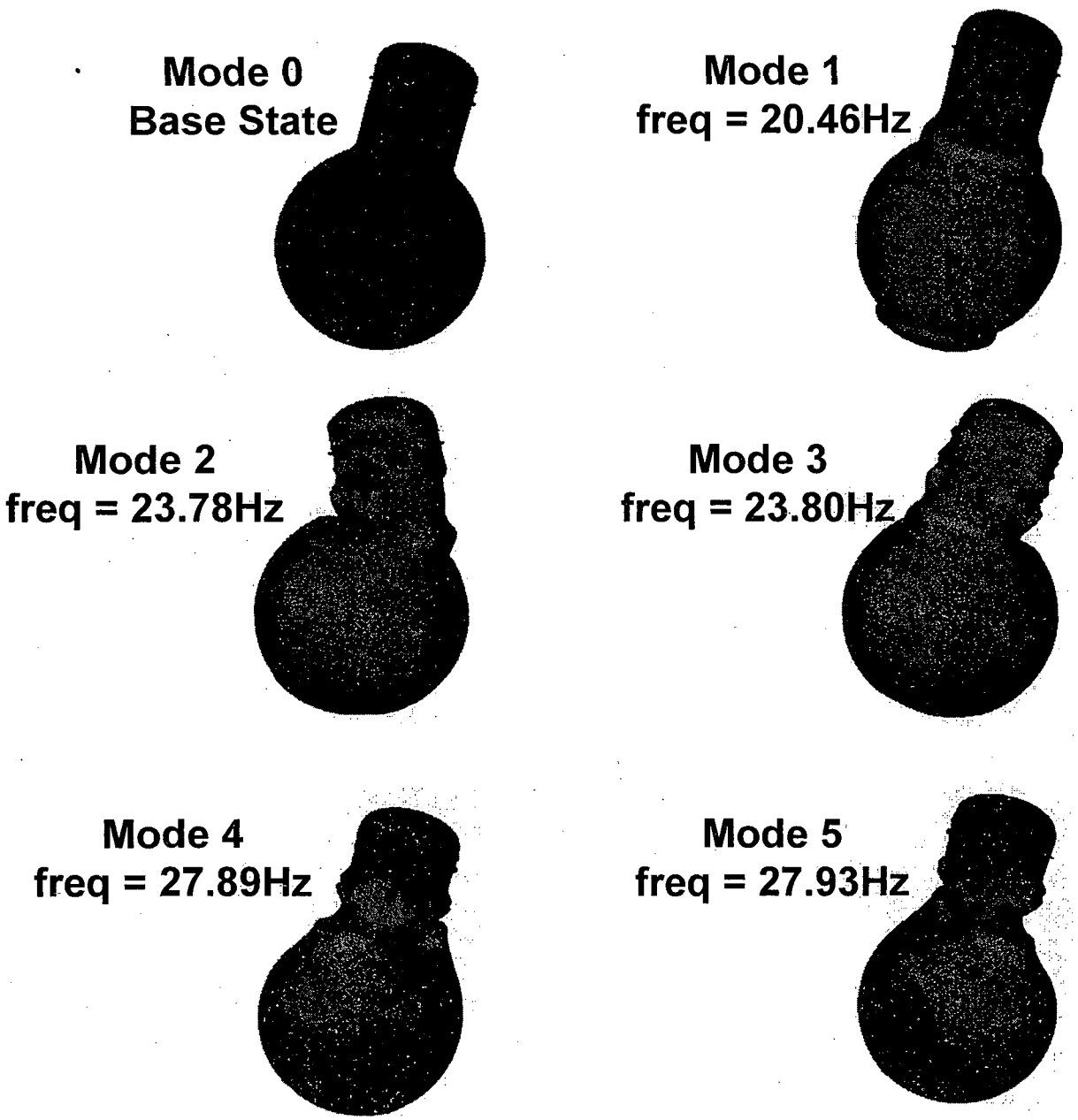

Figure 9-3. Base State and the First 5 Frequencies and Mode Shapes for the Drywell Containment with No Degradation

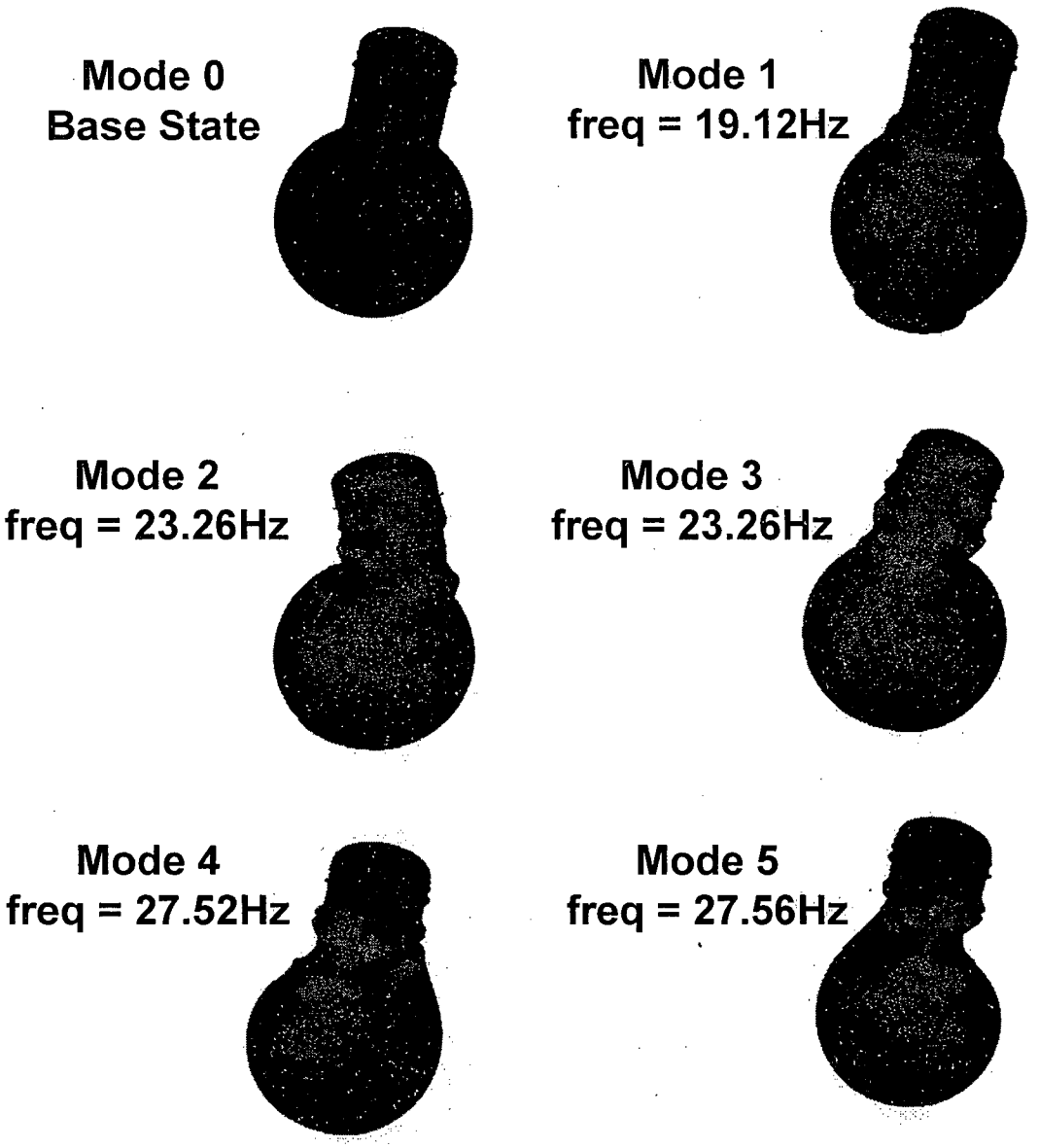

Figure 9-4. Base State and the First 5 Frequencies and Mode Shapes for the Drywell Containment with Degradation

Table 9-2. Summary of the First 5 Natural Frequencies for Drywell with and without Degradation

Mode	Frequency - No Degradation, Hz	Frequency - Degraded Model, Hz
1	20.46	19.12
2	23.78	23.26
3	23.80	23.26
4	27.89	27.52
5	27.93	27.56

10. Appendix B – Sandbed UT Measurement Data and Shell Thickness Development

For modeling the degradation in the sandbed region, the lower sphere was divided into 10 regions to be assigned uniform thicknesses. These regions extend from the centerline of one ventline to the centerline of the adjacent ventline. Each of these regions contains one-half of the two different, but adjacent, bays. This was done in order to avoid placing the thickness discontinuity at the centerline between the ventlines, since this is typically the location of the highest stresses. If the thickness jump was placed at this location, the stresses of interest would be difficult to interpret. An example of the bay combinations is illustrated in Figure 10-1. Here, half of Bay 1 and half of Bay 2 are combined to create Bay Combination 1-3. The measurement points indicated on the images (GPU Nuclear, 1993) were taken from the outside of the containment shell prior to the application of the epoxy coating. For Bay Combination 1-3, Points 8, 9, 15, 18, and 19 were taken from the left half of Bay 1 and Points 1, 2, 3, and 7 were taken from the right half of Bay 3, and averaged. The thicknesses for these points were reported in the GPU Nuclear calculations (GPU Nuclear, 1993) and are provided in Table 10-1. This average was assigned as a uniform thickness to the region highlighted in light red in Figure 10-1 and shown on the model in Figure 2-30. The points that fall within the "bathtub" region (Points 1, 2, 3, 4, 5, 10, 11, 12, 13, 20, and 21) under the ventline in Bay 1 were not included in the average for the adjacent bay combinations. The minimum measured thickness (Point 3) in this region was assigned to the entire Local Bay 1 region as outlined in Figure 10-1 and shown on the model in Figure 2-31.

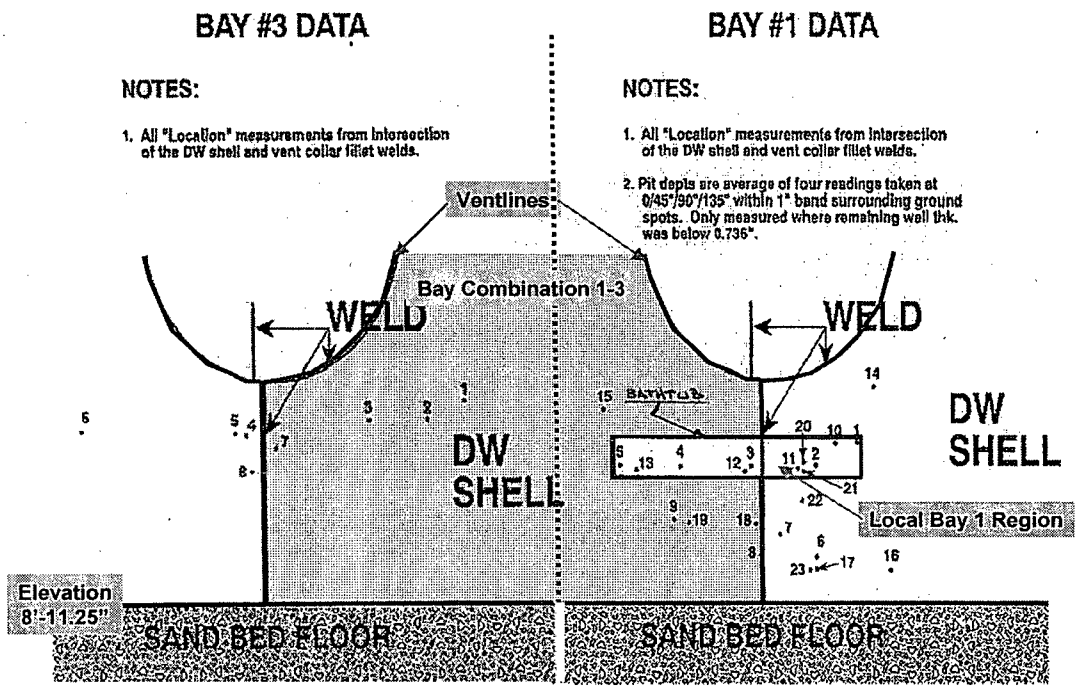

Figure 10-1. Bay 1 and Bay 3 UT Measurement Locations Taken from Outside of the Containment (Images Extracted from GPU Nuclear Calculation Sheet, 1993)

Table 10-1 through Table 10-4 and Figure 10-2 through Figure 10-11 provide the individual datapoints (GPU Nuclear, 1993) and the grouping used to compute the averages for all of the bay combinations summarized in Table 2-7. The bay combinations are assembled and averaged in the same manner as for Bay Combination 1-3 in Figure 10-1. The Local Bay 13 is shown in Figure 10-8 with thickness provided in Table 10-4. As with the Local Bay 1 region, the minimum measured value (Point 7) in the defined region was assigned as a uniform thickness.

Table 10-1. UT Measurement Data for Bay Combinations 1-3, 3-5, 5-7, and 7-9.

Bay Combination 1-3		
Bay	UT Point	Shell Thickness, in
1	8	0.805
1	9	0.805
1	15	1.156
1	18	0.917
1	19	0.89
3	1	0.795 (min)
3	2	1.00
3	3	0.857
3	7	0.826
1-3	average	0.894
Bay Combination 3-5		
Bay	UT Point	Shell Thickness, in
3	4	0.898
3	5	0.823
3	6	0.968
3	8	0.78 (min)
5	1	0.97
5	2	1.04
5	3	1.02
5	4	0.91
5	5	0.89
3-5	average	0.922
Bay Combination 5-7		
Bay	UT Point	Shell Thickness, in
5	6	1.06
5	7	0.99
5	8	1.01
7	1	0.92 (min)
7	2	1.016
7	3	0.954
7	4	1.04
5-7	average	0.998
Bay Combination 7-9		
Bay	UT Point	Shell Thickness, in
7	5	1.03
7	6	1.045
7	7	1.00
9	1	0.96
9	2	0.94 (min)
9	3	0.994
9	4	1.02
7-9	average	0.998

Table 10-2. UT Measurement Data for Bay Combinations 9-11, 11-13, and 13-15.

Bay Combination 9-11		
Bay	UT Point	Shell Thickness, in
9	5	0.985
9	6	0.82
9	7	0.825
9	8	0.791
9	9	0.832
9	10	0.98
11	1	0.705 (min)
11	2	0.77
11	7	0.831
11	8	0.815
9-11	average	0.835
Bay Combination 11-13		
Bay	UT Point	Shell Thickness, in
11	3	0.832
11	4	0.755
11	5	0.831
11	6	0.800
13	1	0.672 (min)
13	2	0.722
13	3	0.941
13	4	0.915
13	9	0.924
13	13	0.932
13	17	0.807
13	18	0.825
13	19	0.912
13	20	1.17
11-13	average	0.859
Bay Combination 13-15		
Bay	UT Point	Shell Thickness, in
13	12	0.885
13	16	0.829
15	1	0.786 (min)
15	2	0.829
15	3	0.932
15	4	0.795
13-15	average	0.842

Table 10-3. UT Measurement Data for Bay Combinations 15-17, 17-19, and 19-1.

Bay Combination 15-17		
Bay	UT Point	Shell Thickness, in
15	5	0.85
15	6	0.794
15	7	0.808
15	8	0.77
15	9	0.722
15	10	0.86
15	11	0.825
17	1	0.916
17	2	1.15
17	3	0.898
17	4	0.951
17	5	0.913
17	9	0.72 (min)
17	10	0.83
15-17	average	0.857
Bay Combination 17-19		
Bay	UT Point	Shell Thickness, in
17	6	0.992
17	7	0.97
17	8	0.99
17	11	0.77
19	1	0.932
19	2	0.924
19	3	0.955
19	4	0.94
19	5	0.95
19	8	0.753 (min)
19	9	0.776
17-19	average	0.904
Bay Combination 19-1		
Bay	UT Point	Shell Thickness, in
19	6	0.86
19	7	0.969
19	10	0.79
1	6	0.76
1	7	0.70 (min)
1	14	1.147
1	16	0.796
1	17	0.86
1	22	0.852
1	23	0.85
19-1	average	0.858

Table 10-4. UT Measurement Data for Local Bay 1 and 13 Regions.

Local Bay 1 Region		
Bay	UT Point	Shell Thickness, in
1	3	0.705 (min)
1	4	0.76
1	5	0.71
1	12	0.724
1	13	0.792
1	1	0.72
1	2	0.716
1	10	0.839
1	11	0.714
1	20	0.965
1	21	0.726
1	min	0.705
Local Bay 13 Region		
Bay	UT Point	Shell Thickness, in
13	5	0.718
13	10	0.728
13	14	0.868
13	6	0.655
13	7	0.618 (min)
13	8	0.718
13	11	0.685
13	15	0.683
13	min	0.618

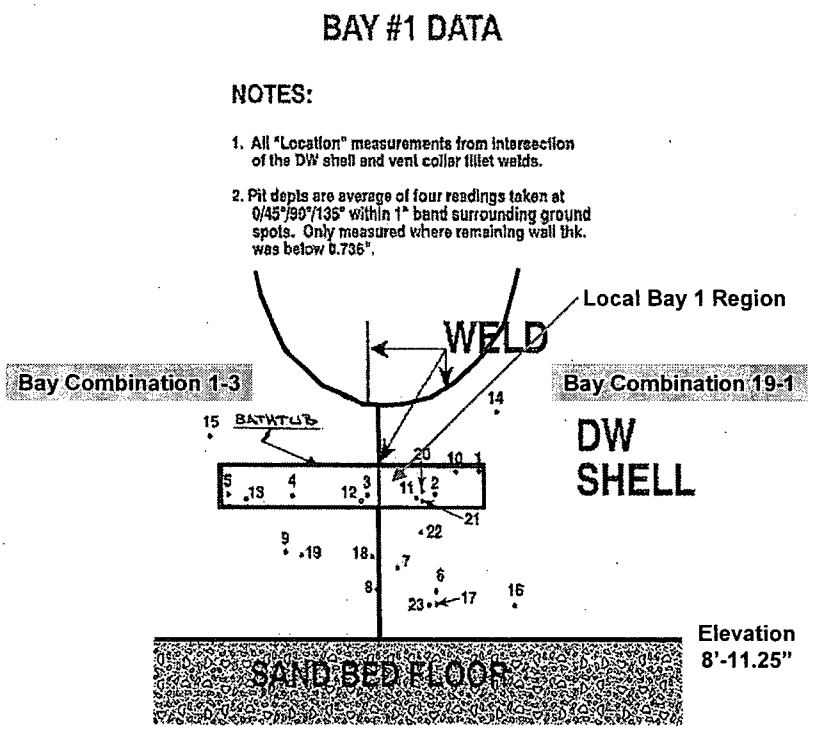

Figure 10-2. Bay 1 UT Measurement Locations Taken from Outside of the Containment (Image Extracted from GPU Nuclear Calculation Sheet, 1993)

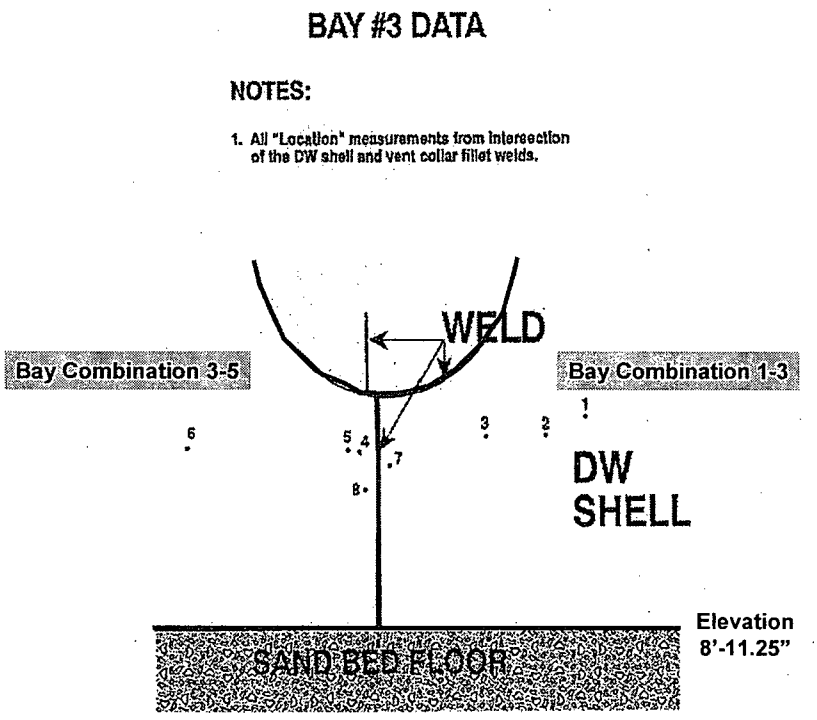

Figure 10-3. Bay 3 UT Measurement Locations Taken from Outside of the Containment (Image Extracted from GPU Nuclear Calculation Sheet, 1993)

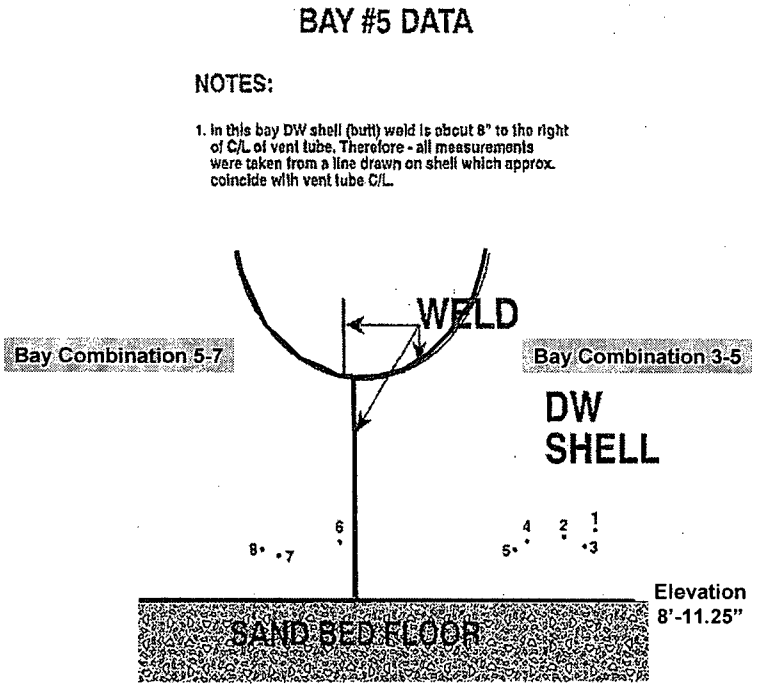

Figure 10-4. Bay 5 UT Measurement Locations Taken from Outside of the Containment (Image Extracted from GPU Nuclear Calculation Sheet, 1993)

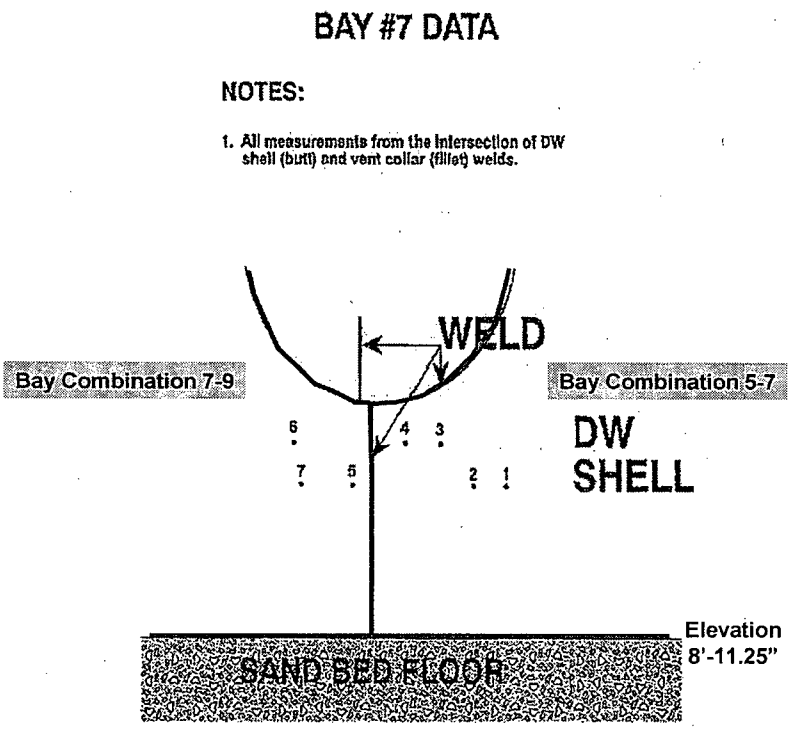

Figure 10-5. Bay 7 UT Measurement Locations Taken from Outside of the Containment (Image Extracted from GPU Nuclear Calculation Sheet, 1993)

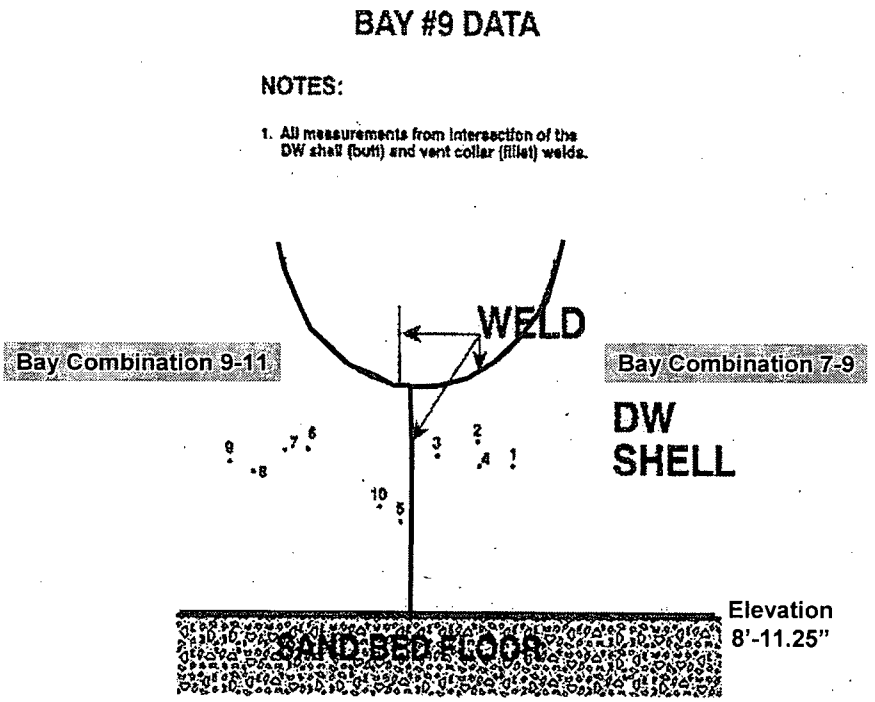

Figure 10-6. Bay 9 UT Measurement Locations Taken from Outside of the Containment (Image Extracted from GPU Nuclear Calculation Sheet, 1993)

Figure 10-7. Bay 11 UT Measurement Locations Taken from Outside of the Containment (Image Extracted from GPU Nuclear Calculation Sheet, 1993)

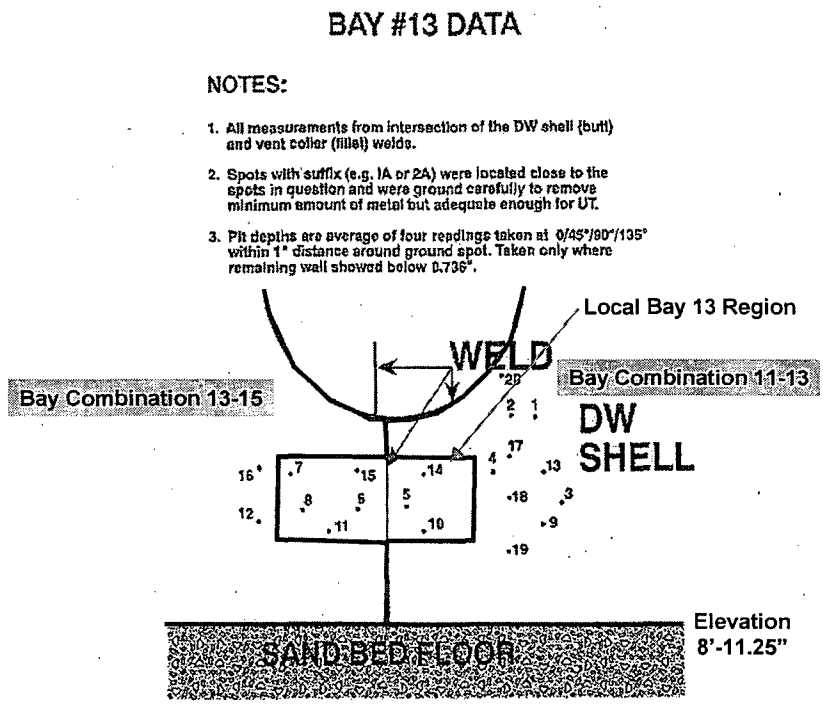

Figure 10-8. Bay 13 UT Measurement Locations Taken from Outside of the Containment (Image Extracted from GPU Nuclear Calculation Sheet, 1993)

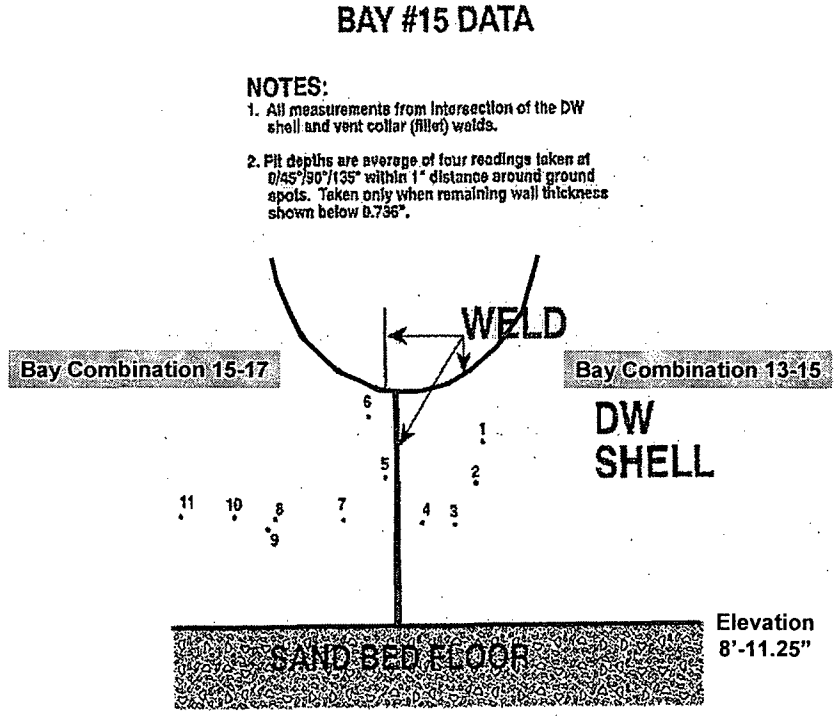

Figure 10-9. Bay 15 UT Measurement Locations Taken from Outside of the Containment (Image Extracted from GPU Nuclear Calculation Sheet, 1993)

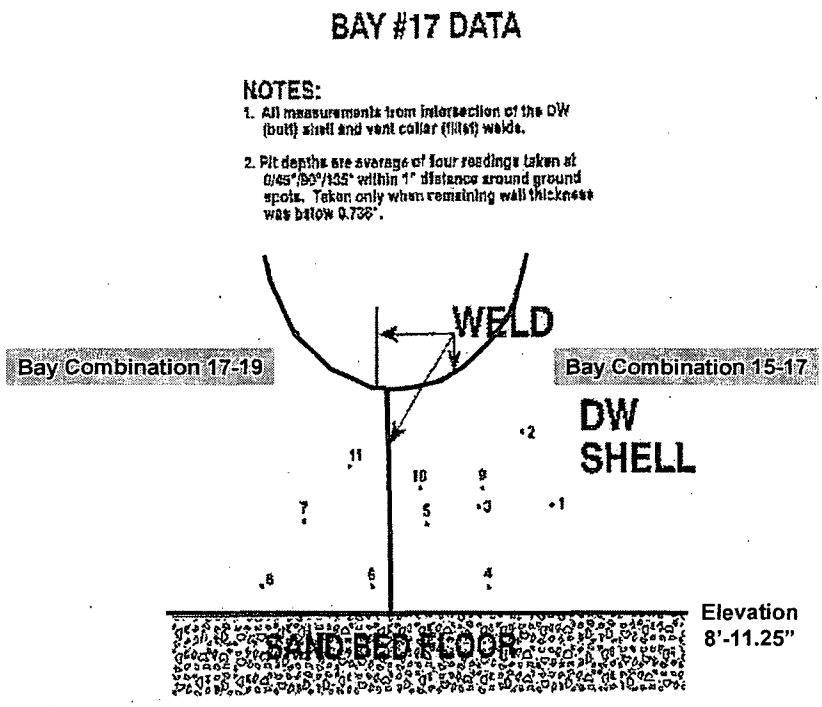

Figure 10-10. Bay 17 UT Measurement Locations Taken from Outside of the Containment (Image Extracted from GPU Nuclear Calculation Sheet, 1993)

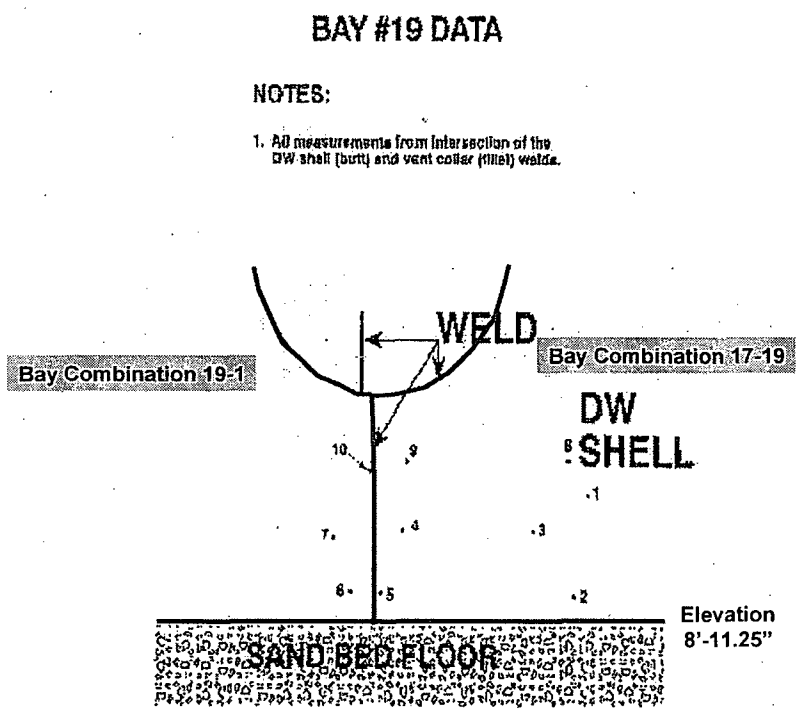

Figure 10-11. Bay 19 UT Measurement Locations Taken from Outside of the Containment (Image Extracted from GPU Nuclear Calculation Sheet, 1993)

DISTRIBUTION

1 P.T. Kuo
U.S. Nuclear Regulatory Commission
Mailstop: O-11F1
Washington, DC 20555-0001

1 Louise Lund
U.S. Nuclear Regulatory Commission
Mailstop: O-11F1
Washington, DC 20555-0001

1 Donnie Ashley
U.S. Nuclear Regulatory Commission
Mailstop: O-11F1
Washington, DC 20555-0001

1 Noel Dudley
U.S. Nuclear Regulatory Commission
Mailstop: O-11F1
Washington, DC 20555-0001

1 Patrick Hiland
U.S. Nuclear Regulatory Commission
Mailstop: O-9E3
Washington, DC 20555-0001

1 Sujit Samadar
U.S. Nuclear Regulatory Commission
Mailstop: O-9D3
Washington, DC 20555-0001

1 Hans Ashar
U.S. Nuclear Regulatory Commission
Mailstop: O-9D3
Washington, DC 20555-0001

1 Samir Chakrabarti
U.S. Nuclear Regulatory Commission
Mailstop: O-12D5
Washington, DC 20555-0001

1 Sally Adams
U.S. Nuclear Regulatory Commission
Mailstop: O-12E5
Washington, DC 20555-0001

1 Randolf Blough
U.S. Nuclear Regulatory Commission
474 Allendale Road
King of Prussia, PA 19406-1415

1 Richard Conte
U.S. Nuclear Regulatory Commission
474 Allendale Road
King of Prussia, PA 19406-1415

1 Michael Modes
U.S. Nuclear Regulatory Commission
474 Allendale Road
King of Prussia, PA 19406-1415

1 Timothy O'Hara
U.S. Nuclear Regulatory Commission
474 Allendale Road
King of Prussia, PA 19406-1415

5 MS 0744 Jason Petti, 6764
1 0744 Mike Hessheimer, 6764
1 0748 Matt Turgeon, 6764
1 0718 Jeff Smith, 6765
1 0736 Marianne Walck, 6760
2 9018 Central Technical Files, 8944
2 0899 Technical Library, 4536

Exhibit 61

Memorandum from Rudolf H. Hausler to Richard Webster, Esq.

Subject: Further Discussion of the External Corrosion on the Drywall Shell in the Sandbed Region. (September 13, 2007).

CORRO-CONSULTA

8081 Diane Drive
Tel: 972 962 8287 (office)
Tel: 972 824 5871 (mobile)

Rudolf H. Hausler
rudyhau@msn.com

Kaufman, TX 75142
Fax: 972 932 3947

Memorandum

Richard Webster, Esq.
Rutgers University Law Clinic
Newark, NJ

13-Sept.-2007

Subject: **Further Discussion of the External Corrosion on the Drywell Shell in the Sandbed Region.**

I. Introduction

The objective of this discussion is to put a few misconceptions, erroneous statements and poor judgment in perspective. We never used the "wrong data the wrong way". We used AmerGen's data a different way, which we think, and will show below, leads to more concise conclusions. In the forefront of this discussion are the contours, or response surfaces, which we generated on the basis of the most accurate external (and in one case internal) UT measurements reported by AmerGen. It turns out, and is discussed below in meticulous detail, that the differences between Tamburro's methodology and that of the response surface methodology, is simply one of greater consistency and reduced arbitrariness.

I would like to highlight a statement which, to some extent, exemplifies the errant logic involved in much of AmerGen's testimony (Ref. 9, A7).

> *The contour plots presented by Dr. Hausler are not accurate* [1]*. The contours generated by Dr. Hausler show drywell thinning that has not been observed or measured by AmerGen.* [This testimony is ascribed to all members of this particular rebuttal group; see Ref. 9, at A7].

The above quote is a recurring theme in AmerGen's rebuttal testimony and therefore needs to be put in perspective.

At no point in time have we attempted to make the corrosion of the drywell shell to look more severe or extensive. While we have in the past deplored the fact that the external UT measurements had not been extended to a larger area, we have evaluated

[1]) Messrs Gallagher, Ouaou, and Dr. Metha, have not shown in their testimony how our contours are not accurate. It is an incredible disservice to the professionalism of these proceedings to promulgate such unsubstantiated accusations.

the data generated by AmerGen (and earlier by GPUN) by means of a standard well known method which, as it turns out, bears some similarities to Tamburro's procedures, but are far more systematic and much less prone to observer bias. The fact that averaging (which is also Tamburro's methodology) results in numbers, which have not been measured is inherent in the process of averaging. In fact, the entire approach of AmerGen is based on averages. AmerGen can hardly claim that Tamburro's averages are valid, while mine are not.

> Mr. Polaski, Dr. Harlow, Mr. Abramovici, Mr. Tamburro, and Mr. McAllister completely misunderstand (or are not familiar with) the process of generating iso-response line in a two-parameter field when they assert that *we have inappropriately statistically treated the external UT data (Ref. 10, at A 2).*

Let's be very clear about this, establishing the contour plots is only a statistical process to the extent taking averages is a statistical process. Both Tamburro and I use averaging to represent the surface, because there is no reasonable alternative approach. In this case I used the mathematical routine developed by the SAS Institute, Inc, (formerly known as Statistical Analysis Software, Inc.) in the Statistical Discovery Software, Ver. 3.1, Chapter 3, page 23, pg 443 of the User's guide. The process it uses was described in detail in previous submissions [2].

> The gentlemen listed above assure us that *these data cannot represent the thickness of the drywell shell. First, there are two few of them for the points to be statistically representative of the shell as a whole. Second they are biased toward the thin side.* And finally, we understand that we have *ignored the limited number of data points,* and that we *have performed our calculations and computer contouring assuming that these external locations were selected at random and, thus, could be representative of the condition of the drywell shell in the sandbed region.* AmerGen Rebuttal Test. Part 3 A38-41.

However, AmerGen is once again being entirely inconsistent. It is precisely the external data, which have been used for the last 15 years to convince the NRC that the shell is still in serviceable condition. Although it was assumed that the most severe corrosion had been identified and that the rest of the sandbed area was less corroded, that assumption has never been verified [3], and was designed solely to satisfy the NRC.

All parties to the proceeding are by now well aware of the paucity of data available, but we have to work with what we have. It is AmerGen that has to show that it can use the available data for the purpose of providing reasonable assurance that the drywell shell meets the CLB. It is therefore rather ironic that AmerGen has now decided that there are too few external measurements to be statistically representative

---

[2] R. H. Hausler Memorandum to Richard Webster, Esq., July 18, 2007 page 5 par. Chapter VI, The development of Contour Plots.

[3] Indeed the task would be difficult. One must visualize an access hole (or canal) of 2 feet in diameter

of the shell as a whole. I have attempted to provide the best analysis possible given the limitations of the data. The ideal would probably be to combine all the data on a contour plot. Unfortunately, because the plot provided of all the data is at such a small scale and does not give exact locations, I have been unable to combine the locations of the internal data with those of the external data. The other alternative is to conclude that because neither the external measurements nor the internal measurements are representative of the drywell shell thickness, there is no reasonable assurance of compliance with the acceptance criteria or the ASME code. Unfortunately, instead of combining all the data, AmerGen has chosen to try to ignore the external data. This makes no sense, because when data is sparse, one should try to extract as much information as possible from what is available. And if there are apparent contradictions within the data it should be taken as and opportunity to learn more rather than a reason to discard one or the other of the data sets non representative.. Furthermore, AmerGen has ignored the trench data, which also contains valuable information.

AmerGen has stated in the past that the internal grids are not representative of the shell as a whole. I agree with this because the 600 odd internal UT grid measurements are not evenly (or randomly) spread over the area of the sandbed, but are in each bay centered on small 6" by 6" areas at height 11'3".. These grids cannot capture the severity of corrosion in the bathtub ring in some of the most corroded Bays because they are located too high. They therefore systematically over-represent the average thickness in some of the most critical Bays. This is one of the reasons that the external UT measurements were required by NRC in the first place. The internal data also cannot be used to evaluate whether the drywell meets the local area acceptance criterion. [4]

It has been asserted by AmerGen time and time again that the locations for the external UT measurements were made visually and by micrometer measurements for the purpose of selecting the "thinnest" wall locations. The examples for Bays 1 and 13 to be discussed below clearly show that this assertion does not hold across the board.

And finally, we learn from AmerGen that in order to establish meaningful contour plots, the points of measurement would have to be selected randomly in order to represent the drywell shell in its entirety. AmerGen Rebuttal Test. Part 3 at A40. There is absolutely no such a priori requirement in the use of contour plots. As we have pointed out earlier, the only assumption that is being made in the interpretation of the contour plots (also sometimes called the response surface) is that the remaining wall thickness between two measured points can be represented by the average of the two points, or more accurately, by the slope of the line between the two points. That is exactly the same approach taken by Tamburro, as is explained below.

---

[4] The fact that there are 49 data points in the internal grids versus at best 20 in the external data sets does not make the internal measurements any more representative of the rest of the bay than the external measurements, as AmerGen and the NRC might want to have it. More points on a smaller area simply do not increase the confidence for the state of the whole.

We have not assumed anything, other than that the points measured by UT and presented by AmerGen were reliable data. The contour plotting routine is an averaging routine and there is no up-front requirement for the data to have been gathered randomly. We have in fact questioned whether the available data would be representative of the drywell shell, which AmerGen has assured us they were, because there was apparently no need for additional measurements in areas where there might be any doubts.

To be absolutely clear about the intentions of this discussion: Our only intention is to try and answer the question as to how much confidence one can have in the integrity of the drywell shell. For that purpose we have among other things resorted to contour plots solely for the purpose of visualizing what one actually knows. In doing that we have done the same thing Mr. Tamburro has done, only using computers to the maximum extent possible rather than using largely manual methods, and have come to quite similar conclusions. Once the obvious errors in Mr. Tamburro's calculations are corrected, they broadly agree with mine within the range of the large uncertainties that remain.

To extrapolate beyond the area that was measured, one can use the response surface routine in the JMP module to extrapolate and predict the remaining wall thickness in the remaining areas of the sandbed region. I have now done this to show just how simplistic AmerGen's approach to this issue is. Although the results outside the measured area are spatial extrapolations from the data, and are therefore less certain than the contours within the measured area, they are better estimates than assuming no degradation in these areas.

II. Discussion of Bay 1

The attached Table 1 shows the external UT data for Bay 1 with the coordinates associated with each point. There were several sources for these data, which were reconciled. However, it turned out that point 6 had the same coordinates as point 17 (-48 vertical and 16 horizontal) but the reported measurements differed by 115 mils. We thought at first that point 6 should perhaps be at –16 horizontal, i.e. on the other side of the centerline. But then we found a graph where the positions of 6 and 7 were reversed to the right of the center line (positive coordinates) and finally there were representations were point 6 was indeed slightly higher and to the left of point 17. We therefore felt justified to change the coordinates from –48 and 16 to –44 and 14 as suggested by most of the graphical presentations.

The resulting contour plot is shown in Figure 1. We have inserted the measurement ID's for each point as well as the respective remaining wall thicknesses. Additionally, we have superimposed Mr. Tamburro's evaluation, which is merely a coarse manual version of the contour plot.

Tamburro in Fig. 1-2 (Ref. 4) defines three areas as shown in Fig.1 below for individual evaluation. Thus Area I contains points 5, 9 and 13 for an "average thickness of 718 mils in an area of 22 inch by approx. 30 inch, or 4.6 sq. feet. Strangely, in Fig 1-6 of Tamburro's work, the same area (referenced in Fig. 1-2) was narrowed and elongated to also contain points 4 and 19. The average residual thickness now was increased to 751 mils, while the estimated area was reduced to 23" by 16" or 2.6 square feet. Fig. 1 below, illustrates that the crude manual estimation by Tamburro is a coarse approximation to the surfaces generated by contouring. The advantage of using the computer is that the manual method is vulnerable to observer bias and does not provide an objective test of whether the results meet the local area acceptance criterion.

The important feature to recognize in all this is that both the contouring process and that used by Tamburro use averaging. However, the contouring is the preferred approach because Tamburro manually defines areas and then calculates average residual wall thickness from the measurements contained in this area, whereas the contours do not select specific areas, but use the measured point as a totality to calculate most likely average wall thicknesses between measured points.

Next, Tamburro defines in Fig. 1-2 an area, which he dubs the "Bathtub Ring". Curiously, he does not include points 11, 2, and 21 in this area even though they are clearly part of the bathtub ring (see Fig. 1 below), but includes these points in another area, which we identified as area III in Fig. 1 below. But when this area (Area III in our Fig. 1) is discussed by Tamburro in his Fig 3-1 (page 30 Ref. 4) he is not consistent in the dimensions. Nevertheless, he identifies this area as the 736 mil boundary and inserts in the same graph a 636 mil boundary somewhat arbitrarily in the middle. Now, Tamburro has identified an area of 14 x 18 inches in his Fig 1-3 as having an average wall thickness of 696 mils (points 7, 11 and 21) and being 1.75 sqft in area. But curiously, point 6 (clearly a companion point to 7 and certainly part of a corroded area) is left out of this exercise.

The peculiar thing about this is that we have been accused of *using the wrong data the wrong way*. The contours are calculated by triangulating between all the points. Tamburro averages (a primitive form of triangulating) across a few points. Please note that point 7 is a good 16 inches removed from points 21, 11 and 2, with other measurements (point 22) in between. The contours indicate that there is not a straight-line slope between point 7 and the others as Tamburro assumes, but that there is in fact a "hump" over point 22. Consequently, the interpretation of the external UT measurements by means of the response surface methodology results in a less severe picture than the one Tamburro arrives at.

There are, however, other, more serious slights of hand in the Tamburro evaluation. In Fig 1-4 (Ref. 4 pg 31) he compares the area covered by points 2, 7, 11 and 21 to the local buckling criterion. He tells us that the area covered by these points is 7 inch by 4 inch or only 0.2 sq feet, when it can easily be seen from our Fig 1 below that the

area attributed to these points would be of the order of 18 by 14 inches or nearly 2 sq feet. Figure 1-4 is therefore incorrect. The same error is repeated in Tamburro's Fig 1-5.

And when it comes to the bathtub ring (Fig. 1-6) and an assessment of points 5, 13, and 4 he conveniently adds points 9 and 19 (see Fig. 1 below) to arrive at an average wall thickness of 751 mils. There is no obvious justification for including point 19 in the bathtub ring. Without it the average would have been 722 mils over an area of about 14 by 14 inches or 1.4 sq ft.

When all is said and done, Tamburro rearranges the data again in Fig. 1-7 and finds an area of 9 sq feet that has a residual wall thickness of 696. However, as clearly shown on Figure 1 this Fig. 1-7 is again incorrect because the area selected must actually be at least 42 inches by 36 inches to capture all the points show on Fig. 1-7, which is considerably larger than 9 square feet.

The question now is how one can reconcile these results with the local buckling criteria. This was, and still is the objective of the external UT measurements (see Tamburro's Figs. 1-4 and 1-5).

1. Originally the local wall thickness criteria derived from the GE sensitivity study (AmerGen Ex. 39) which found that if a local area of 0.5 sq. ft. in two adjacent Bays has a residual wall thickness of 536 mils and then tapers back to a uniform 0.736 inches, the load factor is reduced by 9.5% compared with the load factor found for a uniform wall thickness of 736 mils over the sandbed area (which gave an EFS of 2.0 for the refueling case). Similarly if the 0.5 sq. ft. central area in each Bay has a residual wall thickness of 636 mils, the load factor is reduced by 3.9%. These reduced load factors correspond to EFS's of 1.81 and 1.92. It was stressed that this sensitivity study assumed that the local thinning would gradually over a distance of a foot taper up to the 736 mils specified for the general limiting buckling wall thickness. From these general local buckling wall thickness criteria resulting from the sensitivity analysis it was left to the individual engineer to decide whether a particular corroded area would violate the one or the other of these two cases. The problem is this, the area of reduced wall thickness below 736 mils was never conveniently in the shape of the modeled cut-outs. Therefore, it is unclear what is to be done with an area that measures say 6.9 sq feet with an average wall thickness of 704 mils (total bathtub ring area in Fig. 1 below) and which tapers asymmetrically on one side toward 800 mils and on the other side toward 1150 mils. If the intention was that the cut-outs would bound the corroded areas, the dimensions of the bath tub ring, which is 10 inches wide by 66 inches long exceed the boundaries of the cut-outs and therefore presumably must violate the acceptance criterion for local areas.

2. While the definition for the local buckling criterion used in the various revisions of Calc 24 has varied, in Rev. 2 a more restrictive definition was promulgated in: *If an area is less than 0.736 inches then that area shall be greater than 693 mil*

thick and shall be no larger than 6 inch by 6 inch. (It was admitted that Calc. 024 had previously positioned an area of this magnitude in Bay 13 [5]*).* It is clear, however, that areas of this magnitude exist with wall thicknesses less than 693 mils all through the sandbed area (see above discussion). Consequently, Mr. Tamburro devised a way whereby the measured corroded areas were broken up into separate "mini areas" of which it could be shown that, even though severe corrosion in excess of 736 mil residual wall thickness had been observed, these areas were small enough such that they would satisfy the local buckling criteria. The advantage, of course, of this formulation of the criteria was that one could choose the areas for analysis almost arbitrarily. The disadvantage is that the decisions are left to the judgment of the engineer, which may be biased or influenced by considerations other than the need for an objective assessment of the data. In the end, comparing the Tamburro assessment with Figure 2, we see that Tamburro's assessment is a crude version of the assessment produced by the more sophisticated analysis.

3. Figure 1-7, perhaps inadvertently, illustrates that, according to Tamburro, an area of average thickness 0.696 inches extends over an area that is larger than 9 square feet. Based on this assessment, Tamburro should have concluded that the drywell failed the local area acceptance criterion he was using, which required contiguous areas that are thinner than 0.736 inches on average to be less than 9 square feet in extent. It is unclear why he arbitrarily labeled the area as 36 inches by 36 inches.

The triangulation, on the basis of which the response surfaces are generated, first generates the equations (correlation functions) used to draw the contours. These same equations can then also be used to define a grid larger than the area that had actually been covered by measurements, and to extend the contours for the purpose of predicting, in this case, the extent of corrosion one might expect outside the measured areas. This was done in Figure 2 below for Bay 1. The reason why this was done was because it was suspected that the bathtub ring might extend away from the vent line into the center of the bay. Indeed, as can be seen from Figure 2, a large area of about 15 by 20 inches might exist with a residual wall thickness of less than 750 mils and might actually extend into Bay 19. This is a prediction based on the existing data, and if verification of this prediction is outside the scope of the present intervention, it is certainly a better prediction than the assumption that corrosion stopped with the evaluation of points 5 (680 mils), and 9 (745 mils) 30 to 35 inches below the top of the sandbed.

We also see from Figures 1 and 2 that at the top of the sandbed essentially no corrosion occurred. This is in agreement with the internal grid measurements which essentially showed the same thing, **and which is in part the reason why we have concluded earlier that the internal grid measurements do not reflect the corrosion in the sand bed area and are not in anyway representative of the corrosion of the drywell liner.**

---

[5] This criterion is also repeated in Calc. C-1302-187-E310-041, pg. 11, 12/15/06.

III. Discussion of Bay 13

Table 2 below lists all the data for Bay 13 external UT residual wall thickness measurements. The original data were somewhat confusing. On 1/8/93 an initial set of 8 readings were obtained and listed from 1 through 8 with the associated coordinates. Then on 1/11/93 an additional set of 19 readings were obtained and again listed from 1 through 19 with the associated coordinates. Some of these readings from the second set were new, others were at or near the old coordinates. For this reason all the readings from 1/11/93 were given the suffix a. It appears that additional measurements were made at or near some of these older ones with only minimal grind of the surface (to better place the UT probe). However, these repeat or confirmatory measurements, which differed from the previous ones considerably, did not have the coordinates associated with them and could therefore not be officially included in the data set. (Nevertheless, attempts to insert these measurements at reasonable shifts of the coordinates might have better revealed the "pimpled nature of the surface.")

In 2006 it was reported that a number of the location identified in 1992 could not be "found" and therefore no 2006 data were reported for these locations. This was most unfortunate, because it appeared that one could not now deal with the spots of severe corrosion in the upper right hand corner of Figure 3. However, since it had been observed that on average all 2006 data were 20 mils lower than the 1992 results, the missing 2006 data were filled in with the corresponding 1992 data reduced by 20 mils. These "calculated" measurements are shown in the last column in Table 2 below in italics. Since there were duplicate measurements at the same coordinates, in some cases the coordinates of the second set of data were slightly shifted in order to include all data in the contours [6)]

Figure 3 below thus shows the response surface for the 2006 external UT measurements in the sandbed region. Superimposed are the three areas, I, II, and III,which Tamburro proposed in order to analyze Bay 13 corrosion in greater detail. Tamburro locates all measured points in an approximate graph of Figure 13-1 on page 63 of Ref. 4. It is noted first of all that the relative position of the individual points is distorted when compared to Fig. 3 below which is drawn with the accurate coordinates. Second, as one looks at the numbering of the points it is hard to believe that an argument could be made that the points to be measured **had not been selected at random**. Finally, we also notice that all measuring locations are indicated in Fig. 13-1, however, as we proceed to examine Tamburro's individual areas we find that for some unexplained reasons some of the most corroded points are left out. Thus within the three areas Tamburro proposes to discuss in Fig. 13-2 we find that points 1 and 2 and 1a and 2a are missing. Clearly, the absence of these heavily corroded areas from Tamburro's analysis grossly distort his conclusions.

[6)] When two points have the same coordinates, one set will be dropped from the triangulation even though the values may be different. By shifting the coordinates ever so slightly the particular location in question will be given more weight as it should be because of the additional data.

Tamburro and AmerGen have insisted all through these discussions that the most heavily corroded areas had been selected for UT measurements, and that their evaluation were conservative. However, in the final analysis the most heavily corroded areas are simply overlooked. It turns out that the bathtub ring in Bay 13 is not horizontal, but tilted toward the center of the bay.

Figure 4 shows the predictive contours derived from the triangulation correlations. Note, that the areas predicted to have less the a residual wall thickness of 750 mils (dark green shading) extend all the way up to 0 on the scale of vertical coordinates, a few inches below the "internal grid measurements." Three internal grids had been measured in this Bay (Ref. 11, Section 6, Table 6) with average residual wall thicknesses of 846 (13A). 904 (13D bottom), 1047 (13 B top) and 1142 (13 C). Thus, it is likely that the internal measurements are mostly above the angled bathtub ring, which is tapering out at 11'3" or thereabouts. **Clearly, however, none of the Internal Grid UT measurements reflects the severity of the actual corrosion in the sandbed area below 11'3" in Bay 13.**

IV. The Relationship between the Internal and External UT Measurements

Finally we find the need to comment on the comparison between the internal UT measurements in Bay 17 and their relationship to the external and trench UT measurements. It has been said that if we had chosen the internal grid measurements 17 D instead of 17 A the comparison between the external and trench measurements would have turned out different, and we might have concluded that the internal grid measurements actually did represent the overall corrosion damage of Bay 17 or in fact of all Bays (AmerGen Rebuttal testimony, part 3, pg 3.). As a consequence we have augmented Figure 4 from our Memo of April 25, 2007 to include both sets of internal grid measurements. The results are shown in Figure 5 below. Indeed the horizontal averages plotted as function of the elevation for the data 17 D show considerably more reduced wall thickness than those for 17 A. Now, one needs to remember that the lateral position in the Bay of these data is not represented in the Figure 5, in fact we don't know what the lateral position is because it has not been reported with any precision. Nevertheless, Fig. 5 clearly demonstrates the uncertainty of the assessment of the corrosion damage in the sandbed area if one were to rely on only one set of data, namely the internal grid data. This has earlier also been demonstrated by means of an analysis of the results for Bays 1 and 13.

V. Conclusions

The above discussion has shown that:

- Developing contours is not using "the Wrong Data the Wrong Way", but is in fact the most rational approach to visualizing the external UT measurements in the sandbed area.

- The response surfaces showing the correlations as well as the raw data present a more comprehensive way towards deciding whether certain corroded areas are within the acceptance criteria.
- The approach Tamburro took of dissecting the totality of the measurements for each Bay into mini areas, for the purpose of demonstrating agreement with the acceptance criteria, appears to be rather arbitrary and self-serving. At best, it is a crude approximation of the contouring which is carried out in an objective manner by a computer.
- The correlation equations on the basis of which the response surfaces are calculated allow extrapolation into areas of no measurements. **For certain, prediction on the basis of these equations as shown in Figures 2 and 4 carries more weight than the blanket assertion that there is no severe corrosion outside the areas examined. These predictions show that areas of severe corrosion are probably present at precisely the locations that AmerGen has admitted are most vulnerable to buckling.**
- Finally, reexamination of the data for Bay 17 show just how questionable the assertion is that the internal grid measurements are representative of the entire corrosion damage which may have occurred in the sandbed area.

References

A. Data Sources

1. GPU Nuclear; Calculation C-1302-187-5320-024 Rev. 1, 1/12/93, this revision contained the original raw data on pages 67 to 117,
2. GPU Nuclear, Calculation C-1302-187-5320-024, Rev. 0, 1/12/93, this document explains in detail the rational for the "Evaluation Thickness".
3. Passport 0054604907 (AR A2152754 E09), 11/2/06; this document contains the results of the 2006 external UT measurements.
4. Exelon Nuclear; Calculation C-1302-187-5320-024 Rev. 2, 3/28/07; this document also contains the rational for acceptance within the "acceptance criteria" of the areas which were most corroded.
5. IR 0553792-02 Drywell Structural Integrity Basis IR21 Inspection, 11/06/06, Document contains all 2006 internal Grid data

B. Rebuttal References

6. NRC Staff Rebuttal Testimony of H. G. Ashar, Dr. J. A. Davis, Dr, Mark Hartzman, T. L. O'Hara, A. D. Salomon.
7. NRC Staff Response to Initial Presentations and Response to Board questions.
8. Affidavit of Mark Hartzman, PhD, Aug. 23,2007, par. 2
9. AmerGen's Pre-filed Rebuttal Testimony, Part 2, Acceptance Criteria, by M.P. Gallagher, A. Ouaou, H. S. Metha, PhD,

AmerGen's Pre-Filed Rebuttal Testimony, Part 3, Available Margin: by F. W. Polaski, D. G. Harlow, PhD, Julien Abramovici, Peter Tamburro, and M. E. McAllister.

11. 2006 Inspection Report for ACRS

Bay 1 UT Measurements for External Corrosion.

Measurement ID	Vertical Position inches	Horizontal Position inches	Remaining Wall Thickness 1992 inches	Remaining Wall Thickness 2006 inches	Comments
1	-16	30	720	710	
2	-22	17	716	690	
3	-23	-3	705	665	
4	-24	-33	760	738	
5	-24	-45	710	680	
6	44	14	760	731	location given as -48/16 - duplicate of 17 not likely, therefore moved closer to point 7
7	-39	5	700	669	
8	-48	0	805	783	
9	-36	-38	805	754	
10	-16	23	839	824	
11	-23	12	714	711	
12	-24	-5	724	722	
13	-24	-40	792	719	
14	-2	35	1147	1151	
15	-8	-51	1156	1160	
16	-50	40	796	795	
17	-48	16	860	846	
18	-38	-2	917	899	
19	-38	-24	890	856	
20	-18	13	965	912	
21	-24	15	726	712	
22	-32	13	852	854	
23	-48	15	850	828	

Bay 13 UT Measurements for External Corrosion.

Measurement ID	Vertical Position inches	Horizontal Position inches	Remaining Wall Thickness 1992 inches (1)	Vertical Position inches	Horizontal Position inches	Remaining Wall Thickness 2006 inches (1)	Comments
1a	1	45	672	1	45	***652***	
2a	1	38	727	1	38	***705***	
3a	-21	48	941	-21	48	923	
1	-6	46	814	-6	46	***873***	
2	-6	38	615	-6	38	***595***	
3	-26	42	934	-26	-42	***914***	
4	-12	35	914	-12	-35	***894***	
4a	-12	36	915	-12	36	873	
5	-26	6	735	-26	6	***715***	
5a	-21	6	713	-21	6	708	
6	-24	-8	683	-24	-8	***663***	
6a	-24	-8.5	655	-24	-8	658	
7	-17	-23	632	-17	-23	***612***	
7a	-17	-23	616	-17	-23	602	
8	-22	-20	744	-22	-20	***724***	
8a	-24	-20	718	-24	-20	704	
9a	-28	41	924	-28	41	915	
10a	-28	12	728	-28	12	741	
11a	-28	-15	685	-28	-15	669	
12a	-28	-23	885	-28	-23	886	
13a	-18	40	923	-18	40	814	
14a	-18	8	868	-18	8	870	
15a	-20	-9	683	-20	-9	666	
16a	-20	-29	829	-20	-29	814	
17a	-9	28	807	-9	28	***787***	
18a	-22	38	825	-22	38	***805***	
19a	-37	38	912	-37	38	916	

Calc. 24, Rev. 1 measurements 1/8/93

The numbers with postsript (a) are dated 1/11/93 and are in part duplicate measusrements from the previous entry and in part new measurements

bold numbers in italics are numbers missing in the 2006 survey. They have therefore been calculated by subtracting 20 mils from the 1992 measurements.

This was necessary because otherwise the upper right hand corner of the plot would have been grossly and erroneously distorted.

Bay 1 Contour Plot for 2006 External Measurement Data

Individual Evaluation Areas from Tamburro Analysis superimposed [see Calc. 24 Rev. 2 Fig. 2-1]

Figure 1

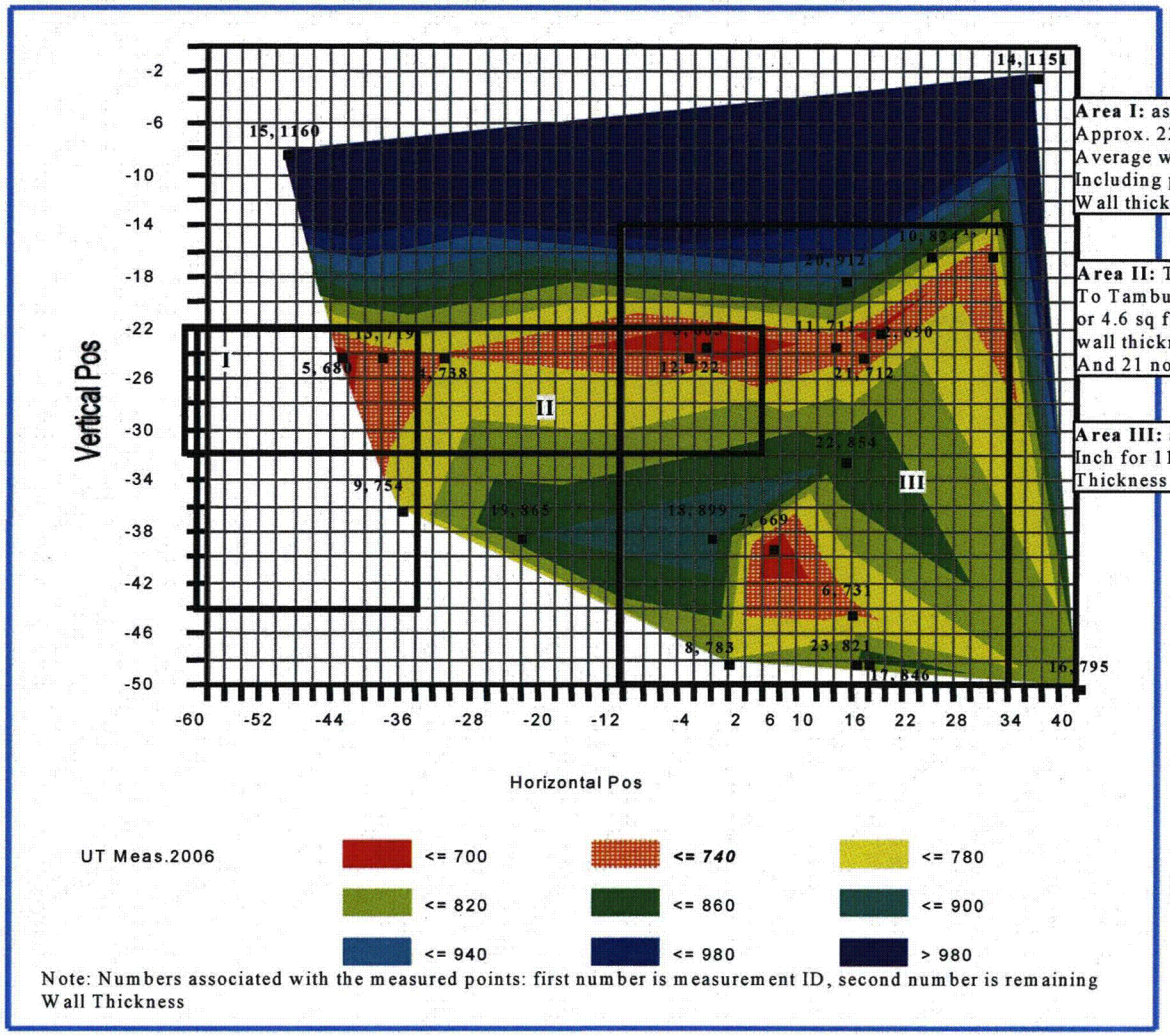

Area I: as defined by Tamburro
Approx. 22 x 30 inch for 4.6 sq feet
Average wall thickness 718 mil
Including pts 2 and 19 results in average
Wall thickness of 751 mils

Area II: The Bathtub ring, according
To Tamburro approx. 10 inch by 66 inch
or 4.6 sq feet for an average residual
wall thickness of 705 mils, except pts 11, 2,
And 21 not included in this area

Area III: according to Tamburro 36 inch by 44
Inch for 11 sq feet and an average residual wall
Thickness of 695 mils

Note: Numbers associated with the measured points: first number is measurement ID, second number is remaining Wall Thickness

Bay 1 Predictive Response Surface Calculated from Triangulation
External UT Measurements 2006

Figure 2

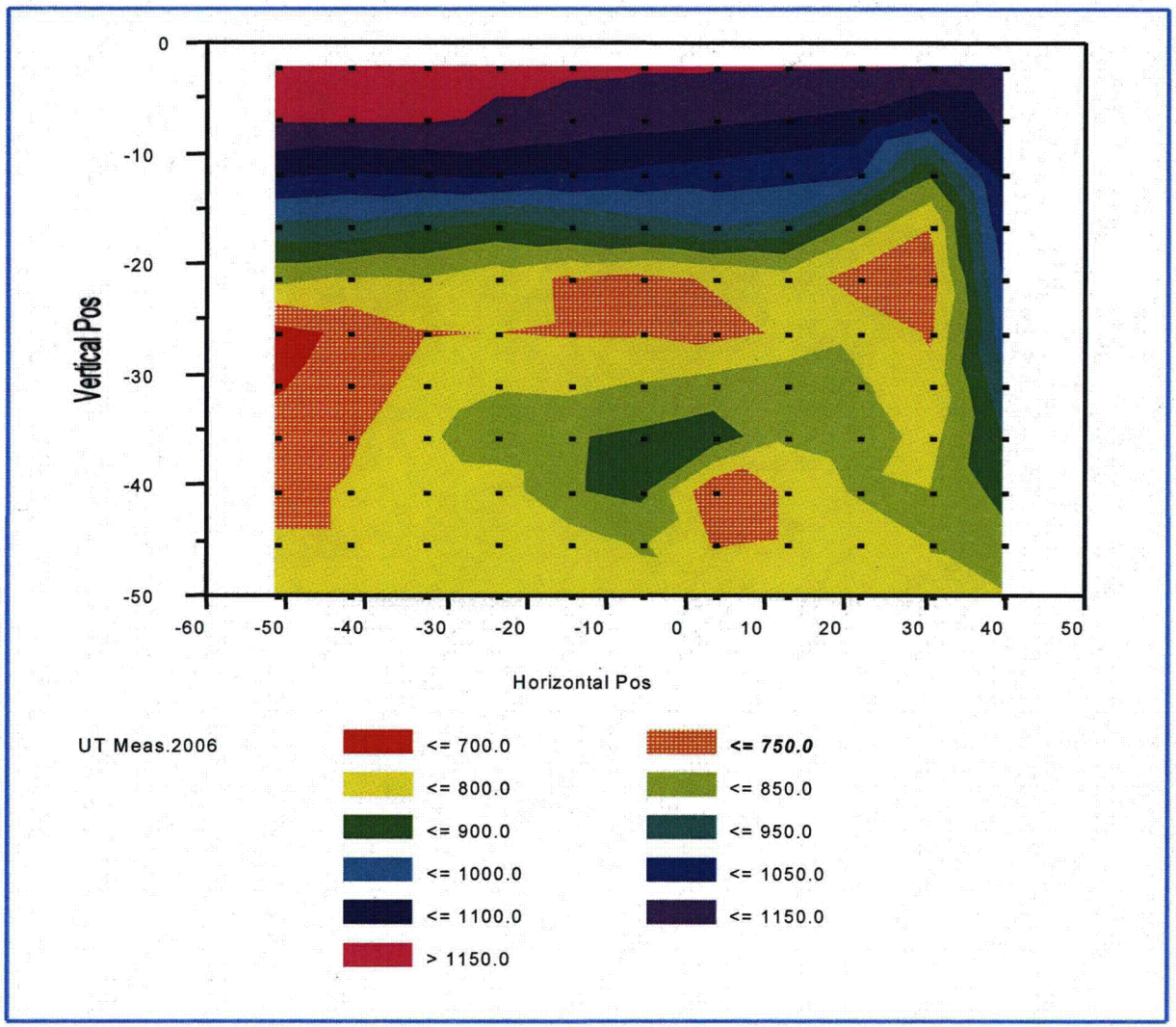

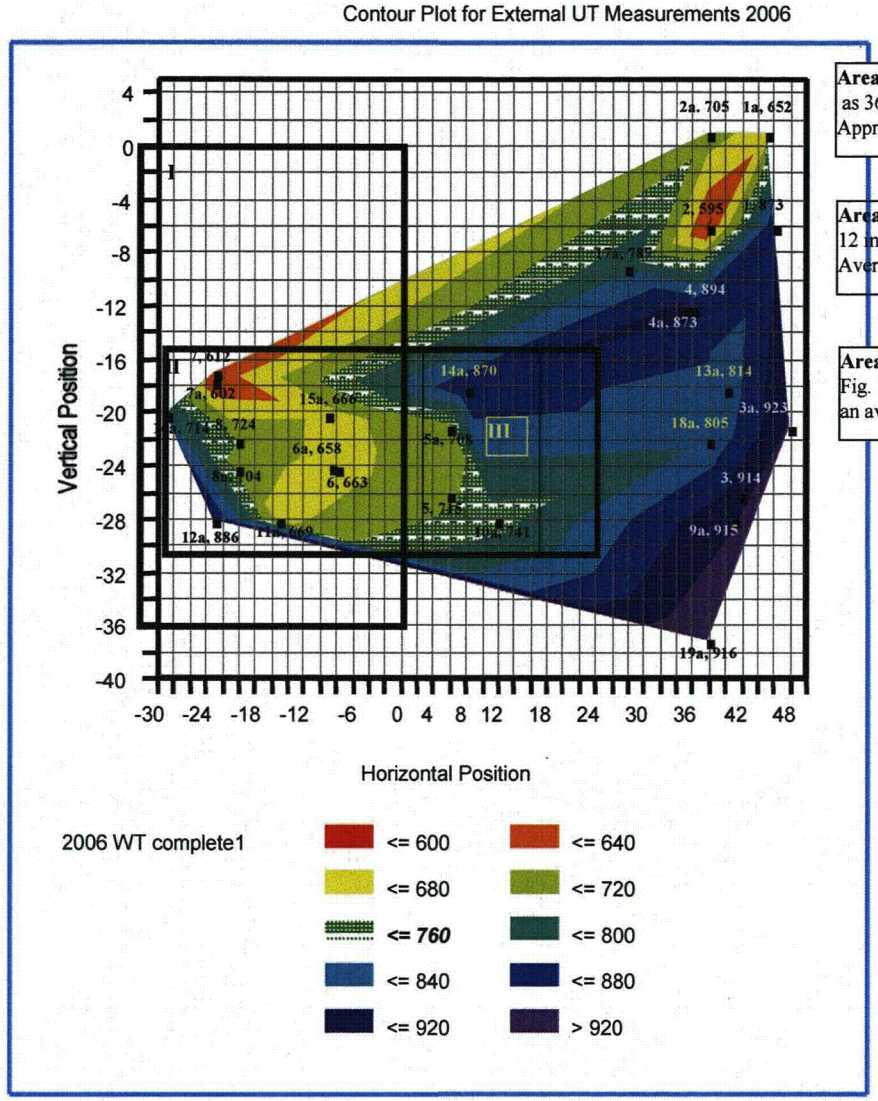

Area I: Defined by Tamburro's Fig. 13-2 as 36 inches by 36 inches. 36 inches is Approximately the height of the sandbed.

Area II: Defined by Tamburro's Fig. 13-2 12 inches by 54 inches, 4.5 sq feet with an Average residual wall thickness of 710 mils

Area III: Defined by Tamburro Fig. 13-2 and Fig. 13-6 actually contains 4 measurements with an average residual wall thickness of 758 mils

Figure 3

Figure 4

Predicted Response Surface for area of Bay 13
Contiguous Areas which are less than 725 mils about 12 sqft
Bordered by the dark green areas.

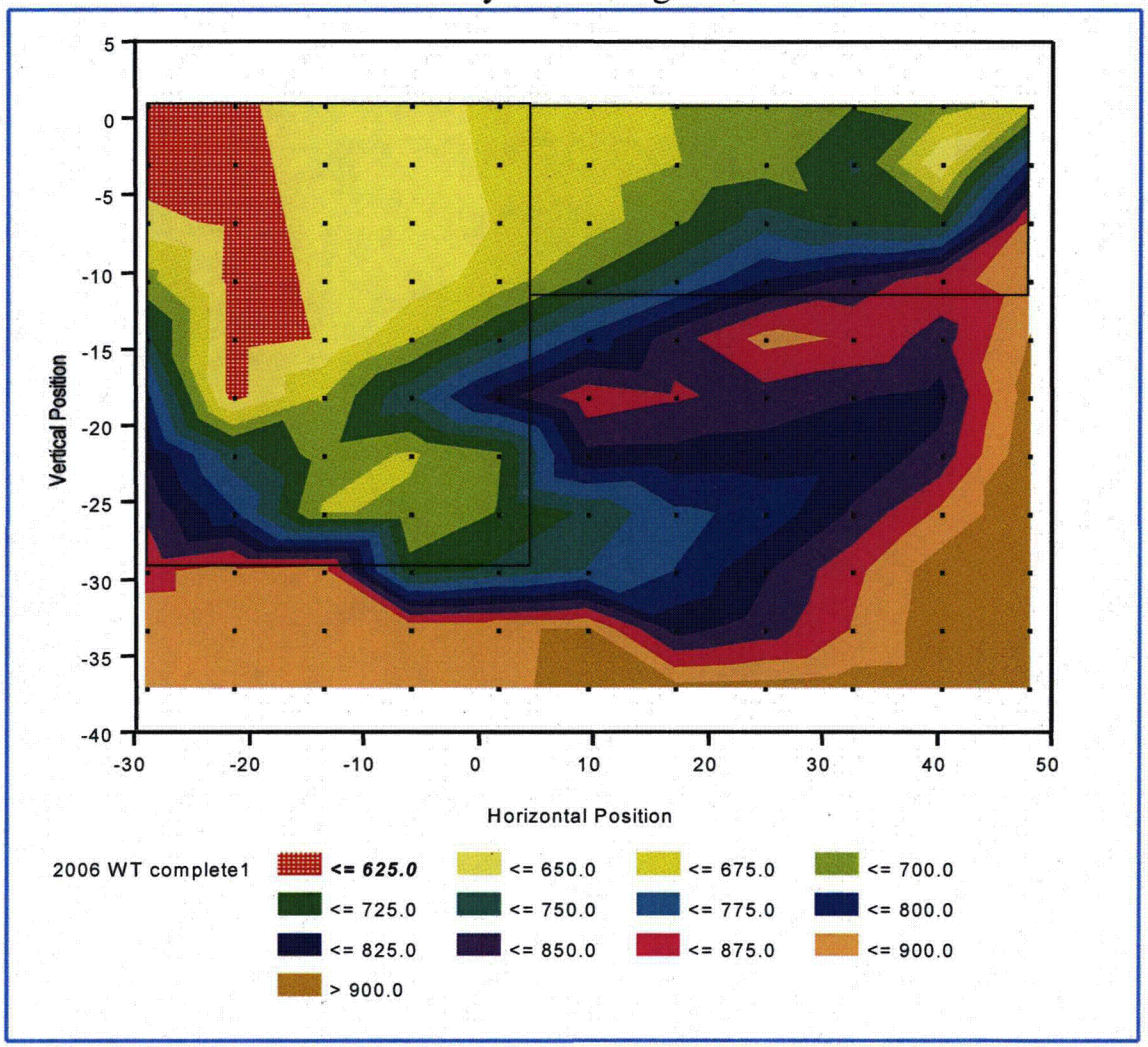

Figure 5

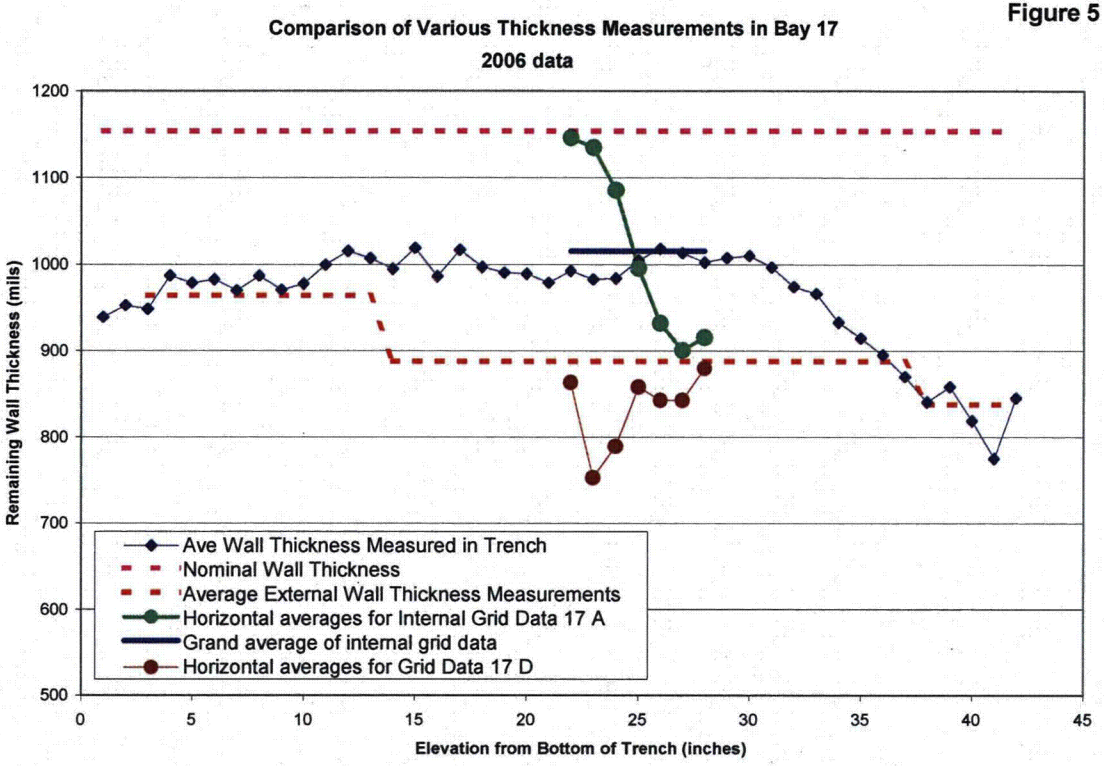
Comparison of Various Thickness Measurements in Bay 17
2006 data
Remaining Wall Thickness (mils)
1200
1100
1000
900
800
700
600
500
0
5
10
15
20
25
30
35
40
45
Elevation from Bottom of Trench (inches)
Ave Wall Thickness Measured in Trench
Nominal Wall Thickness
Average External Wall Thickness Measurements
Horizontal averages for Internal Grid Data 17 A
Grand average of internal grid data
Horizontal averages for Grid Data 17 D

Exhibit 62

Transcript excerpt from:

Official Transcript of Proceedings

Nuclear Regulatory Commission

Advisory Committee on Reactor Safeguards

485th Meeting held on September 6, 2001

. . .

DR. WALLIS: So you have some sort of acceptance criterion which says that the uncertainty has to be within some limits or something, or you just guess?

MR. ULSES: Well, actually, let me jump in here. Basically, what that statement is intended to mean is that if you look at the review of the kinetics package in its entirety, including both the test problem that -- called the GE validation against experimental data on all of the other work that we did, basically the bottom line conclusion was that the effect of any of the -- well, I am just thinking how best to put this.

That was really intended to discuss the fact that as Ralph said, we did have some -- well, some malingering differences in the prediction of power for the sample problem.

However, the effect of those differences on the bottom line answer for AO transients, which is the effect on changes in the minimum critical power ratio, was effectively nil, and actual what I mean by nil, was that it was basically almost impossible to see the effect.

But that's the relevant output of all of these transients. We do all this stuff with all these big codes, and we get one number out of it.

DR. WALLIS: What number did you get for uncertainty?

MR. LANDRY: Well, this is just looking at this transient.

MR. ULSES: Right. This is how it is applied in actual licensing of the plants. I mean, that's what they use to set the operating limits of the plant.

DR. WALLIS: I see. Well, the criteria for accepting this code are that there is reasonable models over physics, and that is part of it. But the other part of it is that when you make a prediction, you can also predict the uncertainty.

Now, that is the requirement for the best estimate code isn't it? Now, what the staff does with that I think is still up in the air. The use of the code may be able to do all the things with CSAI and predict all these uncertainties.

But I don't think the staff has really thought through what it is going to do with these uncertainties when it gets them, and that's where I think we have also mentioned in our letters that, yes, our codes are doing all these things that we have asked them to do, and you need a measure of the predictions, and the answer, and the causes of all the answers and all of that.

But what are you going to do when you have got that? I mean, there has still got to be some relationship with these uncertainties to margins and acceptance criteria, and so on.

I am not sure that the staff really has thought that through. Do you have any comments on that?

MR. LANDRY: At this point, we would just have to say we are continuing to study that, and we are trying to define.

DR. WALLIS: Well, that's typical. I mean, you see, there must be a criterion, some acceptance criterion, when they want to uprate the power to some point where it is meeting some boundary.

Then how big the uncertainties are in the code are very important to know, and whether you may step over that boundary or not. So it seems to me that maybe the acceptabilities then are going to depend upon the use.

Yes, they have got a good code, and they have an assessment of uncertainty, and then look at something like power uprate, and start using this code, and then you can figure out perhaps how big the uncertainty or what is the effect of the uncertainty on your decision about whether or not they should be allowed to uprate power.

MR. CARUSO: Dr. Wallis, this is Ralph Caruso from the staff. We do actually have some criterion in this area for AOOs. For example, we set a safety limit minimum critical power ratios to ensure that 99.9 percent of the rods don't undergo boiling transition.

I think that your question is what does reasonable assurance mean, and I think that the ACRS has had this discussion with the Commission in the past about what reasonable assurance means, and I don't think there has ever been any definition that everyone has agreed to.

This is an eternal question that we try to deal with, and it comes out of judgment to a large extent at this point. When we can quantify it, for example, and say setting safety limit MICPRs, we try to do that.

We are trying to do our regulation in a more risk-informed manner, and that is another attempt to do it in a more quantifiable way. But right now these are the words that the law requires us to use to make a finding.

So those are, unfortunately, the words that we use and they are not well defined.

DR. WALLIS: But the law requires you to make a finding with 95 percent confidence.

MR. CARUSO: No, the law requires us to make a reasonable assurance finding.

DR. WALLIS: If your criterion is 95 percent confidence, then the fact that they have evaluated these uncertainties enables you to make that assessment.

MR. CARUSO: We could say that a 95 percent confidence does define reasonable assurance, but --

DR. WALLIS: That is the thing that I think is not being worked out yet. I mean, you have got the tools to do it, but if someone comes around like tomorrow and says reasonable assurance is 99 percent, then you have still got the tools to do it, but where you come out on allowing some change in the plant may be different.

MR. CARUSO: I really hate to pass the buck on this, but I do believe that this has been the subject of some extensive discussions with the Commission about the definition of reasonable assurance, and I don't believe that anyone has come up with an acceptable definition for all the parties involved.

DR. WALLIS: So maybe my --

MR. CARUSO: This is a little bit beyond my pay grade as they say.

DR. WALLIS: -- saying that you have got a good tool is, but the staff isn't quite sure how to use it, is a true statement.

MR. CARUSO: I can't explain why. I don't want to get into philosophy on this particular issue.

DR. WALLIS: It is not philosophy. It is really very real.

DR. KRESS: Yes, and in a number of our letters, we have commented that the staff needs to get more into formal decision criteria, and this is exactly what we mean by formal decision criteria. How do you use these uncertainties to make our decision.

And you would come up with some sort of a technical definition of reasonable assurance that way, and we said that in a number of letters. And I think it could be repeated over and over. I think it is needed.

DR. WALLIS: And the reasonable assurance probably should be risk-informed. If it is not important to risk, then you can do it with less assurance perhaps.

MR. CARUSO: And there is a lot of effort going on in that area for a formal decision.

DR. KRESS: And that would be part of the formal decision process.

DR. WALLIS: That is part of a broader picture. So, maybe we should move on.

DR. KRESS: But I don't think that is these guys' job. They just have to be sure that the code can -- well, I agree with you that if there is reasonable assurance that it does the uncertainty correct, then they have got a basis for saying its okay for this.

MR. CARUSO: As a lower level engineer, I would be thrilled if someone could define the term for me, but I have not seen it defined yet.

MR. LANDRY: Okay. Moving on to experience . . .

Official Transcript of Proceedings, Nuclear Regulatory Commission - Advisory Committee on Reactor Safeguards, http://www.nrc.gov/reading-rm/doc-collections/acrs/tr/fullcommittee/2001/ac010906.html (last visited Sept. 13, 2007) (transcript excerpt from the 485th Meeting held on September 6, 2001).

Exhibit 63

Diagram of Oyster Creek Lower Drywell / Sandbed Region.

AmerGen

An Exelon Company

LOWER DRYWELL/SANDBED REGION
DETAIL C

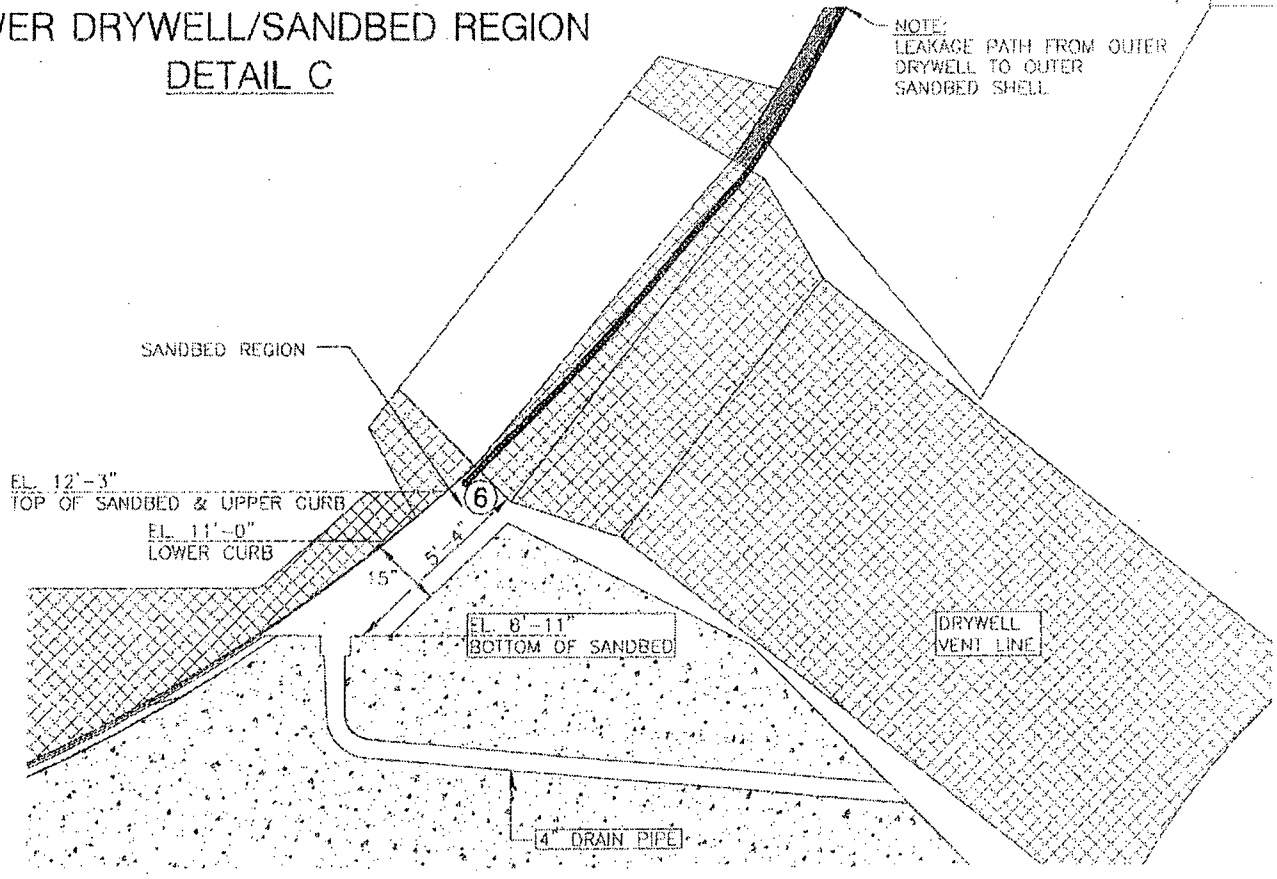

Exhibit 64

E-mails ending in e-mail from Gordon to Licina

[redacted]

redacted to non-proprietary as agreed with Amerigen - a/14/07 R. Wolf

From: Barry Gordon
Sent: Tuesday, October 24, 2006 13:29
To: George J. Licina
Subject: RE: UT Measurement Results - Questions
George,

Thanks. Note that my discussion with Gary Alkire is not related to Fred Polaski. The previous corrosion rate in the sand bed region was 20 mpy. Gary used the highest rate measured. The rates varied from 0.2 to 6 mpy.

[redacted]

Barry

From: George J. Licina
Sent: Tuesday, October 24, 2006 12:57 PM
To: Barry Gordon
Subject: RE: UT Measurement Results - Questions

I will respond to you, based upon the information you sent, presumably for my information (only).

1. If the drywell actually is wet on both sides, corrosion from both sides should be considered. A rate of 3 mpy per side seems awfully high. As a corollary to your statement that a truly dry drywell will not experience any corrosion, it should also be pointed out that the corrosion rate will (also) be zero at locations where the coating is intact. A corollary to that corollary statement is that the life of a coating will typically be less than 40 years.
2. My position on determining rates from a single UT thickness measurement is similar to that of the Regulators. That is, a loss of thickness of X mils, determined after Y years of service, really only indicates that X mils were lost due to degradation. In the absence of anything else, a rate = X/Y can be used, but only as a very rough approximation. That apparent rate, and the significance of a loss of X mils, can also be used to help define the interval until the next inspection.
3. Once a second thickness measurement is made (as appears to be the case for OC), the rate can be approximated better, however, the time that any corrosion is operative is still somewhat unknown, the time of active corrosion during the first time interval remains unknown, and the time dependence of the metal loss is unlikely to be 1. For the form(s) of corrosion under discussion for the OC drywell, a time dependence less than 1 is much more likely; 1 can be used as an upper bound (plus mechanical engineers can actually convert rate to metal loss when a linear rate is used).
4. The fact that OC has UT thickness measurements at more than one time, hopefully at the same locations, and that some areas appear to be getting thinner while others are getting thicker, with the general trend toward some metal loss, implies that the drywell has corroded, probably a little bit, since the last thickness measurements, at a low rate. Those measurements, and the scatter in them, provide data that can be used to estimate an upper bound on metal loss. The extreme value statistics recommended by Hausler would use such data. Any statistical analysis would use those data to come up with predictions of worst case (defined statistically) metal loss and metal loss rate.

I hope that these are useful.

George Licina
Chief Materials Consultant
***Structural Integrity** Associates, Inc.*
Experts in the prevention and control of structural and mechanical failures
3315 Almaden Expressway, Suite 24
San Jose, CA 95118-1557
Phone: 408-978-8200
Fax: 408-978-8964
E-mail: glicina@structint.com
Web Site: http://www.structint.com/

[redacted]

[redacted]

to this e-mail is strictly prohibited and may be unlawful. If you have received this e-mail in error, please notify the sender immediately and permanently delete the original and any copy of this e-mail and any printout. Thank you for your cooperation.

From: Barry Gordon
Sent: Tuesday, October 24, 2006 10:28
To: Gary.Alkire@exeloncorp.com
Cc: howie.ray@exeloncorp.com; sharon.eldridge@exeloncorp.com; james.hallenbeck@exeloncorp.com; Marcos Herrera; Rich Bax; George Licina
Subject: RE: UT Measurement Results - Questions

Gary,

Since I am not familiar with the code minimum wall for the drywell, I cannot comment on it. However, SI has been discussing this type of structural analysis with Ahmed Ouaou and Chris Cooney. We will be happy to help you with it.

By definition, a truly dry drywell will not experience any corrosion.

The only Oyster Creek UT thickness discussions I have had since 1986 occurred today with Peter Tamburro.

Barry

From: Gary.Alkire@exeloncorp.com [mailto:Gary.Alkire@exeloncorp.com]
Sent: Tuesday, October 24, 2006 9:59 AM
To: Barry Gordon
Cc: howie.ray@exeloncorp.com; sharon.eldridge@exeloncorp.com; james.hallenbeck@exeloncorp.com
Subject: UT Measurement Results - Questions

Barry....

So if we take the 6 mil per year corrosion rate (attack from both sides) and apply it to the drywell liner for the remaining life of the plant (assuming life extension) do we violate Code minimum wall? What is Code minimum wall for the drywell shell?
OR
Do we assume that the drywell will not get wet again and assume 3 mils ....what does that do for us???

One thing that Regulators questioned us at Peach Bottom was that we averaged corrosion rate over a long period of time.....(similar to this report) ....but what if the wall loss occurred in the last year? Do we have interim UT data points that show that we have had thinning or no thinning over the years? Peach Bottom was able to show that data and convince the NRC that this was not an overnight corrosion wall loss.

Have you been part of any of these discussions with the UT data evaluators?

Gary

> -----Original Message-----
> **From:** Barry Gordon [mailto:Bgordon@Structint.com]
> **Sent:** Tuesday, October 24, 2006 11:25 AM
> **To:** Alkire, Gary
> **Subject:** RE: Activity Report - Not True
>
> Gary,
>
> It was nice to chat with you today. Attached please find the latest revision.
>
> Barry

[redacted]

[redacted]

<<Oyster Creek Drywell Corrosion BMG06015 R06436R0b.doc>>

From: Barry Gordon

Sent: Tuesday, October 24, 2006 9:09 AM

To: Gary Alkire

Subject: Activity Report - Not True

Hi Gary,

Addressing you activity comment:

"I would like to see the Chemistry department's position on activity being 4 times less than for active leakage in this report somewhere to help support the above Calcium position. Talk to Chemistry for details or forget this comment if this statement can no longer be supported by Chemistry."

The BXWT report states the following under the section **"Previously Circulated Conclusions and Why Conclusion No Longer Valid":**

"The presence of short-lived radionuclides and a 511 keV peak in the trough sample and their absence in the trench samples indicates that the trough water is fresher and the trench water is 'older.' The 511 keV peak is due to fluorine-18 that has a 1.8 hour half life. The trench samples are four orders of magnitude lower in activity than the trough samples. This indicates the water in the trench is not refreshed with short-lived radionuclides as is the water in the trough.

a. OC isotopic data shows 511 keV peak in only the Drywell 1-8 Sump and Drywell CRD Leak samples." (and not in either the trough or trench water)

I added the UT data to my report. However, the tracer results are unknown.

Barry

>

[redacted]

Exhibit 65

E-mails from O'Rourke to Herrara

[redacted]

redacted to non-proprietary as agreed with AmerGen

9/14/07

L. Wh

From: O'Rourke, John F.
Sent: Wednesday, February 07, 2007 10:56 AM
To: Marcos Herrera (E-mail)
Cc: Ray, Howie; Tamburro, Peter
Subject: Current Contract Base Case Definition

Marcos: Based on our conference call from last night, here is the definition I put together for your review and comment, as well as Howie and Pete's review/comment. [redacted]

[redacted]

For now, please review the following so we can all agree on the wording.

1. The following are the base cases that are part of the current contract:
   a. Determine the current factors of safety for the Oyster Creek Drywell as it is currently configured with the wall thicknesses measured during the 2006 refueling outage per the guidance provided by Pete Tamburro (draft of his calculation due to SI on 2/7/07). This analysis is performed with the increased capacity reduction factor identical to the factor used in the GE Analysis (current license basis analysis) and all load combinations as required by the current licensing basis. Note: any values above a safety factor of 2 (Code compliance) for the buckling in the sandbed region and above a safety factor of 1.67 for the operational/accident condition represents additional margin.
      i. The wall thicknesses to be provided by Pete Tamburro in a revision to the 024 calculation will be based on the external UT measurements in each bay. Pete will define an area of localized thinning with a thickness equal to the average of the thin points in that area and blend the wall out to the average of the remaining non-thin points in the bay (general wall thickness). The general wall thickness calculated based on the non-thin external points will be no greater than the internal grid measurements or, if the internal grid average measurement is less than the average of the non-thin external points, the internal grid average will be used for the general wall thickness for that bay (i.e., the lesser of the average of the external non-thin measurements and the average internal grid measurements will be used as the general wall thickness).
   b. For the 2029 base case, uniformly reduce the wall thickness in all areas by an agreed upon (AmerGen/SI) mils per year from 2006 to 2029 and reperform the item 1a analysis to determine the factors of safety for the Drywell in 2029. Other than uniformly reducing the wall thickness, no other changes are made to the item 1a input data. All load combinations analyzed are as required by the current licensing basis.

2. Although not defined in item 1 above as a base case, the current contract will not conclude without performing an analysis to determine the minimum general wall thickness for the current configuration required to meet Code requirements (Buckling factor of safety of 2, operational/accident factor of safety of 1.67). This case is defined as follows:
   a. Using the current configuration as a base, reduce the wall thickness uniformly in the sandbed region while maintaining all wall thicknesses outside of the sandbed region constant until a factor of safety of 2 is obtained. This will identify the minimum general thickness required to meet Code requirements. A value less than 736 mils is expected. Need to determine size of step reductions (10 mils suggested). All load combinations need to be looked at to ensure that the operational/accident

[redacted]

[redacted]

factor of safety of 1.67 is not reached before the buckling factor of safety of 2 for any load combination.

[redacted]